AGARDograph ~~Number~~

One Hundred and Thirty Three

The Effects of Gravity and Acceleration on the Lung

GLAISTER, D. H

11.70

The Advisory Group for

Aerospace Research and

Development. NATO

Author

D.H. GLAISTER, Ph.D., M.B., B.S., R.A.F.
Royal Air Force Institute of Aviation Medicine,
Farnborough,
Hampshire,
England

with chapters contributed by

J. Milic-Emili, A.C. Bryan and J.B. West

Published by

Technivision Services
Slough, England
A Division of Engelhard Hanovia International Ltd.

Library of Congress Number 78 - 108672

International Standard Book Number 0.85102.027.5

Contents

Chapter		Page
1	Acceleration and the centrifuge	13
2	Ventilation and the mechanics of breathing	19
	Pulmonary ventilation Anatomical dead-space Total lung capacity and its subdivisions The diaphragm Thoracic compliance Airway resistance Work of breathing	
3	Distribution of ventilation	37
	J. Milic-Emili	
	Regional ventilatory lung function Factors determining regional distribution of gas within the lung Causes of uneven ventilation distribution in general	
4	The effects of acceleration on ventilation distribution	55
	A.C. Bryan	
	Positive acceleration Forward acceleration Zero gravity	
5	The effect of acceleration on the cardiovascular system	69
	Systemic circulation Pulmonary circulation	
6	Regional distribution of blood flow	82
	J.B. West	
	Normal distribution of blood flow Cause of the uneven distribution of blood flow Features of the unperfused zone 1 Features of zone 2 Features of zone 3 Zone of interstitial pressure	
7	Effects of acceleration on the distribution of pulmonary blood flow	103
	Positive acceleration Forward acceleration Other acceleration vectors Weightlessness Interstitial and alveolar oedema	

8 Acceleration atelectasis 121

Oxygen toxicity
Oxygen solubility
Alveolar oedema
The demonstration of unventilated alveoli in the lower lung
Factors modifying the development of acceleration atelectasis
Mechanism of acceleration atelectasis
Forward acceleration

9 Ventilation-perfusion ratio inequality and gas exchange 151

Positive acceleration
Forward acceleration

10 The effect of acceleration on gas exchange, arterial oxygen saturation and alveolar shunting 159

Gas exchange
Arterial oxygen saturation
Right-to-left shunt
Transient changes in arterial oxygen tension following acceleration
The effect of acceleration on gas stores in the body

11 Summary and conclusions 181

Lung mechanics
Regional ventilation
Intrapleural pressure
Regional perfusion
Regional ventilation-perfusion ratio
Methods for increasing G-tolerance

References 193

Index 211

Acknowledgements

The author wishes to acknowledge the collaboration of the following contributors:

J. Milic-Emili, M.D., of the Department of Physiology, McGill University, Montreal, A.C. Bryan, Ph.D., M.B., B.S., of the Canadian Forces Institute of Environmental Medicine, Toronto (now at the Department of Anaesthetics, Toronto General Hospital) and J.B. West, Ph.D., M.D., of the Postgraduate Medical School, London (now at the Department of Medicine, University of California). While each has contributed his own chapter an additional measure of their contribution to pulmonary physiology is afforded by the frequent reference made to their work throughout the text.

The author has great pleasure in recording his indebtedness to Air Vice-Marshal H.L. Roxburgh, C.B.E., Ph.D., Ch.B., F.R C.P. (Edin), F.R.Ae.S., Commandant, Royal Air Force Institute of Aviation Medicine, for the opportunity of carrying out much of the work described, and also for the chance of putting it into a coherent form. He also wishes to thank past and present members of the Acceleration (now Biodynamics) Section of the Institute of Aviation Medicine for their frequent co-operation as experimental subjects; for data analysis and for much helpful advice and criticism as the work progressed. He is grateful to the Drawing Office and Photographic Section for the preparation of most of the illustrations, and to the Typing Pool and Mrs. I.J. Isles for the preparation of typescript from an often illegible draft.

The author wishes to thank the Director-General of Medical Services, Royal Air Force, for permission to submit this work for publication; and the Ministry of Defence (Air Force Department), for permission to reproduce figs. 2-1, 4-8, 5-2 to 5-4, 5-6, 7-8, 8-1 and 10-1 to 10-3 from the relevant FPRC Reports.

The work described in chapter 5 was supported by the Medical Research Council.

1

Acceleration and the centrifuge

By its own weight made steadfast and immovable Congreve

Newton's first law states that a body will remain in a state of rest or uniform motion in a straight line unless acted upon by a force. Gravity is such a force, for it will cause an unsupported body to fall with an acceleration of 32.2 feet per second per second. A body constrained to go round in a circle, such as a stone swung round at the end of a piece of string, is also acted upon by a force called the centripetal acceleration, which constantly deflects it from a straight path. The magnitude of this force is given by v^2/r, where v is the circumferential velocity and r the radius. If the units are ft./sec and ft, respectively, then the resulting acceleration is given in ft./sec^2. This acceleration can be converted into G by dividing by 32.2 (the gravitational constant). Thus, a centrifuge with a radius of 30ft. will impose a radial acceleration of five G when the gondola is travelling at about 70 ft./sec. Since the distance travelled each revolution is 2π r, or approximately 190 ft., the arm will have to rotate at 22 rev/min. It must be noted that the acceleration imposed upon a subject within the gondola will be rather more than five G (about 5.1 G), since this is the resultant of the radial acceleration and the perpendicular one G of gravity. The subject may be lined up along this resultant by the simple expedient of having a free-swinging gondola, its centre of gravity being below the pivot point. All accelerations given in the text refer to the resultant experienced by the experimental subject.

When a man is subjected to a centripetal acceleration, it is the reaction or centrifugal force which is sensed, in the same way that a motorist is pressed back against his seat as his vehicle accelerates forwards. A man seated in a centrifuge with his head towards the centre of rotation is subjected to a headward acceleration, but the inertial force is acting towards his feet and it is there that blood will tend to pool. Because this inertial force is similar to the force of gravity, it is referred to as positive or $+G_z$, the subscript z denoting that the force acts along the longitudinal axis of the body. This is the strict definition, but the terms positive acceleration and $+G_z$ acceleration are so widely used and accepted that they will continue to be employed throughout the text. Provided that it is appreciated that the terms actually refer to the inertial force and that this force is, by Newton's third law, equal and opposite to the applied acceleration, confusion should not result. Many other descriptive terms have been evolved, since none is wholly satisfactory. For a full account of these equivalents the reader is referred to the table compiled by Gell (92) and fig. 1-1 has been redrawn from this source to illustrate the most commonly used terms.

If a centrifuge subject lies down facing the centre of rotation, then the acceleration is forward and the $+G_x$ inertial force acts towards the spine. Again several equivalent terms exist (Fig. 1-1). The seated and supine postures are the commonest positions adopted in centrifuge experiments, for they simulate, respectively, the major accelerations experienced in aviation and space flight. The term

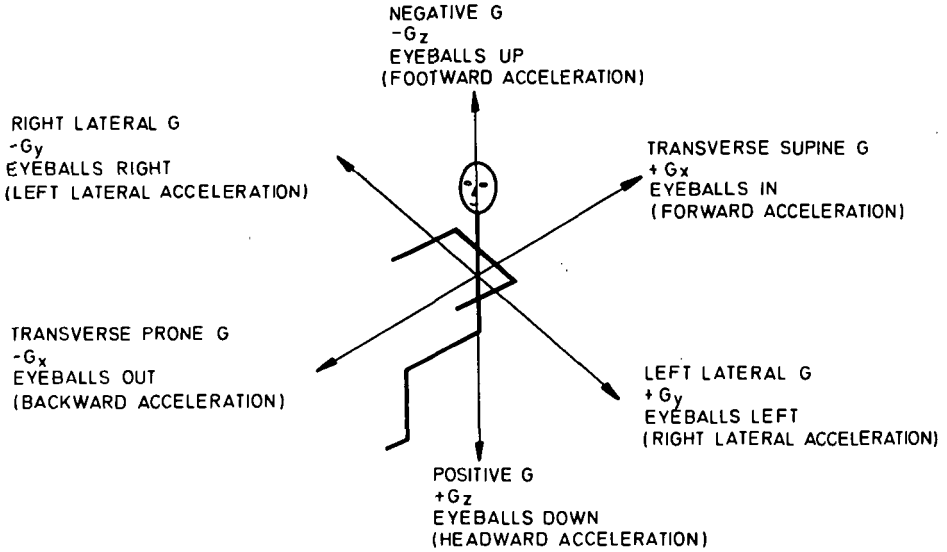

Fig. 1-1 Nomenclature used to describe the direction of the inertial force vector which results from differing axes of acceleration. The terms underlined are those employed in the text. Terms in brackets refer to the direction of the imposed acceleration. (Modified from Gell (92)).

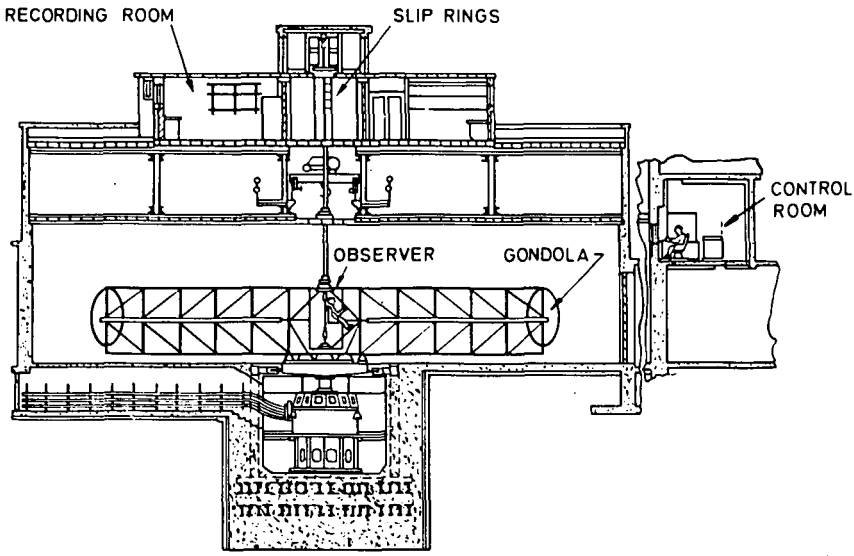

Fig. 1-2 The layout of the man-carrying centrifuge at the R. A. F. Institute of Aviation Medicine. Note the distance separating the experimental subject in the gondola from the recording equipment, and the necessary intervention of slip-rings for electrical signals. The centrifuge has a working radius of 30ft.

transverse acceleration is also widely used to refer to all axes of acceleration perpendicular to the long axis of the body. It has also been used specifically to refer to a forward ($+G_x$) acceleration,but this usage is discouraged.

Interest in the effects of acceleration upon the lung has been stimulated by a number of observations in the fields of general physiology and medicine, as well as in the newer fields of aviation and space medicine. A Frenchman, Piorry, in 1826 (209) noted that "in syncope, the heart continues to beat, but the beats have not force enough to overcome the resistance which is given by gravity". The translation is due to Hill, who subsequently investigated the effect of body position on systemic vascular pressures in animals, and concluded that the changes seen were caused by hydrostatic pressure gradients (126). This work provided experimental support for Piorry's similar conclusion, based on the observation that an unconscious victim of a street accident recovered when lain flat on his back. The same mechanism is responsible for the difference in human tolerance to $+G_z$ and $+G_x$ accelerations on the centrifuge. In 1887, Orth, a German physician, applied similar logic to the pulmonary circulation when he suggested that the frequent apical localisation of tuberculosis might be caused by ischaemia at the top of the lungs (198); the hydrostatic pressure gradient due to gravity being even more significant in the pulmonary vessels than in the higher pressure systemic circulation.

The effects that changes in body position have upon the lungs have been studied since the early beginnings of respiratory physiology. Hutchinson, in 1849 (138),demonstrated that the vital capacity was reduced by 11.5 percent when the posture was altered from the erect to the supine position, and this before the invention of the spirometer. Since the erect posture is equivalent to an acceleration of $+1G_z$ and the supine to $+1G_x$, it is apparent that accelerations of greater magnitude should have profound effects on lung mechanics. For the same reason, a study of the inverted posture is of great value in elucidating the part played by gravity (or acceleration) on lung function, since the gravitational vector is thereby simply reversed ($-1G_z$). Several such studies will be described in the following chapters.

Aviation made little early impact on research into the effects of acceleration on the respiratory system, since it was soon apparent that tolerance to $+G_z$ acceleration was limited by the circulatory system, in particular by the inadequacy of the blood supply to the retina and brain,and that breathing was largely unaffected. Man-carrying centrifuges were built in the mid 1930s in both Germany and North America, but observations made in the next 15 to 20 years did not extend much beyond noting changes in the rate of breathing, and measurements of pulmonary ventilation and lung volumes. Several studies carried out in the 1950s, however, indicated that acceleration did have important respiratory effects,with Henry (122) showing that in man, $+G_z$ acceleration caused a reduction in the oxygen saturation of arterial blood. The bias of acceleration research was also changing at this time, from $+G_z$ to $+G_x$ studies, for it was demonstrated that in order to withstand the prolonged accelerations imposed by rocket flight, (initially in aircraft such as the Bell X-15, later in space-flight simulations), the circulatory system had to be protected by adopting the supine position (212, 276). In this posture, tolerance is dictated by the subject's ability to breathe and by the falling arterial oxygen saturation already referred to.

Further impetus to respiratory research was given by the observation that Royal Air Force pilots, exposed to $+G_z$ accelerations while breathing oxygen, often developed symptoms of chest pain and difficulty in taking a deep breath (147). These symptoms were associated with radiological evidence of lung collapse, and were attributed to absorptional atelectasis.

The development of techniques which allow the distribution of ventilation and blood

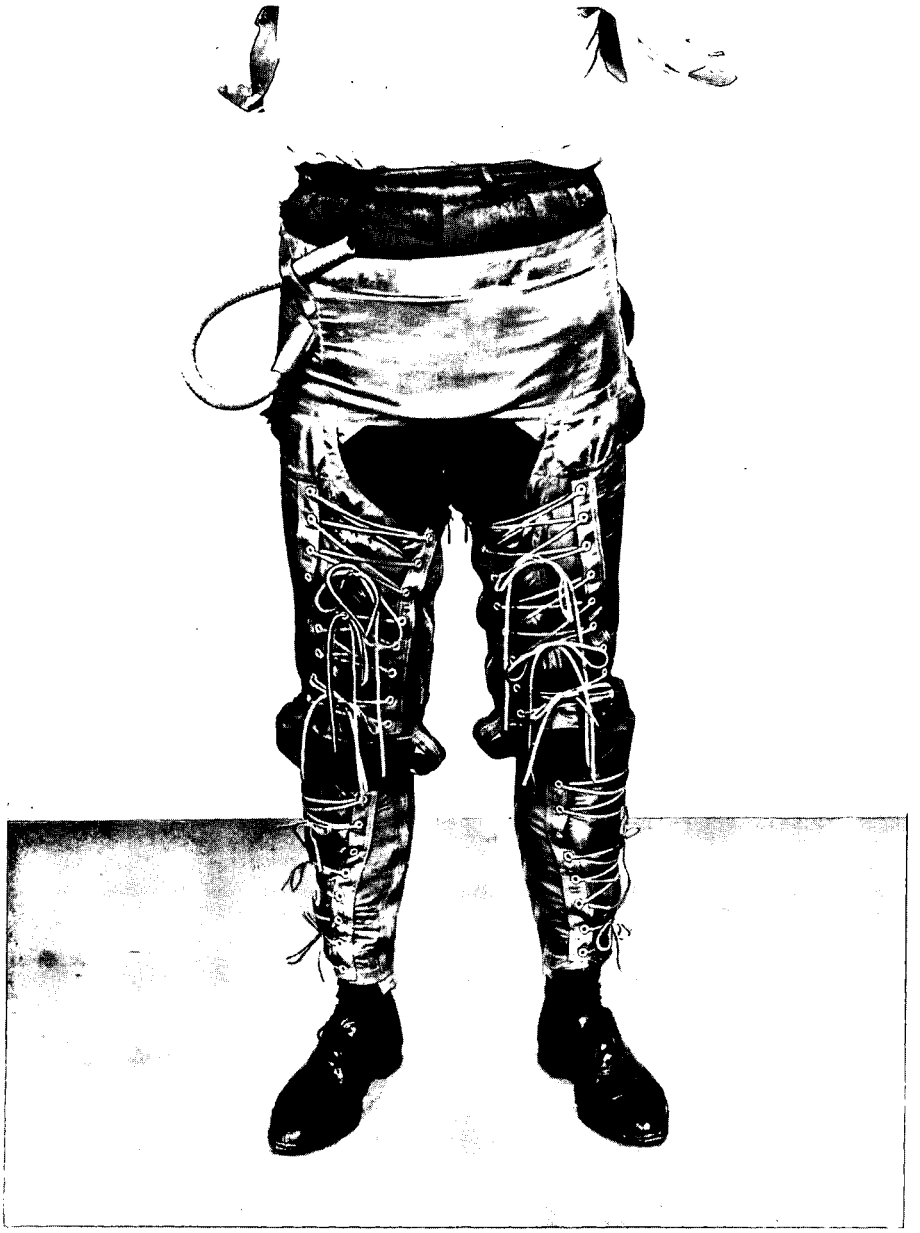

Fig. 1-3 The R. A. F. Mk 5 anti-G suit. Air under pressure is applied through the hose to bladders over the abdomen, thigh and calf. The bladders are held in place by non-stretch material and adjustable lacing.

flow to be studied within the lung using radioisotopes (11, 74), provided tools which were soon modified for use on the human centrifuge. The information so obtained is significant, not only in relation to the mechanisms of arterial hypoxaemia and lung collapse which occur during flight, but also in affording a better understanding of the influence that gravity has upon the normal function of the lung.

If one considers a typical, man-carrying centrifuge (Fig. 1-2), it is apparent that its use imposes complications which do not exist in a conventional laboratory. The most obvious problem is that measuring equipment mounted within the gondola is also subjected to acceleration, and precautions must be taken that artifacts are not thereby introduced. Pressure sensors may respond to acceleration because of the weight of their diaphragms, while hydrostatic pressure gradients in fluid filled catheters need to be precisely allowed for. A good example of such precision is provided by the work of Wood and his colleagues (233). A second problem is caused by the necessary isolation of the subject, for not only are most centrifuges too small to carry more than one man in the gondola, but it is questionable whether an experimenter in this position would be of much use, since he too would be exposed to inertial forces. For these reasons the experimental subject must perform many operations which would normally be done by a second person - turning taps, making injections, putting in pressure calibrations and so on. Apparatus must be designed to make such one-man operation possible, and to minimise the additional work load placed upon the subject. Care must also be taken that any necessary subject participation does not unduly affect the results. This problem is usually overcome by making the subject his own control, the same experiment being run with the centrifuge stationary. While remotely controlled apparatus can be employed, in respiratory studies most measurements have to be timed to the subject's breathing pattern, so that only the subject can initiate the manoeuvres required.

A corollary of the subject's isolation is that recording apparatus is also isolated, and at a considerable distance from the subject (Fig. 1-2). This makes setting-up procedures difficult and requires that most measurements are converted into electrical signals. It has been found that the use of a multichannel instrumentation tape recorder allows a greater flexibility in recording, so that many of these problems can be minimised.

An additional complication that occurs in $+G_z$ centrifuge studies results from the low tolerance set by failing retinal and cerebral circulations. In a relaxed subject, blackout develops at about +3 to $+4G_z$ and unconsciousness at about +5 to $+6G_z$; though unconsciousness may occur as low as $+3G_z$ during a respiratory manoeuvre such as a Valsalva, which impedes venous return. An upper limit of about $+3G_z$ is, therefore, set for many experiments. If the abdominal muscles can be tensed without interfering with the measurements being made, then the upper limit can be extended to, perhaps, $+6G_z$. Transverse acceleration studies ($\pm G_x$) are not affected to the same extent, since the cerebral circulation is protected. However, total lung capacity is dramatically reduced in the supine posture, the expiratory reserve volume disappearing at levels of acceleration which are easily tolerated. This reduction in functional residual capacity must also be taken into account in the interpretation of results.

Tolerance to positive ($+G_z$) acceleration can also be increased by the use of an anti-G suit, but this too is associated with a reduction in the functional residual capacity of the lung (231). An anti-G suit is worn by pilots flying high performance aircraft and consists of an abdominal belt and leggings containing air bladders (Fig. 1-3). The garment is close fitting, so that inflation of the bladders with air at a pressure of about one pound per square inch per G applies pressure to the calf and thigh musculature as well as to the abdomen. Blackout threshold is raised by more than one G, largely due to a reduction in the amount of fluid pooled

in the lower limbs; the induced rise in intra-abdominal pressure also displaces the diaphragm upwards and so reduces the FRC.

A further inescapable feature of centrifugal acceleration is disorientation, which often results from the complex angular accelerations also imposed upon the subject, especially at the beginning and end of the run. Vestibular stimulation may be sufficient to induce nausea or even vomiting, especially if several runs are carried out in succession.

These problems, all by-products of centrifugal acceleration, are mentioned, not as an apology for the sometimes less than adequate standard of acceleration research, but rather as points that must be considered in the interpretation of any results obtained from human centrifuges. Fortunately, by using a small number of highly trained and well motivated subjects, by careful design of apparatus and by restricting the acceleration to an easily tolerated upper limit, it is usually possible to perform the desired experiments and to have confidence in the results so obtained.

In the chapters which follow, the effects of acceleration on the mechanics of the lung are first considered. Ventilation and perfusion are then taken separately, the factors affecting their normal distributions being discussed before considering the influence of added acceleration.

Relevant cardiovascular changes are also considered. Acceleration atelectasis is given its own chapter because of its unique position in aviation medicine, and this is followed by a chapter in which the relationships between regional ventilation and perfusion,and their effect on gas exchange, are discussed. A further chapter deals with measurements of gas exchange and blood gases, with particular reference to pulmonary shunting.

This breakdown of the subject matter has necessitated a considerable amount of overlap. For example, the normal distribution of pulmonary blood flow could not be discussed without reference to the role of gravity, nor could acceleration atelectasis be considered without reference to airway closure. It was decided, however, to accept a certain amount of duplication in order to make each chapter capable of standing on its own. Standard symbols in respiratory physiology (204) have been used wherever possible. Other symbols are explained in the text.

2

Ventilation and the mechanics of breathing

Pulmonary ventilation

Positive acceleration leads to little respiratory embarrassment, at least up to the limits of +4 to $+5G_z$ set by a failing cerebral circulation. This contrasts with the effect of forward acceleration (subject supine), where tolerance is dictated by mechanical failure of respiration, but at much higher levels of acceleration. Some difficulty in breathing is experienced at +4 to $+5G_z$, however, and an increased inhalation/exhalation ratio and increased frequency of breathing may be detected at only +2 to $+3G_z$ (6).

Pulmonary ventilation is increased by exposure to $+5G_z$, by as much as 150% of the resting value (10, 169), but our own observations suggest that low levels of acceleration *per se* have little effect on ventilation, for, in subjects used both to centrifugation and to the experimental procedures involved, there is little change in the pattern of breathing at least up to $+3G_z$ (Fig. 2-1). The modest increase in pulmonary ventilation which is seen is a combination of an increased rate and depth of breathing. The increase in ventilation that occurs immediately upon return to resting conditions, apparent in fig. 2-1, will be considered later, in chapter 10. Rosenhamer found an increase in resting ventilation of 75% at an acceleration of $+3G_z$, though during the performance of standard work loads, smaller percentage increases were noted (228). Under resting conditions, the increase was mainly due to an increase in tidal volume, but during exercise it resulted more from an increase in the rate of breathing. These observations were made under steady-state conditions (after five minutes of acceleration), whereas those made on the R.A.F. centrifuge were obtained during briefer acceleration exposures. The significance of the duration of exposure to acceleration in affecting gas exchange will be considered in chapter 10. The larger increases in ventilation found by other workers may be attributed to secondary factors, such as the increased energy cost of muscular activity, discomfort, apprehension or even nausea, all of which are commonly seen during centrifugation. Breathing is still possible at an acceleration of $+10G_z$.

Babushkin and co-workers (9, 10) attributed the increase in ventilation which they recorded during exposure to $+5G_z$ to a combination of an increased oxygen requirement and true hyperventilation, since they recorded an increase in oxygen uptake and a reduction in the concentration of carbon dioxide in the expired gas. It will be shown later (chapter 8), that a reduction in expired carbon dioxide concentration is secondary to an increase in dead space which results from the development of an unperfused zone (alveolar dead-space) in the lung.

In anaesthetised animals, slowing of respiration is the rule (30, 116), but hyperventilation may be seen. Anaesthetised dogs usually become apnoeic on initial exposure to positive acceleration; but if the acceleration is maintained, respiration recovers and may then be less than, equal to; or even greater than the pre-accele-

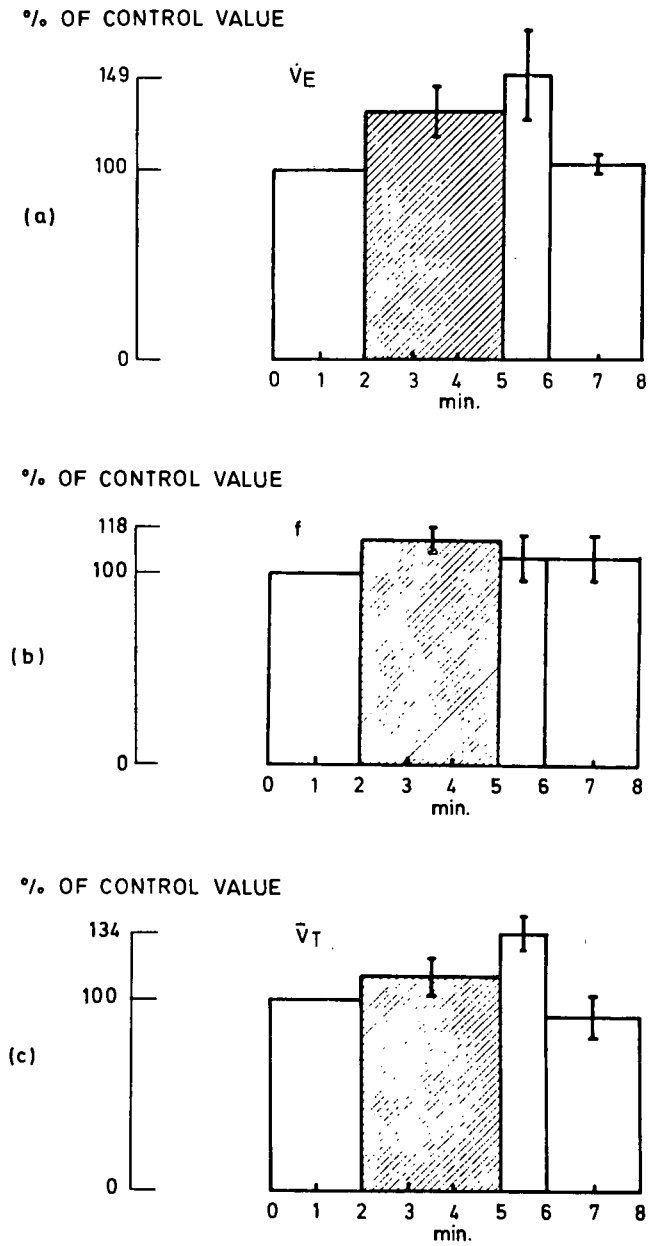

Fig. 2-1 The effect of positive acceleration on (a) pulmonary ventilation ($\dot{V}_E$); (b) respiratory rate (f); and (c) tidal volume ($\bar{V}_T$). The three minute period of $+3G_z$ acceleration is indicated by shading. Control values are taken as 100% and barred vertical lines indicate plus and minus one standard deviation.

ration value. A typical response is illustrated in figure 10-15 (p. 176). The initial apnoea is abolished by vagotomy and replaced by hyperventilation; this response in turn is abolished by section of the sinus nerves (20). The findings suggest that the ventilatory response to positive acceleration is a balance between vagal inhibition from stretch receptors in the lung and stimulation from the effect of hypotension on the carotid baroreceptors. Arterial hypoxaemia may also stimulate respiration during exposure to acceleration (see chapter 10). Owing to this conflict of centrally acting stimuli, the outcome is unpredictable even in anaesthetised animals, so that the variable result reported in conscious human subjects, with the added influence of emotional factors, is hardly surprising.

Fewer data are available on the effects of forward acceleration, but an increase in minute volume has been reported at $+5G_x$ (46) and this increase continued at levels of acceleration up to $+8G_x$, though there was little further change at $+12G_x$ (279). The increase in pulmonary ventilation took place despite a reduction in tidal volume - at $+12G_x$ this averaged only 318 ml, compared to the control value of 580 ml - as there was a relatively greater increase in the rate of respiration (to 39 breaths/min at $+12G_x$). Even on the assumption of an unchanged anatomical dead-space, alveolar ventilation would have been less at $+12G_x$ than at one G.

More recently, Golov found that the respiratory minute volume was less at $+12G_x$ than in the same subjects at $+8G_x$, due to the fact that the tidal volume reached a maximum value at $+8G_x$ and then started to fall, though the respiratory rate continued to rise up to the highest level of acceleration investigated (109). Other studies (45) have suggested a similarity between the effects of forward acceleration and those of negative pressure breathing, and the application of a positive pressure to the airways (two to three millimetres of mercury per G) was shown to increase time tolerance to an acceleration of $+12G_x$ by 67% (264). Backward acceleration (subject prone, $-G_x$) appears to produce less respiratory embarrassment than when the same subjects are supine, while the volume of ventilation is well maintained at up to $-8G_x$ (227).

Anatomical dead-space

Measurements, made using a rapid response carbon dioxide gas analyser, have shown that the anatomical dead space increases during exposure to $+3G_z$ acceleration. This increase was twice as great as would be predicted from the simultaneous increase in lung volume. However, the absolute increase was only 11 ml, rather less than the standard deviation of the observations. The anatomical dead space is also increased by exposure to forward acceleration (141), though here the increase occurs despite a decrease in FRC. The changes found were small and variable, however, ranging from -3 to +39 ml at an acceleration of $+3G_x$, to -7 to +50 ml at $+6G_x$.

Total lung capacity and its subdivisions

The vital capacity (VC) of the lung was measured during exposure to acceleration using a standard water-filled spirometer, after allowing some 30 seconds for stabilisation at each level of acceleration. By careful attention to balancing, this instrument functioned well at up to 8G,and at 5G during normal breathing the pressure swing recorded at the mouth was less than two centimetres of water (100). Residual volume (RV) was determined by a rapid helium-dilution technique (23), and the resulting subdivisions of lung volume, averaged for five subjects at accelerations of up to $+4G_z$, are given in fig. 2-2. There is little change in any volume up to $+3G_z$, but at $+4G_z$ the total lung capacity (TLC) is reduced by an average of five per cent, due to a reduction in inspiratory capacity (IC). The residual volume shows no change

b*

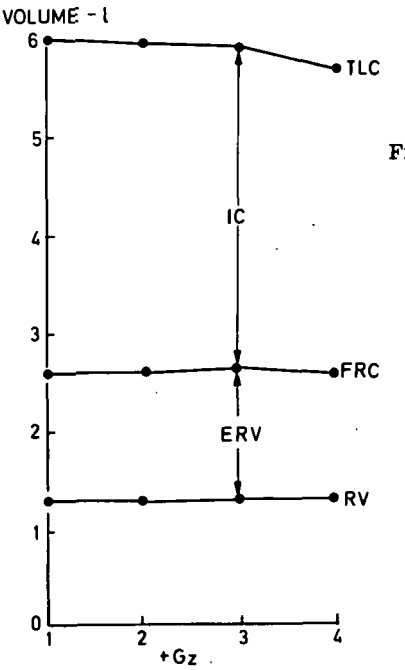

Fig. 2-2 The effect of positive acceleration on total lung capacity (TLC) and its subdivisions - inspiratory capacity (IC), functional residual capacity (FRC), expiratory reserve volume (ERV), and residual volume (RV). Average results from five subjects. Volumes in litres at BTPS.

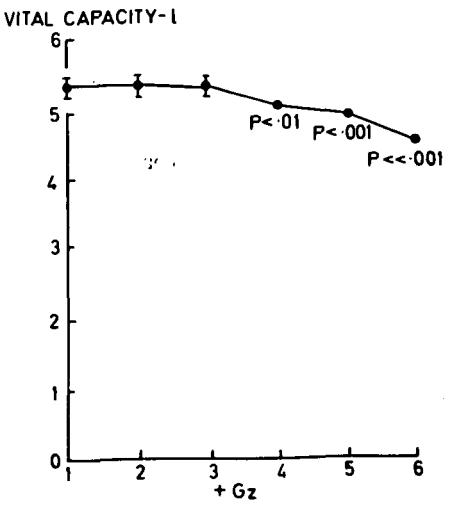

Fig. 2-3 The effect of positive acceleration on vital capacity in a single subject. Standard deviations and levels of significance are indicated.

up to $+4G_z$. Extension of measurements to $+5G_z$ showed a further reduction in IC, while the VC was reduced by 15%. Repeated determinations of VC in a single subject, at accelerations up to a maximum of $+6G_z$, showed a small but consistent increase at $+3G_z$, possibly due to a reduced central blood volume, and a progressive decrease from +4 to $+6G_z$ (Fig. 2-3), the reductions being statistically significant. Other subjects showed a small decrease in VC at $+3G_z$.

Exposure to forward acceleration restricts inspiratory capacity to a greater extent than does the same level of positive acceleration, the expiratory reserve volume (ERV) being markedly reduced. The VC falls by 32% at $+4G_x$ (45) and by as much as 73% at $+5G_x$ (46). Similar changes have been recorded on the R.A.F. centrifuge, and fig. 2-4 shows how IC and ERV decrease during exposure to accelerations of up to $+6G_x$. The ERV virtually disappears at +5 to $+6G_x$; and at these levels of acceleration, lung volume at end-expiration becomes equal to residual volume, an observation of importance in relation to the development of acceleration atelectasis (chapter 8). The degree to which the vital capacity is reduced depends upon the precise posture adopted, it is greater with the trunk absolutely horizontal than when it is inclined slightly towards the acceleration vector. Thus, VC with the trunk inclined forwards by 25° fell to 1.5 litres at $+8G_x$, but with the trunk horizontal it had fallen to 1.5 litres at only $+6G_x$ (278). With increasing acceleration stress the vital capacity continues to fall, and at $+12G_x$ it may measure little more than the tidal volume (45). Similar reductions in vital capacity are not seen in subjects lying prone and the VC is well maintained at accelerations of up to $-6G_x$ (227). This observation explains the easier respiration already noted during $-G_x$ acceleration. Residual volume is not significantly altered by exposure to forward acceleration up to $+4G_x$ (45).

The reduction in inspiratory capacity seen during exposure to both positive and forward accelerations ($+G_z$ and $+G_x$) may be attributed to the increased effective weight of the chest wall, which has to be lifted during inspiration. In addition, exposure to forward acceleration restricts descent of the diaphragm, since the abdominal viscera are forced up against it. The differing effect of the weight of the abdominal viscera explains the changes in expiratory reserve volume, the diaphragm tending to fall during exposure to positive acceleration and to rise during forward acceleration (see below). Simple mechanical considerations suggest that the weight of the chest wall should have a greater effect in reducing vital capacity and tidal volume in a supine subject than in a seated one. In fact, there is little vertical movement of the anterior chest wall in a seated subject during quiet respiration, and it is least marked over the range of normal tidal breathing. Thus, the sternum was found to rise by only 1.2 mm during a tidal inspiration at $+1G_z$, though a similar lung volume change made near to maximum expiration or maximum inspiration resulted in vertical displacements of eight and nine millimetres respectively. By contrast, the antero-posterior movement of the sternum is greater during normal tidal breathing, and is related to lung volume in a nearly linear manner (100).

The constancy of the residual volume, seen during exposure to positive as well as forward acceleration, is of interest and suggests that RV is a function of the intrinsic properties of the lung, and is not limited by the muscular effort available, nor by restricted movement of the thoracic cage. A similar conclusion was reached by Campbell (41).

The functional residual capacity (or because of the constancy of residual volume, the expiratory reserve volume) is the fraction of the total lung capacity which exhibits the greatest mobility with changes in body posture (271). The same may be said of it in relation to acceleration and fig 2-5 illustrates the effect of differing axes and levels of acceleration (from $-1G_z$ through $+1G_x$ to $+5G_z$) on the resting end-tidal lung volume of a relaxed subject. The greatest change (700 ml.) occurs

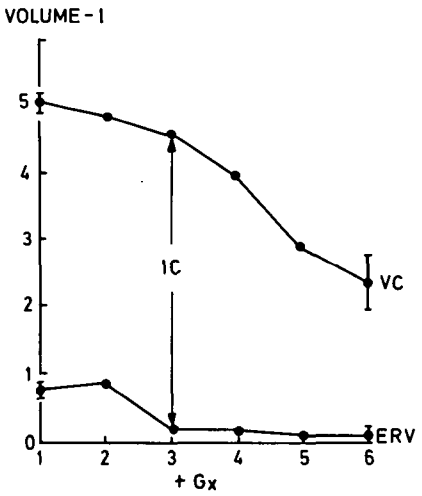

Fig. 2-4 The effect of forward acceleration on vital capacity (VC), inspiratory capacity (IC), and expiratory reserve volume (ERV). Plus and minus one standard deviation of the +1 and +6G_z values are indicated by barred vertical lines. Compare with the same subject's response to +G_x (Fig. 2-3).

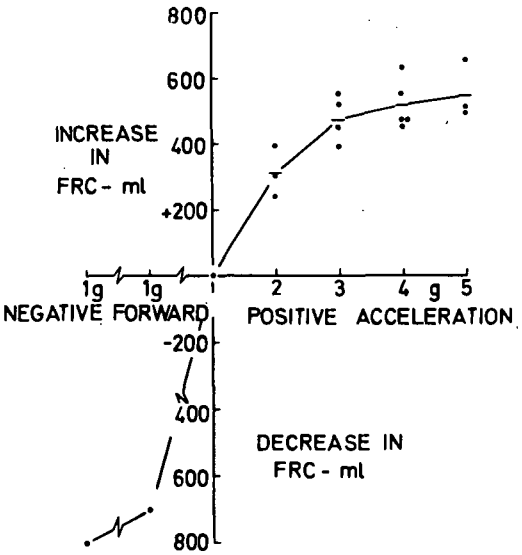

Fig. 2-5 Change in functional residual capacity (FRC) of subject exposed to varying axes and levels of acceleration. Values are given in millilitres at BTPS, and average values obtained during positive acceleration are shown by short horizontal lines.

between $+1G_x$ and $+1G_z$, and changes of similar magnitude have been reported following passive tilting head up from the horizontal (53). Increasing levels of positive acceleration produce continued but lessening changes in lung volume as does the change from $+1G_x$ to $-1G_z$. Assuming that the largest single factor determining lung volume is the resting level of the diaphragm (271), which will be demonstrated later, then the diaphragm behaves like a weight mounted on the centre of a spring fixed at both ends. Movement about the equilibrium point requires little force (or acceleration), but movement towards either extreme is made against a far greater restoring force. The cephalad portion of the spring is represented by the elasticity of the lung and thorax, the weight by the abdominal viscera, and the caudad portion of the spring by the elasticity of the anterior abdominal wall. The diaphragm presumably also contributes its own restoring force, either by muscular effort or, at the extremes of its movement, by its inherent elasticity.

The diaphragm

The resting level of the diaphragm moves to a considerable extent with changes in body posture. Wilson (271), using fluoroscopy, showed that when a standing subject lay supine, the dome of the diaphragm was displaced 3.7 cm. towards the head. Centrifugal acceleration in cats and monkeys ($+G_z$), as well as aircraft induced positive acceleration in man, has been shown to bring about a fall in the resting level of the diaphragm (90). In animals, the level of the diaphragm is unaffected by $+G_x$ acceleration if a small $+G_z$ component is introduced by inclining the body forwards by 10 to 15 degrees (139).

In order to investigate the relationships involved, a technique was developed which allowed the level of the oesophageal hiatus of the diaphragm to be recorded directly (94). The hiatus lies between the crura of the diaphragm, about halfway between the tendinous dome and its posterior attachments, so that about half the excursion of the dome should be recorded at this point. The technique of recording is illustrated in fig 2-6. A thick walled latex balloon is swallowed and passed down into the stomach, where it is inflated hard to give it a transverse diameter of three centimetres. It is then drawn back until its upwards passage is prevented by the crura of the diaphragm. A spring maintains its position riding up against the diaphragm, while subsequent movement is recorded using a low-torque potentiometer.

A recording of diaphragm movement obtained during breaths of differing tidal volume is illustrated in figure 2-7. When the level of the diaphragm is plotted against the corresponding change in lung volume for each second interval of this recording, the relationship is found to be linear, with inspiratory and expiratory points falling on the same straight line. There is no evidence of lag or hysteresis in the recording system. Figure 2-8 shows a graph of diaphragm level plotted against lung volume change for breaths with tidal volumes of up to four litres. The relationship remains linear for volumes of up to 2.5 litres, after which the degree of diaphragm movement becomes reduced. During quiet respiration the diaphragm moves about 8 mm, and during maximal breathing, about 4.5 cm. These results may be compared with radiographic measurements, where the dome of the diaphragm moves 1.5 cm. and 7 to 13 cm. respectively under similar conditions (261). These findings confirm the two to one relationship between dome and crural movement predicted anatomically.

Figure 2-9 shows the effect of accelerations of +3 and $+4G_z$ on the level of the diaphragm, acceleration being applied at a rate of one G per second and maintained for 20 seconds. The diaphragm falls with acceleration, so drawing air into the lungs and increasing the functional residual capacity. Average results were a fall of one centimetre at $+2G_z$ and of two centimetres at $+4G_z$; these displacements were associated with an increase in lung volume of 300 ml. and 500 ml. respectively.

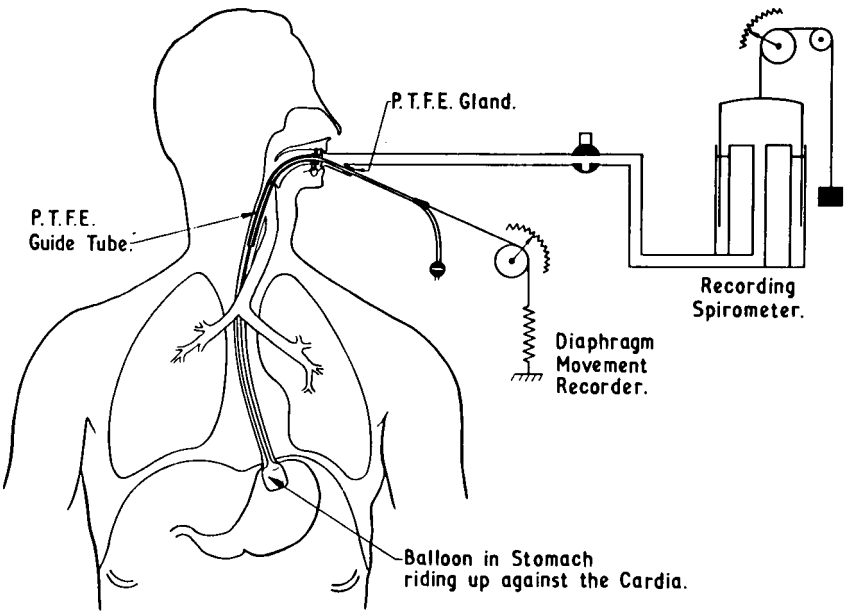

Fig. 2-6 Diagram showing the apparatus used for recording movement of the diaphragm at the oesophageal hiatus. Movement is transmitted to a rigid balloon and thence to a drum driving a low-torque potentiometer. Tension is maintained on the balloon by means of a light spring.

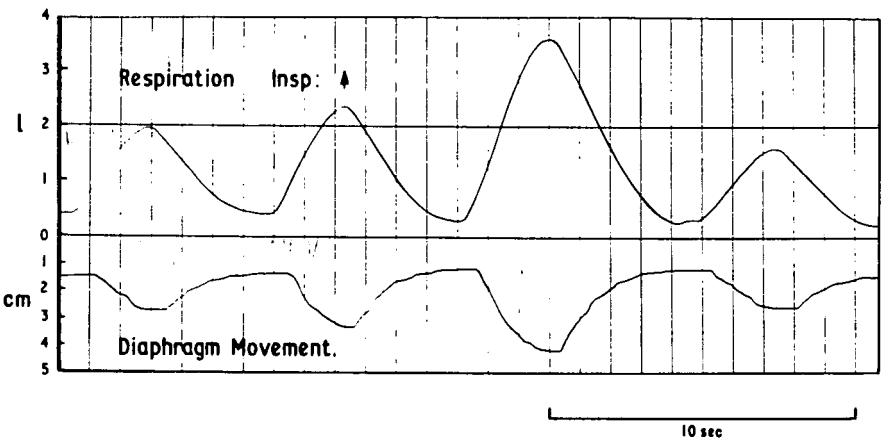

Fig. 2-7 Recording of diaphragm movement and of simultaneous changes in lung volume during four graded breaths.

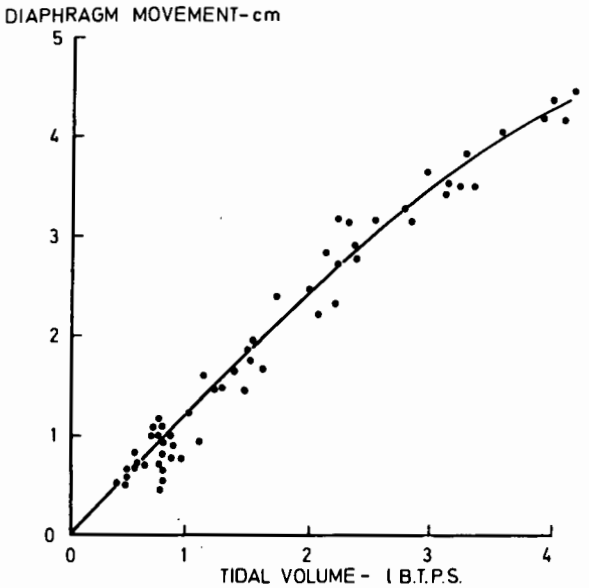

Fig. 2-8 Diaphragm movement plotted against the corresponding change in lung volume, for breaths with tidal volumes of up to four litres.

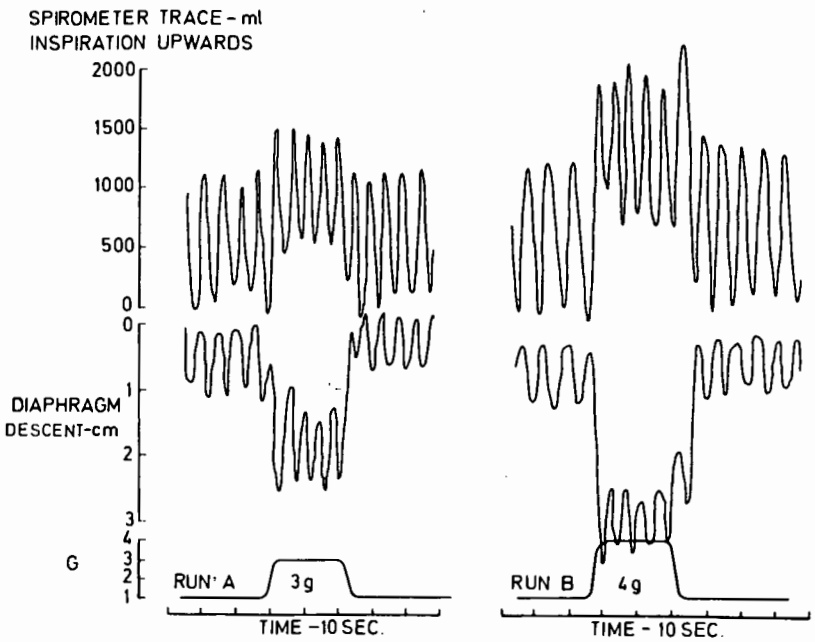

Fig. 2-9 Recordings showing the effect of 20 seconds exposures to +3 and +4G_z on the spirogram (upper trace), and on the level of the diaphragm. Note the rapidity with which changes in level are completed.

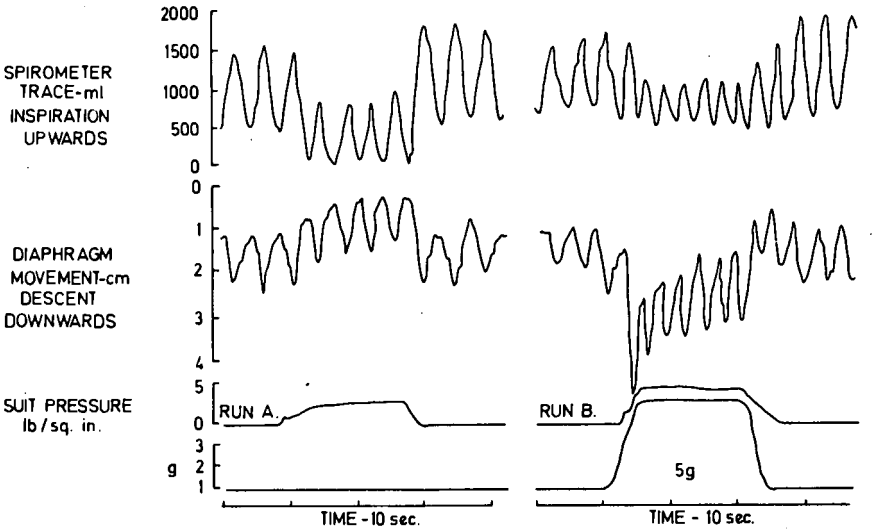

Fig. 2-10 Recordings showing the effect of anti-G suit inflation on the spirogram and on the level of the diaphragm. Run A, inflation of the suit to 3lb./sq. in. Run B, inflation during exposure to acceleration of $+5G_z$.

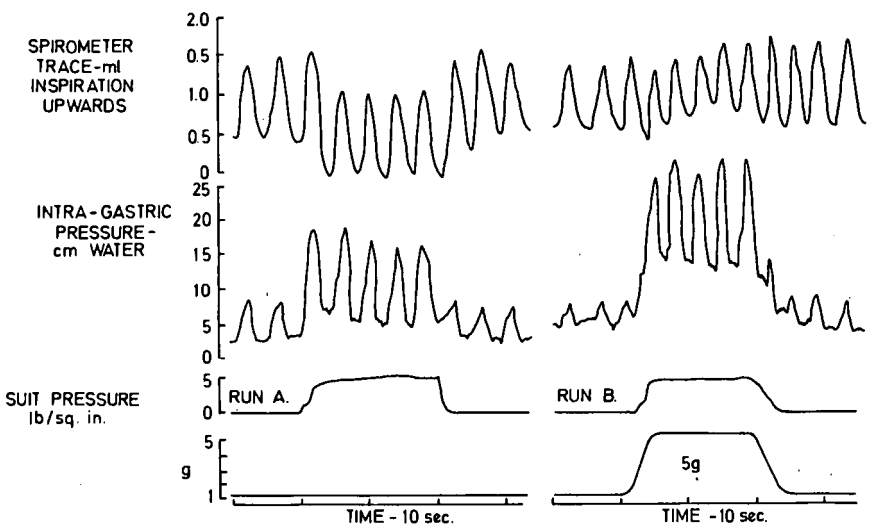

Fig. 2-11 Recordings showing the effect of anti-G suit inflation on the spirogram and on intragastric pressure. Run A, inflation of the suit to 5lb/sq.in. Run B, inflation to the same pressure during exposure to an acceleration of $+5G_z$.

This is the same as the relationship between diaphragm movement and lung volume found by Wade (261), so it appears that positive acceleration leads to the whole diaphragm moving downwards like a piston in a cylinder, with the crura being displaced to the same extent as the dome. In animals, experiments which involved staged evisceration have demonstrated that the displacement of the diaphragm is caused, in the main, by the inertia of the liver mass (139).

The effect on diaphragm level and lung volume of inflating an anti-G suit is shown in fig. 2-10, both on its own (run A) as well as during exposure to an acceleration of $+5G_z$ (run B). Inflation of the suit to a pressure of three pounds per square inch forces the diaphragm upwards by one centimetre, and decreases lung volume by 500 ml. When inflated during acceleration, the descent of the diaphragm is not prevented, but its fall is far less than in an unprotected run (compare with fig. 2-9). With the combination of acceleration and anti-G suit inflation, the tidal volume is decreased, and the rate of breathing is increased. The action of the anti-G suit is mediated through a rise in intra-abdominal pressure (231), and this has been confirmed by recording intragastric pressure (Fig. 2-11). These studies also show that the abdomen becomes stiffer during exposure to positive acceleration, since the pressure swing caused by quiet breathing is increased. The following results were found. The end-expiratory intragastric pressure was increased by exposure to $+3G_z$ from 6 to 12.5 cm. water. The slope of the pressure change recorded during inspiration became steeper at $+3G_z$, the resting value of nine centimetres of water per litre being increased to 16 cm water/ l. The areas of pressure-volume loops recorded during tidal and deep breaths were approximately doubled by exposure to $+3G_z$, so that the work done by the respiratory muscles in displacing abdominal viscera was increased twofold.

Thoracic compliance

Total thoracic compliance is the change in lung volume which results from a unit change in pressure applied to the airways. It is made up of components contributed by the lung and chest wall and can be measured simply, in trained subjects, as the airway relaxation pressure. This is the pressure, positive or negative, which develops within the airways when the subject relaxes at any predetermined lung volume. The effect of positive acceleration on the relaxation pressure curve is illustrated in fig. 2-12, and in plotting the points, lung volumes have been referred to the one G resting end-expiratory level. At $+1G_z$, the intrapulmonary pressure is equal to atmospheric pressure at the resting lung volume. As the volume of the lung is increased, the relaxation pressure becomes more positive; the slope of the linear portion of the curve giving a value for total thoracic compliance of 140ml/cm water. At an acceleration of $+3G_z$, the curve follows a similar pattern, but the resting lung volume is increased by 450 ml and the relaxation pressure curve is less steep. The application of a pressure of one centimetre of water to the airways would only increase the volume of the thorax by 95 ml (total thoracic compliance = 95 ml/cm water). Similarly, at lung volume less than functional residual capacity, higher intrathoracic pressures are developed at $+3G_z$ than at $+1G_z$, only here they are negative (subatmospheric), since the thorax is tending to expand.

Repeated determinations of total thoracic elastance (the reciprocal of compliance) show that this increases linearly with acceleration up to $+4G_z$, at a rate of 2.4 cm water/l. per G (Fig. 2-13). This curve can be extrapolated backwards to zero G to give a 'weightless' elastance of four centimetres of water per litre. In this way, total thoracic elastance can be separated into two components, a true elastic component of four centimetres of water per litre and a gravity dependent component, due to the mass of the thorax, of 2.4 cm. water/litre per G.

The slopes of static relaxation pressure-volume curves are unaffected by forward

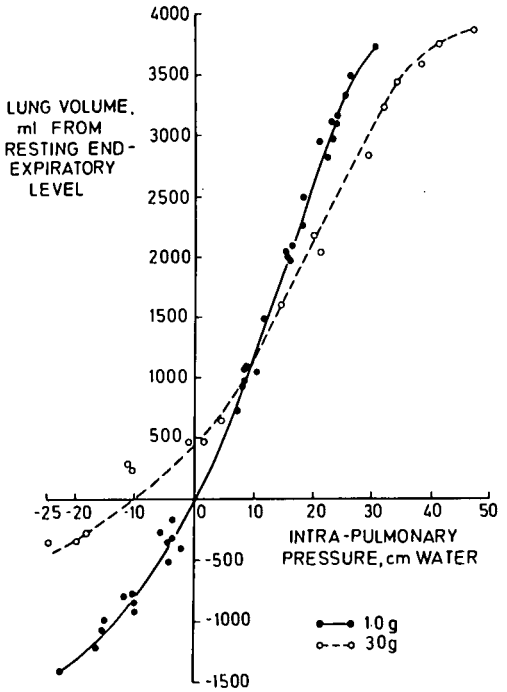

Fig. 2-12 The effect of an acceleration of $+3G_z$ on the relaxation pressure curve of the thorax. Lung volumes, in millilitres, BTPS, are referred to the one G resting end-expiratory level.

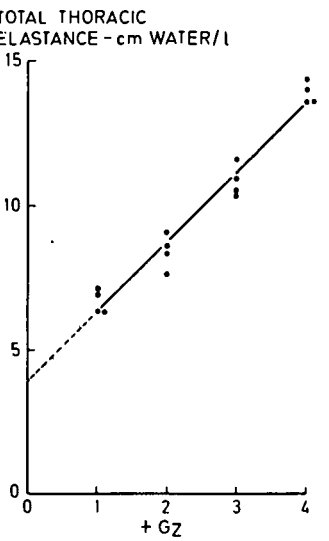

Fig. 2-13 The effect of positive acceleration on total thoracic elastance. Each point represents the slope of the linear portion of a relaxation pressure curve.

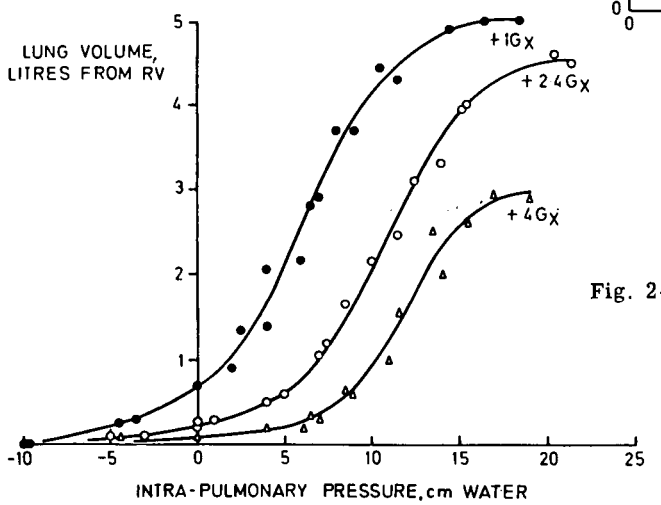

Fig. 2-14 The effect of forward acceleration on the relaxation pressure curve of the thorax. Points are from duplicated runs on a single subject.

acceleration up to $+4G_x$, but the curves are shifted to the right, and intrapulmonary pressures at all lung volumes are increased by four to five millimetres of mercury (5.7 to 7 cm water) per G (46). We have recorded somewhat smaller shifts, but have confirmed the constancy of the slope at up to $+4G_x$ (Fig 2-14).

The lung volume at which the relaxation pressure is zero (equal to atmospheric pressure) is the relaxation volume, or functional residual capacity. Reference to figure 2-14 shows that a natural outcome of the shift to the right of the relaxation pressure curve is a reduction in FRC and VC. At a lung volume two litres above RV, the intrapulmonary pressure is increased by approximately three centimetres of water per G. This rise is simply explained by the anterior chest wall having an effective weight of three grammes square centimetre. The greater shifts referred to above were probably recorded in subjects having thicker chest walls.

While the slope of the linear portion of the relaxation pressure curve is unaffected by forward acceleration, inspiration normally starts from the relaxation volume. In order to increase lung volume by one litre, a pressure of four centimetres of water is required at $+1G_x$, but this is increased to 7.5 cm water at $+2.4G_x$ and to 10.5 cm water at $+4G_x$ (Fig. 2-14). Thoracic compliance over a one litre tidal volume range is therefore reduced to some 40% of normal, by a forward acceleration of $+4G_x$.

Lung compliance may be calculated from the intra-oesophageal pressures recorded at the moments of zero flow during normal breathing (dynamic compliance), or during stepwise increases and decreases in lung volume (static inflation and static deflation compliance). Intra-oesophageal pressure measurements are subject to errors due to distortion of the oesophagus by the balloon used or because structures in the mediastinum press on the oesophagus (188, 256). Artifacts from mediastinal compression have been used to explain away the apparent influence of posture on lung compliance (149), while in a study using body plethysmography, no change in lung compliance was found with change in posture (167). The apparent effect that anti-G suit inflation has on lung compliance has also been attributed to an artifact arising from mediastinal compression (28). Bondurant (27) found that lung compliance fell at +3 to $+3.5G_z$ and at +4 to $+5G_x$ (the lung becoming stiffer), but, insofar as these results were based on intra-oesophageal pressures, they too could be subject to error. In fact, errors in oesophageal pressure measurement have been shown to be exaggerated by forward acceleration (142).

Inflation and deflation lung compliances were determined in four subjects at $+1G_z$ and $+3G_z$, taking care that the past inflation history of the lung was identical on each occasion, since this too may alter the compliance of the lung (83). When pressures were measured from a balloon lying in the middle third of the oesophagus, exposure to acceleration was found to have no effect on the compliance of the lung, which remained at a constant average value of 169 ml/cm water. It was concluded that the changes in compliance previously reported to take place during exposure to acceleration were due to mediastinal pressure artifacts. The decrease in total thoracic compliance found during both positive and forward acceleration must, therefore, be attributed to a decrease in the compliance of the chest wall.

Airway resistance

The increase in anatomical dead-space which occurs during exposure to acceleration ($+G_z$ or $+G_x$), suggests that the resistance of the airways to gas flow is unlikely to increase. This outcome is also suggested by the constancy of the non-elastic component of the work of breathing at $+4G_x$ (45), since this component includes the resistance of the airways. Measured by the interruptor technique, airflow resistance is constant at up to $+7G_x$ (260). Using the same technique on the RAF centri-

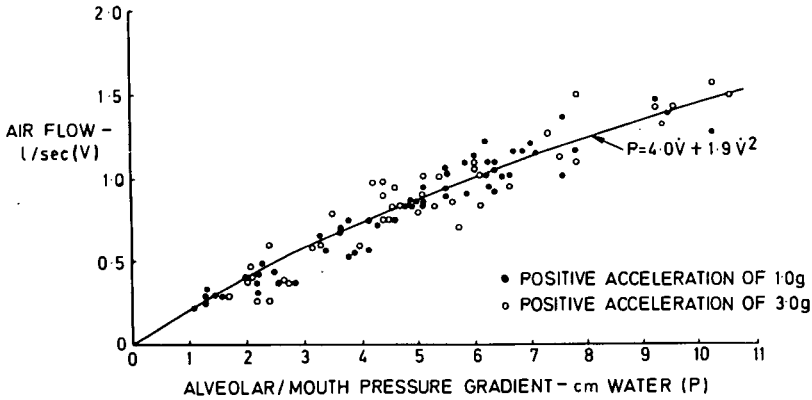

Fig. 2-15 Alveolar-mouth pressure gradients, obtained during brief interruptions to airflow, plotted against the airflow present prior to each interruption. Points were obtained during quiet breathing at one G and at $+3G_z$. The regression line is drawn to the equation $P = 4.0\dot{V} + 1.9\dot{V}^2$ and the single curve fits both sets of data satisfactorily.

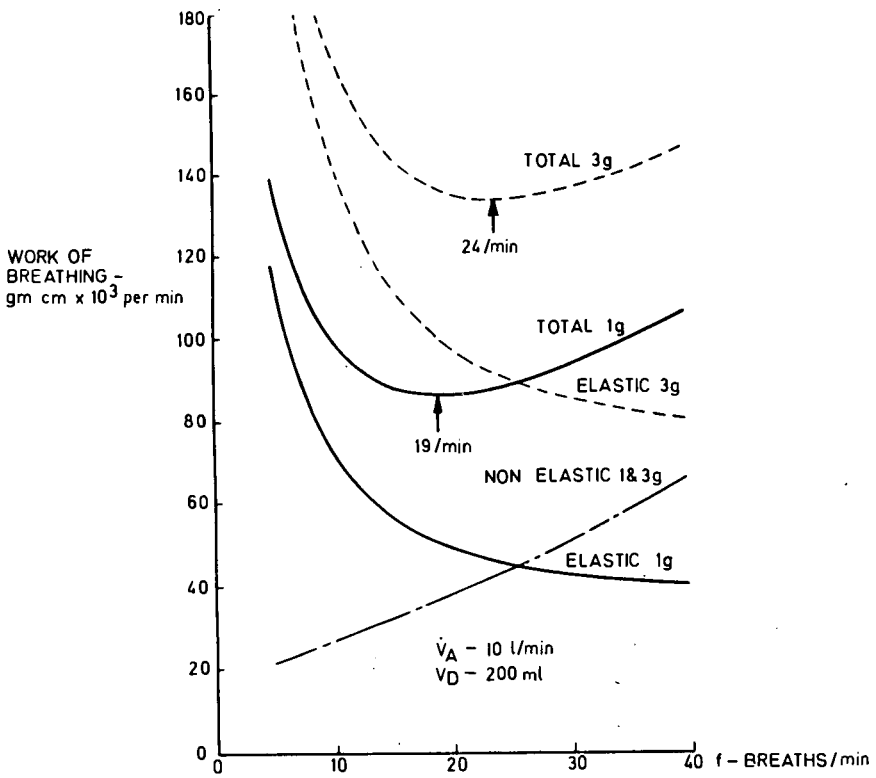

Fig. 2-16 Theoretical relationship between respiratory rate (f), and the total work of breathing and its components at $+1G_z$ (solid lines), and during exposure to an acceleration of $+3G_z$ (dashed lines). Non-elastic work remains constant, but elastic work is doubled at $+3G_z$ so that the optimum rate of breathing increases from 19 to 24 breaths per minute.

fuge, the resistance to airflow was found to be unaffected by exposure to $+3G_z$.

This finding is illustrated in fig. 2-15, where the alveolar-mouth pressure gradient, measured by the change in mouth pressure which occurs during a brief interruption to airflow, is plotted against the flow present immediately prior to each interruption. The curve follows the form of $P = a\dot{V} + b\dot{V}^2$, where a and b are constants for laminar and turbulent flow respectively. As may be seen, the $+1G_z$ and $+3G_z$ points lie on the same regression line. Similar results were found in three subjects, but a fourth subject showed a change in airway resistance with the direction of gas flow (the resistance rising during inspiration), as well as with acceleration (the resistance increasing at $+3G_z$). While the change in the laminar flow constant with acceleration was probably significant in this subject ($P = < .05$), the change was small and suggests only a very modest degree of bronchoconstriction. The effect, seen in only one of the four subjects investigated, was too small and inconstant to constitute a physiologically significant increase to the work of breathing.

The interruptor technique used for the measurement of airflow resistance (202) has been criticised on the theoretical basis that the resistance measured includes a lung tissue viscance component (182). The present results confirm this view, since the values found were similar to the total resistance (airflow resistance plus lung tissue viscance) determined from pressure-volume loops. These loops were obtained by plotting intra-oesophageal pressure against lung volume, and allow the work done on the lung to be calculated, since the area of such a loop has the dimensions of work. Pressure-volume loops were recorded for breaths of several different tidal volumes at $+1G_z$ and $+3G_z$, and their areas were found to be unaffected by acceleration. It is concluded from this observation, and from the airway resistance measurements previously described, that the work done on the lungs is not increased by acceleration, at least up to $+3G_z$.

Cherniack and co-workers concluded that the non-elastic component of the total work of breathing was unaffected by a forward acceleration of $+4G_x$ (45), while we have come to a similar conclusion in studies on positive acceleration ($+3G_z$). As already mentioned, however, the elastic component of the total work of breathing is increased at both $+4G_x$ and $+3G_z$. Since the elastic component is related to tidal volume, and the non-elastic component to the frequency breathing, it follows that there is an optimum relationship between rate and depth of breathing for any given ventilation (200), as well as for any given acceleration.

Figure 2-16 illustrates the theoretical relationship between breathing rate and work of breathing, assuming a constant alveolar ventilation of 10 l/min and a constant anatomical dead-space. The same figure (dashed lines) illustrates the effect of doubling the elastic component of the work of breathing, as would occur during exposure to accelerations of the order of $+3G_z$ or $+4G_x$. As may be seen, acceleration increases the optimum frequency of breathing from 19 to 24 breaths per minute, and the total work done at the optimum frequency rises by 55%. During mild exercise sufficient to raise the ventilation to 25 l /min, the optimum rate of breathing increases from 30 to 40 breaths per minute and the total work of breathing goes up by 40%.

Calculations based upon the work of Otis (199), show that, at $+3G_z$, the respiratory muscles will require an additional 10 ml of oxygen each minute, in order to maintain a ventilation of 25 ml /min. These calculations assume that expiration is a passive process, energised by the elastic recoil of the chest wall and lung. In practice, energy stored in this way is in excess of requirements, even at one G, so it has to be absorbed by prolonging inspiratory muscle activity into early expiration (115). During acceleration, even more energy will be stored because of the increase in the elastic component of the work of breathing, and more muscular effort will be required during expiration to absorb this excess. For this reason, the actual

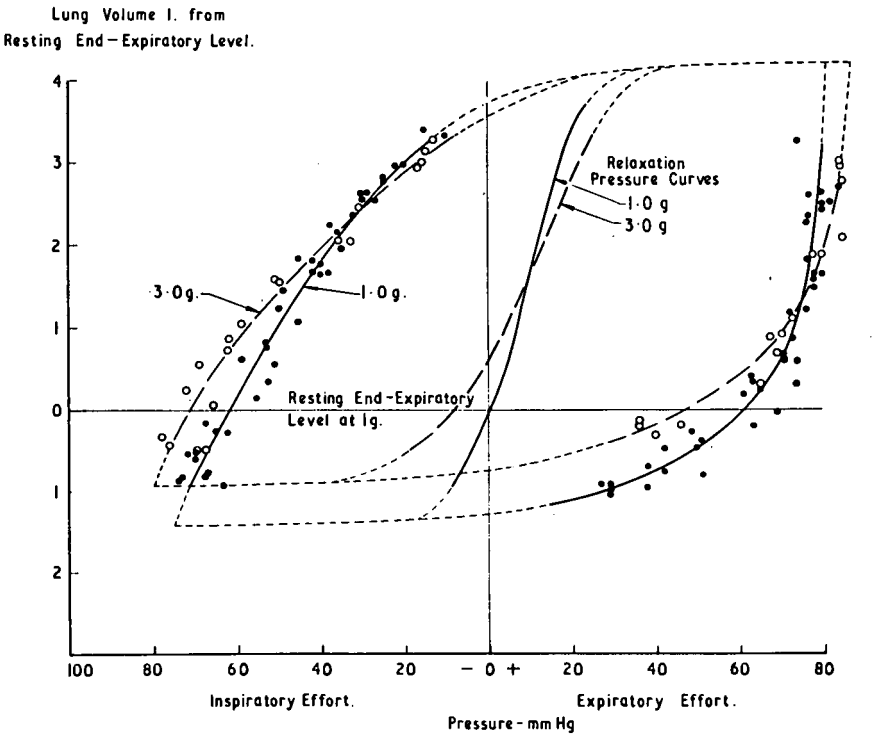

Fig. 2-17 Effect of $+3G_z$ acceleration on maximum voluntary inspiratory and expiratory pressures at different lung volumes. The relevant relaxation pressure curves have been redrawn from fig. 2-12. Lung volumes are given at BTPS and are referred to the one G resting end-expiratory level. Developed pressures are given by the horizontal distance between the maximum pressure curve and the corresponding relaxation pressure curve.

cost of acceleration on the work of breathing will be greater than that calculated above. The increase in the frequency of breathing predicted during exposure to both positive and forward acceleration is borne out by the breathing patterns actually recorded under these conditions.

There remains the possibility that, by distorting the thorax and diaphragm, acceleration could render the respiratory muscles less efficient in bringing about pressure changes within the lungs. This possibility was investigated during exposure to a positive acceleration of $+3G_z$, by having a subject make maximal inspiratory and expiratory efforts over the whole range of lung volumes (Fig. 2-17). Because of the compressibility of the contained gas,the development of high pressures, positive or negative, changes lung volumes significantly, and appropriate corrections have to be made. For the same reason, it is not possible to determine the maximal inspiratory effort at full expiration, nor the maximal expiratory effort at full inspiration, so these points on the curve must be completed by extrapolation. At full inspiration, no further inspiratory effort can be made, and at full expiration, no further expiratory effort can be made; the recorded curves cross the zero pressure line at these volumes. The resulting pressure-volume loops have areas which measure the maximum amount of work which could be carried out in a single respiratory cycle.

To help the interpretation of fig. 2-17, the relaxation pressure curves from the same subject have been added from the data given in fig. 2-12. Lung volumes are referred to the one G resting end-expiratory level. Inspiratory as well as expiratory pressures are modified by exposure to positive acceleration, but only to the same extent as the relaxation pressures. The effect is therefore passive, and does not imply any altered efficiency on the part of the respiratory musculature. The area of the maximum work loop obtained at $+3G_z$ is less than that recorded at one G, by virtue of a reduction in vital capacity, but such a reduction could not be significant in normal breathing nor even in exercise. The much greater reduction in vital capacity which results from forward acceleration does, however, lead to a decrease in the work available for breathing, which limits tolerance to this axis of acceleration to about $+12G_x$.

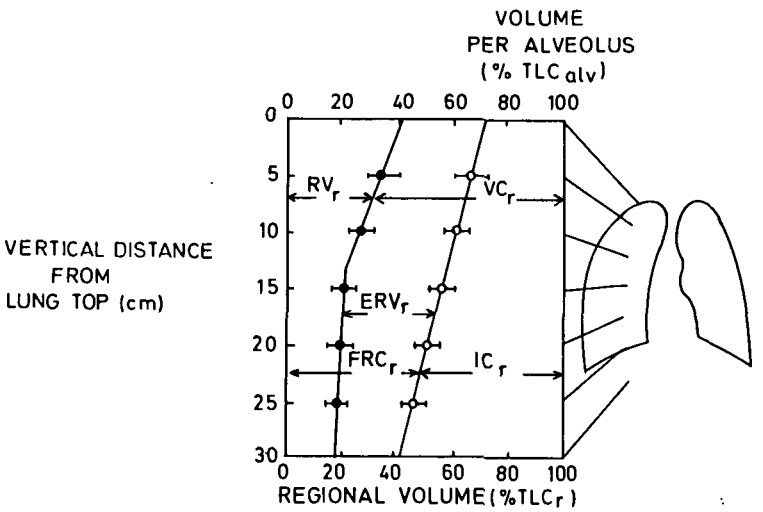

Fig. 3-1 Regional subdivisions of lung volume in seated men. Filled and open circles represent average results obtained on eight healthy young subjects at RV and FRC, respectively. Bars indicate 2 SE. RV_r = regional residual volume; IC_r = regional inspiratory capacity; ERV_r = regional expiratory reserve volume; VC_r = regional vital capacity

3

Distribution of ventilation

J. MILIC-EMILI

Davy in 1800 (63) was the first to investigate the distribution of gas within the lung. He used hydrogen to study mixing of gases in a closed lung-spirometer system, and concluded that respiration produced "a uniform mixture of residual gas with the gas inspired". His views were shared by most workers throughout the nineteenth century, but later workers using more refined methods concluded that inspired gas is not distributed equally among the various lung units, even in healthy subjects. This conclusion was reached independently in studies using radiological, bronchospirometric and inert gas methods. These methods have been extensively used during the first half of this century and have provided considerable information concerning the distribution of gas within the lung (22, 29, 87). This information, however, consisted of a great number of seemingly isolated findings.

In 1955, Knipping *et al.* (148) introduced radioactive gases in the study of the distribution of gas within the lung. Since then, there has been a renewed interest in the study of this apsect of physiology, and it now seems that the factors controlling the normal distribution of ventilation are beginning to be understood. Clearly, much work is needed before this complicated subject is fully understood. Nevertheless, the recent advances in this field have produced a lung model which, in spite of its limitations, allows the integration of many of the seemingly isolated findings reported in the literature into a coherent picture. Accordingly, this is an opportune moment for review.

This chapter is concerned first with a description of the regional ventilatory function of the normal lung. Much of this information was obtained in recent studies with radioactive gases using external counters over the chest. These results will be interpreted through the use of a simple mechanical model. Second, the validity of the model will be analyzed, and finally, the causes of uneven ventilation in general will be briefly discussed.

Regional ventilatory lung function

Regional subdivision of lung volume

Usually, most accounts of the overall ventilatory function of the lung start with a description of the total lung capacity (TLC) and its subdivisions. Accordingly, it seems logical that this account of the regional ventilatory function of the lungs should start with a description of the regional subdivision of lung volume. One of the methods most commonly used to measure overall subdivisions of lung volume, the helium method, is based on the gas-dilution principle. Measurements of the regional subdividions of lung volume are also based on the gas-dilution principle, but radioactive xenon (^{133}Xe) is used instead of helium (185). Figure 3-1 illust-

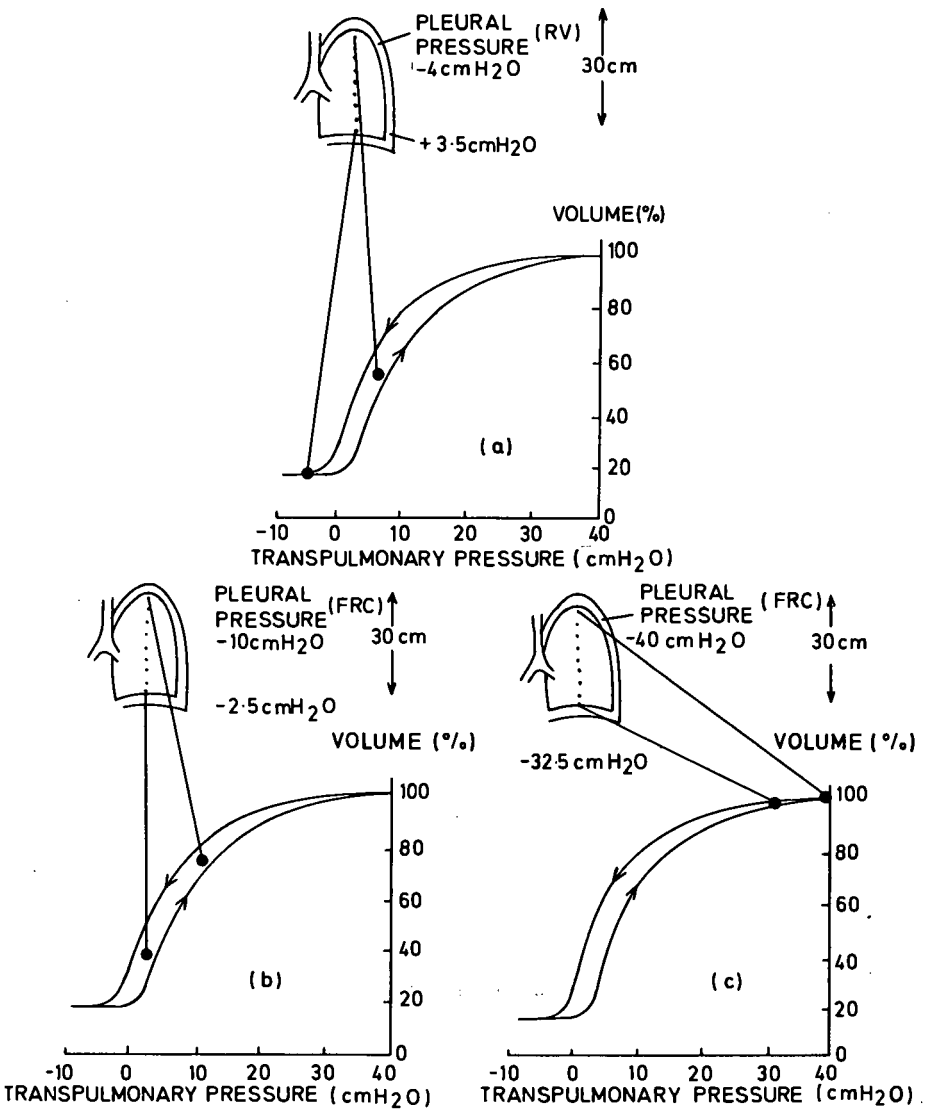

Fig. 3-2 Effect of pleural pressure gradient on the volume distribution of gas within the lung. The pressure is assumed to increase at a constant rate of 0.25 cm water/cm vertical distance. The elastic properties, as shown by the S-shaped static volume-pressure curves in the lower part of each panel, are assumed to be uniform throughout the lung. Values of pleural pressure at the apex and base existing at three lung volumes (RV, FRC and TLC) are shown in the upper part of each panel. In C, at full inspiration (TLC), all lung regions are expanded virtually uniformly, in spite of the pleural pressure differences down the lung. On the contrary, at RV and FRC (A and B, respectively), the pleural pressure gradient causes the upper lung regions to have a greater volume than the lower zones.
(From (186) by courtesy of J. nucl Biol. Med.)

rates the regional subdivisions of lung volume in eight seated normal young men. Regional volumes are expressed as a percentage of the volume of each region at TLC, i.e., TLC_r, r denoting 'regional parameter'. Thus TLC_r is the volume of gas contained by a region at full inspiration. Since at TLC the volume of the lung units (alveoli) is probably uniform throughout the lung (107, 185), regional lung volumes expressed as a percentage of TLC_r are also an expression of the volume of the alveoli. The volume per alveolus, expressed as percent of the alveolar volume at TLC (i.e. TLC_{alv}), is also shown on the upper abscissa of fig. 3-1.

It is apparent that at the end of both a normal expiration (FRC) and a maximal expiration (RV), the apical lung regions are more expanded than the basilar lung zones, so the regional FRC and the regional RV are relatively greater in the upper zones of the lungs. Regional FRC (FRC_r) decreases approximately linearly with distance down the lung, whereas regional RV (RV_r) decreases progressively from the lung top to roughly the mid-level of the lung, thereafter remaining substantially constant. These regional differences in lung expansion have been explained by a mechanical model, based on the combination of vertical gradient in pleural pressure and the static volume-pressure curve of the lung (185, 186).

In the upright man there is a gradient in pleural pressure down the lung, with the more negative values towards the apex. Although its nature is not well understood, the gradient appears to be gravity-dependent, i.e., related to the weight of the lung (see below). Figure 3-2 shows how the gradient in pleural pressure, combined with the elastic properties of the lung (which are assumed to be uniform) can account for the regional differences in lung expansion observed in ^{133}Xe studies. At full inspiration (TLC), all lung regions are expanded nearly uniformly, despite the vertical gradient in pleural pressure (Fig. 3-2c). This is because, near full inflation the slope of the static volume-pressure curve of the lung is nearly flat, with the result that the pleural pressure differences down the lung do not cause appreciable regional differences in expansion. As lung volume decreases below TLC, the lung regions operate on a progressively steeper part of their static volume-pressure curve, so that the vertical gradient in pleural pressure causes marked differences in expansion down the lung. Indeed, at both RV and FRC, the apical lung units are much more expanded than those near the lung base (Fig. 3-2a, b). This behaviour is reflected in the results obtained using ^{133}Xe (Fig. 3-1).

It should be noted that, at residual volume, pleural pressure in dependent lung zones exceeds airway pressure, i.e., it is positive (Fig. 3-2a). When pleural pressure exceeds airway pressure, the airways collapse and gas is trapped behind the closed airways (43, 252). Therefore, airway closure sets a limit to expiration from the dependent lung zones (185, 252), the volume of trapped gas representing their minimal volume. The observation that the regional RV is virtually constant from lung middle to bottom (Fig. 3-2) suggests that at full expiration, all lung units in the lower half of the lungs have attained their minimal volume. By contrast, the upper lung units do not appear to have attained their minimal volume at the end of a maximal expiration.

The lung model presented in fig. 3-2 can also be used to explain the effect of changes in body position on distribution of gas within the lung. In the supine position, in which the differences in pleural pressure between lung apex and base are diminished, the distribution of gas between apex and base becomes more uniform (34). In this position, however, there is a gradient in pleural pressure between the upper (ventral) and dependent (dorsal) aspects of the lungs. Accordingly, it is not surprising that in the supine position there are differences in expansion between the ventral and dorsal parts of the lungs (Fig. 3-3). Similar results are obtained in the prone position as well as in lateral decubitus. In all of these postures, the upper lung regions (which are exposed to more negative pleural pressure) tend to be more expanded than the lower lung zones (146). It should be emphasized that the pleural pressure gradient and the resulting differences in lung expansion tend

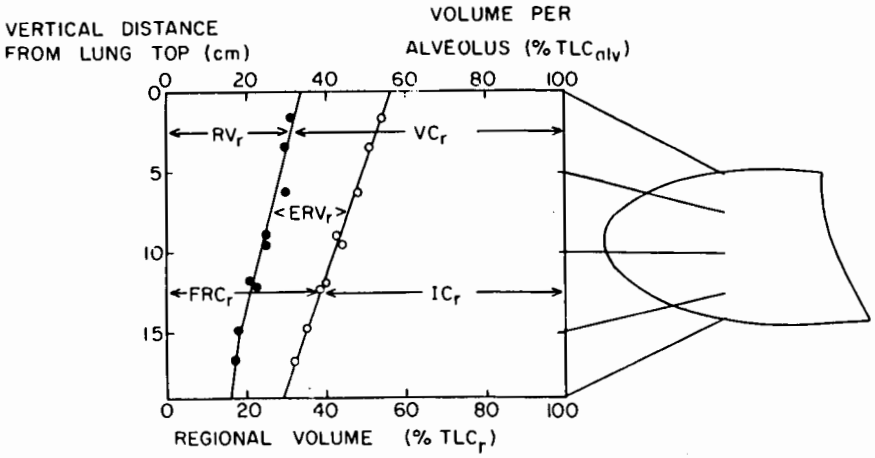

Fig. 3-3 Regional subdivisions of lung volume in a supine normal young man. Symbols as in fig. 3-1.

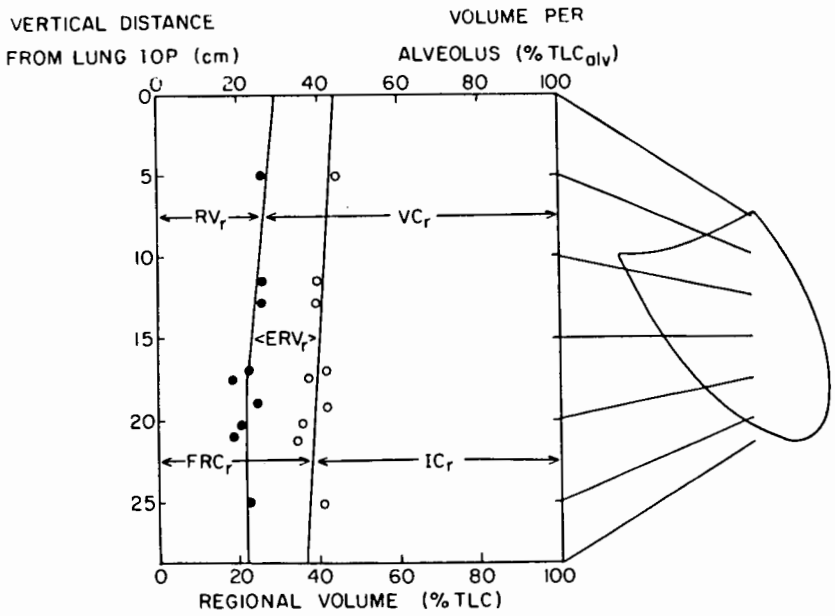

Fig. 3-4 Regional subdivision of lung volume in a healthy young man in the head-down (60° from horizontal) position. Symbols as in fig. 3-1.

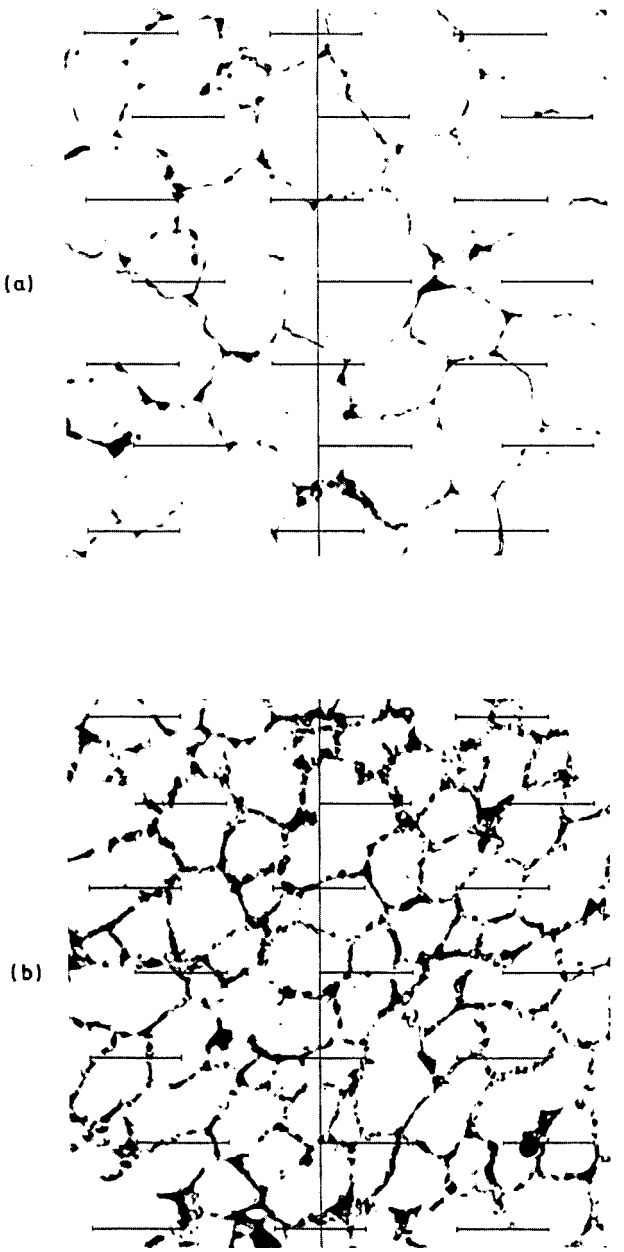

Fig. 3-5 Sections of lung from apex (a) and from 20 cm lower down the lung (b) of a greyhound dog frozen in the vertical (head-up) position. Each line is equivalent to 100μ.
(From Glazier *et al* (107), by courtesy of J. appl. Physiol).

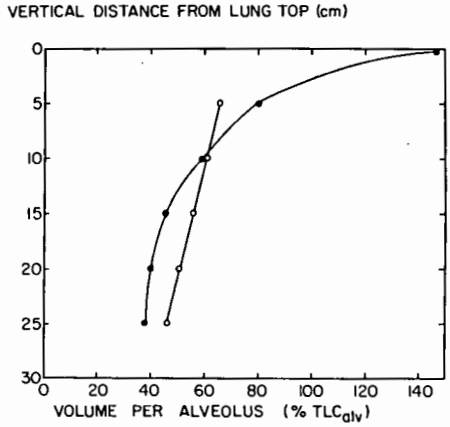

Fig. 3-6 Relationship between vertical distance and alveolar volume in greyhound dogs frozen head-up at FRC (solid circles). From data of Glazier ***et al*** . Open circles indicate results obtained on normal seated men at FRC from fig. 3-1.

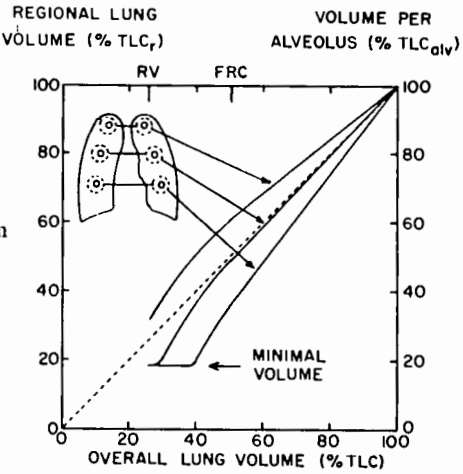

Fig. 3-7 Average relationship between regional (or alveolar) and overall lung volumes in four healthy young men sitting upright. Results from three lung regions (4.5, 13.8 and 22.5 cm from lung top). The broken line (line of identity) indicates regional (or alveolar) percentile expansion equal to that of the entire lungs. (From (252), by courtesy of J. appl. Physiol).

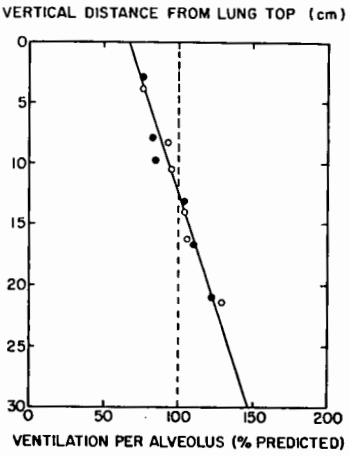

Fig. 3-8 Relationship between vertical distance from lung top and ventilation per alveolus in a seated man. Open circles, right lung; filled circles, left lung. Dotted line indicates uniform distribution of ventilation per alveolus throughout the lung.

always to occur vertically, (i.e. in the direction of gravity), while along the horizontal axis of the lung the regional distribution of gas is virtually uniform (146, 185).

In the head-down position, the distribution of gas within the lung may be much more uniform than in the head-up (upright) position (Fig. 3-4), whereas the differences in expansion between upper and dependent lung regions are about the same in the supine and prone positions, or in the left lateral and right lateral decubitus (146). This discrepancy may be due to the fact that in the head down position, the vertical gradient in pleural pressure is virtually abolished, whereas this is not the case for the other postures. The reason for this will be discussed later (see also chapter 11, p. 183).

In the past, systematic topographical differences in expansion of the lung have not been reported in the numerous morphometric studies of the lungs. In most cases the lungs had been inflated outside the chest before fixation and therefore, the measurements did not reflect the state of the lungs inside the chest. Recently, a vertical gradient of alveolar size has been directly demonstrated by Glazier *et al*, (107) in histological sections, by freezing whole dogs and thus fixing the lungs *in situ* without alteration of the pleural pressure relationships produced by opening the chest. Figure 3-5 shows sections of lung from the apex and 20 cm lower down the lung of a dog, frozen at FRC in the vertical (head-up) position. The apical alveoli are considerably more expanded than the lower alveoli.

From sections such as those shown in fig. 3-5, Glazier *et al* were able to compute the relative volume of alveoli at different levels of the lung. In the erect lung, at functional residual capacity, they found a marked vertical gradient of alveolar size. No significant difference in size was found when the dogs were frozen with their lungs inflated by 30 cm water positive-pressure applied at the mouth, a result which supports the contention that at full inflation the alveoli are expanded nearly uniformly throughout the lung.

Figure 3-6 depicts the relationship between distance down the vertical lung and alveolar volume existing in dogs frozen at FRC. Alveolar volumes are expressed as percentage fractions of their volume at TLC (i.e. at 30 cm water positive-pressure inflation). The apical alveoli are about 3.7 times larger than the basilar alveoli, the major part of the gradient of alveolar size being present in the uppermost 10 cm of the lung. Also shown in this figure is the volume of the alveoli at different levels of the lungs in normal seated men at FRC, as measured using ^{133}Xe. Considering the limitations of both methods used, the agreement between the two sets of data is reasonably good, except in the upper 10 cm of the lung where the alveolar volumes computed on frozen dogs are considerably larger than those determined in the ^{133}Xe studies. This discrepancy could be due to differences in species and/or techniques used. In this connection it should be noted that the specific lung compliance is greater in dog than in man. Furthermore, the vertical dog lung is much narrower than the human lung. Both of these factors could affect the vertical gradient of alveolar size (107, 187).

The results of the frozen dog experiments would indicate that the apical alveoli actually decrease in size when lung volume is inflated from FRC to 30 cm water. This peculiar finding cannot be investigated using ^{133}Xe, since at the apex of the lung no adequate radioactive counting is possible.

Glazier *et al* (107) also showed that in the horizontal lung, alveolar size was the same at the apex and base, but the uppermost alveoli were larger than the dependent ones. Furthermore, in inverted (head-down) dogs, alveolar size was uniform from apex to base. These results are in good agreement with our ^{133}Xe data.

Regional distribution of ventilation

West and Dollery (267) reported that when a normal seated man took a single breath of CO_2 labelled with radioactive oxygen ($^{15}O_2$), the ventilation per unit gas volume was greater in basilar than in apical lung regions. Similar results were obtained by Ball *et al* (11), and Glaister (102). Bryan *et al* (34), using ^{133}Xe, also observed that ventilation per unit gas volume becomes more uniform if inspired volume is increased from resting tidal volume to maximal inspiration. In all of these studies inspiration was started from resting end-expiratory lung volume.

A more complete analysis of the regional distribution of gas within the lung has recently been obtained by measuring regional lung volumes at different overall lung volumes, encompassing the entire range of the vital capacity (146, 185). Such measurements, in four normal young seated men, are shown in fig. 3-7, in which regional volumes (V_r) existing at three different vertical levels of the lungs are plotted against overall lung volume (V). These results were obtained under quasi-static conditions (airflow < 0.5 litres/sec). If the alveoli of all regions had expanded uniformly, the volume of each region (expressed as a percentage of regional TLC) should always be the same as the overall lung volume (expressed as a percentage of regional TLC) i.e., the relationship between regional and overall lung volumes should be given by the line of identity (slope = 1), which is shown as a broken line. Clearly, this is not the case: the lung units in the upper regions appear to be more expanded than those in the lower zones at all lung volumes, except at full inspiration.

Since, in normal subjects at full inspiration, the lung units are nearly equal in volume throughout the lung, expression of regional volumes as percentages of TLC_r can be considered as a particularly useful baseline of comparison, or denominator. Indeed, in normal subjects, differences in regional volumes expressed in these terms simply reflect differences in volume (size) of the lung units (alveoli). Similarly, differences in regional volume changes, when expressed as percentage of TLC_r, simply reflect differences in ventilation per lung unit, or ventilation per alveolus.

The slopes $\Delta V_r / \Delta V$ of the curves in fig. 3-7 indicate the rate of filling and emptying (or ventilation) of the lung units in the various lung regions in relation to volume changes of the lung as a whole. It is apparent that, at lung volumes above FRC, the proportion of ventilation delivered to any lung region is substantially constant, as shown by the linear relationships between regional and overall lung volumes. Thus, in this range of lung volumes, the various lung zones do not fill sequentially. However, the slope of the curves is greater in dependent than in upper lung zones, indicating that the dependent lung units are relatively better ventilated. In brief, these results suggest that when a normal subject takes a breath from FRC, the ventilation per alveolus is greater in dependent than in upper lung regions, but that the relative distribution of ventilation is independent of the volume inspired, i.e., the difference in ventilation between upper and dependent alveoli is proportionately the same whether the subject takes a resting tidal breath or a maximal inspiration.

It should be noted that the data in fig. 3-7 were obtained during relatively slow inspirations. Recent radioactive xenon studies have shown that at lung volumes greater than FRC, the regional distribution of gas within the lungs is substantially independent of the speed of inspiration (225). Thus, a plot of the slopes of the linear portion of the curves in fig. 3-7 against vertical distance down the lung, will describe the regional distribution of ventilation per alveolus for breaths of any magnitude and speed; provided that breathing takes place over the range of lung volumes where the relationship between regional and overall lung volumes is linear. Such a plot for a normal seated man is provided in fig. 3-8, where ventilation per alveolus is expressed as a percentage fraction of the value predicted assuming uniform distribution of ventilation to all lung units. As shown in this figure, ventilation per

alveolus increases approximately linearly with vertical distance down the lung. The slope of the line in fig. 3-8 is an expression of the relative change in ventilation per alveolus per centimeter descent down the lung. As shown in table 3-1, this value is about the same in all body positions indicated.

Table 3-1. Change in ventilation per alveolus (expressed as per cent predicted) per centimeter descent in the lungs, in normal young men in various body positions. Values are means, with ranges in parenthesis.

Posture	Number of subjects	Change in ventilation per alveolus/cm lung descent	Reference
Seated	9	2.3 (1.9 to 3.6)	(185)
Supine	3	2.3 (2.0 to 2.6)	(146)
Prone	3	2.0 (1.9 to 2.1)	(146)
Left lateral	3	2.2 (1.9 to 2.7)	(146)
Right lateral	3	3.1 (3.0 to 3.2)	(146)

In the head-down position, ventilation per alveolus appears more uniform than in the other postures. It should be noted that the difference in ventilation per alveolus, between the uppermost and the most dependent parts of the lungs, tends to be smaller in the supine and prone positions then when seated or in lateral decubitus. This is a consequence of the greater vertical lung length in the latter postures. Similarly, the difference in ventilation per alveolus, between the uppermost and lowermost lung units, should be more pronounced in subjects with greater lung dimensions.

It is of particular interest that, in the range of lung volumes where breathing normally takes place, the distribution of ventilation is (a) preferential to the dependent lung zones and (b) independent of the volume inspired and of the speed of inspiration, i.e., of the breathing pattern. The former feature is important because blood flow normally is also distributed preferentially to the dependent lung zones (see chapter 6). Thus, ventilation and blood flow are relatively well matched in the normal lung and consequently, gas exchange is more efficient than would be the case if ventilation distribution were uniform. The latter feature would also appear to be functionally significant, considering the importance of ventilation distribution to gas exchange and the considerable variability of the pattern of normal breathing.

The preferential distribution of ventilation to the dependent lung zones, when breathing is in the normal range of lung volumes, can also be explained as a combination of the vertical gradient in pleural pressure and the uniform elastic properties of the lungs. As shown in fig. 3-9b, at FRC the lower lung units operate on a steeper (more compliant) part of the static volume-pressure curve than the upper lung zones. As a result, during inspiration started from FRC, the difference in compliance between the lower and upper parts of the lungs favours greater tidal volumes in the dependent zones. The independence of ventilation distribution on the breathing pattern is more difficult to explain. Possibly, this behaviour is a consequence of the exponential character of the static volume-pressure curve of the lungs and of uniform

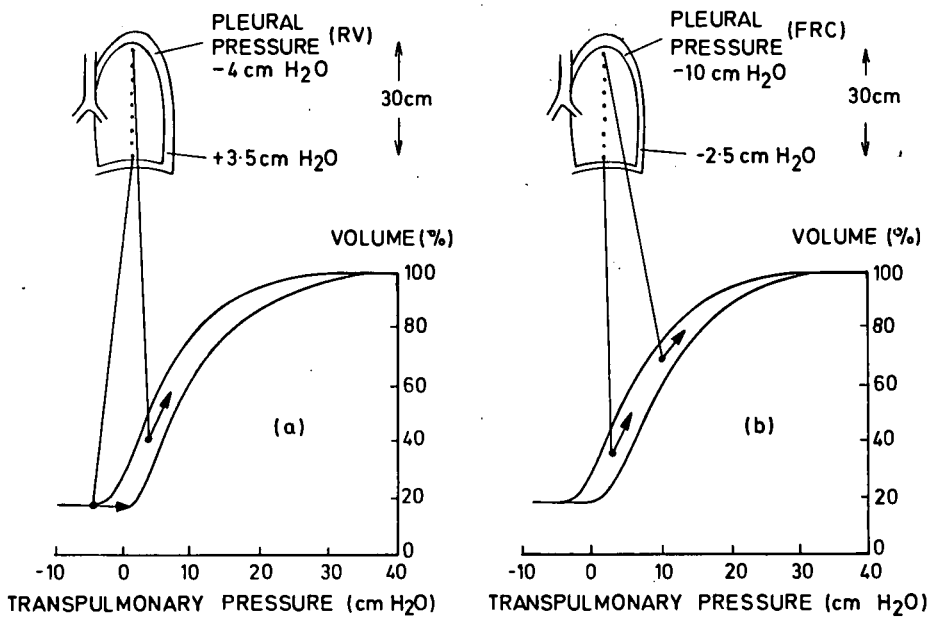

Fig. 3-9 Effect of pleural pressure gradient on distribution of ventilation. In (b), at the beginning of a normal inspiration (FRC), the basilar lung regions are operating on a steeper part of the compliance curve of the lungs than the apical lung zones. As a result, during tidal volume respiration, the ventilation is greater in the basilar lung regions, as shown by the arrows. By contrast, in (a) at residual volume (RV), pleural pressure at the lung base is positive (+ 3.5 cm water) and as a result the lower alveoli are not ventilated because of airway closure (trapping). Under these conditions, the lung apex ventilates better than the base. (From (186) by courtesy of J. nucl. Biol. Med.).

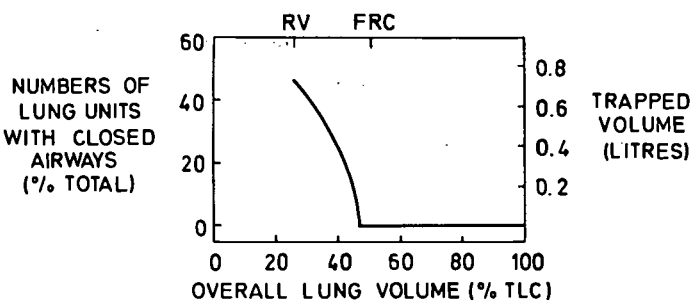

Fig. 3-10 Number of lung units with closed airways (%total number) and trapped volume (litres), as a function of overall lung volume (%TLC). Average results on four healthy young men sitting upright.

changes in pleural pressure with changes in overall lung volume (185, 252).

If breathing takes place at lung volumes less than FRC, the distribution pattern of ventilation is entirely different. Indeed, as shown in fig. 3-7, when lung volume is reduced below FRC, the slope $\Delta V_r / \Delta V$ increases progressively in all regions shown, until regional volume reaches a value of about 19 percent TLC_r, which corresponds to the regional minimal volume. Once the minimal volume is reached (at about 40 percent TLC for the lower zones and 30 percent TLC for the middle zones), regional volume remains constant despite further reduction in overall volume.

As pointed out above, minimal volume is caused by airway closure. The progressive increase in the slope $\Delta V_r/\Delta V$ of the curves in fig. 3-7, when lung volume is reduced below FRC, can also be explained by airway closure. This commences in the most dependent parts of the lung, (which are exposed to more positive pleural pressure) and progresses upwards in the lung till RV is reached (66, 128) (Fig. 3-9a). If the airways to part of the of the lung close, the slopes $\Delta V_r/\Delta V$ of the remainder of the lung would be expected to increase. As shown in fig. 3-10, in normal seated young subjects the airways begin to close at about 46 percent TLC (i.e. just below FRC). The extent of airway closure increases progressively with further decrease in lung volume, until at RV airway closure affects about half of the lung units. Figure 3-10 also shows the volume of gas trapped behind closed airways at different overall lung volumes. It can be seen that at RV, the volume of gas trapped amounts to about 0.75 l.

As shown in fig. 3-7, at low lung volumes (i.e. near RV), the slope of the curves relating regional to overall lung volume is steeper in the upper than in the dependent lung zones. Accordingly, the ventilation distribution is reversed, lung units in upper regions being better ventilated than those in dependent zones. Furthermore, during inspiration from RV, the proportion of gas delivered into the upper units decreases progressively as inspiration proceeds, whereas the opposite is true in the dependent lung zones. Thus at low lung volumes the distribution of ventilation is not only reversed but the various lung regions also fill (and empty) sequentially. In this connection it should be pointed out that at low lung volumes, the distribution of gas within the lungs changes with the speed of inspiration, i.e. with increasing inspiratory airflow the distribution of inspired air becomes more uniform(225). Therefore, the relationships between regional and overall lung volumes below FRC shown in fig. 3-7 do not apply at high flow rates.

Again, these results can be explained by the simple model based on the vertical gradient in pleural pressure and on uniform elastic properties of the lungs. At lung volumes below FRC, however, the regional distribution of ventilation is further complicated by gas-trapping. As shown in fig. 3-9a, when lung volume approaches RV, the transpulmonary pressure in the dependent lung zones is negative (i.e. pleural pressure exceeds airway pressure). As a result the dependent-zone airways collapse, causing gas-trapping in these units. Thus, when a small breath is taken from RV, the trapped units receive none of the inspired air until transpulmonary pressure reaches the critical value (opening pressure) required to reopen the closed airways (43, 128, 252). If inspiration is slow (low airflow), transpulmonary pressure follows the static volume-pressure relation of the lung; hence the critical opening pressure is attained at relatively high lung volumes. On the contrary, if inspiration is rapid, the critical opening pressure is reached at lower lung volumes. As a result, during rapid inspiration distribution of inspired gas is more uniform (225).

The reversal of ventilation distribution at low lung volumes is of considerable interest. Indeed, in many physiological and pathological conditions (e.g. obesity, submersion in water, chest-strapping, anti-G suit, negative pressure breathing)

the reduction in FRC at times may be large enough to cause airway closure in the dependent lung zones (and hence a reversal of ventilation distribution) in the resting tidal volume range (see chapter 8). In this connection it should also be pointed out that in the horizontal positions (supine, prone and lateral decubitus), the FRC is considerably lower than in the standing or seated positions. Accordingly, dependent-zones airway closure should occur more readily in the former than in the latter positions. Recent work by Abernethy *et al* (1) indicates that this is probably the case, at least during prolonged recumbency. On the basis of measurements of urinary-alveolar nitrogen differences, they concluded that the unevenness of the ventilation-perfusion ratio is greater in recumbency than in the erect position. By contrast, previous work with radioactive gases (34, 146) has suggested that the ventilation-perfusion ratio distribution is more homogeneous in recumbency. It should be noted, however, that in the experiments of Abernethy *et al* , the urinary and alveolar gas samples were collected at least one hour after the subject lay down, during which period the subject breathed quietly. Under these circumstances, airway closure in the dependent lung zones may well have occured, and could explain, at least in part,the increased ventilation-perfusion ratio unevenness. The radioactive-gas studies, on the contrary, involved repeated maximal inspirations, and dependent-zones airway closure may have been minimized, leading to a more even $\dot{V}_A/\dot{Q}$ distribution.

Factors determining regional distribution of gas within the lung

In the preceding section of this chapter, a simple mechanical model of the lung was used to explain the uneven distribution of gas within the normal lung. In this section, the validity of the model will be analysed in some detail.

In theory, uneven regional distribution of gas in the lung can be caused by regional differences in flow-resistance, compliance and pleural pressure. All of these factors probably contribute to the uneven distribution of gas in the diseased lung. In the normal lung, however, regional differences in airway resistance probably contribute little to the unevenness, at least at lung volumes greater than FRC. Indeed, in this volume range, lung compliance is independent of frequency in most normal subjects (64, 181, 201). For this to occur, the various parallel pathways within the lung must fill and empty synchronously over a wide range of breathing frequencies. This condition, which is obviously essential for efficient gas exchange, could be achieved if the time-constants (the product of resistance and compliance) of the various lung units were the same thoughout the lung (201). This rather rigorous requirement can hardly be met in the lung, considering (a) the different length of the multitudinous parallel pathways (229) and (b) the marked differences in expansion of lung tissue at different vertical levels caused by gravity.

Recently, an alternative explanation has been proposed by Macklem and Mead (172). They pointed out that most of the flow-resistance is in a common path (trachea and upper airway), while the resistances and time-constants of the parallel lung units are rather small. Under these conditions, there could well be considerable variation in the time constants of these lung units. This would affect neither lung compliance nor gas distribution until respiratory frequencies exceeded physiological limits. It appears that in normal man, at lung volumes greater than FRC, the uneven regional distribution of ventilation is not caused by regional differences in airway resistance, a conclusion that is also supported by ^{133}Xe studies (34, 185, 225). Severinghaus *et al* (239) and Newhouse *et al* (191) have suggested that local hyperventilation resulting in local hypocapnia causes local bronchoconstriction, with consequent diversion of ventilation to better perfused alveoli. This homeostatic mechanism appears to play no role under normal conditions, but in lung disease may be important. At lung volumes lower than FRC, where airway closure is present in the dependent lung zones, airway resistance probably plays an

important role in determining distribution of gas within the lung (225). Indeed, at low lung volume, lung compliance has been shown to be frequency dependent (189).

Regional differences in the intrinsic static volume-pressure relations of the lung is another factor which could conceivably cause uneven distribution of gas. Frank (88) and Faridy *et al* (82) have shown that there is a small but significant difference in the static volume-pressure relationship between upper and lower lobes of dogs, while within each lobe the elastic properties are properties appear to be uniform. In human lungs, the intrisic elastic properties are probably uniform throughout the lung (252). Changes in pulmonary blood volume and its distribution within the lung may also contribute to uneven distribution of gas (107, 277). Under normal conditions, however, this is probably only a small factor contributing to the distribution inequality of gas.

From the above considerations it follows that the observed differences in regional distribution of gas must be caused chiefly by regional differences in pleural pressure. Several investigators have reported that pleural pressure increases down the lung. Wood *et al* (272) and Bryan *et al* (34) suggested that this vertical gradient of pleural pressure may cause regional differences in alveolar expansions. Indeed, by combining the vertical pleural pressure gradient and the static volume-pressure curve of the lung, it should be possible to compute the vertical gradient of alveolar size. Unfortunately, the results of direct measurements of the pleural pressure gradient vary considerably, gradients ranging between 0.2 and one centimetre of water per centimetre distance down the lung having been reported (62, 153, 188, 232, 251, 272).

In view of the many potential sources of error inherent in measurements of pleural pressure, either with devices inserted into the pleural space or in the oesophagus, these discrepances are not surprising. Fortunately, the ^{133}Xe studies have provided independent measurements which can be used to predict the distribution of pressure along the lung surface, so providing an independent test of the validity of the various results reported in the literature. By combining the ^{133}Xe data and measurement of static volume-pressure relations of the lungs, it was possible to predict the regional differences in pleural pressure which would have to exist to account for the observed differences in regional distribution of gas in man (146, 185). Such predictions indicate that in the upright and horizontal positions, the uneven distribution of gas as measured using ^{133}Xe would be caused by a vertical pleural pressure gradient of 0.2 to 0.3 cm water/cm descent down the lung. As shown in fig. 3-11, the predicted gradient is steeper in the upper than in the lower lung regions. In the head-down position, on the contrary, the differences in alveolar expansion down the lung are small (Fig. 3-4), and hence pleural pressure should be substantially uniform.

Glazier *et al* (107), using an entirely different approach, also computed the vertical pleural pressure distribution which would account for the gradient in alveolar size observed in the frozen dogs. Their predicted gradients for the vertical (head-up) position are greater than those computed from the ^{133}Xe data, but they also found that the gradient is considerably steeper in the apical parts of the lung. The discrepancy between the gradient predicted by Glazier *et al* and those computed from the ^{133}Xe studies may be due to differences in geometry and/or mechanical properties between the dog and human lung (107, 187). Glazier *et al* also reported that, in the head-down position, the vertical pleural pressure gradient should be virtually abolished, a conclusion which is consistent with the results of some of the ^{133}Xe studies.

The nature of the vertical pleural pressure gradient is not clearly understood. Krueger *et al* (153) have suggested that the lung behaves as a fluid of the same density as lung tissue. The mean density of lung tissue at FRC is about 0.2 to

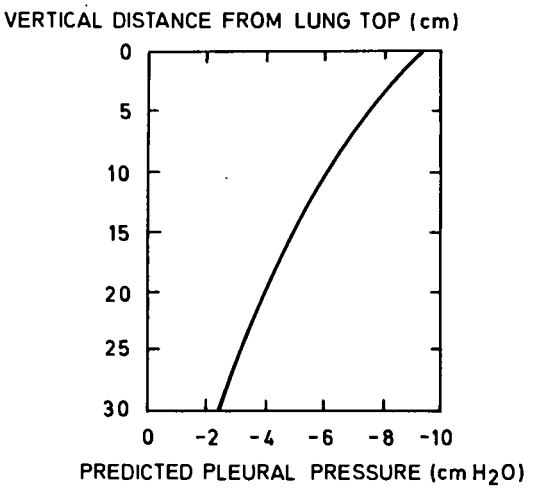

Fig. 3-11 Vertical distribution of pleural pressure which would have to exist to account for differences in regional distribution of gas measured using ^{133}Xe in seated men at FRC.

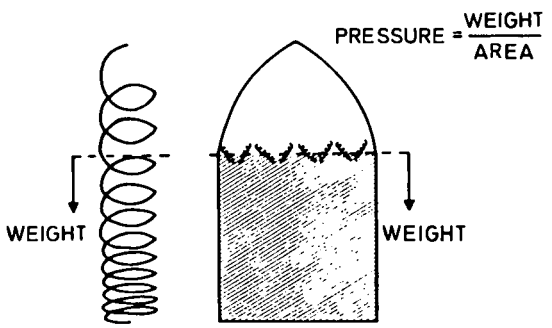

Fig. 3-12 Model to account for the vertical differences in pleural pressure caused by gravity. In a spring supported at the top, the distending force is determined by the weight of the spring below any point. By analogy, the weight of the lung below any horizontal plane is supposed to be taken by the parenchymal fibres in the plane, so that the distending pressure is the dependent weight divided by the cross-sectional area.
(From West, (266), by courtesy of J. Nucl. Biol. Med.).

0.3 g/cm^3, which is consistent with some of the directly measured pleural pressure gradients (62, 153, 188). Turner (257) has proposed that the differences in pleural pressure down the lung are due to differences in supporting forces along the lung surface. Figure 3-12 illustrates a simple model which could account for the pleural pressure gradient. If the lung is supported by its superior surface, the pleural pressure component due to gravity at any lung level can be taken as equal to the weight of the lung below this plane, divided by its cross-sectional area (W/A). In the head-up position, W increases up the lung while A decreases. Accordingly, at the apex where the W/A ratio is high, there will be a large negative pleural pressure. On the contrary, in the inverted (head-down) position, both W and A increase at approximately the same rate up the lung, and accordingly the pleural pressure is more uniform. This model is compatible not only with the observed differences in alveolar volume in the upright position, but also in the inverted position. Although attractive, this hypothesis has several limitations (107), and it is too early to say whether it is entirely valid (see also chapter 11 p. 183). Clearly, further work is needed for a better understanding of the factors which determine the distribution of pleural pressure. Whatever its precise nature, the vertical gradient in pleural pressure appears to be gravity-dependent, i.e., related to the weight of the lungs, since it increases during acceleration (see chapter 4).

On the basis of these considerations, it appears that in the normal lung, the gravity-dependent pleural pressure gradient is the major determinant of the uneven regional distribution of gas. It should be noted, however, that the effect of this gradient on distribution of gas depends on the elastic properties of the lungs. Indeed, as shown in fig. 3-2, the regional distribution of gas depends on the combination of the gradient with the static-volume pressure curve of the lung. Thus any change in the elastic properties of the lungs will necessarily affect the distribution of gas (187). For example, with ageing, the elastic recoil of the lung decreases, and this has been shown to have a profound effect on regional ventilation distribution within the lung (128).

In conclusion, the simple mechanical model of the lung used to explain the uneven distribution of gas involves several approximations which may not be entirely valid, and more information is needed, particularly regarding the topography of pleural pressure. Nevertheless, this simple model has been found useful for predicting ventilation distribution under a variety of conditions, e.g., breathing at low lung volume (129), old age (128), and acceleration (see chapter 4). Furthermore, by this model gravity is for the first time taken into consideration. It has long been recognized that gravity is the main factor determining the regional distribution of blood flow within the lung. There now appears to be little question that gravity is also the main factor determining the regional distribution of gas. This has important functional significance, in the sense that the re-distribution of ventilation which occurs with changes in body posture appears generally to follow the same direction as the shift of pulmonary blood flow. In this way pulmonary ventilation and perfusion remain reasonably well matched in most body positions, a fact that is clearly important in terms of the overall efficiency of gas exchange within the lung.

Causes of uneven ventilation distribution in general

In the preceding sections of this chapter, only regional ventilation distribution was considered. Although regional differences in ventilation are probably the major source of ventilation inhomogeneity within the normal lung, they are not its sole source. This section deals briefly with the problem of uneven ventilation distribution in more general terms. A more complete analysis of this topic can be found elsewhere, (29,87).

Two main theories have been proposed to explain the uneven distribution of ventilation within the lung: the parallel and the series, or stratification ventilation theory. These theories take into account the complex arrangement of the various and multitudinous anatomical units within the lung.

Parallel ventilation

The parallel ventilation theory states that separately located spaces in the lung may be ventilated at different rates, independently of one another and in parallel (224). Such different ventilation rates are indeed present at different vertical levels of the lungs, as described in the preceding sections of this chapter. In addition to these gravity-dependent differences of ventilation distribution between regions, there is probably some ventilation unevenness within each region. The latter differences cannot be revealed by the conventional radioactive-gas methods, which describe the behaviour of relatively large areas of the lung, but presumably can be detected by the analysis of inert gas wash-out curves (110, 190). The integrated use of the latter methods and of the radioactive-gas techniques is clearly indicated in order to obtain more precise information concerning the sources of uneven distribution of ventilation.

Uneven ventilation distribution can be caused not only by differences in volume-expansion of the various parallel lung units, but also by their asynchronous behaviour, i.e., by local differences in the time course of inspiratory filling and expiratory emptying. Asynchronous (sequential) behaviour of the lung units, at different vertical lung levels, is indeed present when breathing takes place at lung volumes less than FRC, and under these circumstances may be an important cause of uneven ventilation distribution. Above FRC, the various vertical lung regions do not appear to fill (or empty) sequentially. Thus, according to the radioactive-gas data, in the lung volume range where breathing normally takes place in seated subjects, this mechanism probably contributes little to the uneven distribution of gas. It should be stressed again that the radioactive gas measurements describe the overall behaviour of relatively large areas of the lung, and accordingly, the results of these studies do not exclude asynchronous behaviour of parallel elements within each region studied. Recent work by Sikand ***et al*** (240) and Read (218, 219) based on analysis of expired gas, suggests that the parallel units within each lung region also behave synchronously, at least in normal subjects breathing above FRC. Again this is consistent with the frequency-independence of lung compliance, as described in the previous section of this chapter.

The synchronous behaviour of the normal lung appears to be a useful feature, not only in relation to total ventilation distribution (i.e., total ventilation distribution is independent of the breathing pattern), but also in relation to the distribution of dead-space gas within the lung. As pointed out by Fowler (87), asynchronous volume behaviour should result in uneven distribution of dead-space gas, and hence of the effective ventilation. Under these conditions, the efficiency of gas exchange within the lung could be reduced. In this connection, it should be noted that uneven dead-space gas distribution may also be caused by differences in bronchial pathway length. The length of the bronchial pathways, and hence dead-space volume, is greater in the peripheral than in the central (perihilar) lung units (229, 230). Accordingly, the effective (total minus dead-space) ventilation per alveolus should decrease from the centre to the periphery of the lung. Thus, although in any horizontal plane of the lung total ventilation distribution appears to be substantially uniform, there is probably a gradient of effective ventilation distribution with the lowest values in the most peripheral lung units. It is of interest that perfusion distribution per alveolus has also been reported to decrease from the central to the peripheral parts of the lung (33). Thus, the $\dot{V}_A/\dot{Q}$ distribution is more homogeneous than would be the case had perfusion distribution been uniform in any given

horizontal plane in the lung. However, other studies, also involving the use of a gamma camera (192), have not confirmed this observation.

Series ventilation

Krogh and Lindhard (152) suggested that the more deeply situated air spaces (e.g., alveoli) would receive less inspired gas than more central spaces (e.g., alveolar ducts), implying that, at any given instant in the respiratory cycle, gas concentrations might be different at various depths within each terminal lung unit. This theory has been termed the 'stratification ventilation theory' since it suggests layering of gas within the terminal lung units; or the 'series ventilation theory', as it represents the lung as being ventilated like two or more spaces in series, each with a different ventilation rate. Making certain anatomical assumptions, Rauwerda (217) calculated that, within the primary lobules, any gas concentration difference would decrease to 16 percent of the initial difference within less than 0.3 sec. This implies that the gas tensions within the primary lobules of the normal lung are nearly uniform at all physiological breathing frequencies. Rauwerda's work has often been quoted in the past as evidence against the concept of stratified ventilation distribution.

The study of gaseous diffusion within the lung has recently gained new impetus (59, 60, 143, 218, 219, 240). The results indicate that stratification of ventilation within the secondary lobules of the lung may contribute substantially to the unevenness of ventilation seen in the normal lung, a finding consistent with the anatomy of the secondary lobule. Because of stratification, the effective ventilation of the most distal alveoli within the secondary lobule must clearly be less than that of the more proximal alveoli. It is of interest that a similar gradient of diminishing blood flow along the axis of the secondary lobule has also been reported (263). This perfusion gradient reduces the potential magnitude of $\dot{V}_A/\dot{Q}$ inhomogeneity within the secondary lobules, and must again improve the efficiency of gas exchange within the lung.

In conclusion, several potential causes of uneven distribution of ventilation within the lung have been documented, and under certain conditions each may play an important role. Under normal conditions, gravity appears to be the major cause of the uneven ventilation seen in the human lung, although stratification probably plays a more important role in determining this unevenness than has been previously recognized.

4

The effects of acceleration on ventilation distribution

A. C. BRYAN

In the previous chapter, it was shown that the observed distribution of regional lung volume and ventilation could be explained by the mechanical properties of the lung. Because of the existence of a pleural pressure gradient, and because of the shape of the pressure-volume curve, there are predictable regional differences in regional volumes and ventilation. The cause of the pleural pressure gradient is not certain, but from postural data, both direct (153) and indirect (185), it appears to be primarily related to the weight of the lung. The alterations in lung mechanics which occur during acceleration have been described in chapter 2, but the relevant facts will be reviewed here as the changes in ventilation distribution during acceleration are the direct result of these mechanical changes.

If the pleural pressure gradient is primarily due to the weight of the lung, then, since weight is effectively a function of acceleration, the gradient should vary with acceleration. This has been shown to be true both for oesophageal pressure in man during $+G_z$ acceleration (36, 103) and for pleural pressure in dogs during G_x acceleration (233). In all these studies, the gradient increased directly and approximately linearly with acceleration.

Positive acceleration

Acceleration, at least up to moderate levels, does not appear to alter the elastic properties of the lung. Bondurant (27) reported that dynamic compliance fell at $+3G_z$, but as there are good reasons to believe that acceleration produces asynchronous emptying of the lung, dynamic compliance may be reflecting this, rather than a change in the true elastic recoil (201). Measurements of the expiratory static compliance curve during acceleration do not show any significant change in the shape of the curve, i.e., the elastic recoil is the same, but the curves are displaced due to the change in regional pleural pressure (Fig. 4-1). These measurements have only been made at low levels of acceleration, as they are difficult to perform accurately at higher levels. At higher accelerations, it is possible that there is some change in the regional elastic recoil due to changes in blood-flow distribution, and if the acceleration is prolonged, some pulmonary oedema. Despite this caution it does appear that, in the range of interest, acceleration does not significantly affect the elastic properties of the lung.

Under these conditions, as originally suggested by Wood (272), the dependent alveoli should get smaller, and those at the top of the lung larger, as the acceleration increases. Furthermore, with a known gradient and known elastic properties, these changes should be predictable. Unfortunately, there is no agreement as to the magnitude of the pleural pressure gradient. Most of the evidence, both direct and indirect (36, 103, 146, 153, 185) suggests that the

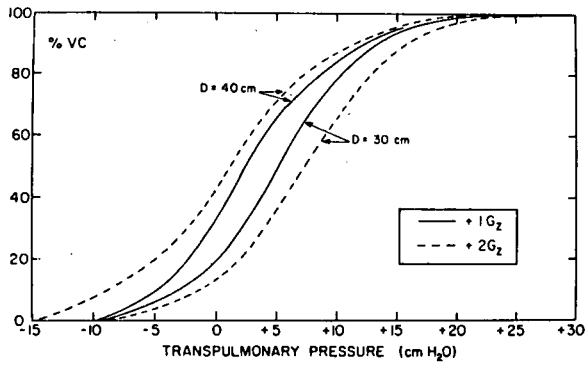

Fig. 4-1 Ordinate: overall lung volume expressed as % VC.
Abscissa: transpulmonary pressure in cm water.
Static deflation pressure-volume curve in one subject at $+1G_z$ (solid curve) and $+2G_z$ (dotted curve) with the top of the balloon 30 and 40 cm from the nares.
(From (36), by courtesy of J. appl. Physiol).

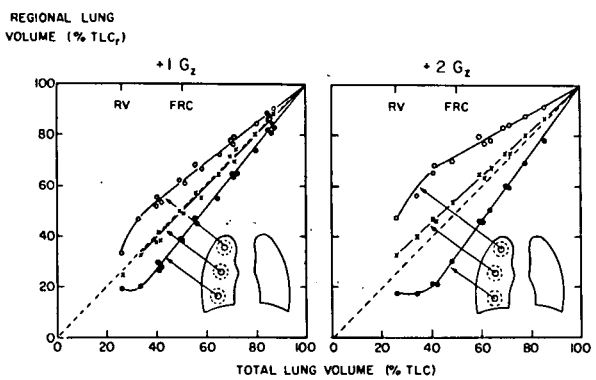

Fig. 4-2 Ordinate: regional lung volume expressed as a percentage of the regional total lung capacity.
Abscissa: overall lung volume, expressed as a percentage of total lung capacity. Results obtained in a subject using ^{133}Xe at $+1G_z$ and $+2G_z$. The vertical distance from the top of the lung to the centre of the counters was 4.5 cm (open circles), 13 cm (crosses), and 23.5 cm (solid circles). Broken lines (slope = 1) indicate regional percentile expansion equal to the overall percentile expansion.
(From (36), by courtesy of J. appl. Physiol.).

gradient is about 0.2 cm water/cm in the upright position. However, Wood and his co-workers (232, 233) have consistently shown a gradient two or three times as large, measured with open fluid filled catheters in the supine dog. Permutt has suggested that this large gradient may be due to an artifact inherent in the method of measurement (208), and certainly such a large gradient seems inconsistent with the mechanical behaviour of the lung.

The data on the changes in the distribution of regional volume and ventilation are not extensive and are mainly confined to $+G_z$ acceleration, but in general they tend to confirm the theoretical predictions, based on changes in lung mechanics. It is convenient to deal with the results as events above functional residual capacity and events below, as below FRC the situation is complicated by asynchronous emptying and terminal airway closure, as discussed in chapter 3.

Lung volume greater than FRC

Using ^{133}Xe, regional lung volumes at different overall lung volumes have been measured at +1, +2 and $+3G_z$. A typical result is shown in figure 4-2. At $+2G_z$ it can be seen that at all levels of lung inflation (except at TLC), the upper units are larger and the lower units smaller than at $+1G_z$.

Furthermore, at $+2G_z$ the slopes of the lines (dVr/dV) - rate of volume change or ventilation - are linear, indicating that each zone is accepting a constant aliquot of gas; that is, the ventilation is still synchronous. However, the slopes of the lines have changed (Fig. 4-3), producing a higher ventilation to the base and a decreased ventilation at the apex. The conjunction of the volume change and the ventilation change means that there is a very considerable alteration in the ventilation per unit volume. Similar changes were found in all subjects. The slopes of the lines in fig. 4-3 are linear and can be expressed by the equation $dVr/dV = a + bD$ and the values for the constants a and b are given in table 4-1. Of particular interest is the value Di, the point around which these curves rotate, or the level at which ventilation does not change with acceleration, and this must be the iso-volume and hence the iso-pressure point in the lung.

Table 4-1. Values of the constants a and b of the equation $dVr/dV = a + bD$, and vertical distance down the lung to the isovolume point Di. From (36).

Subject	$+1G_z$ a	$+1G_z$ b	$+2G_z$ a	$+2G_z$ b	$+3G_z$ a	$+3G_z$ b	Di, cm
MG	0.74	0.020	0.45	0.040			25
PN	0.76	0.021	0.33	0.044			15
JS	0.67	0.025	0.39	0.036			19
CB	0.72	0.016			0.42	0.039	13

Note: Di is calculated from the following expression: $a + bD = a^1 + b^1D$, where a and b are the values of the constants of the equation $dVr/dV = a + bD$, at $+1G_z$, and a^1 and b^1 are the corresponding values during increased acceleration.

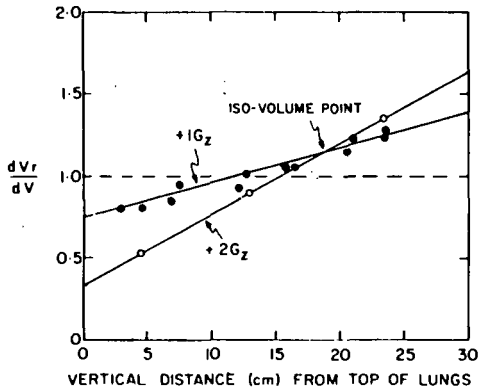

Fig. 4-3 Ordinate: slope (dVr/dV) of the linear portion of the curves in fig. 4-2, or ventilation.
Abscissa: vertical distance from the top of the lung. The broken line (slope = O) indicates uniform ventilation. Data from one subject at $+1G_z$ (solid circles) using twelve vertical counters, and at $2G_z$ (open circles) using three vertical counters.
(From (36), by courtesy of J. appl. Physiol.).

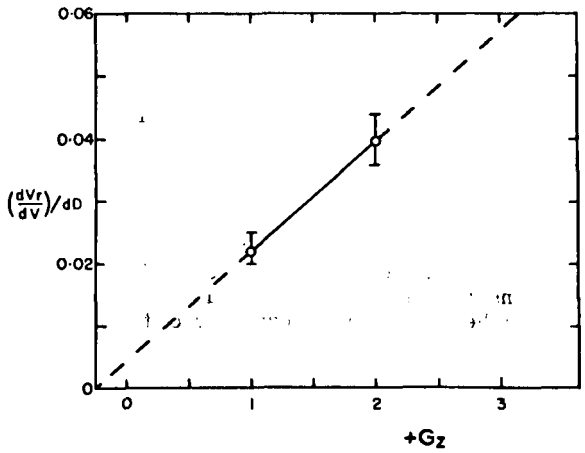

Fig. 4-4 Ordinate: slope d(dVr/dV)dD, or the difference in ventilation between top and bottom of the lung, of the curves shown in fig. 4-3.
Abscissa: $+G_z$ acceleration. Mean values and range on three subjects. Note the very small difference in regional ventilation on extrapolation to zero G.
(From (36), by courtesy of J. appl. Physiol.).

The slopes of the lines in fig. 4-3 are plotted against acceleration in fig. 4-4. The expression d(dVr/dV)/dD is formidable, but simply expresses the difference in ventilation between the top and bottom of the lung. It can be seen that the difference nearly doubles at $+2G_z$, and Glaister (98) has shown that the difference triples at $+3G_z$. The particular interest of this graph is that, if the line is extrapolated back to zero G, there appears to be very little difference in regional ventilation. The validity of this extrapolation is supported by the finding that complete inversion of the body leads to a reversal of the $+1G_z$ pattern of ventilation (102). In this position, however, lung geometry and the supporting forces do appear to modify the distribution of pleural pressures (178, 257), and in the dog, the gradient of alveolar size is not reversed by inversion (107). These apparently conflicting findings will be discussed in chapter 11.

The ^{133}Xe data can also be used to calculate an approximate pleural pressure gradient. Knowing the regional volume and the subject's static pressure volume curve, the local pressure required to produce the regional volume can be determined. At $+1G_z$, the mean gradient in five subjects was 0.16 cm water/cm, and at $+2G_z$ it doubled to 0.33 cm water/cm (36). This is obviously an approximation, as it combines the errors of ^{133}Xe counting and errors inherent in oesophageal pressure measurement. However, it is probably a more accurate way of estimating pleural pressure than most of the direct measurements that have been made. In fig. 4-5, the pleural pressure gradients calculated at $+1G_z$ and at $+2G_z$ have been extrapolated back to zero G, and the gradient then disappears. This again suggests that the gradient of pleural pressure is primarily due to the weight of the lung.

Lung volumes less than FRC

As described in the previous chapter, the pattern of distribution of inspired gas is entirely different at lung volumes less than functional residual capacity. As the volume falls below FRC, there is a progressive closure of terminal airways. The exact mechanics of the closure are not fully understood. Clements (51) has suggested, on the basis of surface forces, that a duct will collapse when a bubble blown on the end of it has twice the radius of the duct (by the Laplace relationship). Assuming that the bubble started as a hemisphere, as it gets smaller the radius increases and closure of the duct will occur at 20 percent of the initial volume. However, this hypothesis requires a very exact geometry which is probably not realistic in the lung. An alternative hypothesis is that, as the units get smaller and their elastic recoil approaches zero, the point at which airway pressure equals pleural pressure must approach the terminal airway (180). Downstream of this point, pleural pressure will exceed airway pressure and airway closure may occur. The closure occurs first in the most dependent parts of the lung, where the pleural pressure is highest and the alveoli least distended. Closure commences at about 46 percent of total lung capacity, and as residual volume is approached, the zone of closure spreads up the lung. Closure occurs when the regional volume is approximately 20 percent of the regional total lung capacity.

Under increased acceleration it has been demonstrated that the pleural pressures, in the dependent parts of the lung below the iso-pressure point, become more positive. On this basis, one would predict that closure should occur at a higher lung volume and involve more of the lung. Studies of regional lung volume close to residual volume are technically rather difficult, but what data exists supports this prediction. In fig. 4-2, at $+1G_z$, the lower zone starts filling at 30 percent TLC, whereas at $+2G_z$ filling does not start until about 40 percent TLC. This 'lower zone' is not quite at the bottom of the lung, as the centre of the counter was actually 24 cm from the lung apex, and it is of interest to predict what is happening at the bottom. This can be done by a linear extrapolation of the lines in fig. 4-3

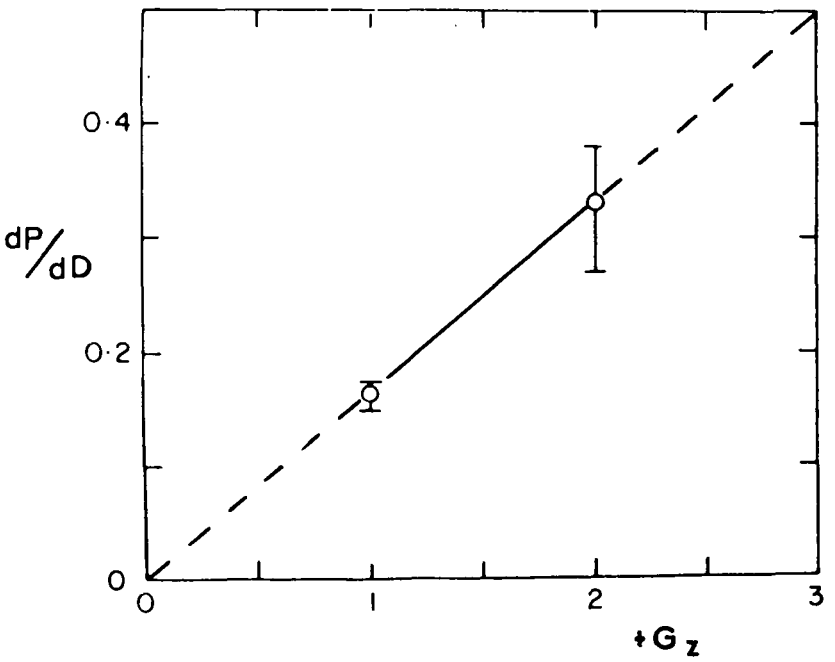

Fig. 4-5 Ordinate: Pleural pressure gradient (dP/dD), in cm water/cm, predicted from regional lung volumes.
Abscissa: $+G_z$ acceleration. Mean and range on three subjects. Note the absence of a pleural pressure gradient on extrapolation to zero G. (From (36), by courtesy of J. appl. Physiol.).

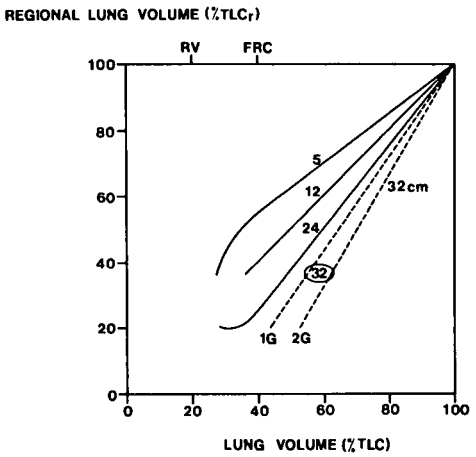

Fig. 4-6 Ordinate: regional lung volume expressed as a percentage of regional total lung capacity.
Abscissa: overall lung volume expressed as a percentage of total lung capacity. The solid lines are taken from fig. 4-2, the figures being the vertical distance of the three counters from the top of the lung. The dotted lines are the predicted volume-expansion curves at the base of the lung (32 cm) at $+1G_z$ and $+2G_z$, obtained by extrapolation of data in fig. 4-2.

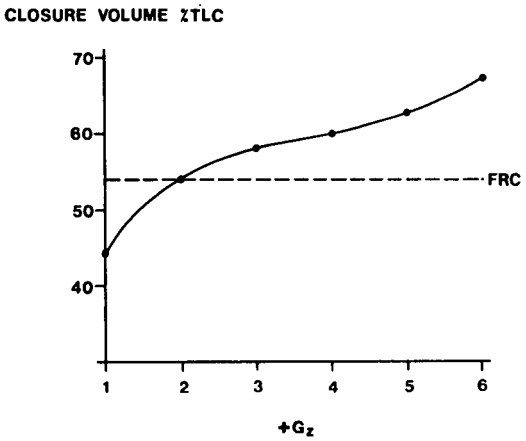

Fig. 4-7 Ordinate: predicted closure volume at the base of the lung, assuming that closure occurs at $20\%TLC_r$, obtained from fig. 4-6.
Abscissa: $+G_z$ acceleration. Events at higher acceleration were obtained by extrapolation. The dotted line indicates functional residual capacity, which is assumed not to change.

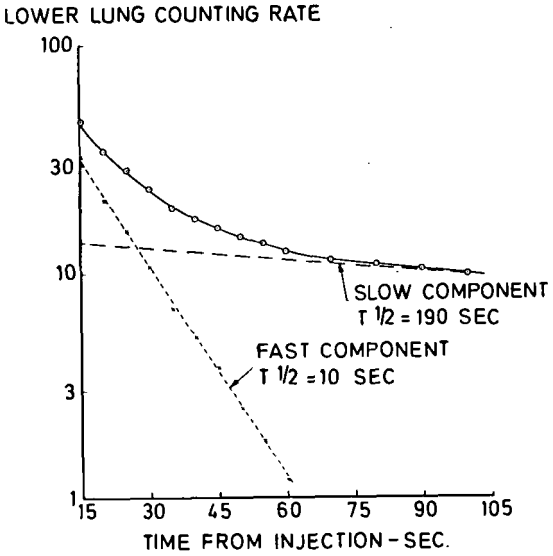

Fig. 4-8 Ordinate: zenon-133 count rate over a lower lung field plotted on a logarithmic scale (open circles).
Abscissa: time following the intravenous injection of a bolus of ^{133}Xe. Subtraction of the slow wash-out component from the overall wash-out yields a fast wash-out component

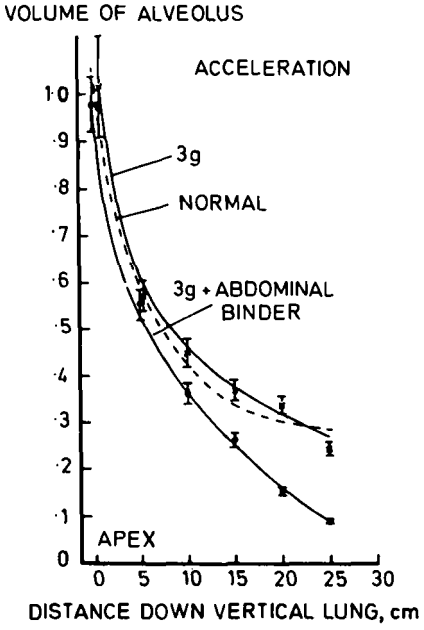

Fig. 4-9 Ordinate: relative alveolar size measured in frozen dog lung.
Abscissa: vertical distance down the lung. Dotted curve is the normal $+1G_z$ distribution, the two solid curves are from dogs frozen at $+3G_z$ with and without an abdominal binder (from 107).

to 32 cm, the overall lung length, obtaining the slope dVr/dV and replotting this hypothetical line, as has been done in fig. 4-6. If closure occurs at 20 percent of regional total lung capacity, at $+1G_z$ this will be reached at 44 percent TLC. At $+2G_z$ closure will start to occur at 54 percent TLC, i.e., almost at functional residual capacity. It is obvious that at any higher acceleration, closure will occur at a lung volume greater than FRC. By another linear extrapolation of the curve in fig. 4-4, the closure volume at higher accelerations can be approximated (Fig. 4-7). From this it is apparent that at higher accelerations, these units will be closed and unventilated for an increasing part of the tidal volume range.

Glaister (98) has conclusively demonstrated this closure during tidal breathing at high $+G_z$ acceleration, by following the wash-out of injected ^{133}Xe. At $+1G_z$, the wash-out of intravenously injected ^{133}Xe from the lung approximates to a single exponential with a time-constant proportional to the regional ventilation per unit volume (33). However, during $+3G_z$ acceleration, the basilar wash-out has two obvious components (Fig. 4-8). The fact that ^{133}Xe evolved into the lung must indicate that the alveoli themselves were not collapsed. The appearance of a large, very slow component in the wash-out must indicate a large population of alveoli with very poor ventilation, presumably due to airway closure, possibly with intermittent opening (see also p. 129).

It is unfortunate that an anti-G suit, which is so helpful in supporting the systemic circulation, aggravates the gas-trapping in the dependent part of the lung. The abdominal bladder of the suit increases intra-abdominal pressure, elevates the diaphragm and reduces the FRC (chapter 2). As a result of this, the subject breathes closer to residual volume and dependent airway closure will occur at a higher lung volume for any given acceleration. The important influence of an anti-G suit will be further discussed in relation to acceleration atelectasis (chapter 8).

Direct demonstration of the changes in alveolar size during increased acceleration has been obtained by morphometry of frozen intact dogs (107), fig. 4-9. Exposed to $+3G_z$, there was almost no change in alveolar size because of the unopposed descent of the diaphragm and increase in lung volume. With an abdominal binder in place, analogous to a conscious man's abdominal musculature, or perhaps to an anti-G suit, marked changes in alveolar size were produced. The alveoli at the base were very small, the apex to base ratio being 11:1, compared to 3.7:1 at $+1G_z$. The volume of the alveoli at the base of the lung was the same as the minimal volume of alveoli obtained from the pressure volume curve of an excised dog lung. Closure was not demonstrated histologically, but the fact that the units had reached their minimal volume strongly suggests that closure must have occurred. As the dog was frozen at about FRC, minimal volume (or closure) was occurring in the tidal volume range. At first sight, the curvilinearity of the alveolar size-distance relationship illustrated in fig. 4-9 is disturbingly different from the linear relationship shown with ^{133}Xe. However, the xenon technique used gave no information about the top five centimetres of lung, where most of the alinearity occurs, and the fit below this level is reasonably good.

The occurrence of closure in the tidal volume range is of critical importance in the genesis of the gas exchange failure that occurs during acceleration. Acceleration increases the blood flow to the dependent parts of the lung and decreases the blood flow above. Before closure occurs, exactly the same changes take place in the distribution of ventilation per alveolus, thus tending to make the $\dot{V}_A/\dot{Q}$ distribution more uniform. However, as soon as closure occurs, units with a very high blood flow become unventilated, or only intermittently ventilated, and with a $\dot{V}_A/\dot{Q}$ approaching zero these units act as a 'blood-shunt' (chapter 10). Conversely, there is an increase in ventilation per alveolus to the poorly perfused upper units whose $\dot{V}_A/\dot{Q}$ will approach infinity and act as an 'air-shunt'.

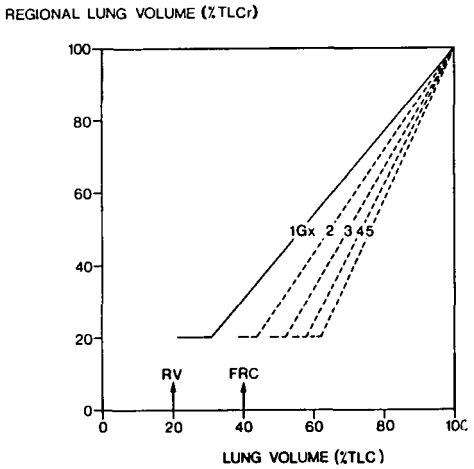

Fig. 4-10 The solid line represents the regional expansion of the dependent part of the lung from data of Kaneko ***et al*** (146). Dotted lines are extrapolations of the volume expansion at higher levels of $+G_x$ acceleration.

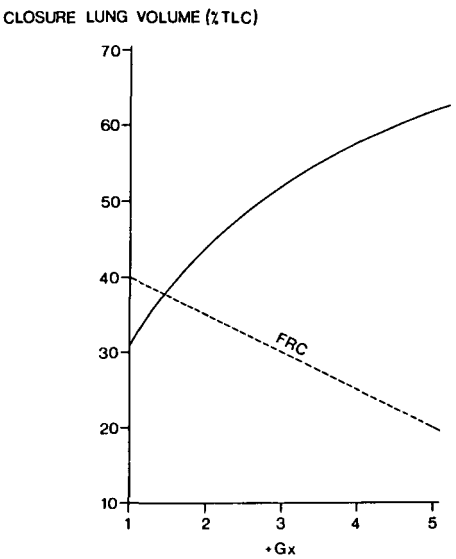

Fig. 4-11 Ordinate: predicted closure volume in the dependent part of the lung (assuming that closure occurs at 20% TLC_r) obtained from fig. 4-10. Abscissa: $+G_x$ acceleration. The dotted line indicates predicted changes in functional residual capacity.

Forward acceleration

Until recently, no data has been available on the distribution of ventilation during forward acceleration, although in many respects it is more interesting and of greater practical importance than that which occurs during headward acceleration. Gas exchange failure is hardly likely to be a limiting factor in tolerance to $+G_z$ acceleration, but it may well be limiting in prolonged exposures to $+G_x$ acceleration. It is possible to predict the order of magnitude of the changes that might occur in forward acceleration. The distribution of ventilation in the supine position appears to obey exactly the same laws as the upright distribution (146), and closure appears to occur at the same regional minimal volume. Increasing the acceleration will increase the pleural pressure gradient and, if the iso-pressure point is assumed to be in mid-thorax, it is possible to predict a new set of regional volumes. Figure 4-10 shows that the critical regional closure volume will be reached at a progressively higher lung volume as the acceleration increases. At the same time there is a progressive reduction in the functional residual capacity (chapter 2). The combination of these two effects (Fig. 4-11), closure during tidal breathing, should be more marked during $+G_x$ than during $+G_z$ acceleration.

The ^{133}Xe lung scanning technique (67) has recently been used to study the distribution of ventilation during $+G_x$ acceleration, and the results confirm the above predictions. Figure 4-12 illustrates the regional distribution of the first one and two litres of the vital capacity, as a fraction of the regional lung volume. This represents ventilation per unit lung volume for tidal breaths of one and two litres at an expiratory reserve volume of zero, and was chosen for study since the residual volume is the only stable compartment of the lung during $+G_x$ acceleration (chapter 2).

When one litre of gas is inspired from RV (Fig. 4-12 upper graph), the anterior regions of the lung receive approximately equal fractions but, even at $+1G_x$, alveoli in the most posterior two centimetres of lung are less well filled. At $+3G_x$, this effect is exaggerated and ventilation falls off over the posterior five centimetres of the lung. At $+5G_x$, ventilation decreases over the posterior seven centimetres of the lung, and no gas at all goes to the back four centimetres. Thus, at $+5G_x$, even at one litre above RV, alveoli in the most dependent four centimetres of the lung remain at their minimal lung volume. When two litres are inspired from RV, the pattern of distribution is similar (Fig. 4-12, lower graph), but the zone of diminished ventilation is smaller, and a non-ventilated region appears only at the extreme back of the lung at $+5G_x$. While the FRC was somewhat variable, at $+5G_x$ all five subjects whose results are averaged in fig. 4-12 were breathing, at rest, with an end-inspiratory lung volume within one litre of RV (average value 740 ml BTPS). In other words, these subjects were all ventilating at lung volumes below those at which the ^{133}Xe distributions were measured : even more of the lung would have been unventilated than suggested by these results.

The uniform distribution of gas going to the anterior parts of the lung seen in fig. 4-12 appears to contradict the prediction that ventilation should increase with distance down the lung, and that this effect should be enhanced by acceleration. Indeed, accelerations of +3 or $+5G_x$ appear to have little or no effect on the distribution of gas over the anterior 10 cm of lung at either lung volume studied. It must, however, be appreciated that two conflicting processes are governing regional ventilation under these conditions. With distance down the lung (from front to back), the rising pleural pressure will cause an increase in the ventilation of functioning alveoli. Against this, an increasing fraction of alveoli will remain at their minimal volume and be unventilated.

A comparison of the one litre and two litre distributions illustrated in fig. 4-12 shows that a much greater fraction of the second litre has gone to opening up units

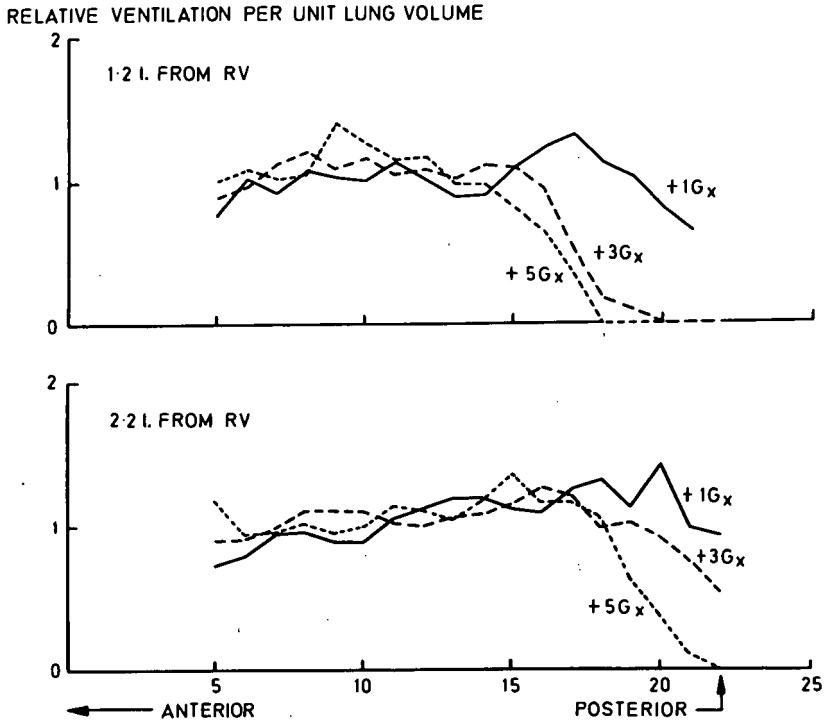

Fig. 4-12 The effect of forward acceleration on the regional distribution of the first one litre (upper graph) and two litres (lower graph) of inspirate from residual volume. Average results from five subjects.

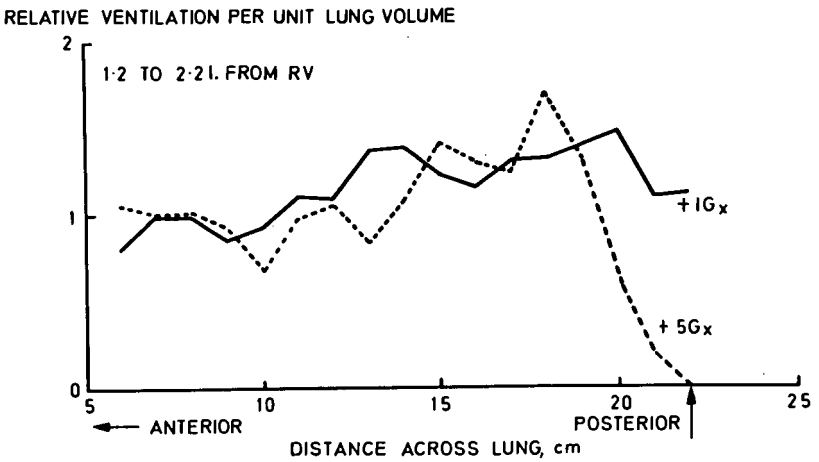

Fig. 4-13 Regional distribution of the second litre of inspirate from residual volume, plotted as in fig. 4-12. Ventilation per unit lung volume is increased in the region where alveoli are being inflated from minimal volume.

in the dependent lung, and this is illustrated in fig. 4-13. It is apparent that the distribution of ventilation during normal breathing will depend critically upon the fraction of the lung remaining at its minimal lung volume at end-expiration and end-inspiration, and this in turn will depend upon the FRC, the tidal volume and the level of acceleration. Under these conditions, it is not surprising that $+G_x$ acceleration is accompanied by a severe gas exchange failure, nor that 100 percent oxygen does not prevent this, since a shunt has been created (chapter 10).

During $-G_x$ acceleration (subject prone), the lung volume at which closure occurs will increase in approximately the same way. However, during $-G_x$ acceleration, as the inertial forces are not acting directly on the compressible anterior chest wall and abdomen, the FRC does not decrease and may even increase (243).

Therefore, one would expect much less closure during tidal breathing at equivalent levels of acceleration. This prediction is strongly supported by the slight fall in oxygen saturation seen in $-G_x$ acceleration, compared to the substantial fall seen at the same level of $+G_x$ acceleration (243), and illustrated in fig. 10-6 (p. 164).

Zero gravity

No studies of ventilation distribution have been conducted during weightlessness. However, on the basis of the hypothesis developed here, that regional differences in ventilation are primarily due to the weight of the lung, during weightlessness the distribution of ventilation should be uniform. This prediction is supported by linear extrapolation, to zero-G, of data obtained at varying levels of positive acceleration. Such extrapolations have been carried out in figs. 4-4 and 4-5.

5

The effect of acceleration on the cardiovascular system

Systemic circulation

Before considering the effects of acceleration on the pulmonary circulation, it is necessary to discuss the changes which take place within the systemic circulation, since the two systems cannot be divorced one from the other. The systemic response to acceleration is determined in the main by two factors, one physical the other physiological. The physical factor is the intravascular hydrostatic pressure gradient, and its dependence upon gravity and acceleration.

Intravascular hydrostatic-pressure gradient

In 1826, Piorry described his management of an unconscious patient who was being propped up by his comrades. He caused him to be laid flat and the patient recovered (209). Piorry concluded that blood pressure at heart level was insufficient to overcome the hydrostatic pressure gradient between heart and brain. Hill investigated the effect of posture on the distribution of blood pressure in animals, and also concluded that the changes observed were largely due to hydrostatic pressure effects (126).

At one G, a column of blood 30 cm tall (equal to the vertical distance between heart and brain in a seated or standing man) exerts at its base a pressure equal to that of a 31.8 cm column of water (the specific gravity of blood being taken as 1.06), or 23 mm Hg. At four G, this pressure will rise to 92 mm Hg. Looked at the other way, if a pressure of 115 mm Hg is applied at the bottom of a column of blood, the pressure 30 cm up will be reduced by the hydrostatic pressure gradient, to 92 mm Hg at one G and to 23 mm Hg at four G. Therefore, if the pressure delivered by the left ventricle remains constant at 115 mm Hg, at $+4G_z$ the pressure in the retinal arteries will fall to equal the intra-ocular tension (20 to 25 mm Hg), retinal blood flow will cease and loss of vision (blackout) ensue. Complete collapse of the central retinal arteries and exsanguination of the disk has been noted during acceleration induced blackout in man (162), in confirmation of the above prediction. At $+5G_z$, arterial pressure at head level will fall further to equal atmospheric pressure and, in theory, there will be no further cerebral blood flow and the subject will become unconscious. It is, therefore, difficult to carry out experiments on conscious man at levels of acceleration greater than $+5G_z$, and if vision is required, at levels greater than $+4G_z$.

Intravascular pressures at levels in the body below the heart will be increased by the hydrostatic pressure gradient, and the enormous range of pressures which exist over the height of the body, due simply to the existence of this gradient, illustrates the extreme importance of defining precisely the level at which any measurements are made. A six foot tall man, standing at $+1G_z$ and with a left ventricular pressure of 115 mm Hg, would have arterial pressures which ranged from 90 mm Hg

at the head to 230 mm Hg at the feet. At $+5G_z$, if standing were still possible, the range would be from zero millimetres of mercury at the head to 1, 275 mm Hg at the feet. Seated, the range of pressures would be somewhat less, from zero to about 500 mm Hg. Similar pressure gradients will be present in fluid filled catheters, so that recorded pressures will be referred to the level of the pressure transducer, rather than to the position of the catheter tip.

A corresponding hydrostatic pressure gradient exists within the venous system and, theoretically, arteriovenous pressure differences are constant at all levels in the body. However, if the transmural pressure at the venous end of any capillary falls below its critical closing pressure (39), then blood flow will become independent of venous back pressure. This, the waterfall effect, will be discussed in greater detail in the next chapter, in reference to blood flow through the capillaries of the upper lung (see p. 94). If the transmural pressure rises, distensible capillaries will tend to be dilated passively and their resistance to flow will fall.

While the pressure distribution predicted to occur during exposure of man to acceleration can be demonstrated under certain circumstances (i.e., within a few seconds of exposure to accelerations with a rapid rate of onset (30, 155)), with more prolonged exposures the pressures are modified by physiological factors. Firstly, the pressure developed by the left ventricle does not remain constant during prolonged exposure to positive acceleration, but the level of constant pressure (or of 'hydrostatic indifference') is rather higher up the body, at about the level of the second or third rib anteriorly. The situation is complicated by the fact that the heart and diaphragm drop significantly during exposure to positive acceleration, and the level of hydrostatic indifference should be referred to a fixed point in the vascular system, rather than to a fixed bony landmark.

Circulating blood volume

Secondly, prolonged exposure to positive acceleration causes pooling of blood in the dependent limbs, and possibly also in splanchnic vessels and in the lower lung. It leads also to the filtration of fluid from blood into tissues in regions where transmural pressures are high. Both processes result in a reduction in the volume of circulating fluid. Plethysmography of the calf carried out during exposure of man to accelerations of up to $+5G_z$ (133) showed that the increase in the volume of this segment took place in two phases, a rapid phase due to pooling, and a slow phase attributable to filtration. The overall changes found were, however, small (estimated at 50 ml/G), though greater than those recorded by Lambert (154) - 60 ml after 25 seconds at $+5G_z$. Using the teeter board technique, Garrow (unpublished observation) estimated that, after five minutes exposure to $+2G_z$, 250 ml of blood had been displaced from the upper body to the legs, a figure more in keeping with predictions based upon the effects of posture and cuffing on the distribution of blood volume (7, 123).

Filtration losses can be estimated from changes in haematocrit, and by this means a 3. 6 percent reduction in the effective blood volume was found after five minutes exposure to $+3.5G_z$. This loss increased to 4. 5 percent when the level of acceleration was raised to $+4G_z$ (49), a figure which represents an effective blood loss of 270 ml. The effect may be more pronounced in the dog, where a 20 to 25 percent loss in effective blood volume has been reported following a five minute exposure to 6. 2G (157).

Reflex regulation

A third factor which modifies the circulatory response to acceleration is reflex regulation originating from receptors in the aortic arch and carotid bifurcation. These baroreceptor reflexes function to maintain pressures constant. If acceleration is applied rapidly, at rates of one G per second or more, these reflexes are initially inoperative, with an immediate fall in systemic blood pressures throughout the upper part of the body, greatest within five to ten seconds of attaining peak

acceleration. Then, as compensatory reflexes become effective, pressures recover and may be in excess of those predicted on the basis of simple hydrostatic pressure changes. Finally, compensation may fail due to the continuing loss of circulating blood volume, whereupon the recorded pressures will fall again, either gradually or catastrophically, with classical vaso-vagal slowing of the heart and loss of consciousness. These changes in blood pressure also occur in anaesthetised dogs, and examples may be seen in fig. 4-14 and 4-20. A secondary fall in pressure is illustrated in fig. 10-16 (p.176).

The degree of reflex circulatory compensation which occurs during exposure to positive acceleration may be gauged from changes in peripheral vascular resistance. Forearm blood flow undergoes a considerable reduction at $+3G_z$ (134), and studies using the rate of clearance of radioactive xenon have shown that muscle blood flow may become unrecordable at this level of positive acceleration. In both studies, changes in perfusion pressure were minimised by supporting the arm at heart level. Wood and co-workers (273) found that the total peripheral resistance rose by an average of 40 percent in five subjects during steady-state conditions at $+3G_z$. Recent studies on the distribution of the cardiac output made in dogs during exposure to positive acceleration, using radioactive rubidium (the technique of Sapirstein (236)) have shown significant reductions in kidney, liver and gut blood flows in individual animals at $+4G_z$; though myocardial blood flow was consistently well maintained (106). In one animal, renal blood flow was reduced to only 7 percent of its control value, and this despite a rise in perfusion pressure estimated at 30 mm Hg. These figures suggest that a considerable degree of circulatory adjustment may occur in internal organs during exposure to positive acceleration, as well as in skin and muscle.

Cardiac output

Of more immediate relevance to the pulmonary circulation are changes in cardiac output, since these will be reflected almost immediately by similar alterations in pulmonary blood flow. Changes in cardiac output have been shown to alter the distribution of blood flow within the lungs (267). Unfortunately, few measurements have been made in man during exposure to positive acceleration. Howard (132) determined the cardiac output in two subjects on the R.A.F. centrifuge using the direct Fick technique, and found reductions of 32 percent at $+1.73G_z$ and of 40 percent at $+2.18G_z$, compared to the $+1G_x$ resting position (the maintained $+1G_x$ vector gave resultant accelerations of two G and 2.4G at angles of 30°and 25°from the true G_z axis). Wood and co-workers used the dye dilution technique, and found reductions of seven, 18 and 22 percent at +2, +3 and $+4G_z$ respectively, the measurements being made 20 to 40 seconds after the onset of peak acceleration (273). Rosenhamer (228) also used dye dilution in his extensive studies of the effects of $+3G_z$ acceleration on resting and exercising subjects, and found a 24 percent reduction at rest, and rather lesser reductions, 16 and 13.5 percent, at two levels of exercise (300 and 600 kpm/min respectively).

In dogs, changes in cardiac output appear to be more pronounced, and this may be related to the fact that maintained positive acceleration is outside a dog's normal experience. At +3 to $+4G_z$, the cardiac output of anaesthetised dogs was reduced by 52 percent even in centrifuge runs with a very low rate of onset of acceleration (acceleration increasing by one G every 15 seconds), and after one minute at plateau acceleration (124). The decrease in cardiac output resulted from a 65 percent reduction in stroke volume incompletely compensated by an increase in heart rate. The peripheral resistance rose by an average value of 70 percent. We have observed virtually identical values in dogs at $+4.2G_z$, again after one minute at peak acceleration, cardiac output being reduced by 54 percent and the total peripheral resistance rising by 67 percent (106).

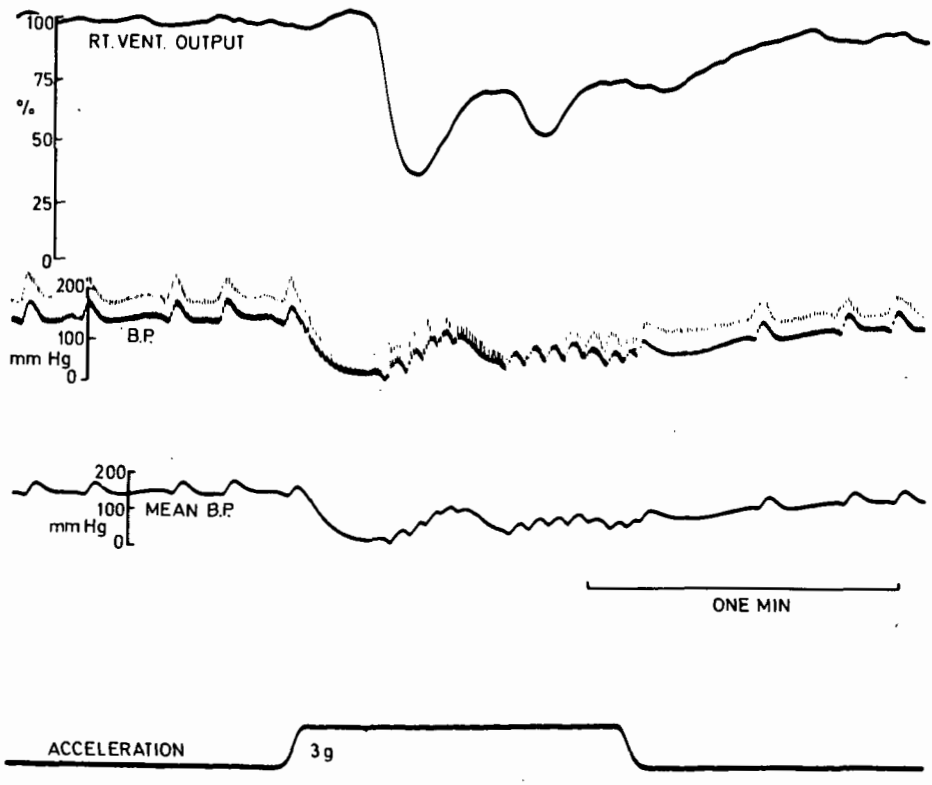

Fig. 5-1 Output of the right ventricle recorded during exposure of an anaesthetised dog to an acceleration of $+3G_z$ for one minute. Blood pressure was monitored from a catheter in the abdominal aorta with a transducer mounted at the level of the left ventricle. There is a close correlation between cardiac output and pressure, the lag in output changes being caused by the technique of measurement employed (see text). (From (104), by courtesy of Aerospace Med.).

All the determinations referred to above were carried out under reasonably steady-state conditions (i.e., during or after several minutes of sustained acceleration), but arguing from the transient changes in systemic blood pressure which take place immediately after the onset of acceleration exposure, grosser fluctuations in cardiac output would be expected within the first 30 to 45 seconds. In order to investigate these acute changes, a modification of the constant-infusion indicator-dilution technique was developed to furnish a second by second index of changes in the output of the right ventricle. The technique has been used in dogs exposed to positive acceleration on the R.A.F. centrifuge and is as follows.

Normal saline containing radioactive xenon gas (^{133}Xe) in solution is infused at a constant rate (40 ml over seven minutes in dogs weighing 13 to 25 kg) into the right atrium and sampled, also at a constant rate (one millilitre per second), from the pulmonary artery. The radioactivity of the pulmonary arterial blood is determined by passing it through a coil in a well scintillation detector. The output of the associated ratemeter (using a time-constant of one second) is recorded on magnetic tape together with systemic blood pressure and a signal indicating the position of the infusion pump syringe barrel. Since the major fraction (90 to 95 percent) of the injected isotope is cleared by the lungs on its first passage through the pulmonary circulation (210), recirculation of the indicator is not a great problem, and may be ignored. The recorded count rate is therefore inversely proportional to the quantity of blood with which the injected isotope was mixed, and this is the same as the output of the right ventricle. The recorded count rate is played back through an analogue computer and its reciprocal, taking the immediate pre-acceleration count rate as unity, re-recorded together with systemic blood pressure.

Figure 5-1 illustrates the effect of exposing an anaesthetised dog to an acceleration of $+3G_z$ lasting for one minute. As can be seen, there is a dramatic fall in the output of the right ventricle to 36 percent of its pre-acceleration value, and this fall commences within a few seconds of attaining peak acceleration (allowing 10 seconds as the time taken for injected ^{133}Xe to reach the scintillation detector). Thereafter, the output closely follows the changes in systemic blood pressure, and a secondary fall is seen in both traces. By the end of the period of acceleration, the output of the right ventricle has recovered to a relatively stable 75 percent of its pre-acceleration value. On return to normal gravity, recovery is complete within 25 seconds. In other animals, recovery was considerably faster than this, and took place with a time course which mirrored the initial fall. In some animals, recovery was accompanied by an overshoot to 110 to 115 percent of the pre-acceleration output, and this overshoot lasted approximately 10 seconds. During more severe acceleration exposures ($+5G_z$ for one minute), right ventricular outputs as low as 18 percent of the pre-acceleration control value were seen, either early in the run, or after 30 to 45 seconds of sustained acceleration. It is interesting to compare the lability shown by the output of the right ventricle with the stability of the recorded pulmonary arterial pressure (i.e., fig. 5-7), and this paradox will be considered later.

The rapidity with which the right ventricular output can change in the dog suggests that in man, measurements of cardiac output could not be made using the Fick principle, or even dye-dilution, within the first minute of acceleration exposure. However, Wood and his colleagues (273) carried out repeated dye injections in man during exposure to accelerations of +2, +3 and $+3.5G_z$, lasting for up to 10 minutes, and found that the later results did not differ significantly from measurements made within the first 20 to 40 seconds. Thus, after three to 10 minutes at $+3G_z$, the cardiac output fell by an average value of 17 percent, a figure almost identical to the 18 percent reduction found in the 20 to 40 second period. They suggested that the results might have been very different had the determinations been carried out within the first 15 seconds of exposure to acceleration "before the initial compensatory cardiovascular response to the stress..... had been completed". It is obviously essential that any measurements of the distribution of pulmonary

blood flow should be carried out taking into account the possibility of early transients in total flow, and ideally at least one minute should be allowed to achieve relative stability. The similarity seen between the systemic blood pressure response and the output of the right ventricle (i.e., fig 5-1), and that between the systemic blood pressure response to acceleration of dog and man, suggests that similar changes in output do occur in man, and that the extent and time course of these changes may be inferred from the recorded blood pressure.

Forward acceleration

From the foregoing discussion on the effects of positive acceleration on the circulation, and the important role of hydrostatic pressure gradients, it would be expected that forward accelerations would have a far less pronounced effect. This is indeed the case, with the exception that cardiac arrhythmias appear to be more common during human exposure to $+G_x$ acceleration (255), the commonest arrhythmia seen being premature contraction arising from either the atrium or ventricle. One subject developed paroxysmal atrial tachycardia at $+10.5G_x$, though a similar arrhythmia was noted during passive head-down tilting in this subject. It was concluded that arrhythmias were associated with over-distension of the right atrium.

With the body supine, hydrostatic pressure gradients are small and the vertical heart-brain pressure gradient is abolished. Blackout does not occur. However, in the attitude which gives least respiratory embarrassment (see chapter 2), that is with hips and knees flexed to 90°and the back raised 25°from the horizontal, a $+G_z$ component is introduced and vision is lost at about 10G (17, 48): subjects become unconscious at 14 to 16G (17). When the back angle is reduced to 10°, blackout threshold is raised to 16G and unconsciousness is not lost until an acceleration of some 20G is imposed (17).

Changes in heart rate are rather variable and appear to depend critically upon the exact posture adopted. Bradycardia may occur when the spine is truly at right angles to the applied acceleration (71, 156), whereas tachycardia is the rule when the trunk is inclined forwards and a $+G_z$ component introduced. Heart rates seen during exposure to forward acceleration may also be affected by the attitude of the head (247), presumably because of altered hydrostatic pressure differences between the heart and the carotid baroreceptors.

Changes in cardiac output are small during exposure to forward acceleration, the output at $+5G_x$ under steady-state conditions increasing by from 11 to 34 percent in five subjects. This apparent lack of circulatory stress was confirmed by measurements of total peripheral vascular resistance, which rose by a mere two to six percent during exposure to an acceleration of $+3.5G_x$, lasting for up to 10 minutes, and by an average of 14 percent during the first three minutes of exposure to $+5G_x$ (273).

Mean aortic pressure, referred to the level of the third intercostal space at the sternum, was found to rise progressively with increasing levels of forward acceleration, and averaged 135 mm Hg at $+5G_x$, an increase of 27 mm Hg above the control value (273). More striking were large increases in right atrial pressure, which in one subject rose to 32 mm Hg at $+3.5G_x$, and in five subjects averaged 23 mm Hg at $+5G_x$: with prolonged exposures these pressures tended to decline. Nolan and co-workers found similar high values of right atrial pressure (32 mm Hg $+5.3G_x$), and stressed the importance of defining precisely the level to which such pressures should be referred (194). They used the midpoint of the antero-posterior dimension of the thorax measured at the third intercostal space at the sternum, and considered that the tricuspid valve lay close to this point. In the dog, during changes in posture, the zero reference point appears to lie within the right ventricle (117). The difference would not be significant, however, except in studies on lateral acceleration ($+G_y$ or $-G_y$). A similar rise in right atrial pressure was predicted from a measurement

made within the superior vena cava, at which point the pressure rose by 20 mm Hg at $+6G_x$. However, the same human subject showed only a minimal increase in pressure at this point when exposed to an acceleration of $-6G_x$ (242). While neither right ventricular nor pulmonary arterial pressures have been recorded during exposure of man to forward acceleration, the raised right atrial pressures referred to above do suggest that pulmonary vascular pressures may be high, a point of interest in relation to the distribution of the pulmonary blood flow (see chapter 7).

Dogs also appear able to tolerate forward accelerations well, and as in man, changes in cardiac output are small. Steiner and co-workers found that exposure of anaesthetised dogs to accelerations lasting from five to ten minutes led to a 14 percent decrease in output at $+6G_x$, and to a 23 percent decrease at both +10 and $+14G_x$ (250). The decrease at the two higher levels of acceleration was statistically significant, even though it lay within the range of normal variation found in resting dogs. The decreases were caused by a reduction in heart rate, the stroke volume remaining virtually unchanged. No progressive changes in output were observed with respect to time, but it was not stated how early in the exposure to acceleration the first determination had been made. Rather greater changes were reported by Sandler, the cardiac output falling by 20 percent at $+5G_x$, by 30 percent at $+10G_x$, and by 37 percent at $+15G_x$ (235). At lower levels of acceleration, the cardiac output may rise as in man, and at +4 to $+6G_x$, a 12 percent increase in output has been reported (124), associated with a 26 percent decrease in total peripheral resistance.

As in man, aortic pressures in the dog rise steadily with increasing levels of acceleration, the rise in systolic pressure averaging 16 percent at $+5G_x$ and 25 percent at $15G_x$ (235). Pressures on the right side of the heart are also increased, mean right atrial pressures rising from control values of zero and three millimetres of mercury in two dogs, to 23 and 23.5 mm Hg at an acceleration of $+15G_x$. In one dog, the systolic pressure recorded in the right ventricle rose to 62 mm Hg at $+10G_x$, though values of about half this were recorded in two other animals at the same level of acceleration (234).

Pulmonary circulation

Owing to the paucity of information concerning normal pulmonary arterial pressures in seated man (most observations being carried out during cardiac catheterisations on supine subjects), measurements were made in a number of normal men, both at rest as well as during exposure to positive acceleration (103). Catheterisations were carried out with the subjects supine, and pressures were subsequently monitored with the subjects seated in the centrifuge gondola, using a strain gauge pressure transducer. Accelerations were applied with an onset rate of one G per second, to plateaux of +2 to $+3G_z$, and were maintained for 45 to 60 seconds. Pressures were referred to the level of the pulmonary trunk as determined by fluoroscopy.

Figure 5-2 shows a recording made during a centrifuge run to $+2.4G_z$. There is an immediate fall in mean pulmonary arterial pressure of 10 cm water (more clearly seen in the damped pressure trace), and this fall is maintained throughout the period of acceleration. The pulse pressure also falls with the onset of acceleration, but tends to recovery gradually towards its control value. It is probable that this recovery represents a return of the right ventricular output towards its control value, following a more severe reduction with the onset of acceleration (see fig. 5-1). The heart rate is increased by acceleration (from 80/min to 96/min) and remains high. With return to normal gravity there is a pronounced overshoot in the pulmonary arterial pressure, and this is followed by a period of bradycardia, with a more gradual return of pressure to its control value. In other subjects, the initial fall in pulmonary arterial pressure was greater, then recovered to a new level which was still below the control value. The immediate post-acceleration changes are shown

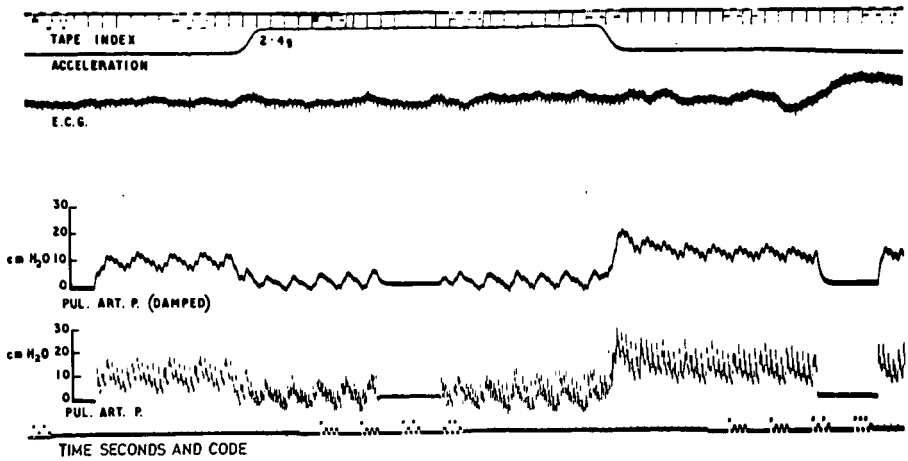

Fig. 5-2 Recording showing response of a human subject to +2.4G_z acceleration. From above, downwards, the traces record tape index, imposed acceleration, electrocardiogram, damped and undamped pulmonary arterial pressures and time. Pressures are referred to the level of the pulmonary trunk, and zero pressure calibrations have been inserted during the course of the run.

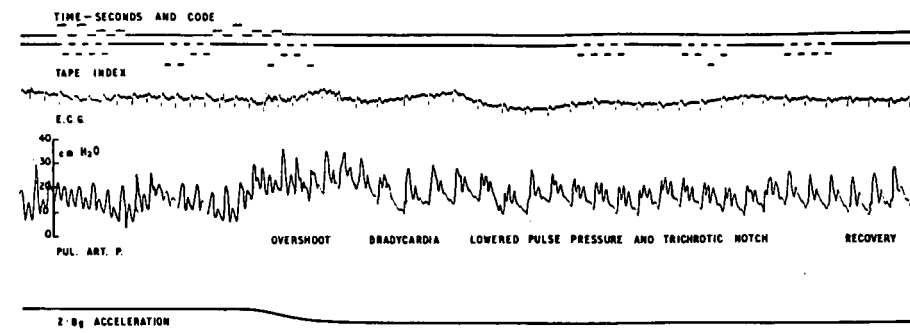

Fig. 5-3 Recording showing the period of recovery following one minute at an acceleration of +2.8G_z. From above, downwards, the traces record time, tape index, electrocardiogram, pulmonary arterial pressure referred to a level eight centimetres below the pulmonary trunk, and imposed acceleration.

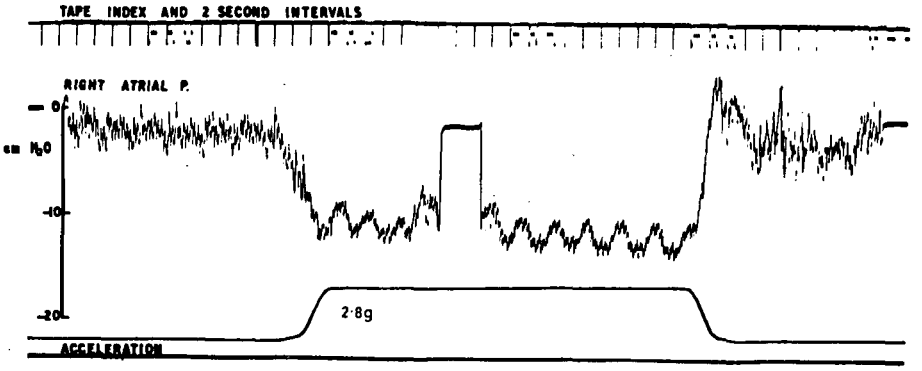

Fig. 5-4 Recording of right atrial pressure during a 40 second exposure to an acceleration of $+2.8G_z$. Pressure is referred to the level of the pulmonary trunk. Note the overshoot which follows return to one G.

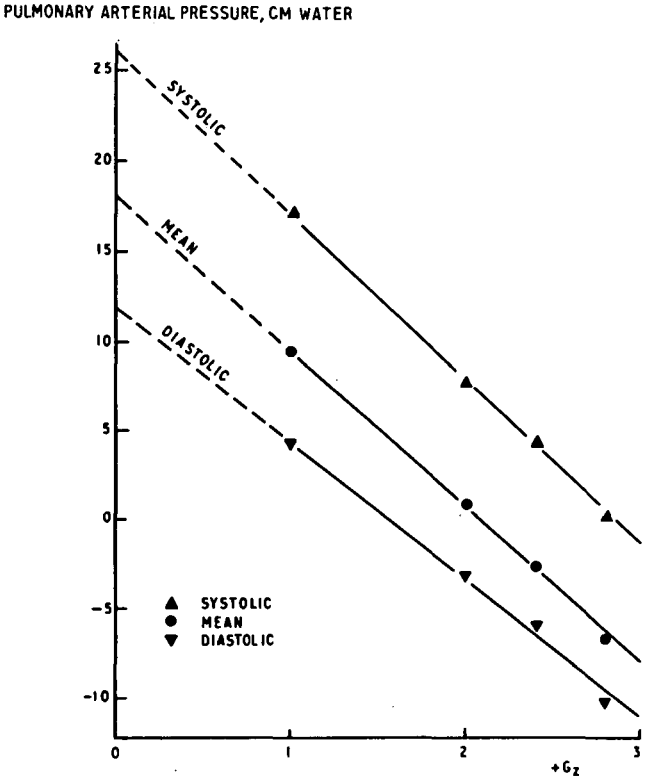

Fig. 5-5 The effect of positive acceleration on systolic, mean and diastolic pulmonary arterial pressures recorded as shown in fig. 5-2. Pressures were measured during the second half of one minute centrifuge runs. Lines are extrapolated back to zero G, to indicate the pressures expected to occur throughout the pulmonary arterial bed during weightlessness.
(From (103), by courtesy of Proc. R. Soc.).

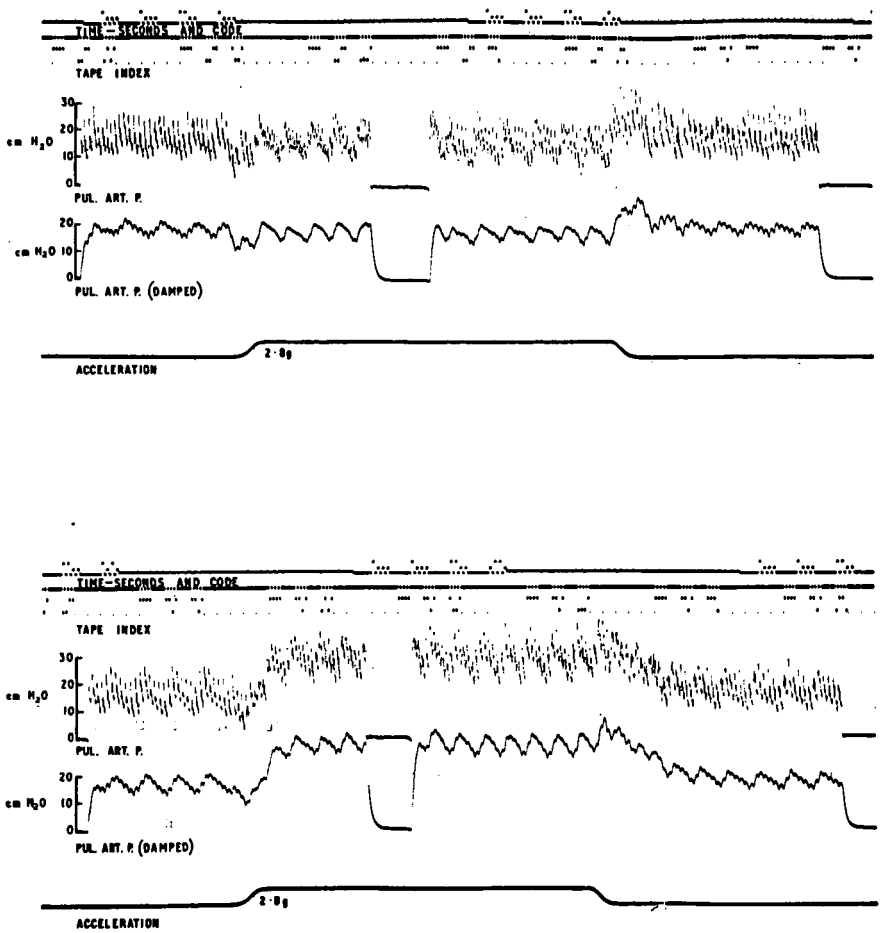

Fig. 5-6 Upper recording. Effect of +2.8G_z acceleration lasting for one minute on undamped and damped pulmonary arterial pressures. The lower record is identical except that the subject wore an anti-G suit. Pressures are referred to a level eight centimetres below the pulmonary trunk.

more clearly in fig. 5-3, which is a recording of the end of a $+2.8G_z$ centrifuge run (illustrated in full in fig. 5-6). In this recording the pressure transducer was mounted eight centimetres below the pulmonary trunk. The period of bradycardia is clearly seen to follow the overshoot in pulmonary arterial pressure, and represents a slowing of the heart in response to the sudden increase in venous return, as blood pooled in the lower limbs returns to the heart. A similar overshoot may be seen in pressures recorded from the right atrium, and a recording is illustrated in fig. 5-4. Respiratory pressure swings (pressure falling with inspiration) are apparent in all recordings from the pulmonary artery or right atrium, and tend to become more pronounced during acceleration.

At $+1G_z$, the mean pulmonary arterial pressure with the subjects at rest and seated upright, averaged 9.5 cm water (7.0 mm Hg) in four subjects. The corresponding systolic and diastolic pressures were 17.2 cm water (12.6 mm Hg) and 4.3 cm water (3.2 mm Hg) respectively. These pressures fell linearly with positive acceleration as illustrated in fig. 5-5, so that at $+2.8G_z$, the mean pressure at the level of the pulmonary trunk averaged 10 cm water below atmospheric pressure. With increasing acceleration, from +1 to $+2.8G_z$, all pressures fell at a rate of about eight centimetres of water per G. At a level eight centimetres farther down the lung the pressures would have been unaffected by acceleration, since at this lower level the recorded fall would be exactly balanced by the increase in hydrostatic pressure. Figure 5-6 was obtained with the pressure transducer mounted at this lower level during an exposure to $+2.8G_z$, and only the transient pressure changes are seen.

However, since the subjects were forced down in their seats to the extent of one to two centimetres per G, and the transducer was mounted rigidly in the gondola, these observations place the level of constant pressure (or hydrostatic indifference) too low, and the best estimate is that this level lies five centimetres below the pulmonary trunk. At this level, the mean pulmonary arterial pressure averaged 14.5 cm water (10.7 mm Hg), and was unaffected by positive acceleration, at least up to $+3G_z$. Taking the vertical height of a human lung to be 25cm and placing the lung hilum 10 cm from the base, mean pulmonary arterial pressure would vary from 20 cm water at the base to minus five centimetres of water at the apex at $+1G_z$, and from 30 cm water at the base to -45 cm water at the apex at $+3G_z$. The significance of these pressure distributions in relation to the distribution of the pulmonary arterial blood flow will be discussed in chapters 6 and 7.

Pulmonary arterial pressures recorded in seated subjects at rest are considerably lower than those reported in the literature for supine subjects, where an average value of 19 cm water (14 mm Hg) was obtained from 68 published determinations. The discrepancy is explicable on the basis of posture since in the erect position the pulmonary trunk will come to lie above the hydrostatic indifference plane, and the recorded pressure will fall. The present results agree well with others obtained in seated men (26), when corrections are made for the respective pressure reference levels.

The effect of the inflation of an anti-G suit on pulmonary arterial pressure is also illustrated in fig. 5-6. Systolic and diastolic pressures at the level of hydrostatic indifference are raised by some 13 cm water, during a centrifuge run at $+3G_z$; this may be compared to the effect of the identical run made without anti-G suit protection, where these pressures remain unchanged. A further comparison, made in another subject at $+2.4G_z$, showed that the mean pulmonary arterial pressure was raised by 11 cm water when the anti-G suit was inflated. Most of this increase in pressure is explicable in simple mechanical terms, since the diaphragm and mediastinum are displaced upwards by inflation of the abdominal portion of the suit (see chapter 2). A realistic figure for this displacement would be three centimetres at $+3G_z$. With a hydrostatic pressure gradient of three centimetres of water per centi-

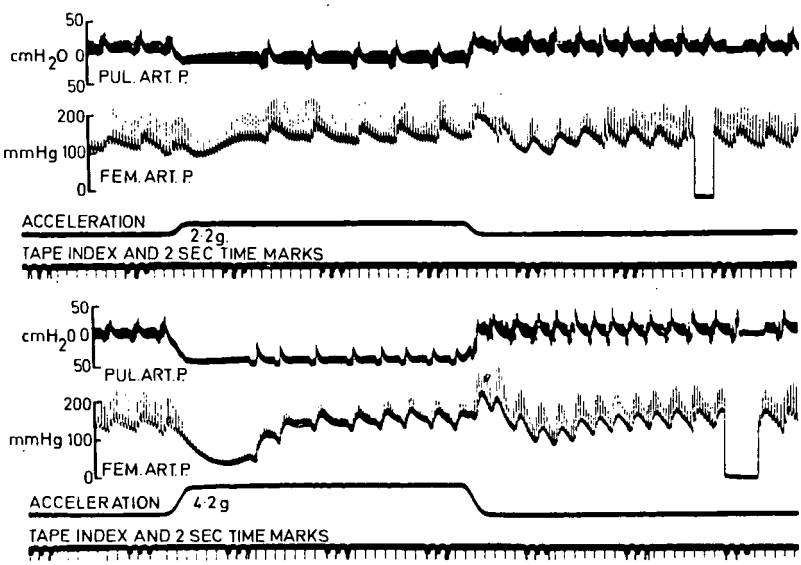

Fig. 5-7 Recordings of pulmonary arterial pressure (Pul. Art. P.) and femoral arterial pressure (Fem. Art. P.), during exposure of an anaesthetised dog to positive acceleration of 2. 2G and 4. 2G, each run lasting for one minute. Pulmonary arterial pressure is referred to the level of the pulmonary trunk, and femoral arterial pressure to the level of the left ventricle.
(From (104), by courtesy of Aerospace Med.).

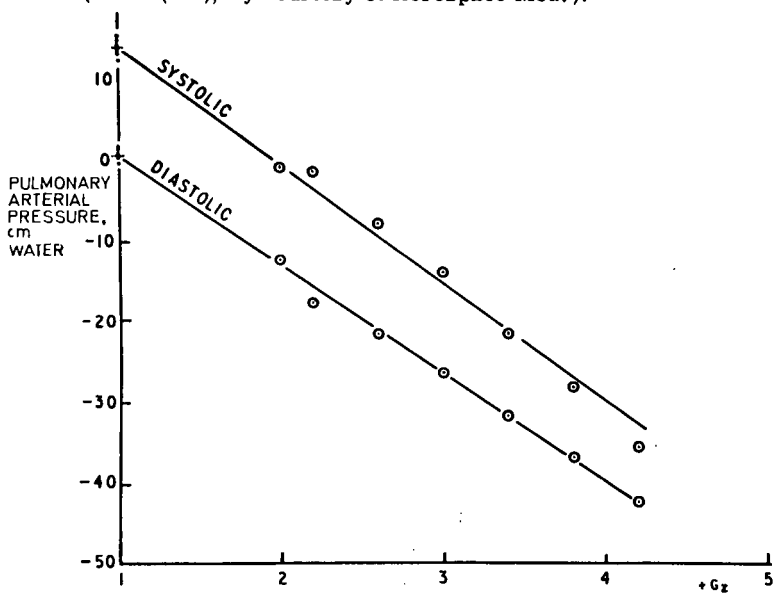

Fig. 5-8 The effect of positive acceleration on systolic and diastolic pulmonary arterial pressures in the dog, recorded as shown in fig. 5-7. Control pressures were measured prior to each centrifuge run, and average values are indicated by short horizontal lines.

metre, the pressure recorded by a fixed pressure transducer should go up by nine centimetres of water.

Pulmonary arterial pressures have also been studied in dogs during exposure to positive acceleration, with results very similar to those just described for man. Figure 5-7 illustrates recordings of pulmonary arterial and femoral arterial pressures obtained from an anaesthetised, spontaneously breathing greyhound, during exposures to +2.2 and +4.2G_z lasting for one minute. The femoral arterial pressure is referred to the level of the left ventricle, and shows an initial drop with the onset of acceleration, followed by recovery as compensatory reflexes become effective. The pressure finally stabilises at a level slightly above the control value. Changes in pulmonary arterial pressure contrast markedly with pressures recorded in the systemic circulation, and appear to mirror the applied acceleration with no evidence of any compensatory adjustment. Indeed, the only change apparent throughout the duration of the acceleration stress is a widening of the pulse amplitude. This corresponds to the rise in systemic pressure, and is presumably related to a recovery in cardiac output and to an increase in total pulmonary blood flow. Following return to normal gravity, the pressure overshoot is minimal, and this again contrasts with the changes recorded in systemic blood pressure. It appears that effective vasomotor changes must be lacking in the pulmonary circulation, and large changes in cardiac output (as illustrated in fig. 5-1) may be accommodated with little or no change in mean pulmonary arterial pressure. A possible explanation for this observation is that the pulmonary vascular bed is not filled under resting conditions (see chapter 6), and a small rise in pressure can open up further capillaries so that the total vascular resistance of the lung will fall.

The effect of acceleration on systolic and diastolic pulmonary arterial pressures is illustrated for one dog in fig. 5-8. As in man (Fig. 5-5), pressures fall linearly with increasing positive acceleration: the hydrostatic indifference plane lies 4.5 cm below the pulmonary trunk. Body displacement during acceleration should be less of a problem than in human recordings (see p.79) owing to the restraint used in the centrifuge gondola, and the recorded level of hydrostatic indifference will not be subject to the same error.

The rise in right atrial pressure already referred to during exposure of man and dog to forward (+G_x) acceleration, suggests a corresponding rise in pulmonary arterial pressure, and the probability is that the hydrostatic indifference point lies fairly far anterior in the chest. It is possible that, despite the smaller antero-posterior dimensions of the lung, vascular pressures in the dependent lung may be greater during exposure to +G_x than to +G_z acceleration. This leads to the possibilities of oedema formation and of a more uniform distribution of blood flow during +G_x acceleration, and these points will be taken up in chapters 8 and 7 respectively.

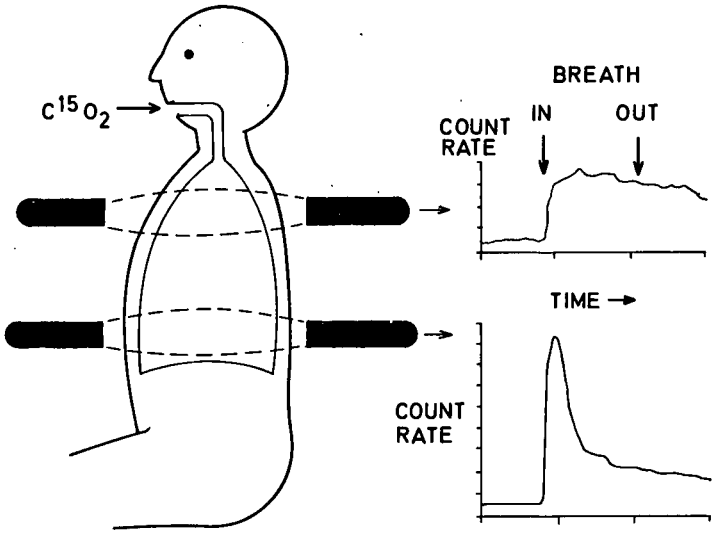

Fig. 6-1a Technique for measuring regional distribution of pulmonary blood flow and ventilation using radioactive oxygen-labelled carbon dioxide. The subject takes a single breath of this gas and the increase in counting rate reflects regional ventilation, while the 'clearance rate' of the radioactive gas during breath-holding measures regional blood flow. (By courtesy of Brit. Med. Bull.).

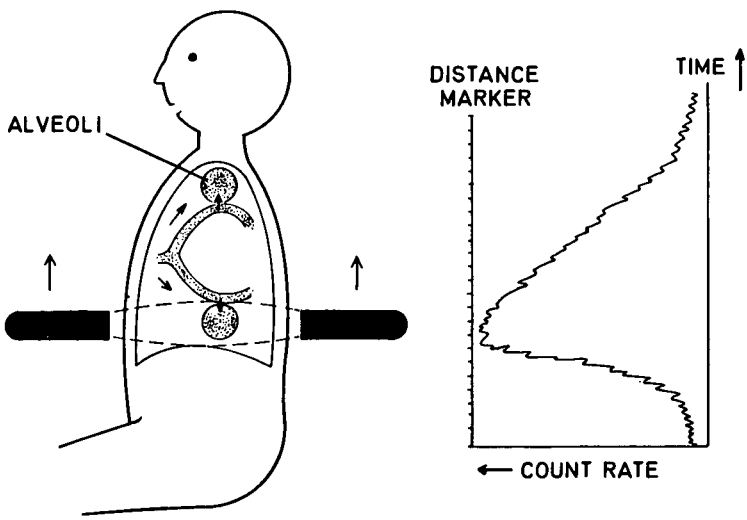

b. Technique for measuring regional blood flow using radioactive xenon. The gas is dissolved in saline and injected into a peripheral vein. When it reaches the lung it is evolved into alveolar gas and the lung is scanned from bottom to top by two opposed counters while the subject holds his breath.

6

Regional distribution of blood flow

J. B. WEST

Until 10 years ago, little attention was paid to the uneven distribution of blood flow in the lung. Although the German pathologist, Johannes Orth (198) was aware as long ago as 1887 that the weight of the column of blood in the lungs might affect its distribution, textbooks of physiology published in the 1950's generally ignored the subject. Now we know that there is a striking inequality of blood flow down the upright lung, that the pattern of distribution can be predicted from the various intrathoracic pressures, and that under some conditions (notably exposure to high levels of acceleration - see chapters 9 and 10), the uneven distribution of blood flow can seriously impair pulmonary gas exchange. The rapid increase in our knowledge began with the introduction of radioactive gas techniques and these will be described briefly first.

Methods

The first method (267) which was used to measure regional blood flow is shown in fig. 6-1a. The subject is seated and pairs of scintillation counters are arranged over upper and lower zones of the lung. He takes a single breath of air containing carbon dioxide labelled with oxygen-15, and holds his breath for some 15 seconds. When the radioactive gas enters the counting field, there is an increase in counting rate which depends on the regional ventilation of the lung and its volume. During the subsequent breath-holding period, radioactivity can only be removed by the blood flow, so that the slope of the tracing, or 'clearance rate', is taken as a measure of regional perfusion.

This technique is simple for the patient, but complicated for the investigator, since oxygen-15 has a half-life of only two minutes and must therefore be prepared on a nearby cyclotron. A more convenient method, which is now used in many laboratories throughout the world, is shown in fig. 6-1. This time the relatively insoluble xenon-133 is used (11). The gas is dissolved in saline and injected into a peripheral vein. When it reaches the lung, it is evolved into alveolar gas because of its low solubility, and it remains there during a short breath-holding period. The distribution of intrapulmonary radioactivity can then be detected by multiple external counters, by scanning each lung from bottom to top with a pair of counters, or by the use of a radiation camera. The most informative technique at the present time is that which makes use of moving counters. The scan so obtained is then compared with another made after mixing xenon uniformly throughout the alveolar gas by rebreathing. In this way, blood flow per unit alveolar volume is derived.

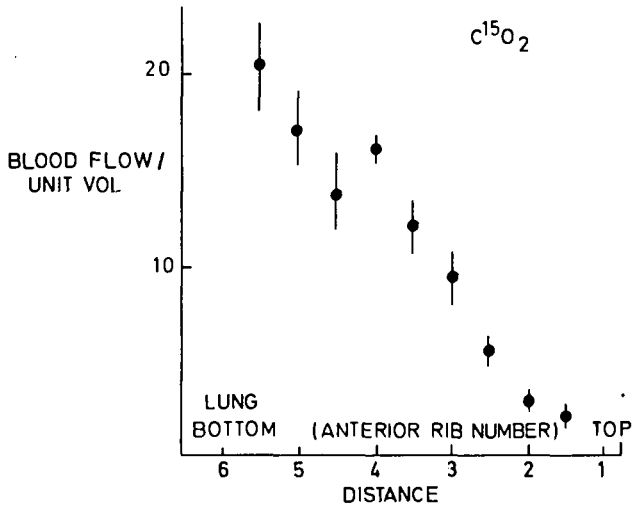

Fig. 6-2 Normal distribution of blood flow in the upright human lung as measured with radioactive carbon dioxide in 16 normal volunteers. Means and standard errors. Note the steady decrease in flow from bottom to top of the lung: flow is almost nil at the apex.
(From (266), by courtesy of J. nucl. Biol. Med.).

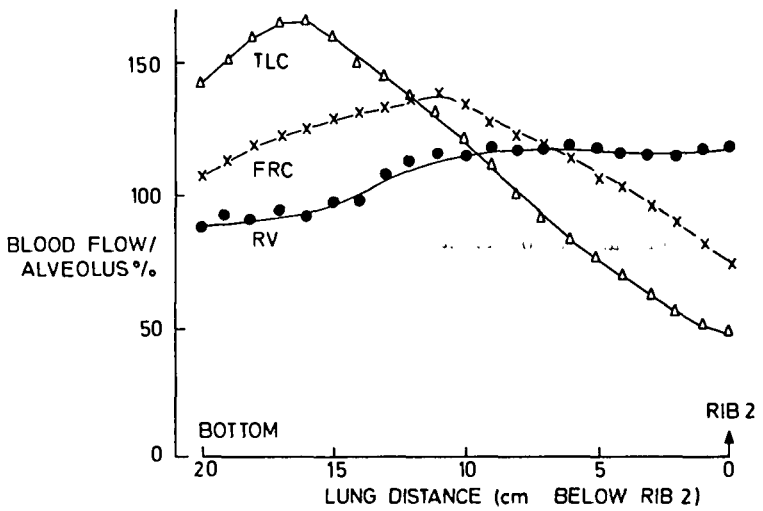

Fig. 6-3 Blood flow per alveolus (as a percentage of that expected if aveoli are perfused equally) plotted against distance down the lung at three lung volumes - total lung capacity (TLC), functional residual capacity (FRC) and residual volume (RV). Points represent the mean values for the right and left lungs of all subjects studied at the volume. Note the reduction of basal blood flow which is more marked at lower lung volumes.
(From (136), by courtesy of Resp. Physiol.).

Normal distribution of blood flow

In the upright lung

Figure 6-2 shows the distribution of blood flow in the normal upright lung (267). These results were obtained from 16 normal volunteers (staff members) using oxygen-15 labelled carbon dioxide as described above. One litre of the gas was inspired from functional residual capacity and the breath was held for about 15 seconds. The mean values with their standard errors are shown for the pooled results of both lungs at nine levels, based on the rib positions in the mid-clavicular line.

It can be seen that blood flow decreases, more or less steadily, from the bottom of the top of the upright lung, reaching low values at the apex. This general pattern has been confirmed using radioactive xenon (11) and also with the radioactive macro-aggregated albumin technique (258).

Effect of changing lung volume

Recently, Hughes and his colleagues (136) have examined the effect of changing lung volume on the distribution of blood flow. The method of Anthonison and Milic-Emili was used to obtain blood flow per alveolus (5). In brief, the ^{133}Xe solution was injected at the lung volume to be studied, and after the counting rate over the lung was steady, the subject inhaled to total lung capacity and the lungs were scanned. The equilibration scans were also made at TLC. The results were expressed in terms of an index which would be 100 percent at each level if blood flow per alveolus were uniform throughout the lung. This method depends on the fact that, at TLC, all alveoli are thought to be the same size (see later).

Figure 6-2 shows the pooled results obtained from nine subjects. It can be seen that, at TLC, blood flow increases down the lung over most of the vertical height, the pattern being similar to that seen in fig. 6-1. However, a small area of reduced blood flow can be seen at the base, and this reduction is statistically significant. At smaller lung volumes, this zone of reduced blood flow extends further up the lung. At functional residual capacity, blood flow begins to decrease four centimetres above the dome of the diaphragm, or about eight centimetres above the very bottom of the lung. At the lung base, blood flow is reduced by some 30 percent, compared with its maximum value at this lung volume. At residual volume, this zone of reduced blood flow has extended right up the lung and now apical flow exceeds basal flow. Thus, the normal gradient in the upright lung has been inverted.

Effects of posture and exercise

In addition to changes in lung volume, other physiological factors affect the normal distribution of blood flow. Figure 6-3 shows that, in the supine position, apical blood flow increases until it becomes very similar to basal blood flow (267). Indeed, Bryan and his colleagues (34) found that blood flow per unit lung volume at the base exceeds that at the apex by some 20 percent, and they attributed this to the downward tilt of the lung caused by the buttocks when a subject lies on a flat table. In the inverted posture, perfusion at the apex of the lung exceeds that at the base (65, 102).

Although apical and basal blood flows become almost the same in the supine posture, the perfusion of the dependent zones exceeds that of the uppermost regions of the lung. This is also true of the left and right lateral, and prone positions (146). However, if account is taken of the differences in regional expansion of the lung which normally exist, and blood flow is expressed as per alveolus, the vertical

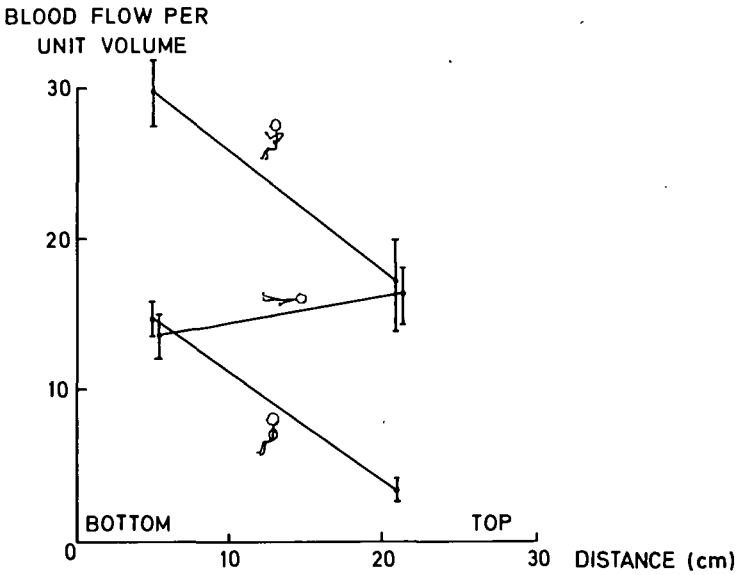

Fig. 6-4 Effects of change of posture and exercise on the distribution of blood flow. Means and standard errors. Note that in the supine position, upper and lower zone blood flows are virtually the same.

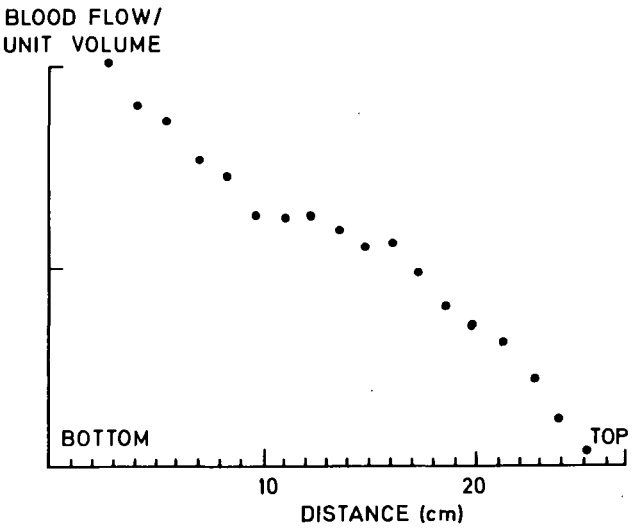

Fig. 6-5 Distribution of blood flow in the isolated dog lung under various conditions. In all three diagrams, blood flow per unit alveolar volume measured with ^{133}Xe is plotted against distance up the lung.

a. Shows the flow distribution found with a normal pulmonary arterial pressure and low venous pressure. Note the similarity to the distribution in the upright human lung shown in fig. 6-2.

b., c. See page 88.

gradient of blood flow is apparently small in the supine and prone positions, but more marked in the right and left lateral positions.

Figure 6-4 also shows that, when a subject exercises in the sitting position, blood flow increases both to the upper and lower zones. The rise in the upper zone may be slightly greater than that to the lower zone (267), but in any event, the proportion of the total pulmonary blood flow going to the apex of the lung is much increased (34). As yet,only low levels of exercise have been studied, partly because of the difficulties of breath-holding at higher levels of work.

Effects of pathological factors

Un-physiological conditions, such as heart disease, also provide evidence about the mechanisms underlying the normal distribution of blood flow in the lung, but the results must be interpreted with caution. In particular, possible regional changes in the structure of the blood vessels should be kept in mind. In diseases which increase the pulmonary blood flow, such as left-to-right intracardiac shunts, flow is more evenly distributed than in the normal lung, though lower zone blood flow still exceeds upper zone flow (69). The pattern found in normal subjects during exercise is therefore reproduced. In conditions in which pulmonary arterial pressure is increased because of a rise in arteriolar resistance, but pulmonary blood flow is not necessarily raised, flow is again more evenly distributed than in the normal lung. In diseases which raise pulmonary venous pressure, for example mitral stenosis, the distribution of blood flow becomes more uniform with moderate disease,but later in the course of the disease the normal distribution of flow may become inverted, so that more flow goes to the upper than to the lower zones (68, 258). Severe long standing mitral stenosis results in structural changes in pulmonary vessels, particularly in the lower zones (70), but this inverted distribution of blood flow is also seen in acute pulmonary venous hyper-tension, for example in left ventricular failure (258).

Cause of the uneven distribution of blood flow

Effects of pulmonary arterial, venous and alveolar pressures

To analyse the role of the various pressures in the pulmonary circulation in determining the pattern of flow, it is necessary to be able to change one pressure at a time and to observe the effect this has on the flow. Such a procedure is difficult or impossible in normal subjects, or in patients, so we have had to recourse to an experimental preparation where this could be done (269). The left lung of a dog is removed, suspended in a lucite box, ventilated with intermittent negative pressure, and perfused with a non-pulsatile flow of venous blood from a second dog. Various features of this preparation, such as its ability to exchange gas, the compliance of the lung, the pulmonary vascular resistance, and the rise in this resistance during hypoxia, demonstrate its normal physiological behaviour.

Figure 6-5a shows the distribution of blood flow, obtained using ^{133}Xe in this preparation, when the pulmonary arterial pressure was approximately normal. It can be seen that blood flow decreases steadily from the bottom of the lung to become virtually zero at the top. The similarity of this distribution to that found in the upright human lung (Fig. 6-2) is striking. Figure 6-5b shows the distribution of blood flow in the same lung a few minutes later, when the pulmonary arterial pressure had been lowered by reducing the blood flow through the lung. Again, blood flow decreases with distance up the lung, but it now falls to zero some two-thirds of the way up the lung and an appreciable part of the apex becomes unperfused. It was possible to determine the level in the lung where pulmonary arterial pressure, as measured at the arterial cannula, equalled alveolar pressure. Here we are referring to the fact that the arterial pressure falls off at the rate of one

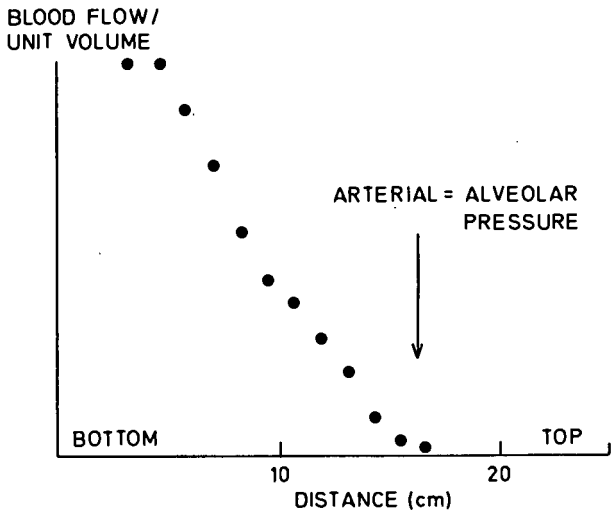

Fig. 6-5b Shows the effect of lowering pulmonary arterial pressure. Note that there is now an unperfused area at the top of the lung, and that blood does not rise above the level at which arterial pressure equals alveolar pressure.

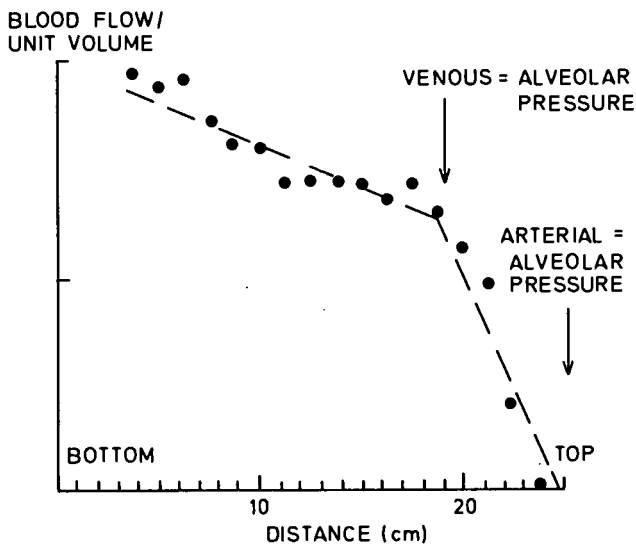

Fig. 6-5c Shows the effect of raising pulmonary venous pressure. The result is to make the flow distribution more uniform below the level at which venous pressure equals alveolar pressure.

centimetre of water per centimetre of distance up the lung because of the hydrostatic effect. Figure 6-5b shows good agreement between the no-flow level and the level at which arterial pressure equals alveolar pressure, and this finding has been confirmed on many occasions.

Figure 6-5c shows the effect on the distribution of blood flow of raising pulmonary venous pressure, which had been kept low in figs. 6-5a and b. It can be seen that the distribution of blood flow in the lower part of the lung becomes more uniform. Instead of the distribution being approximately linear, an inflection is now seen, and other evidence confirms that this occurs at the level where pulmonary venous pressure equals alveolar pressure. More recent work shows that the change in slope shown in this particular example is much greater than that usually seen.

It is possible to account for these and many other similar results found in the isolated lung by means of the simple three-zone model illustrated in fig. 6-6. Many features of this model were proposed by Permutt, Bromberger-Barnea and Bane (207), Banister and Torrance (15) and others. The lung can be conveniently divided into three zones, according to the heights of the pulmonary arterial (Pa), alveolar (PA) and venus (Pv) pressures.

Zone 1 is that part of the lung above the level at which arterial and alveolar pressure are equal. In fig. 6-6, the alveolar pressure has been shown at atmospheric, as it is in man at the end of inspiration or expiration, and the Pa = PA level is therefore the height of the blood in an open-ended manometer in the pulmonary artery. (In fact, because of the pressure drop along the artery and its branches caused by flow resistance, Pa falls off a little more rapidly with height inside the lung compared with the manometer, but this error becomes increasingly small as the Pa = PA level is approached and blood flow falls to zero). Figure 6-6 shows that there is no pulmonary blood flow in zone 1. This is presumably because the collapsible vessels are directly exposed to alveolar pressure. The close correlation between the no-flow level, and the level at which arterial pressure equals alveolar pressure, implies that the collapsible vessels - in this preparation - are neither protected from alveolar pressure nor do they have an inherent tendency to close - but see the effect of volume history later.

Zone 2 is that part of the lung in which arterial pressure exceeds alveolar, but alveolar pressure exceeds venous pressure. Here the vessels behave as Starling resistors (see p. 94), that is, collapsible tubes surrounded by a pressure chamber, and flow is determined by arterial pressure minus alveolar, not by arterial pressure minus venous pressure (Pa - PA in Fig. 6-6; not Pa - Pv). In the lung, PA is the same at every level, while Pa increases steadily down the lung due to the hydrostatic pressure gradient. In this way the increase of flow with distance down zone 2 is satisfactorily explained.

Zone 3 is that part of the lung where venous pressure exceeds alveolar pressure. The present study shows an increase of flow with distance down this zone, though the rate of increase may be less than that seen in zone 2 (Fig. 6-5c). The increase appears to be approximately linear with distance down the lung. Again the distribution of flow in this zone can be explained by mechanical factors. Because venous pressure is higher than alveolar pressure throughout this zone, the pressure inside the collapsible vessels will be everywhere higher than the pressure outside. The vessels will therefore not be flaccid but expanded. Now the pressure difference controlling flow is not Pa - PA but Pa - Pv. At first sight, it appears that there would be no change in blood flow down zone 3, because Pa - Pv is the same at all levels. However, since intravascular pressures increase down zone 3 (the hydrostatic pressure gradient) and alveolar pressure remains constant, the transmural pressure will rise with distance down the zone. If the vessels are distensible, their resistance to flow will fall and blood flow will continue to increase.

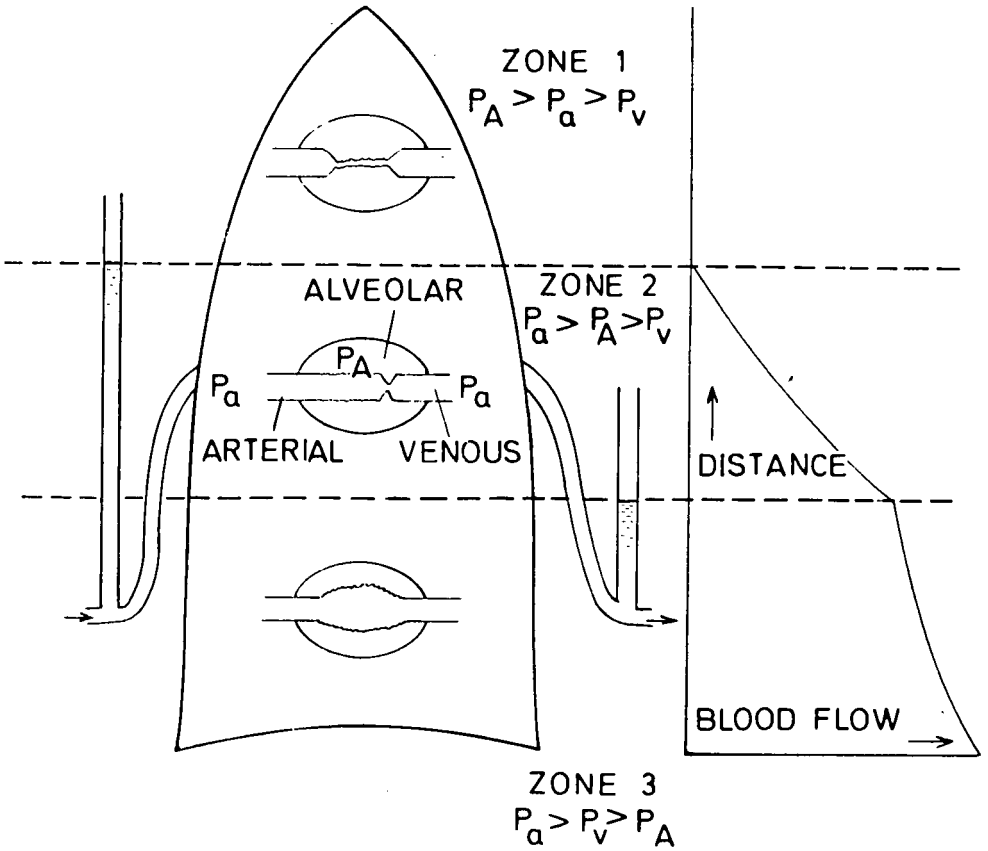

Fig. 6-6 Diagram to show the effects of pulmonary arterial, alveolar and venous pressures on the topographical distribution of blood flow in the lung. The lung is divided into three zones by the relative magnitudes of the three pressures.
In zone 1, arterial pressure is less than alveolar pressure and there is no flow, presumably because collapsible vessels are directly exposed to alveolar pressure.
In zone 2, arterial pressure exceeds alveolar, but alveolar pressure exceeds venous pressure.
Here the vessels behave like Starling resistors and flow is proportional to the difference between arterial pressure (which is increasing down the lung) and alveolar pressure (which is constant).
In zone 3, venous pressure exceeds alveolar pressure and flow is determined by the arteriovenous difference. Flow increases down this zone because the transmural pressure of the vessels increases so that the vessels have a larger calibre.
(From (269), by courtesy of J. appl. Physiol.).

It is not surprising that the slopes relating blood flow and height in zones 2 and 3 may be dissimilar, since they are governed by different factors.

The scheme illustrated in fig. 6-6 accounts for many of the distributions of blood flow so far observed in the human lung. The fact that apical and basal flows become equal in the supine position follows from the evening out of the hydrostatic pressure differences. The more uniform distribution of blood flow on exercise, compared with rest, results from the increased pulmonary arterial pressure, and the same explanation applies to pathological conditions such as left-to-right intracardiac shunts, in which pulmonary blood flow is increased. The fact that the distribution of blood flow becomes more uniform when the venous pressure is moderately raised by the passive rise in pulmonary arterial pressure and the upward extension of zone 3. However, the reduction of blood flow at the base of the normal lung at low lung volumes, and the inverted distribution of blood flow seen in patients with a raised pulmonary venous pressure, cannot be explained in this way.

Features of the unperfused zone 1

The histological appearance of the blood vessels in zone 1 has been studied by Glazier and his colleagues (108). The isolated lung was perfused with a low pulmonary arterial pressure and the surface of the lung suddenly flooded with liquid freon gas cooled to -160°C with liquid nitrogen. A vertical strip of lung about 0.5 cm thick was frozen within a few seconds in this way and pieces of the tissue were freeze-dried, embedded and mounted for histological examination.

Lung from zone 1 shows very thin alveolar septa with collapsed capillaries containing only a few trapped red blood cells. Some of these are elongated as if they are distorted by the pressure around them. Some of the slightly larger vessels in the corners of the alveolar septa are open, suggesting that they are exposed to a pressure less than alveolar pressure. High in zone 1, most of these corner vessels close and even the larger vessels with muscular walls may be distorted because of the very low pressure within them.

Effect of volume history of the lung

Lloyd and Wright (168) and Bruderman and his colleagues (31) showed that, under some conditions, the pericapillary pressure is less than alveolar pressure. There is evidence that this lowering is caused by the surface tension of the alveolar lining layer, and this is substantially affected by the volume history of the lung.

The influence of this factor has been investigated in our laboratory using the isolated lung preparation (203). In one series of experiments (Fig. 6-7), the distribution of blood flow was measured with ^{133}Xe when the lung was inflated by a transpulmonary pressure of 12 cm water, after it had been held in a near deflation state (transpulmonary pressure of three centimetres of water) for one minute. This distribution was compared with one, also obtained at a transpulmonary pressure of 12 cm water, but this time after the lung had been distended for one minute (transpulmonary pressure of 22 cm water). Figure 6-7 shows that, immediately after the lung was inflated from a nearly collapsed state, blood was detected several centimetres higher than when the lung was deflated to the same transpulmonary pressure. The figure illustrates the results of four paired measurements carried out on a single lung. In 26 similar pairs of observations, the mean difference in the height to which blood rose was 4.1 cm (standard error of mean 0.4 cm). When the lung was in its inflation state, blood rose an average of 4.6 cm above the level at which arterial and alveolar pressures were equal, but only rose 0.6 cm above this level in the deflation state. Figure 6-7 also shows that, with time, there was a tendency for the difference in blood flow height between

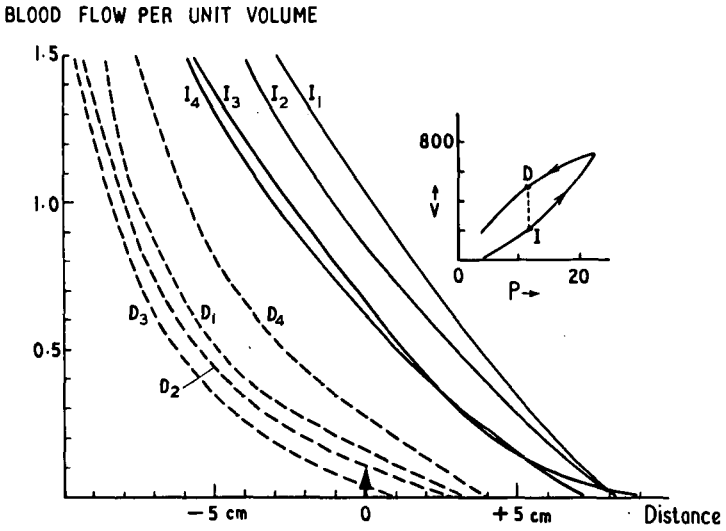

Fig. 6-7 Distribution of blood flow in the inflation state (solid lines) contrasted with the deflation state (dashed lines), both measured at the same transpulmonary pressure. The ordinate shows blood flow per unit alveolar volume, and the abscissa shows distance up the lung referred to the level (marked with an arrow) at which pulmonary arterial and alveolar pressures are equal. Insert shows pressure-volume curve.

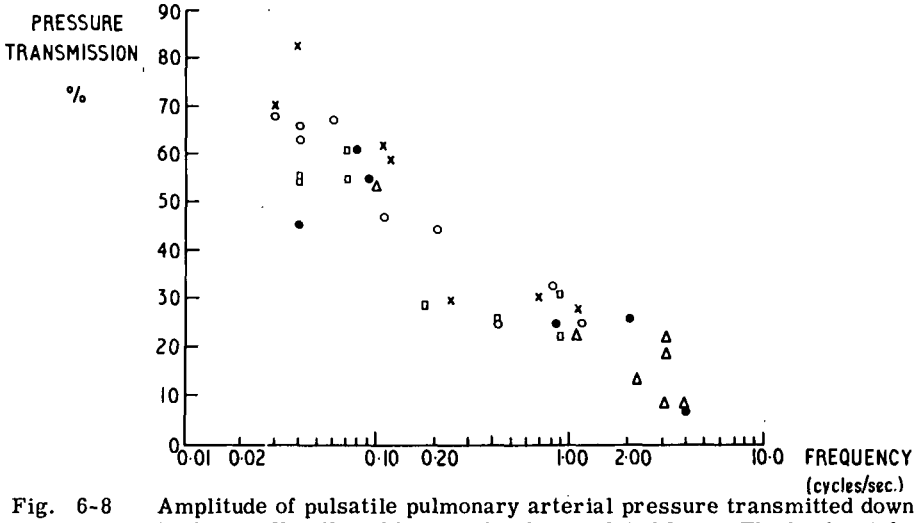

Fig. 6-8 Amplitude of pulsatile pulmonary arterial pressure transmitted down to the small collapsible vessels of an isolated lung. The horizontal axis shows the frequency of the sinusoidal input on a logarithmic scale. Different symbols indicate different preparations. Note that the pressure transmission falls with frequency to reach about 30% at physiological frequencies.
(From (175), by courtesy of Circulation Res.).

inflation and deflation to decrease, possibly because of a change in the properties of the alveolar lining layer.

In some experiments the distribution of blood flow was compared at the same lung volume, rather than the same transpulmonary pressure, under inflation and deflation conditions. Because of the hysteresis of the pressure-volume curve, this meant that the deflation measurements were made at a lower transpulmonary pressure than the inflation ones. In one series of eight measurements, the lung was inflated to a transpulmonary pressure of 18 cm water after near collapse. When the distribution of blood flow was compared with that obtained after deflation to the same volume after near maximal inflation, the average difference in the height to which blood rose was 6.7 cm (standard error of mean 0.7 cm). In a larger series of isovolume comparisons, the difference in height to which blood rose was plotted against the difference in transpulmonary pressure between the inflation and deflation states. Since the slope of a regression line, drawn by the method of least squares, was less than one, and since, under isovolume conditions, the difference in transpulmonary pressure reflects the effect of surface tension on the static recoil force, we concluded that changes in surface tension of the alveolar lining layer exert a greater pressure tending to close the alveoli than they do tending to open the alveolar blood vessels.

It is difficult to imagine how surface forces in the alveolar lining layer could open capillaries situated along the alveolar septa, since these vessels tend to bulge outwards into the alveolar gas spaces (108). This has led some authors to suggest that the vessels which are pulled open are those in the corners of the alveoli (222).

Effect of pulmonary arterial pulse pressure

Up to this point we have been looking at the influence of pulmonary arterial pressure on the distribution of blood flow for conditions of steady flow. For example, the experiments illustrated in figs. 6-5 and 6-7 were all done using a non-pulsatile perfusing pressure. However, the pressure in the pulmonary artery of man and other animals is highly pulsatile. In man, the normal pulse pressure measured in the pulmonary artery is about the same magnitude as the mean pressure. How much of this pulsatile pressure in transmitted to the small vessels of the lung? Do the apical capillaries wink open and shut with each heart beat, or do they see only the mean pressure?

These questions have been studied by Malony, Bergel and their co-workers (175, 176). First, the propagation of pulsatile pressure and flow was measured in an isolated lung preparation of minimal height in order to minimise hydrostatic pressure effects. Arterial and venous pressures and flows were measured with electromanometers and electromagnetic flow meters. It was found that, if the pulmonary arterial pressure was first lowered to a level at which no flow occurred, and was then raised rapidly, delays of up to several seconds occurred before venous flow began. A further one to nine seconds was required before flow reached a steady level. These preliminary experiments showed that the lung was capable of passing only the low frequency components of the applied input.

The transmission of pulsatile flow was measured and found to be greatly attenuated in its passage through the lung at physiological frequencies. Transmission fell from about 75 percent at the very low frequency of 0.03 c/s, to about 10 percent at a frequency of one cycle per second. Transmission was found to be independent of outlet pressure, and there was no difference whether the lung was perfused in the forward (artery to vein) or backward direction.

Pressure transmission down to the small collapsible vessels was also measured, and the results are shown in fig. 6-8. At a frequency of 0.03 c/s, some 60 percent of the pulsatile pressure is transmitted down to the small vessels, but at a frequency

of one cycle per second, the transmission falls to 30 percent. It was concluded from these experiments that the lung passed only the low frequency components of the applied input, and that, in a vertical lung, only 30 percent of the mean to peak pressure pulse would be transmitted down to the small vessels, and affect the distribution of blood flow.

In a further series of experiments (176), the distribution of blood flow was measured in a vertical isolated lung preparation which was perfused by pulsatile arterial pressure. The pattern obtained was compared with that seen when the lung was perfused with a steady pressure equal to the mean value of the pulsatile pressure. It was found that the pattern of blood flow (measured using ^{133}Xe) was altered during pulsatile perfusion and that more blood passed through the upper zones of the lung. As the frequency of the pulmonary arterial pressure waves was increased from 0.03 to 3 c/s, the difference in the flow pattern diminished, and the level to which blood rose in the lung decreased. At the lower frequencies, blood rose to a height approximating to 70 percent of the mean to peak pressure pulse. At the higher frequencies, this was reduced to about 30 percent. These experiments confirm that the transmission of the pulmonary arterial pressure pulse by the blood vessels of the lung is frequency dependent, and that this dependence alters the distribution of blood flow in the lung. Furthermore, the magnitude of the pressure transmission to the small collapsible vessels calculated from the distribution of blood flow agrees well with the pressure transmission observed in the previous experiments using an isolated lung of minimal height.

Features of zone 2

Histology

Rapidly frozen lung from zone 2 shows open capillaries with abundant red blood cells along the alveolar septa. Glazier and his colleagues (108) have shown that the number of red blood cells per unit length of septum increase approximately linearly with distance down zone 2, and this remains true over a pressure range equivalent to a vertical lung height of 35 cm. This observation implies a steadily increasing capillary blood volume per unit volume of lung parenchyma down the zone. The increase in blood volume is partly due to distension of open capillaries, but chiefly to the opening up of new vessels.

Pressure-flow relations

When alveolar pressure exceeds pulmonary arterial pressure, blood flow through the lung is determined by arterial less alveolar pressure, rather than the more usual arterio-venous pressure difference. This observation has been of enormous value in our understanding of the pressure-flow relations of the lung in general, and of zone 2 in particular. Banister and Torrance (15) and Permutt and his colleagues (207) were responsible for the clearest statements on this subject, though several previous authors recognised the importance of the transmural pressure in determining flow through collapsible tubes. The behaviour has been variously called the 'sluice effect', the 'vascular waterfall' or the 'Starling resistor effect', this last because the behaviour resembles that of the resistive device used by Starling in his heart-lung preparation (150).

A Starling resistor consists of a limp-walled rubber tube in a pressure chamber. When the outlet pressure of such a device is higher than chamber pressure, flow is determined by the inflow-outflow pressure difference in the ordinary way. However, if the outflow pressure is reduced below chamber pressure, flow is determined by the difference between inflow and chamber pressures and is unaffected by changes in

outflow pressure. A constriction can be seen to develop in the downstream end of the collapsible tube and the pressure inside the tube at the collapse point is equal to chamber pressure, since the tube does not resist collapse. The large pressure drop across the constriction is dissipated in accelerating liquid through it. In practice, instability often develops and the rubber tube flutters. Frequently, the collapse extends upstream, but the first point of closure is the downstream end.

How far the small collapsible vessels of the lung behave in a similar way is unknown, but certainly, if venous pressure is less than alveolar pressure, blood flow can be shown to be independent of venous pressure. The precise extent of the collapsible alveolar segment in anatomical terms is not known, but is includes the pulmonary capillaries and probably other small vessels up to a diameter of about 30 microns. Whether a definite collapse point develops as it does in rubber tube models, and whether instability occurs in the lung vessels is not known. It should be remembered that the pulmonary capillaries in zone 2 are only just wide enough to allow the passage of red blood cells in any case.

A typical example of the relations between flow and pulmonary arterial pressure under zone 2 conditions is seen in fig. 6-9. These measurements were made on the left upper and middle lobes of a greyhound lung, placed on its side (86). The vertical height of this preparation was less than four centimetres, so that hydrostatic differences within it were kept to a minimum. Perfusing pressure is plotted with respect to alveolar pressure at the bottom of the lung. Since perfusion pressure gradually increases with distance down zone 2 of the lung, this graph could equally well represent the rate of increase in blood flow per unit volume down the lung. It can be seen that the curve becomes progressively steeper as the upstream pressure increases. A similar curve relating blood flow per unit volume to distance down zone 2 in the lung, can also be demonstrated using ^{133}Xe: for example, fig. 6-7. This fall in vascular resistance with increase in perfusing pressure has been observed many times in the past, being usually ascribed to dilatation of vessels due to their increased transmural pressure, and to the opening up of new vessels. Histological measurements show that the opening of new channels is the more important factor in the fall in vascular resistance down zone 2 (108).

Features of zone 3

Histology

The number of red blood cells per unit length of alveolar septum increases down zone 3 over a pressure range equivalent to a vertical lung height of 50 cm, just as it does down zone 2 (108). The increase in capillary pressure causes striking changes in the dimension of the vessels across the septa, and considerable bulging into the alveolar cavities is evident at higher pressures. As in zone 2, new vessels apparently continue to open up down the zone. However, when the capillary pressure exceeds about 60 cm water, capillary blood volume ceases to increase with distance down the zone, suggesting that all the capillaries have opened up and that no appreciable further distension of the vessels can occur.

Pressure-flow relations

These are most easily studied using the preparation described above, in which hydrostatic effects are minimised by lying an isolated lung on its side (86). If pulmonary arterial and venous pressures are gradually raised in steps at the same rate, so keeping the arterio-venous pressure difference constant, the plot of blood flow versus arterial (or venous) pressure corresponds to the change in blood flow with distance down zone 3. Under these conditions, the most useful expression for

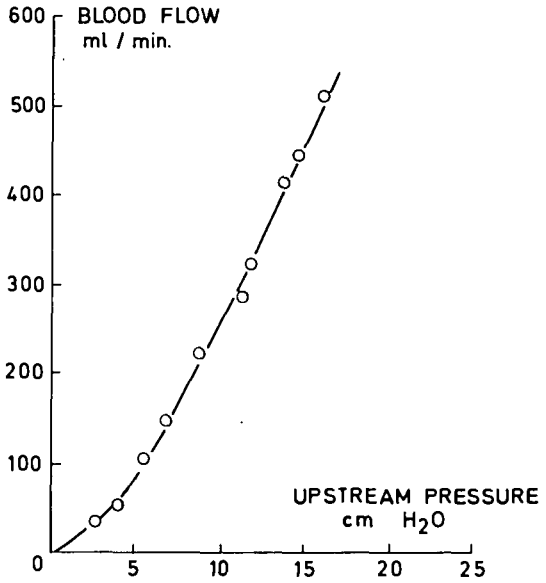

Fig. 6-9 Typical pressure-flow relationship obtained in an isolated lung of minimal height under zone 2 conditions. Note that the slope of the curve increases as pressure rises. The same relationship is found for the increase in blood flow down zone 2 (compare Fig. 6-7).

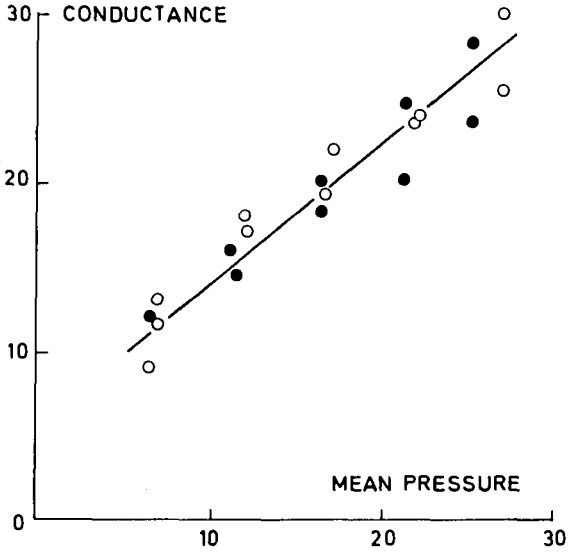

Fig. 6-10 Effect of gradually raising upstream and downstream pressures together, on the conductance of an isolated lung of minimal height, in zone 3 conditions. Solid symbols for forward flow; open symbols for reverse flow. Note the rapid rise in conductance (fall in resistance) as pressure increases, which accounts for the marked increase in blood flow down zone 3.
(From (86), by courtesy of Resp. Physiol.).

resistance is the arterio-venous pressure difference divided by flow. Conductance is the inverse of this.

Figure 6-10 shows the results of a typical experiment. Conductance (in ml/min per cm water) is plotted against the mean of the upstream and downstream pressures for both forward, artery-to-vein flow (solid symbols), and reverse flow (open symbols). It can be seen that conductance increases rapidly and approximately linearly as mean pressure is raised. The mean distensibility of the preparations in zone 3 conditions is most simply reported by giving the percentage increase in conductance which occurred when the mean pressure was raised from 10 to 30 cm water. The values obtained in forward flow ranged from 37 to 110 percent with a mean of 87 percent. This corresponds to the change in blood flow which would be expected over 20 cm of vertical height down zone 3 under appropriate pressure conditions. In a series of 10 measurements of the slope of zone 3 using ^{133}Xe in six separate lungs (269), it was found that blood flow per unit volume decreased by an average of 62 percent over 20 cm of vertical distance from the bottom of the lung. The figure predicted from the pressure-flow measurements on the flat lung is 47 percent, which agrees reasonably well in view of the very different techniques used.

Figure 6-10 also shows conductance during reverse perfusion (vein to artery), and it can be seen that the values were substantially the same as those obtained with forward flow. Indeed, in a series of preparations, the mean change in conductance for forward and reverse flow was the same. In the course of these experiments, mean conductances under zone 2 conditions (between upstream pressures of zero and 20 cm water) were compared with conductances under zone 3 conditions (at a mean pressure of 10 cm water). There was close agreement between the values in the two conditions, indicating that the downstream vessels, which contribute to observed resistance in zone 3 but not in zone 2 conditions, have considerably less resistance than those upstream of the collapse point, irrespective of flow direction. This is consistent with the conclusion reached by other measurements (86), namely, that the major site of vascular resistance in these preparations is in collapsible vessels exposed to alveolar pressure.

On the basis of the pressure-flow relations measured in these flat-lung experiments, it is possible to predict the relative slopes of blood flow versus distance down zone 2 and 3. It is found that the slope of zone 3 is almost as great as that of zone 2, and that unless the radioactive gas measurements were very precise, it would be impossible to detect any difference. This prediction has been borne out in practice (137). These recent measurements suggest that the much flatter slope apparently caused by zone 3 in some earlier preparations (for example, Fig. 6-5c) may have been partly due to the influence of interstitial pressure.

The evidence that is available suggests that the slope of zone 3 in man is also steep; indeed it would be surprising if this were not so in view of the histological similarities between the blood vessels of the human and dog lung. Figure 6-3, for example, shows that at total lung capacity, when the effects of interstitial pressure are nearly abolished, blood flow increases rapidly down virtually the whole of the lung. Although pulmonary venous pressure is not accurately known under these conditions, it is probable that the lower part of the lung is in zone 3. Some authors have claimed that the slope of zone 3 in man is small or absent under some conditions, for example (5, 130), but it is likely that these investigators were seeing the effects of interstitial pressure.

Zone of interstitial pressure

We have seen (Fig. 6-3) that, at lung volumes less than total lung capacity, a zone

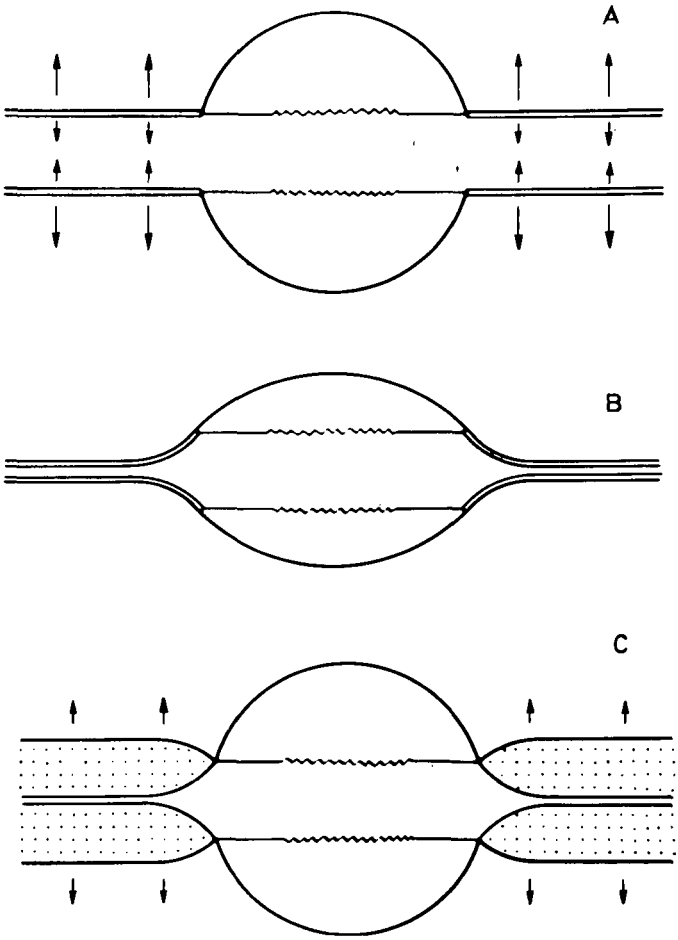

Fig. 6-11 Subdivision of pulmonary blood vessels into alveolar and extra-alveolar components. Alveolar vessels (contained within the circle) are exposed to alveolar pressure (modified by surface forces). Extra-alveolar vessels are surrounded by a low interstitial pressure developed by expansion of the lung parenchyma. Diagram B shows that in the collapsed lung, extra-alveolar vessels close because of the inherent tension in their walls. Diagram C shows that, in the presence of oedema fluid in the perivascular space, vessels are isolated from the normal expanding pull, and close.
(From (268), by courtesy of Circulation Res.).

of reduced blood flow can be detected in the dependent regions of the normal human lung. It is impossible to explain this on the basis of the inter-relationships between pulmonary arterial, venous and alveolar pressures as shown in fig. 6-6. It is true that if the resistive vessels were indistensible and no new channels opened up in response to an increasing transmural pressure, it would be theoretically possible to have a uniform distribution of blood flow down zone 3, though in the event blood flow is found to increase rapidly. However, there is no conceivable combination of these pressures which could cause a reduction of blood flow in the lower zones.

We believe that the cause of this zone of reduced blood flow lies not in the blood vessels exposed to alveolar pressure, which we have been considering up till now, but in larger vessels outside the influence of alveolar pressure.

Alveolar and extra-alveolar vessels

Macklin filled the vessels of excised lungs with a latex suspension, and showed that the volume of the larger vessels increased as the lungs were inflated, and decreased with deflation (174). Howell and his colleagues extended these observations using kerosene, a fluid which fills only the larger vessels and does not penetrate to the capillaries (135). These authors showed that the effect of lung inflation on the pulmonary vascular bed varied, depending upon the portion studied. With positive pressure inflation (that is, alveolar pressure rising with respect to vascular pressures), the small vessels unfilled by kerosene were compressed, but the larger kerosene-containing vessels were expanded. It was found that, although the volume changes in the larger vessels were small, surprisingly negative pressures could be developed within them as the lungs were inflated.

Figure 6-11 shows, diagramatically, the two types of vessels. Outside the influence of alveolar pressure, the extra-alveolar vessels are shown as being held open by a pressure developed by the expansion of the lung parenchyma. Permutt (205) has obtained evidence that the pressure outside the extra-alveolar vessels may be very low, even lower than pleural pressure, and that it becomes lower as the lung is further expanded. The mechanism by which a low perivascular pressure can be developed is not fully understood, but Mead (179) has argued recently that the effective distending pressure on the larger vessels is related to the departure of the volume of any vessel from the volume which it would achieve if it distended identically with its surroundings.

The precise anatomical location of the alveolar vessels is not known, but histological measurements of rapidly frozen lung show that the capillaries in the alveolar septa are exposed to alveolar pressure. There is evidence that the somewhat larger vessels in the corners of the alveoli are exposed to a slightly lower pressure, and it seems likely that vessels of 100μ diameter and larger are truly extra-alveolar.

Figure 6-11 also shows that the extra-alveolar vessels tend to close because of tension in their walls which can be attributed to the elastic and muscle tissue present. Indeed, there is accumulating evidence that the calibre of the extra-alveolar vessels is determined by the balance between several forces. The negative pressure developed by the expanded lung tends to open the vessels, and this force is opposed by the inherent tension in the walls of the vessels and by any fluid accumulation in the perivascular space (Fig. 6-11c).

Perivascular space of the extra-alveolar vessels

An important feature of the extra-alveolar vessels is the interstitial tissue around them with its potential perivascular space. Von Hayek has given a clear account of the anatomy of the spaces around the pulmonary arteries, veins and bronchi of the human lung (120). According to Marchand (177), the fascial sheaths which envelop

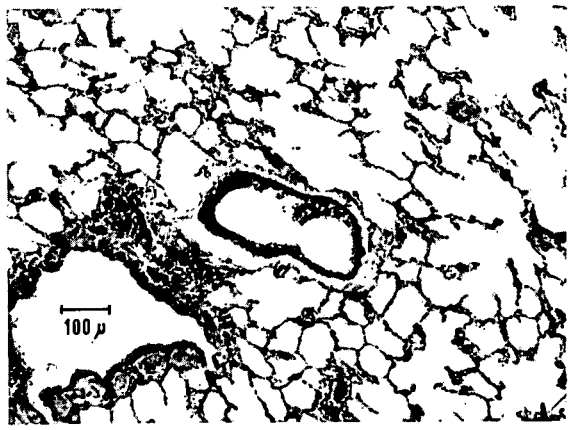

Fig. 6-12 Photomicrograph showing a small pulmonary artery accompanying a bronchus. Note the interstitial tissue around the vessel (perivascular space), but not around the airway.

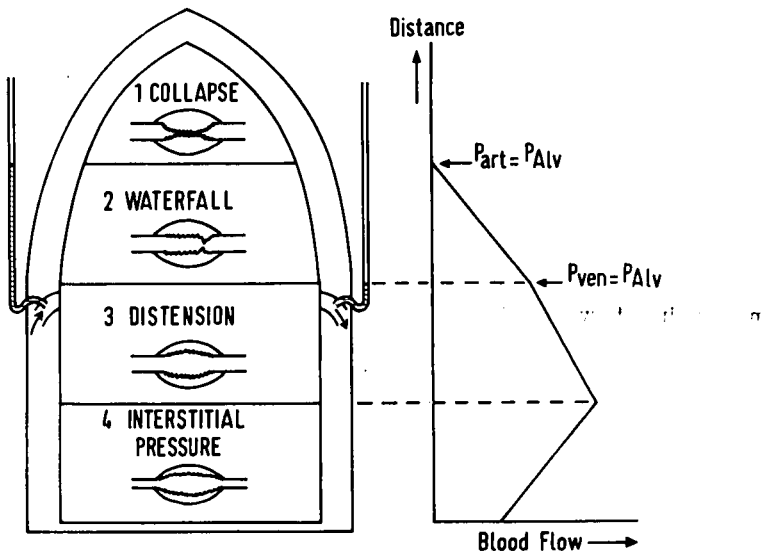

Fig. 6-13 How the three zone diagram of fig. 6-6 can be modified to take account of the reduction of blood flow of the most dependent zone of the lung as a result of a raised interstitial pressure. The first three zones correspond to those featured in fig. 6-6, and to these has been added a fourth zone where the vascular resistance of the extra-alveolar vessels becomes significant because of a rise in interstitial pressure. This occurs in the normal lung at volumes below total lung capacity because of the relatively poor expansion of lung parenchyma in dependent zones. (From (136), by courtesy of Resp. Physiol.).

the perivascular and peribronchial interstitial tissue are a direct extension, into the lung, of the peritracheal and peri-oesophageal fascial layer. This interstitium contains loose alveolar tissue with fine radial collagenous fibres. There is also an abundance of lymph vessels, and indeed most of the lymph from the lung parenchyma drains towards the hilum in the perivascular and peribronchial spaces. Because the interstitial tissue is surrounded by a well defined fascial sheath, any accumulation of oedema fluid, blood or air produces a clearly recognisable perivascular or peribronchial space.

Figure 6-12 shows a small pulmonary artery (about 300 by 100 μ) accompanying a somewhat larger bronchus. A narrow space can be seen around the artery, though not around the bronchus, and it is typical that the interstitium extends further peripherally along the arteries than along the bronchi. The pulmonary veins also have a perivascular space, but according to von Hayek, the veins are not accompanied by large perivascular lymph vessels and the space is accordingly smaller.

One of the striking features of the perivascular space is the ease with which oedema fluid, blood and air can track along it. Macklin (173) overinflated small regions of the lungs of cats and showed that the air which leaked from ruptured alveoli was transported along the peri-arterial and perivenous spaces to the hilum. Tocker and Langstrom injected barium solution into the peri-arterial and perivenous spaces in the hilar region in dogs, and showed that it tracked peripherally to the 'most minute branchings of the vessels' (254). Marchand injected dye under the pretracheal fascia in cadavers, and demonstrated by dissection that it found its way into the perivascular and peribronchial regions of the lung. He regarded these perivascular and peribronchial spaces as a 'highway connecting the lung to the mediastinum', and attributed the batwing shadow, often seen in radiographs of hypertensive heart failure, to distension of this space by oedema fluid (177).

Interstitial pressure and regional blood flow

Figure 6-3 showed that, at lung volumes less than total lung capacity, a zone of reduced blood flow could be detected in the dependent regions of the normal lung. How can this be explained on the basis of an increase in resistance of the extra-alveolar vessels? There is now good evidence that the lung parenchyma is less well expanded at the base of the normal upright lung than in the upper zones (see chapter 3). These regional differences in lung expansion will cause regional differences in the resistance of extra-alveolar vessels. Just as these vessels are pulled open by the low pressure developed around them by expansion of the lung parenchyma, so with lung deflation these extra-alveolar vessels will contract. The walls of the vessels contain elastic tissue, and also muscle in a state of tone, so that, if the normal expanding force on the vessel is removed, they will constrict because of the inherent tension in their walls (Fig. 6-11b). The result is that a zone of relatively high vascular resistance is seen in the dependent region of the lung.

Additional evidence for this mechanism is that the vascular resistance of the excised lung which is poorly expanded is high, and indeed, lung which has been allowed to collapse completely shows a critical closing pressure - that is a perfusing pressure at which no flow occurs (266).

The zone of reduced blood flow in the dependent lung, due to interstitial pressure, has been extensively studied in isolated preparations where the various factors affecting extra-alveolar vessels have been altered separately. Thus, the zone of reduced blood flow can be exaggerated by reducing lung volume, by infusing vasoconstrictor drugs or by loading the vascular system of an intact dog, so moving fluid into the interstitial space and raising its pressure. By contrast, the zone can be decreased by increasing lung volume, or by infusing vasodilator drugs.

An interesting point is why the isolated lung should have a dependent zone of high vascular resistance at all since, unlike the lung *in vivo*, all the alveoli of the excised lung are approximately the same size. A possible explanation is that the pressure in the perivascular space is higher at the bottom of the lung than at the top. The space contains lymph vessels, and it is reasonable that it would therefore have a hydrostatic pressure gradient. Indeed it is possible that pressure inside the space increases faster than one centimetre of water per centimetre of distance towards the bottom of the lobes, because tissue fluid is continually draining through the space to the hilum. The fact that some of the measurements on the isolated lung show a region of high interstitial pressure at the bottom of the middle and upper lobes, as well as the lower lobe, supports this hypothesis.

Figure 6-13 shows how the three-zone diagram of fig. 6-6 can be modified to take account of the reduction of blood flow to the most dependent tissue (136). In the three upper zones, it is the relations between arterial, alveolar and venous pressures on the alveolar vessels which determine the differences in blood flow. In addition, there may be a zone where the vascular resistance of the extra-alveolar vessels become significant, because of a rise in interstitial pressure. As we have seen, this occurs in the normal lung at volumes below total lung capacity, because of the relatively poor expansion of the lung parenchyma in dependent zones. Furthermore, a pathological rise of interstitial pressure caused, for example, by interstitial oedema, can exaggerate this zone of reduced blood flow.

7

Effects of acceleration on the distribution of pulmonary blood flow

In the previous chapter, it was shown that hydrostatic forces caused gradients of pressure within the pulmonary vessels, and that three zones of perfusion could be defined, according to the relative magnitude of the arterial, venous and alveolar pressures. The vascular pressure gradient, expressed in centimetres of water per centimetre vertical distance, is equal to ρG, where ρ is the density of whole blood. Little error is introduced by taking this as 1.0 (actually 1.06), so that the pressure change becomes equal to the vertical distance in centimetres, times the applied acceleration in G. Figure 7-1 shows how pressures would vary throughout an upright lung at $+3G_z$, taking the mean pulmonary arterial pressure to be 15 cm water at a level five centimetres below the hilum of the lung (the level of hydrostatic indifference established in chapter 5), and assuming venous pressure to be 10 cm water lower. The effect of $+3G_z$ would be to increase the extent of zone 1 (the region of zero blood flow); to shrink zone 2 (the waterfall zone) to one third of its normal depth - although the gradient of blood flow down it would increase threefold; and marginally to reduce the extent of zone 3 (the passive distension zone).

In the supine position, the vascular hydrostatic pressure difference between the apex and base of the lung disappears, to be replaced by a gradient between the anterior and posterior surfaces. The mean arterial pressure is about 17 cm water, with reference to a point five centimetres deep to the insertion of the fourth rib into the sternum (26). If this pressure were unaffected by acceleration, it would be sufficient to perfuse the entire lung at about $+5G_x$ (taking the anterior chest wall to be 1.5 cm thick). At greater levels of acceleration, the upper level of blood flow would drop away from the anterior surface of the lung and a zone 1 would appear.

Figure 7-2 summarises the extents of the zone 1 expected for different postures, at accelerations of one and five G. It assumes that the mean pulmonary arterial pressure remains at a constant 15 cm water on a line where two possible planes of hydrostatic indifference intersect (five centimetres below the hilum of the lung and five centimetres deep to the anterior chest wall). The third, lateral, plane will be considered later. As already mentioned, a significant zone 1 is present at $+1G_z$, and would increase markedly at $+5G_z$, as indicated in the right hand diagram. Due to the low placement of the pressure reference point, more lung would be perfused in the inverted posture, and even at $-5G_z$ (assuming this level of negative acceleration to be tolerable), only lung in the costo-phrenic angles would be without blood flow. With the lung lain on its front or back, the entire organ would be perfused at one G ($-1G_x$ or $+1G_x$), but a zone 1 would appear in either posture at five G. However, due to the anterior placement of the pressure reference point, this zone would be more extensive in the prone position ($-5G_x$) than in the supine position ($+5G_x$).

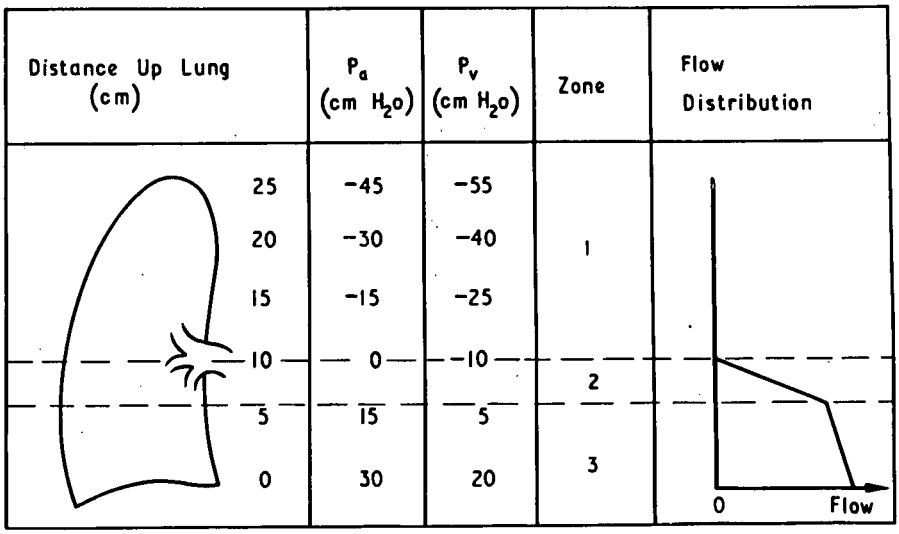

Fig. 7-1 Theoretical pressure-flow relationships in the lung at $+3G_z$. P_a, mean pulmonary arterial pressure; P_v, mean pulmonary venous pressure.

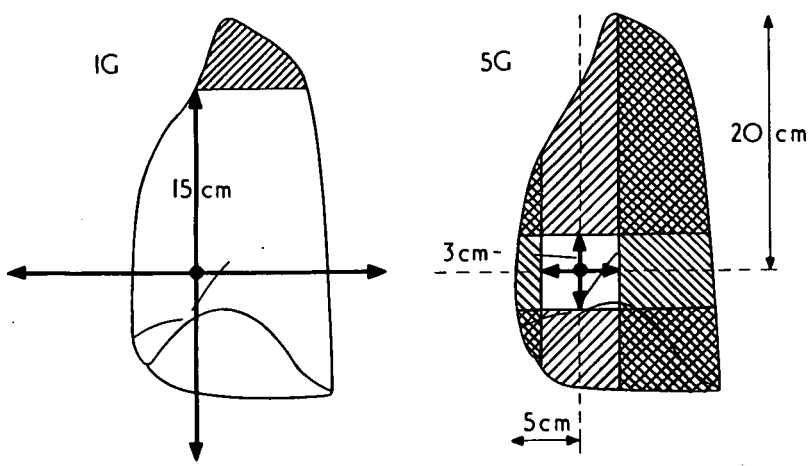

Fig. 7-2 Inner aspect of the right lung to show the level to which blood will rise at one and five G. Mean pressure at the reference point (black dot) is taken as 15cm water. Hatched areas indicate unperfused zones in various postures.

By making use of the same basic assumptions, the regions of lung subject to zone 2 or zone 3 flow conditions may also be calculated for the other postures. In each case, zone 2 would have a vertical extent of 10 or two centimetres at one or five G respectively, and any remaining lung would constitute a zone 3. The degree to which these theoretical predictions are supported by experimental evidence will now be considered.

Positive ($+G_z$) acceleration

Zone 1

By injecting solutions of xenon-133 intravenously at end-inspiration, and then monitoring the radioactivity of the upper lung, blood flow could be detected at $+1G_z$ and $+2G_z$, but became undetectable at $+3G_z$ (98). Since the scintillation counter used in these studies had a field of view two inches in diameter and was centred one inch below the clavicle, this observation suggested the development of a quite extensive zone of zero blood flow at the higher level of acceleration. This finding confirmed earlier calculations based on studies of expired carbon dioxide, which showed that up to one third of the ventilated lung volume comprised alveolar dead space at $+3G_z$ (96).

Bryan (35) carried out more detailed centrifuge studies in which solutions of macro-aggregated albumin, labelled with radioactive iodine (^{131}I-MAA), were injected intravenously during exposure to accelerations of up to $+4G_z$. The large albumin molecules form micro-emboli in pulmonary capillaries, and the distribution of these labelled emboli, and hence that of blood flow at the time of the injection, can be obtained by scanning the chest with a scintillation detector (262). An advantage of this technique is that only the injection requires to be carried out on the centrifuge, since the distribution of radioactivity remains constant for several hours. It is, however, difficult to correct the count rates for regional variations in lung volume or counting geometry. Results obtained at up to $+4G_z$ are shown in fig. 7-3, and also included is the distribution of radioactivity obtained when the injection of ^{131}I-MAA was made into a subject lying supine. Here, the apex to base distribution of blood flow should be uniform and the scan becomes, in effect, a measure of the volume of lung seen by the detector. In theory, this scan could be used to correct the other scans for this variable, but it should be noted that each scan was carried out on a different subject, and precise corrections would be invalid.

As may be seen from fig. 7-3, the greatest fall in apical perfusion occurs between $+1G_z$ and $2G_z$, with smaller falls at $+3G_z$ and $+4G_z$. This hyperbolic relationship between the height to which the blood flow rises and acceleration is to be expected since, as already stated, this height is proportional to the reciprocal of the acceleration.

Further ^{133}Xe studies were carried out employing a system in which the resolution with which the isotope was detected within the lung was improved by the use of a flat-beam collimator (101). This consisted of a stack of nine tapering slots, and isocount curves, obtained by moving a small source of ^{133}Xe within a lung phantom, are illustrated in fig. 7-4, superimposed upon a section of the lung. There is some widening of the field of view close to the collimator, due to the unavoidable scattering of radiation by the anterior chest wall (see p. 117). Despite this scattering, the sensitivity falls off by 90 percent at a distance of only one centimetre above and below the collimator axis. The resolution of the system, when used for scanning the lung at a speed of three centimetres per second, was 1.5 cm.

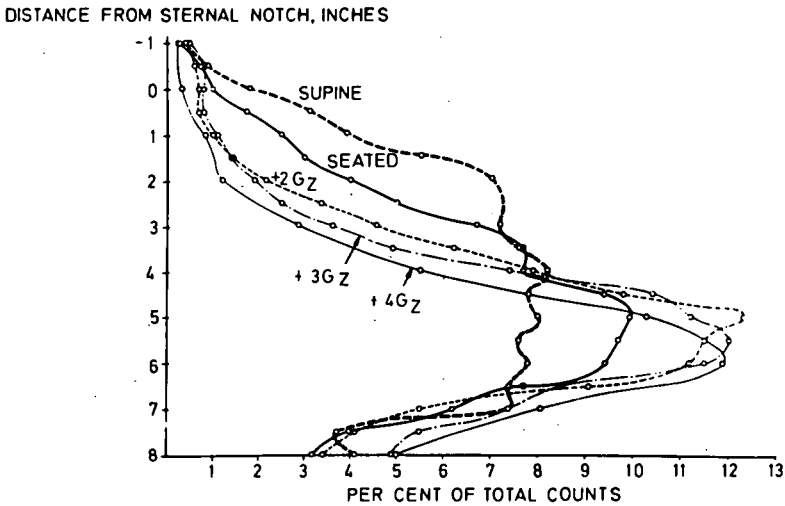

Fig. 7-3 The distribution of ^{131}I - MAA following i.v. injection in subjects supine, seated and at +2, +3 and $+4G_z$.

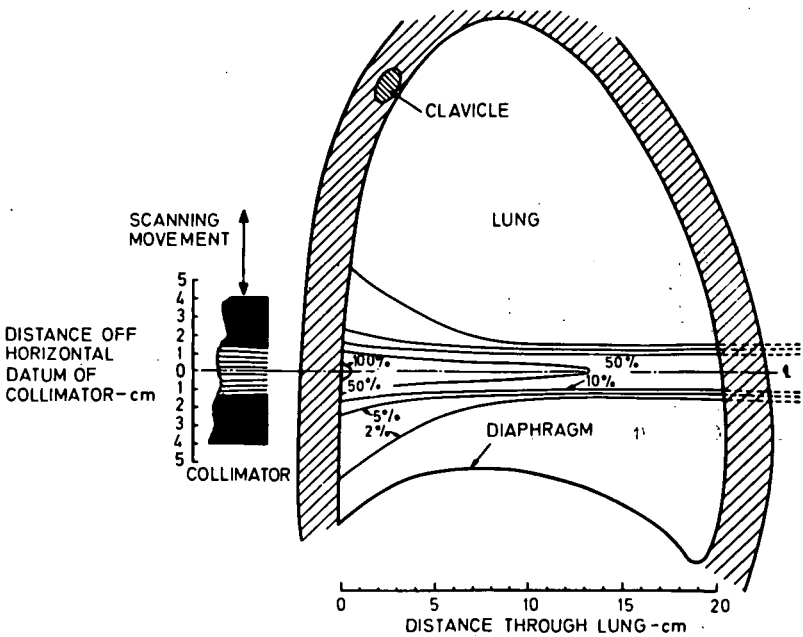

Fig. 7-4 Isocount curves, shown in relation to the chest wall and underlying lung, obtained by moving a small source of Xe within a lung phantom Movement is restricted to the vertical plane of the flat-beam collimator used for scanning the lung, and the peak response, just within the chest wall, is taken as 100%.
(From (103), by courtesy of Proc.R.Soc.).

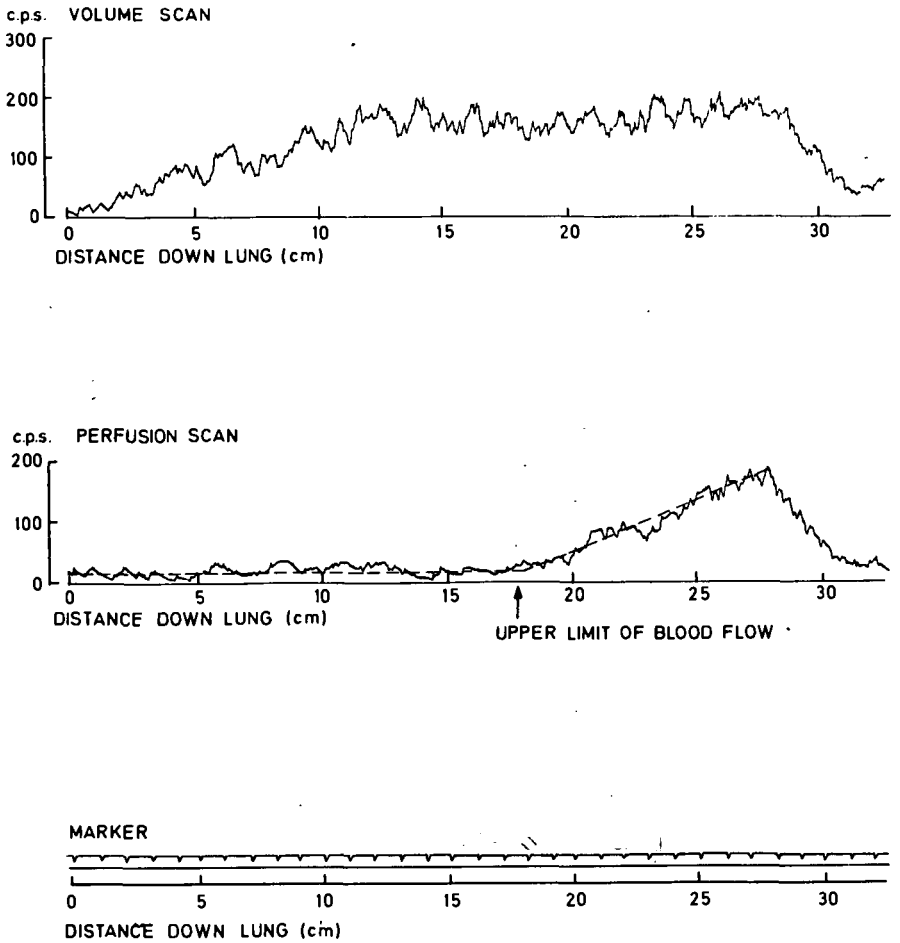

Fig. 7-5 Distribution of radioactivity down the right lung at $+3G_z$. The lower scan was made during breath-holding after an intravenous injection of ^{133}Xe in solution, and represents vertical distribution of blood flow. The upper scan was made at the same lung volume after a period of re-breathing ^{133}Xe, and is used to correct the perfusion scan for regional lung volume and counting geometry.

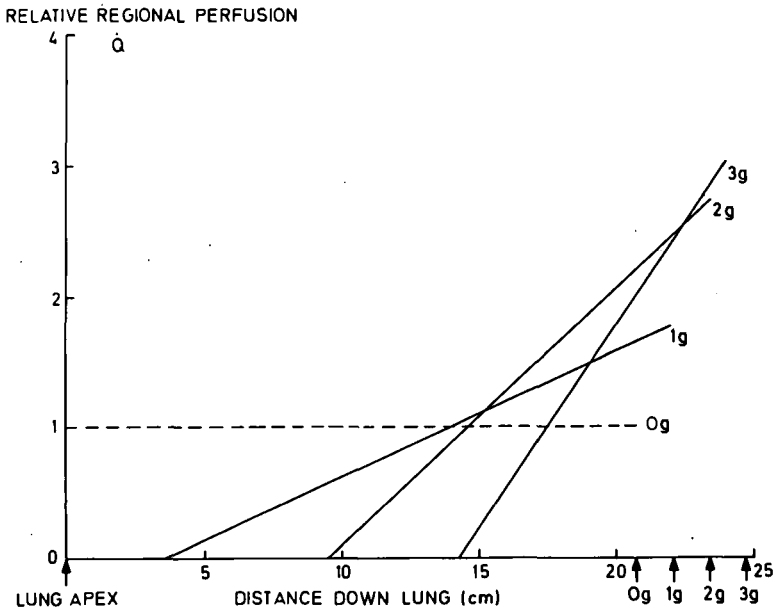

Fig. 7-6 The effect of $+G_z$ acceleration on the distribution of pulmonary blood flow. The ordinate gives the relative regional blood flow per unit lung volume, and the abcissa, the distance down the lung in centimetres. Extrapolation of the slopes to zero G indicates that blood flow would be uniformly distributed during weightlessness (dashed line).

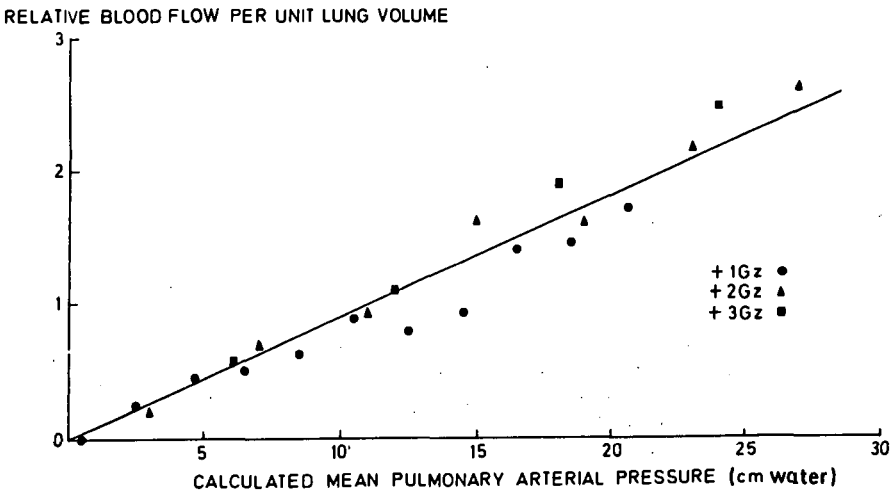

Fig. 7-7 Relationship between regional blood flow (derived from the distribution of injected ^{133}Xe) and calculated mean pulmonary arterial pressure (assuming zero pressure at the upper limit of blood flow, and a pressure gradient of 1.0 cm water/cm per G). Points are for one subject at $+1$ to $+3G_z$.

When this system was used to determine the distribution of pulmonary blood flow, the upper level to which perfusion rose could be clearly defined as that point along the scan where the count rate suddenly increased (Fig. 7-5). On average, in subjects seated at one G, the uppermost 3.5 cm of lung were unperfused (representing 13 percent of the ventilated lung volume). At $+2G_z$, 10 cm were without perfusion and at $+3G_z$, the uppermost 14 cm, or 45 percent of the ventilated lung volume comprised an unperfused zone 1. Pulmonary arterial pressures were measured in the same subjects during subsequent centrifuge runs. (The results have already been noted in chapter 5, see p. 79). At $+1G_z$, the level in the lung at which the hydrostatic pressure gradient would have reduced the mean arterial pressure to equal alveolar (atmospheric) pressure, corresponded accurately with the upper level of blood flow as defined using ^{133}Xe. At $+2G_z$ or $+3G_z$, the agreement was less good, but the discrepancies were explicable in terms of small shifts in body position as the effective body weight increased (103). It appears that other factors which might affect the level to which blood rises in the lung, such as pulsatile vascular pressures (176), or surface forces acting from within the alveoli (31), do not exert a large effect, at least in healthy man during normal breathing.

Zone 2

Owing to the difficulty in correcting for regional changes in lung volume and counting geometry already alluded to, the ^{131} I-MAA studies do not allow a precise analysis of the way that blood flow varies down zone 2, other than showing that it does increase (Fig. 7-3). The ^{133}Xe-lung scanning technique does allow such an analysis, since a regional lung volume correction scan is applied and results are calculated in terms of blood flow per unit lung volume (67). At all levels of acceleration investigated, blood flow increased linearly down the lung and, as predicted, the rate of increase was doubled at $+2G_z$ and trebled at $+3G_z$ (Fig. 7-6). This implies that regional blood flow remains proportional to mean pulmonary arterial pressure, and this relationship is indicated, for one subject, in fig. 7-7. Here flow, in relative terms, is plotted against mean arterial pressure, on the assumption that this pressure was zero at the upper level of blood flow.

Zone 3

Theory suggests (see chapter 6) that, at the level down the lung where venous pressure comes to exceed alveolar pressure, the waterfall effect will cease to operate and blood flow will become proportional to the arterio-venous pressure difference. Since hydrostatic pressure gradients are the same in the arteries as in the veins, flow should thereafter remain constant or increase, solely by virtue of passive distension of pulmonary capillaries, brought about by the rising transmural pressure. A change in slope of the flow curve could, therefore, be expected at this level. In the ^{133}Xe-lung scanning studies, blood flow per unit lung volume remained linearly related to distance down the lung for calculated mean arterial pressures of up to 30 cm water - the lung base at $+3G_z$ (Fig. 7-7). Such high arterial pressures must have been associated with positive venous pressures (though these have not been measured during $+G_z$ acceleration), and it appears that, under the conditions of measurement, zones 2 and 3 had similar gradients of perfusion. There are several possible explanations for this finding.

a) The pulmonary capillaries could be so distensible that resistance to blood flow falls dramatically as the intramural pressure rises (see chapter 6, p.95-6).

b) Flow through the venous end of the capillary could be determined by interstitial, not alveolar pressure. This would have the effect of stretching the waterfall zone, as its lower extent would only be attained at that level down the lung where venous pressure came to exceed

interstitial pressure. Taking a lung with an average density of 0.3gm/cm^3 and height of 25 cm, the interstitial pressure at the base at $+3G_z$ would be 22.5 cm water (0.3 × 25 × 3). This approximates to the venous pressure expected at the base of the lung (Fig. 7-1), and a zone 3 would not be seen.

c) Airways close in the lower lung during exposure to acceleration (see chapter 4) and alveolar pressures might rise. Again the waterfall zone would be stretched, and zone 3 could disappear.

d) Pulmonary capillaries could exhibit a range of critical closing pressures. The venous pressure would then have to exceed this closing pressure plus alveolar pressure, rather than alveolar pressure alone, before zone 3 conditions applied, and this would occur lower down the lung. Recent evidence has shown that, under certain conditions, small vessels in the pulmonary circulation do exhibit a critical closing pressure (170).

It is apparent that the last three mechanisms suggested are all variations of a common theme, namely that the waterfall zone is extended to a region of higher venous pressure, by changes in the precise pressure relationships which govern flow through the pulmonary capillary bed.

e) The cardiac output falls during exposure to positive acceleration. The increase in flow seen at the lung base could merely represent a greater fraction of a smaller total blood flow going to that region. However, for this to have been the complete explanation for the ^{133}Xe findings, the cardiac output would have to have fallen by 45 percent at $+3G_z$, a far greater decrease than has been recorded at this level of acceleration (see chapter 5).

There is one further possible explanation for an increase in blood flow down zone 3, and this is supported by a considerable amount of experimental evidence.

f) The ^{133}Xe studies, which failed to differentiate between predicted zones 2 and 3, measured regional perfusion in terms of flow per unit lung volume. Since one effect of gravity is to cause a gradient in the size of alveoli down the lung (see chapter 3), the number of alveoli per unit lung volume will increase. The density of capillaries will follow the same pattern, and blood flow per unit lung volume will increase with distance down the lung, even if the flow per capillary remains constant.

Anthonisen and Milic-Emili (5) have measured regional blood flow per alveolus, by having their subjects inspire to total lung capacity before the distribution of radioactivity was measured. The quantity of isotope in each alveolus is not affected, but at TLC the alveoli are all of approximately equal size (185). Using the modified technique in various postures at one G, these workers were able to distinguish two regions of lung in which blood flow increased at different rates with vertical distance, but showed that, when blood flow was expressed per unit lung volume, the two regions became indistinguishable (5, 146). These regions may equate with West's zones 2 and 3. The masking effect provided by regional differences in capillary density will be exaggerated by acceleration, since the gradient in alveolar size is also made larger (see chapter 4).

No measurements of blood flow per alveolus have been attempted during positive acceleration, but reference to the $+G_x$ results, to be discussed shortly, suggests that variation in alveolar size is a major determinant of regional blood flow. Some of the increase in blood flow seen at the lung base does appear to be real

however, since it was also observed in the ^{131} I-MAA studies at $+2G_z$, though there was no further increase at higher levels of acceleration. In this technique the lung is scanned in supine subjects at one G and alveoli should be of uniform size from the apex to the base of the lung.

Zone 4

West has described a region of decreased blood flow in the most dependent parts of the lung, and refers to it as zone 4 (see chapter 6). He has postulated that it is caused by an increase in the resistance of extra-alveolar vessels to blood flow. Several mechanisms have been suggested which could be responsible. Normally, dependent alveoli are smaller and have less elastic recoil, so that the radial traction exerted on extra-alveolar vessels by the lung parenchyma may be less. West has described peri-vascular cuffing of these vessels under pathological conditions which may compress them (or allow them to contract). This mechanism could also be important during prolonged acceleration, where high intravascular pressures could lead to the extravasation of fluid into the lung parenchyma. A rise in alveolar pressure following closure of airways in the dependent lung might also promote a zone of decreased blood flow. It is interesting to note that zone 4 is increased at small lung volumes, just as is the tendency for airways to close (see chapters 3 and 8).

In neither the ^{131} I-MAA nor ^{133}Xe studies referred to above has a decrease in blood flow to the dependent lung been demonstrated, but, with ^{133}Xe, regional variations in alveolar size, if extensive enough, could again mask a decrease when flows are expressed per unit lung volume.

Forward ($+G_x$) acceleration

The normal resting distribution of pulmonary blood flow in supine subjects follows a pattern similar to that seen in seated man, when the shorter antero-posterior dimension of the lung is taken into account. Flow per unit lung volume increases linearly from the front to the back of the chest, and the entire lung is perfused. It was considered (146) that the whole lung lay in zone 3, a conclusion based upon the almost uniform distribution of blood flow found when expressed per alveolus.

Until recently, the only direct study of blood flow distribution carried out during $+G_x$ acceleration in man was made using the ^{131} I-MAA technique (130). Runs were carried out at $+4G_x$ and $+8G_x$ in three subjects and it was found, somewhat surprisingly when the marked influence of $+G_z$ acceleration is considered, that forward acceleration had no demonstrable effect. The implications are that, even at $+8G_x$, the lung still lies wholly in zone 3; mean arterial pressure at the back of the lung must be at least 150 cm water; and since the flow at the back of the lung was unaltered despite an increase in pressure there of some 120 cm water, pulmonary capillaries must be virtually indistensible. These findings receive some support from the observation that, in dogs, the anterior pulmonary vasculature is well filled at even $+10G_x$ (234).

Earlier, Jacquemin and co-workers (141) had shown that exposure to $+5G_x$ led to a marked change in the pattern in which carbon dioxide appeared at the lips during a prolonged expiration. We believe that this phenomenon, a downwards sloping plateau of CO_2, is only explicable if there is a region of lung containing little or no CO_2 which empties predominantly late in expiration. This effect will be discussed in detail in chapter 8 (p.131). We have noted a similar change at +5 to $+6G_x$ (Fig.7-8), though it is not seen in all subjects. The finding suggests that alveolar dead space (zone 1) can develop at these levels of forward acceleration. Other evidence for this supposition comes from the finding of a 35 percent reduction in

effective pulmonary capillary blood flow at $+8G_x$ (211), since this is again explicable on the basis of alveolar dead space.

Xenon-133 measurements

In order to resolve these differences, we have recently made measurements scanning the lung, using ^{133}Xe at accelerations of up to $+5G_x$. Subjects were studied supine, with hips and knees flexed to 120°, and supported on rigid, individually moulded couches, so that the posterior chest wall would not be displaced as the effective weight of the body rose. Injections of 133Xe were made at end-inspiration after 30 seconds of maintained acceleration, and the chest was then scanned from the right hand side, the detectors being traversed along an antero-posterior or postero-anterior axis. The perfusion scans so obtained were corrected for regional lung volume and counter geometry by means of repeat scans carried out at the same lung volume after rebreathing ^{133}Xe (67). The collimators used on the scintillation detectors gave a dynamic vertical resolution of 1.5 cm (101) and were developed for the $+G_z$ studies already discussed (Fig. 7-4).

Average results obtained from four subjects are given in fig. 7-9, as graphs of relative regional blood flow per unit lung volume plotted against detector position. At $+1G_x$, the distribution of blood flow is very similar to that reported by Kaneko *et al* (146), but contrary to the ^{131} I-MAA findings, flow to the anterior lung is decreased, and that to the posterior lung considerably increased at $+5G_x$. In two of the subjects, a zone 1 could be identified, and this extended over the most anterior two to three centimetres of the lung. If the upper limit of blood flow in these subjects is taken to indicate a mean arterial pressure of zero, then the pressure at the back of the lung would have been 70 to 80 cm of water. This is similar to values predicted from measurements of right atrial pressure (chapter 5). As with the $+G_z$ results obtained using the same technique, blood flow increased steadily from the front to the back of the lung with no evidence of a zone 3 (a falling off of the slope), nor of a zone 4 (a decrease in flow). Indeed, the perfusion gradient appeared to steepen towards the back of the lung, and this effect was seen in all four subjects (Fig. 7-9). The perfusion gradient was not, however, steepened in direct proportion to the applied acceleration, and in this respect the pattern of flow differed from that found during positive acceleration.

Blood flow over the most anterior 10 cm of lung increased linearly (Fig. 7-9) and could be extrapolated back to a virtual level of zero flow, and hence to a virtual level of zero pulmonary arterial pressure. Hydrostatic pressures could then be inferred for all levels in the lung, and a level was found where this pressure was unaffected by acceleration (a plane of hydrostatic indifference). This process is illustrated for a single subject in fig. 7-10, and the plane of hydrostatic indifference is found to lie seven to eight centimetres deep to the front of the chest, or 15 cm from the back. On average, in the four subjects, the level lay 5.5 cm deep to the front of the chest, or 15.5 cm from the back. While in this small series it is not possible to state whether the level of constant pressure should be related to the back, rather than to the front of the chest, it does seem that this level is further anterior than the level used by most workers for pressure reference (chapter 5). It is, however, close to the level selected by Bevegård and co-workers (26), and the mean pressure found is also similar to that recorded by these workers in supine subjects at one G. Such an anterior placement of the plane of hydrostatic indifference explains the rather even distribution of blood flow found at $+1G_x$ - all the lung being truly in zone 3 - and also explains the apparently slight effect of forward vis-à-vis positive acceleration (Fig. 7-6).

The absence of a clear cut differentiation between zones 2 and 3, even at $+5G_x$ in subjects where a zone 1 can be identified (i.e. Fig. 7-10), can be explained by any of the factors discussed in relation to this phenomenon at $+3G_z$ (p.109). In order

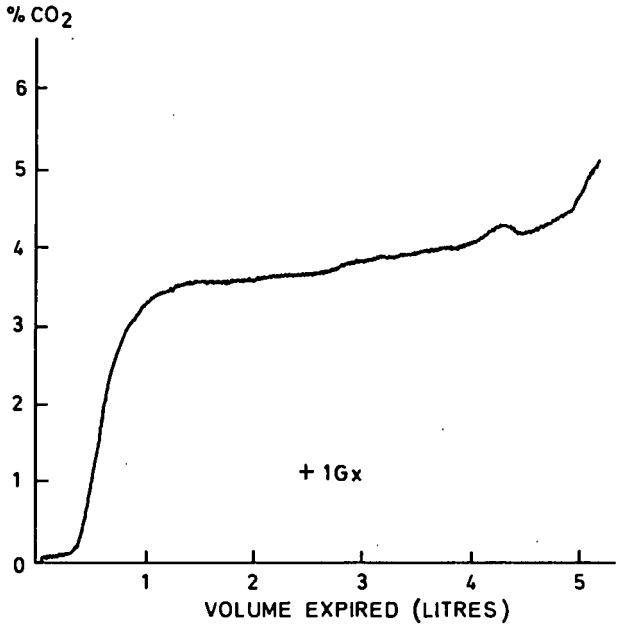

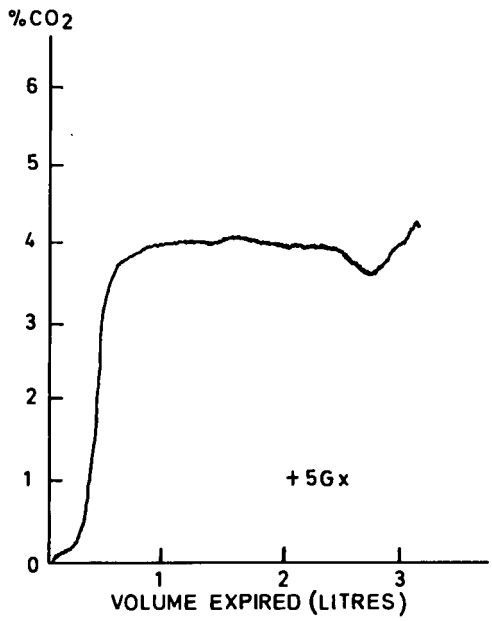

Fig. 7-8 Effect of forward acceleration on the concentration of CO_2 appearing at the lips during a slow, maximal expiration from TLC. Note the falling plateau concentration at $+5G_x$.

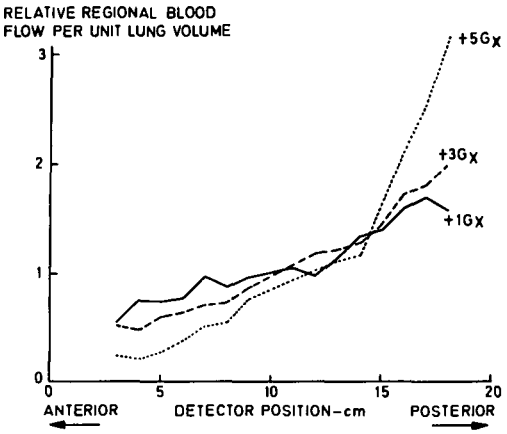

Fig. 7-9 Distribution of blood flow from front to back of the lung during exposure to +G acceleration - average results from four subjects. Flows are expressed per unit lung volume and scaled to an average regional value of 1.0. The position of the scintillation detector is measured from the front surface of the chest.

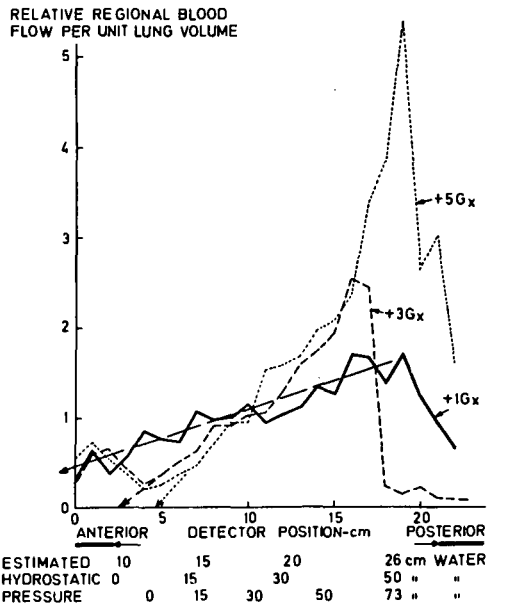

Fig. 7-10 Distribution of blood flow in one subject, plotted as in fig. 7-9. The upper levels of blood flow, obtained by extrapolation of the linear portions of the curves, are taken to represent zero arterial pressure, and hydrostatic pressures are calculated throughout the lung. At a level seven to eight centimetres below the front of the chest this pressure is 15 cm water and is independent of acceleration. The appearance of blood flow in the chest wall is an artifact caused by scattered radiation.

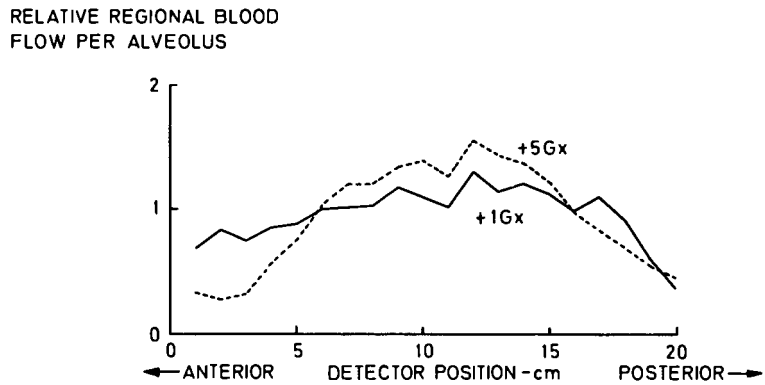

Fig. 7-11 Distribution of blood flow from front to back of the lungs during exposure to $+G_x$ acceleration - average results from four subjects. Flows are expressed per alveolus and are scaled to an average regional value of 1.0. At $+5G_x$, zones 2, 3 and 4 may all be identified.

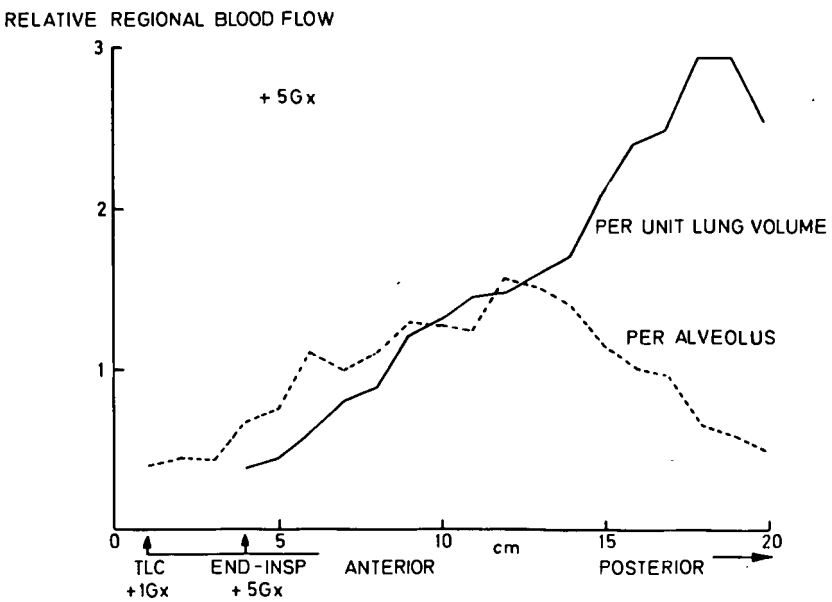

Fig. 7-12 Distributions of pulmonary blood flow at $+5G_x$, expressed per unit lung volume (solid line) and per alveolus (broken line) - average results from three subjects. The appearance of a deeper chest in the flow per alveolus curve is due to the scans being made at TLC.

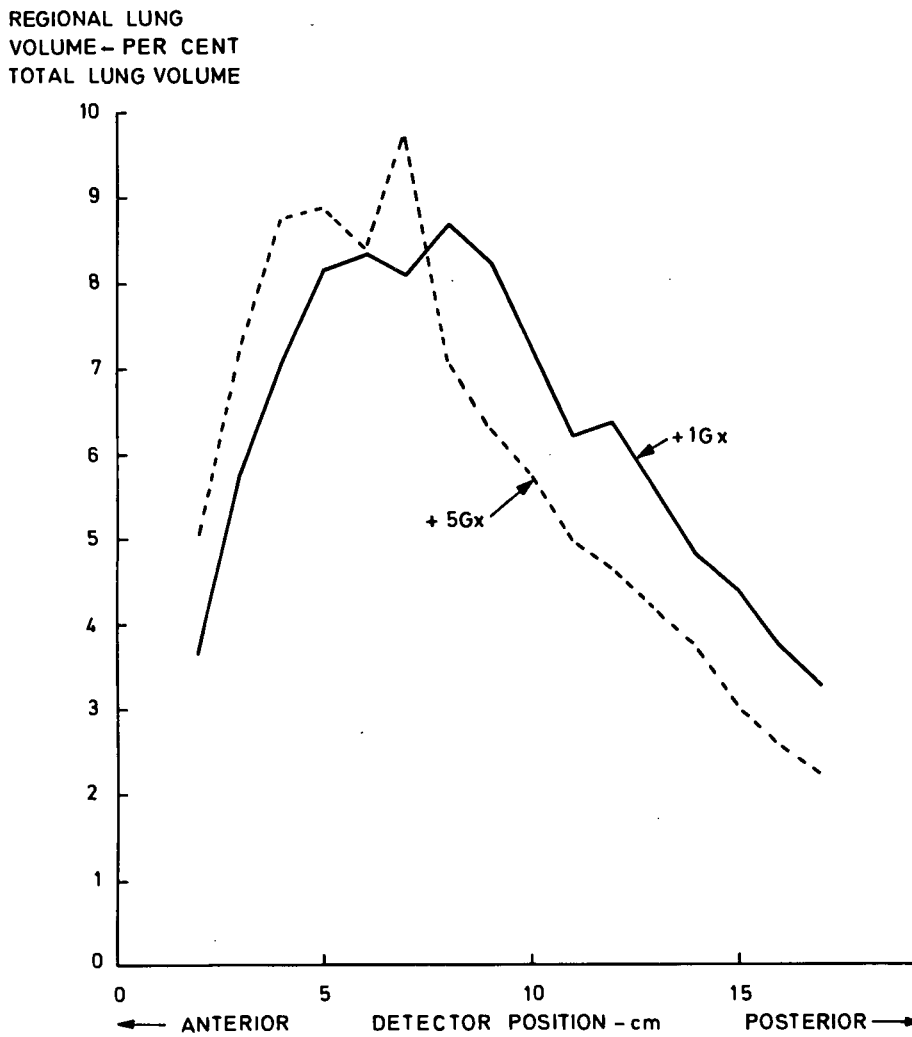

Fig. 7-13 The effect of $+5G_x$ acceleration on the regional gas content of the lung.
Ordinate: regional gas volume expressed as a percentage of the total volume.
Abcissa: distance in centimetres from the front surface of the chest.

to examine the role played by variations in alveolar size, and hence in capillary density down the lung, the ^{133}Xe technique was modified so that regional blood flow could be expressed per alveolus. The subject injected ^{133}Xe at end-inspiration as before, but he held his breath until the centrifuge had been stopped, then inspired to total lung capacity before starting the scan. Under these conditions alveoli should be of uniform size, but the distribution of blood flow recorded will be that present at the time of the ^{133}Xe injection.

The average distribution of blood flow found in four subjects at $+1G_x$ and $+5G_x$ is illustrated in fig. 7-11. Three of the subjects were common to the earlier studies, and fig. 7-12 compares their average distribution of blood flow per unit lung volume and per alveolus at $+5G_x$. It is apparent that great differences arise depending upon the method of measurement employed. Since the only difference can be in the relative size of alveoli at the time of scanning - the distribution of ^{133}Xe to the alveoli being the same in the two experiments - it follows that the effect of stopping the centrifuge and inflating the lungs maximally has been to dilute xenon in the most dependent alveoli by a factor of five. That is to say, at $+5G_x$, alveoli at the back of the lungs must have been compressed to about one fifth of their volume at total lung capacity. This is similar to the ratio of residual volume to TLC for the whole lung (54), and provides further evidence for alveoli in the dependent lung at $+5G_x$ being at minimal volume (see also chapter 4, p. 65). The effect of acceleration on relative alveolar size is also apparent in the lung volume scans, and fig. 7-13 gives the distributions of radioactivity across the lung at $+1G_x$ and at $+5G_x$, with the concentration of ^{133}Xe being rebreathed and the volume of the lung being the same in either case. The quantity of gas present in the anterior lung is increased by acceleration (the alveoli are distended and there is relatively less lung tissue), whereas, at the back of the lung, alveoli are compressed and the proportion of tissue to gas is increased.

Reference to fig. 7-13 shows that, at $+1G_x$, two distinct zones of perfusion may be seen, flow increasing linearly over the anterior 14 cm (zone 3) and then decreasing to the back of the lung (zone 4). At $+5G_x$, a further zone is seen, since flow increases rapidly over the third to seventh centimetre, and then more gradually from the seventh to the 14th cm. These would appear to be zone 2 and 3, and zone 4 occupies much the same volume of lung as at $+1G_x$.

The apparent increase in flow over the most anterior one to two centimetres of lung is an artifact, caused by the counting of radiation scattered by the anterior chest wall. There is, unfortunately, no way in which this effect can be eliminated, since the scattered radiation has an energy only slightly less than that of the primary gamma of ^{133}Xe.

While an increase in blood flow is apparent down zone 3, and this increase is exaggerated by acceleration (Fig. 7-11), it is much less than the increase suggested by flow per unit volume measurements (Fig. 7-9). Indeed, flow per capillary goes up by only 30 percent when the mean vascular pressure is doubled from 20 to 40 cm water. This observation suggests that the pulmonary capillaries are not very distensible (since flow is critically dependent upon vessel radius), and the main factors which determine regional blood flow are the waterfall effect, an increase in capillary density down the lung caused by compression of dependent alveoli, and the factor or factors responsible for the appearance of a zone 4.

Figure 7-11 showed that the extent of zone 4 was not changed significantly by an acceleration of $+5G_x$. This implies that the region is not defined by pressures within the vascular or tissue compartments, for these will all be increased dramatically by acceleration. At $+5G_x$, zone 4 corresponds quite well to a region of rapidly decreasing, or zero ventilation (see Fig. 4-12, p. 66), and the match is reasonable at $+1G_x$ too. It is probable that zone 4 has a mechanical origin, and is

related to the great reduction in alveolar size which occurs in the dependent parts of the lung. This would also be in keeping with its dependence upon overall lung volume (136).

Other acceleration vectors

It was stated earlier in this chapter that a non-central placement of the pressure reference point would lead to alterations in the distribution of the various perfusion zones, depending upon the posture of the body. Thus, the hydrostatic pressure at the back of the lung in a subject lying supine will be greater than that at the front of the lung in a subject lying prone, because the plane of hydrostatic indifference lies rather far forwards in the chest. The only experimental evidence in support of this conclusion is the observation that, in one subject, central venous pressures were measurably lower during $-G_x$ than during comparable $+G_x$ acceleration exposures (243). These pressures may be taken to reflect other vascular pressures within the thoracic cavity.

Lateral accelerations ($\pm G_y$) have not been studied to any great extent and the lateral localisation of the hydrostatic indifference point is unknown. At one G, almost identical distributions of perfusion were found in left and right lateral postures (146), which suggests that, in man, the reference point must lie fairly close to the mid-line.

In dogs, however, pulmonary arterial pressures measured at mid-lung level were greater in the left lateral ($+G_y$) than right lateral posture ($-G_y$), at one and at seven G (259). The values reported indicate that the level of hydrostatic indifference in this species lies about 2.5 cm to the right of the mid-line. In the right lateral posture ($-G_y$), acceleration led to a decrease in the fraction of the cardiac output which went to the superior part of the lung, and to an increase in the fraction supplying the mid-lung. There was, however, little change in the blood flow to the dependent lung region (221). These measurements were based on the distribution of radioactive microspheres injected into the outflow tract of the right ventricle. It was considered that the constancy of dependent lung blood flow at accelerations of up to $-6G_y$ represented an active movement of flow away from a region of developing atelectasis, but it could equally well have been caused by the occurrence of zone 4 flow conditions, since the technique used measured blood flow per alveolus.

The effect of negative acceleration ($-G_z$) is also virtually unexplored, since human tolerance to acceleration, when inverted, is so low. Because of the low placement of the hydrostatic indifference point within the chest, only a small fraction of the lung should comprise alveolar dead space and, as indicated in fig. 7-2, the unperfused zone at $-5G_z$ will be restricted to the costo-phrenic angles. At one G, the distribution of perfusion is more uniform in inverted subjects than in the same subjects upright (65, 102), an observation in keeping with the predicted overall rise in vascular pressures.

Weightlessness (zero G)

Measurements of blood flow distribution, made at differing levels of acceleration, allow the effects of weightlessness to be predicted by extrapolation of the results to zero G. This has been carried out for $+G_z$ acceleration in fig. 7-6, and it may be seen that blood flow becomes uniform. Similar arguments can be applied to the $+G_x$ findings, where non-uniformities in flow are again attributable to inertial forces. If zone 4 is the outcome of a gross reduction in alveolar dimensions brought about by the weight of the overlying lung tissue, this zone, too, should disappear during weightlessness.

Studies employing ^{133}Xe and lung scanning, as well as direct measurements of pulmonary arterial pressure made during exposure to positive acceleration, suggest that, during weightlessness, the mean pressure will be 15 cm water throughout the lung. It is not clear if the lung will be in zone 2 or 3, and indeed Permutt has suggested that it may be in zone 2 during inspiration and in zone 3 during expiration (206). The point is somewhat hypothetical since blood flow will be uniformly distributed in either case. Permutt points out that uniform distribution may be of doubtful benefit, for, compared with the distribution at one G, uniformity can cause little improvement in the efficiency of the lung as a gas exchanger (265), but postural changes in flow may be important in the fluid economy of the lungs.

Interstitial and alveolar oedema

Since a zone 1 has been demonstrated during both $+G_z$ and $+G_x$ acceleration, it is possible to calculate hydrostatic pressures throughout the pulmonary vasculature and to state, with reasonable certainty, what the greatest mean pulmonary arterial pressures are likely to be. At $+3G_z$ the highest pressure will be 30 cm water at the base of the lung (103) and, due to the low placement of the reference point, this pressure would only rise to 40 cm water at $+5G_z$. The colloid osmotic pressure of plasma proteins is of the order of 27 to 44 cm water (237), and in isolated lung preparations, transudation does not take place until the capillary pressure exceeds 38 cm water (89). Transudation should be minimal at even the higher level of $+G_z$ acceleration, and frank oedema is most unlikely to develop.

Taking there to be 13 cm of lung below the level of hydrostatic indifference in the supine posture (see p.112, and allowing for the thickness of the chest wall), the greatest pressure will be 28 cm water at $+1G_x$, 54 cm water at $+3G_x$, 80 cm water at $+5G_x$ and 119 cm water at $+8G_x$. Transudation could, therefore, occur at quite low levels of acceleration and frank oedema (interstitial, or even alveolar) is probable if centrifuge runs are prolonged. In the prone position, however, the greatest pressure would be only 47 cm water at $-8G_x$, and oedema should be far less likely to develop.

8

Acceleration atelectasis

Keefe, in 1958, reported on a number of pilots in the Royal Air Force who had developed respiratory symptons during flight (147). These symptoms consisted of cough, the inability to take a deep breath, and pain in the chest. In many cases there was radiological evidence of basal lung collapse. A survey of 107 aircrew showed cough to be the commonest symptom with an incidence of 38 percent; while cough together with difficulty in breathing were present in 25 percent; and these, plus chest pain in 20 percent (75). The incidence varied with the type of plane and sortie flown, and it was deduced that the condition was in some way related to the breathing of oxygen and to positive acceleration. Two theories were advanced: one postulated the mechanical collapse of intermediate sized airways followed by absorptional atelectasis, the other favoured the formation of oedema in the dependent parts of the lung. Oedema was considered to result from the combination of a raised capillary pressure secondary to acceleration and an increase in capillary permeability secondary to the toxic action of 100 percent oxygen.

Following these preliminary reports, an enquiry was made among tactical fighter pilots in the United States Air Force (158) and 34 cases of the syndrome were found. Of these, 31 (91 percent) had difficulty in taking a deep breath. The symptoms were attributed to absorptional atelectasis, but it was considered that the formation of oedema in the lower lung played an important role. The similarity between this condition and the effects of oxygen toxicity was noted, though the very different time courses of the two conditions were recognised. Later, the important role of an anti-G suit in the development of the syndrome was established and the term 'aeroatelectasis' was introduced (164). Atelectasis was attributed to restricted chest cage expansion with compression and reduced aeration of the lower lung. Proof that the full development of the syndrome required the combination of three factors, namely breathing 100 percent oxygen, exposure to positive acceleration, and wearing an anti-G suit, came from both in-flight studies (114), as well as from centrifuge experiments (140).

Green and Burgess (114) carried out a flight trial on 13 aircrew, each one flying pre-determined sorties in which the effects of acceleration, oxygen and anti-G suit were investigated in various combinations. Lung volumes were measured and chest x-rays taken before and after each flight, and a post-flight questionnaire was completed. After the high-G test sortie (a 30 minute flight including several exposures to +4 to $+5G_z$ each lasting 10 to 20 seconds) in which oxygen was breathed and an anti-G suit worn, 12 out of the 13 pilots experienced the classical symptoms, and the exception, though symptomless, had typical lung volume and x-ray changes. The x-ray findings consisted of obliteration of the costo-phrenic and cardio-phrenic angles, and shadowing at both lung bases which did not conform to the natural anatomical boundaries of the lung. An example is given in fig. 8-1. Total lung capacity was reduced in all subjects, as was inspiratory capacity, but the functional

Fig. 8-1 Chest radiograph of a pilot taken immediately following a flight in which he pulled positive acceleration while wearing an anti-G suit. 100% oxygen was breathed throughout. The shadowing seen at both lung bases is typical of $+G_z$ acceleration-induced atelectasis. (From Green and Burgess (114)).

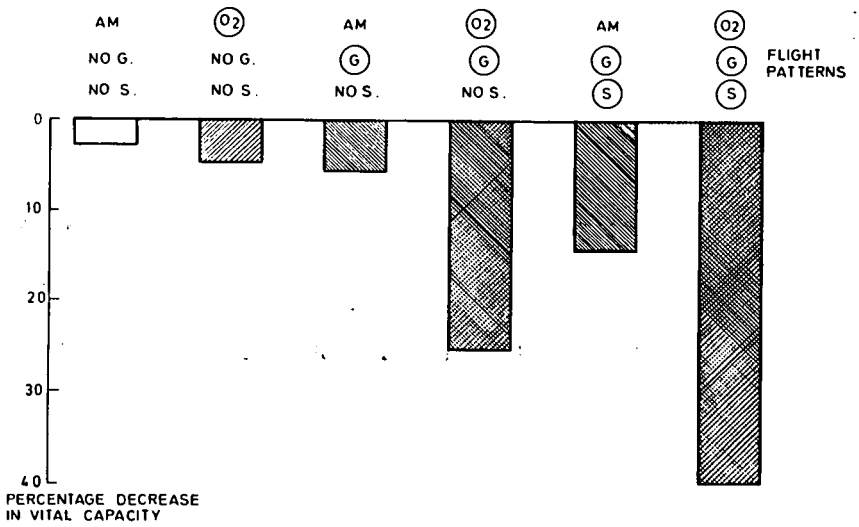

Fig. 8-2 Percentage reductions in vital capacity recorded following flights entailing various combinations of positive acceleration (G), anti-G suit (S) and 100% oxygen (O_2). Note that the reduction in VC is greatest when all three factors are present, and less when the pilots were breathing airmix (AM). (Redrawn from Green and Burgess (114)).

residual capacity was only reduced in two of the six subjects on whom a full analysis was carried out. Residual volume showed no significant change in any subject. Following high-G sorties, there was a greater reduction in TLC when 100 percent oxygen was breathed - this volume falling by an average of 2.15 litres in six pilots - than when the pilots were on airmix (oxygen being added to the inspired air to maintain a sea-level partial pressure of oxygen in the alveolar gas), the reduction then averaging 0.95 litres. The reduction was also greater when an anti-G suit was worn (2.15 litres) than when it was not worn (1.3 litres). In the other conditions investigated, namely $+1G_z$ with 100 percent oxygen or airmix, and high-G with airmix and no anti-G suit, reduction in TLC did not exceed 0.42 litres. The greatest change in lung volumes took place in vital capacity, and the reductions which were found following the six types of sortie are illustrated in fig. 8-2.

Green and Burgess considered that the chest pain was probably due to uneven inflation of the lungs, with localised over-distension and stimulation of vagal afferents in the lung parenchyma, or of pain endings in the mediastinum. It is interesting to note that the site of the pain varies with the site of the atelectasis, so that when atelectasis develops in the apices of the lungs (see p.142), the sensation is deep and central in the upper thorax with more tracheal irritation. With basal atelectasis it is usually sub-sternal (114). In either case it is exacerbated by deep inspiration. Green and Burgess concluded that the reduction in VC, up to 60 percent in some instances, was also reflex in origin, though in some cases it was due to the inspiratory effort being limited by pain or cough. No conclusions were reached as to the nature of the mechanism responsible for atelectasis, but mechanical closure of small airways with distal absorptional collapse was the preferred explanation, closure being considered to result from distortion of the lower lung.

An attempt has been made to measure atelectasis quantitatively following acceleration, by determining the compliance of the lung (113). Compliance was calculated from changes in oesophageal pressure recorded during quiet breathing, and showed a consistent reduction (-17 to -36 percent in seven subjects) after exposure to $+4G_z$ for 75 seconds, the subjects breathing oxygen and wearing anti-G suits. Determinations of vital capacity were made following the oesophageal pressure measurements, and showed a wider scatter, reductions varying from 10 to 50 percent. It was felt that the centrifuge run employed provoked varying degrees of atelectasis in different individuals, and that individuals showed differing vital capacity changes in response to a given compliance change.

Hyde and co-workers (140) carried out a study on the human centrifuge at the Wright-Patterson Air Force Base. The conditions investigated were various combinations of acceleration ($+1G_x$ and $_z$; $+6G_x$ with trunk inclined forwards 12°, hips flexed 78° and knees flexed 90°; +3 to $+3.5G_z$), differing inspired gas composition (100 percent oxygen, air, and oxygen at a positive pressure of 12.5 mm Hg), and anti-G suit utilization. It was assumed that atelectasis had occurred whenever the vital capacity fell by 0.5 litres or more following the test procedure. Experimental conditions were imposed for three minutes on up to 17 subjects, and the results are summarized in Table 8-1.

Studies were also carried out to see if atelectasis could be induced by restricting respiratory movements by loading the chest and abdomen with weights. No changes in VC were provoked, even though oxygen was breathed. It was concluded that three concurrent conditions were required for the development of atelectasis, these being:-

(a) Acceleration *per se*.

(b) Elevation of the diaphragm, inherent in $+G_x$ and caused by anti-G suit inflation during $+G_z$ acceleration.

(c) Breathing 100 percent oxygen.

The causative mechanism was considered to be inertial redistribution of the pulmonary blood volume, with tissue compression and lower airway obstruction, leading finally to absorptional atelectasis. Oedema formation was not implicated. Lung collapse has also been demonstrated radiographically after three minute exposures to forward accelerations of +5.6 to +6.4G_x, with the subjects breathing 99.6 percent oxygen (194), though areas of shadowing were less restricted to the extreme lung base than those seen following positive acceleration.

The term acceleration atelectasis may conveniently be used to describe the syndrome under discussion, although the breathing of 100 percent oxygen appears to be just as essential as either positive or forward acceleration. Indeed, an identical syndrome can be produced in the laboratory without a centrifuge (see p.140), though it is probable that gravitational acceleration is still a factor necessary for its development. Two basic theories attribute the syndrome to oedema, or to absorptional atelectasis (though absorptional atelectasis may also follow oedema). In both cases collapse of lung tissue follows the absorption of oxygen trapped distal to the obstruction (plugs of oedema or mucus, or mechanical closure of small bronchi or alveolar ducts). The basic difference between the two theories is that although each involves 100 percent oxygen, the one invokes its toxicity while the other invokes its solubility. The toxic action of pure oxygen will be considered first.

Oxygen toxicity

Pure oxygen has long been known to exert a toxic action on the lung. Thomas Beddoes in 1796 (24), in describing 'the effect of breathing oxygen air little diluted', wrote 'it is not the defect, but excess of oxygen, that is pernicious' in producing 'fatal mortification of the lung'. In reference to an experiment performed on a kitten exposed to 80 percent oxygen a colleague (Mr. Guillemand, of St. John's College, Oxford) states that 'the lungs were of a florid red colour in the oxygenated kittens ..... the edge of one lobe ..... was marked with livid spots (as in mortification)'. This may be the first post-mortem description of absorptional atelectasis, but it must be noted that the animal had been exposed to the oxygen rich atmosphere for 17 hours. Smith, in 1899, confirmed the pathological action of oxygen on the lungs of mice, and described the condition as a pneumonia. It took an average of 64 hours to develop, however (245).

The toxic action of pure oxygen has since been confirmed many times, but in man, an average exposure of 14 hours is required before obvious symptoms appear (55), though symptoms have been reported after only six hour exposures to 99 percent oxygen (25). Symptoms include substernal distress, a reduction in vital capacity and irritation of the nose and throat. The reduction in vital capacity has been attributed to absorptional atelectasis, radiological evidence of basal lung collapse being found after exposure to oxygen, at a pressure of 418 mm Hg, for seven days (184). Two possible modes of action were suggested:

(a) A direct action on bronchial epithelium with inflammation, exudation, destruction and collapse (16).

(b) An indirect action mediated by a decreased arterio-venous oxygen difference and a resulting reduction in carbon dioxide carrying power. The ensuing change in blood pH leads to dilatation of pulmonary capillaries followed by exudation (197).

Ernsting (75) was able to show a 25 percent reduction in carbon monoxide diffusing capacity after exposures to pure oxygen at atmospheric pressure lasting for only

three hours, and demonstrated that this effect was due to impaired diffusion across the alveolar-capillary membrane. Such changes are, however, too slow to be implicated in the development of acceleration atelectasis, where collapse can follow exposure to positive acceleration after only 15 minutes prior breathing of 100 percent oxygen (113)(see also p. 138).

A reduction in vital capacity has also been reported following a three hour exposure to 100 percent oxygen (37), and the associated symptoms of restrosternal pain aggravated by inspiration, and cough, are identical to those of acceleration atelectasis. It was concluded that atelectasis was due to the absorption of oxygen trapped distal to closed airways, the closure being mechanical in origin. These findings will be discussed later. In a further experiment where oxygen was breathed at a pressure of two atmospheres for 11 hours, the symptoms of cough and chest pain could not be relieved by deep breaths, but got progressively worse. This was attributed to a direct 'chemical' type of oxygen toxicity. The fact that symptoms did not occur when 50 percent oxygen in nitrogen was breathed for three hours at a pressure of two atmospheres (except in one subject with an upper respiratory tract infection) suggests that the partial pressure of oxygen breathed is less important than the absence of an inert gas, a finding which argues against oxygen exerting its atelectatic through a direct toxic action.

Oxygen solubility

The disappearance of air from an obstructed lobe of the lung was demonstrated by Lichtheim in 1879 (166), and the rapidity with which oxygen could be absorbed under similar conditions was determined by Coryllos and Birnbaum in 1932 (57). Oxygen took but 15 minutes compared with the 16 hours required for the complete absorption of the same volume of nitrogen. The same authors (58) refer to 'the nitrogen of the air acting as a physical brake by virtue of its slow absorption into the blood'. Dale and Rahn (61) showed that, initially, the rate of absorption of trapped gas is related to the solubility of that gas, hence the slow absorption of nitrogen. Subsequently, trapped gas equilibrates with mixed venous blood and its rate of absorption becomes proportional to regional blood flow. The driving force which brings about the continued absorption of gas, even when equilibrium has been reached, is equal to the alveolar-arterial oxygen difference less the arterio-alveolar carbon dioxide difference: this is of the order of 54mm Hg under normal conditions. Thus, the sum of the partial pressures of the component gases in the closed-off lung (approximately equal to atmospheric pressure), is greater than that of the gases in the tissues and venous blood. Using dogs, Dale and Rahn showed that oxygen was absorbed 63 times more rapidly than air, in good agreement with the earlier results.

In a similar preparation to that used by Dale and Rahn, Ernsting investigated the influence of environmental pressure and inspired gas composition on the rate of absorption of gas from a lung without effective ventilation (77). The two phases of gas absorption referred to above were confirmed, the first rapid phase representing loss of excess oxygen until the partial pressure of this gas fell to about 120 mm Hg. During this phase, the rate of absorption of gas was independent of nitrogen concentration, and was increased by a reduction in environmental pressure. The second, slow phase of gas absorption, which took place once equilibrium had been attained, was slowed further by both a raised nitrogen concentration and by a reduction in ambient pressure. It was concluded that the protection against acceleration atelectasis afforded by the addition of nitrogen to the inspired gas would be enhanced by a lowered environmental pressure.

The 'nitrogen brake' of Coryllos and Birnbaum may be compared to the marked reduction in atelectasis which results when as little as 20 percent nitrogen is added to the inspired gas prior to acceleration (113). This effect is illustrated in fig. 8-3.

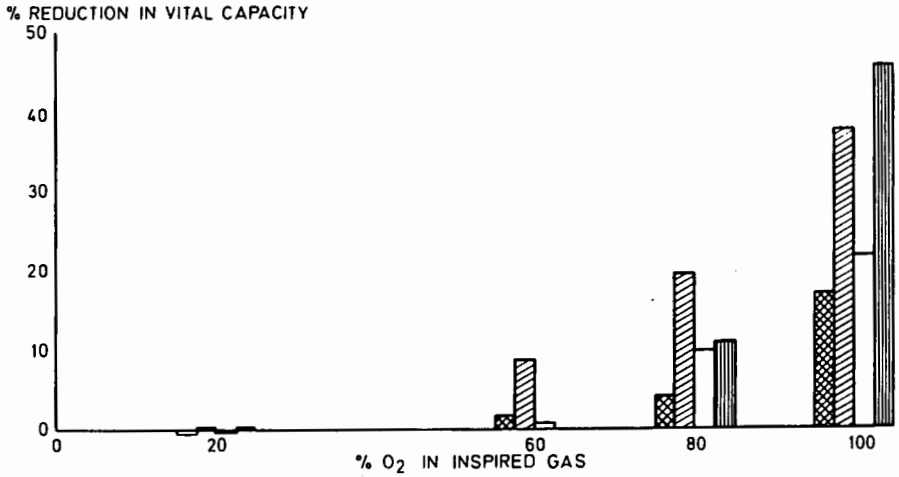

Fig. 8-3 The effect of nitrogen content of the inspired gas on the percentage reduction of vital capacity following exposure to an acceleration of $+4G_z$ for 75 seconds in four subjects.
(Redrawn from Green (113)).

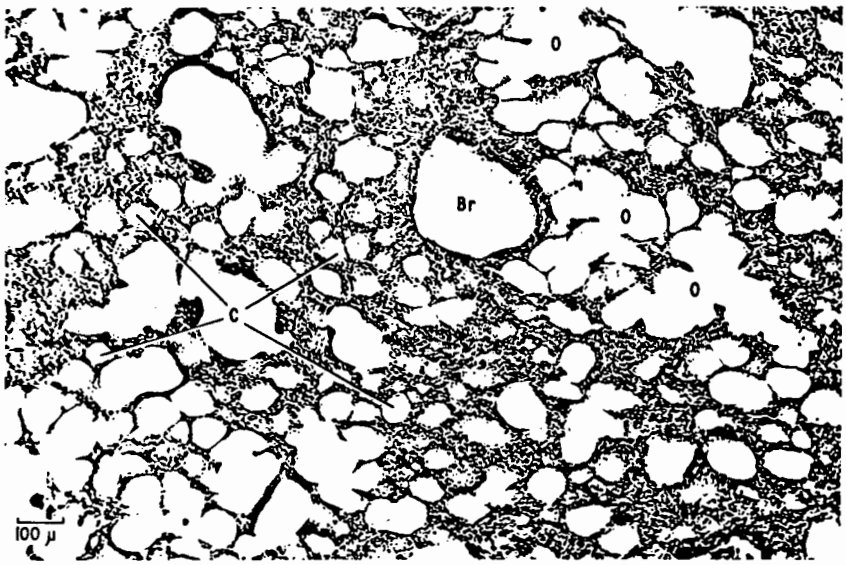

Fig. 8-4 Photomicrograph of a section taken from the base of the lung of a dog following exposure of the intact animal to $+1G_z$ for $4\frac{3}{4}$ hours, and to six, one minute centrifuge runs of up to $+4G_z$. Mixed areas of open (o) and apparently closed (c) alveoli surround a small bronchus (Br). Haematoxylin and Van Gieson's stain.

Addition of nitrogen to inspired gas has been advocated for aircraft cabin atmospheres, in order to reduce the incidence of acceleration atelectasis, 40 percent nitrogen in oxygen being the recommended breathing mixture for cabin altitudes of up to 25,000 ft. (76). It may also be noted here that the addition of as little as five percent nitrogen to the inspired gas was also sufficient to prevent atelectasis in a subject exposed for 72 hours to oxygen at a pressure of five pounds per square inch, though atelectasis did occur when the concentration of nitrogen was 2.5 percent or less (73). As already mentioned, atelectasis did not develop during prolonged exposures to 50 percent oxygen in nitrogen at a pressure of two atmospheres, even though the partial pressure of oxygen was equivalent to that of 100 percent oxygen at sea level.

If trapping of alveolar gas can be demonstrated under the conditions which lead to the development of acceleration atelectasis, then the solubility of oxygen appears adequate to explain the development of collapse, as well as the marked influence upon it of added nitrogen.

A number of further possible mechanisms must, however, be mentioned, if only so that they can be dismissed from further discussion.

Alveolar oedema

Oedema has frequently been invoked to explain the development of acceleration atelectasis. In theory, it could act directly to reduce the volume of aerated lung or, by plugging small airways, it could lead to absorptional atelectasis. As discussed in chapter 7, estimates of pulmonary arterial pressure, made in man during exposure to positive acceleration, suggest that oedema would be unlikely, even at the base of the lungs, at accelerations of less than +5 to $+6G_z$. Furthermore, attempts to obtain sputum from pilots with acceleration atelectasis have been unsuccessful (114). As will be shown later, gross atelectasis can be produced in a susceptible subject even at $+2.4G_z$, and an identical syndrome can be produced at one G by breathing oxygen at a small lung volume (see p.140). Under these conditions pulmonary oedema could not be implicated.

In dogs killed during exposure to positive acceleration, (rapid intra-atrial injection of saturated potassium chloride solution), no macroscopic evidence of pulmonary oedema was seen post-mortem, even after two minutes at $+4.6G_z$, though the dependent parts of the lungs were atelectatic and engorged with blood. Histologically, the lower lung of dogs, exposed to acceleration of up to $+4G_z$ while breathing air, showed gross engorgement of pulmonary capillaries, and the majority of the alveoli resembled closed off vacuoles at differing stages of contraction (Fig. 8-4). There was, however, no evidence of oedema fluid within these alveoli (100). Similar histological changes have been reported in the lungs of dogs following prolonged exposure to high levels ($+14G_x$) of forward acceleration (248). Furthermore, in dogs transfused with blood or dextran, or injected with alloxan to produce pulmonary oedema, filling of alveoli with fluid occurs late, and is not associated with trapping of air. Under these conditions atelectasis is uncommon, although the total volume of each fluid filled alveolus is reduced (246).

It is not, however, possible to rule out oedema as a causative or contributory factor in the development of atelectasis at high levels of acceleration. In chapter 5, it was predicted that capillary pressures would be high in the dependent parts of the lungs during exposure to forward acceleration, and this prediction was supported by the indirect evidence put forward in chapter 7. Vascular pressures in the lowest part of the lung at $+8G_x$ could be as high as 120 cm water (see p.119). Nonspecific areas of increased density were seen in X-ray films from two subjects after exposure to forward acceleration (up to $+6.4G_x$) while breathing 99.6 percent oxygen.

In one of these subjects the areas cleared within five minutes though the coincident linear changes of atelectasis persisted for up to 20 hours. The nonspecific changes were considered to be 'compatible with some degree of pulmonary oedema' (194).

Anti-G suit

The role of the anti-G suit in the development of acceleration atelectasis has already been referred to, its effect being attributed to restricted chest cage movement and diminished aeration of the lower lung (164). Since the lung is freely mobile within the thoracic cavity, it is difficult to see how regional changes in ventilation could be brought about, and this mechanism must be discounted. The influence of an anti-G suit on lung collapse will be considered later, in relation to the change in lung volume also induced (p.140).

Reflex pulmonary atelectasis

Reflex bronchoconstriction has been shown to produce atelectasis in experimental animals (253), the adequate stimulas being pulmonary embolism, intra-abdominal manipulation, or blunt injury to the chest wall. The stimulus required is, however, far greater than could ever occur in normal flight or on the centrifuge. In fact, positive acceleration has little direct effect on airway resistance (chapter 2), so that gross bronchoconstriction can be ruled out during the development of atelectasis.

Pulmonary surfactant

It has been shown that the breathing of 98 percent oxygen by cats and rabbits until death, never more than seven days, leads to an increase in the surface tension of surface active material obtained from the lungs (93). Similar results have been found in dogs (40), and rabbits may show such changes after only three hours exposure to oxygen (118). Loss of surfactant would increase the tendency for alveoli to contract down, and so could lead to atelectasis. This factor may be important in relation to the effects of prolonged oxygen exposure, but its onset is too slow to be relevant to acceleration atelectasis. Loss of surfactant has also been reported to occur in rabbits in which unilateral atelectasis has been produced by pneumothorax. Again, up to eight days is required for the loss to occur (163). It is possible that the increased surface tension found after prolonged exposure to oxygen is secondary to atelectasis rather than a cause of it.

The Demonstration Of Unventilated Alveoli In The Lower Lung

While the lower lung appears to be better ventilated than the upper lung under normal conditions (see chapter 3), Milic-Emili and co-workers (185) have shown that the distribution of inspired gas is sensitive to lung volume: at small lung volumes the normal distribution is reversed and the first part of an inspiration from residual volume goes to the upper lung. In other words, alveoli in the lower lung are poorly ventilated at small lung volumes. Slagter and Heemstra measured airway resistance at differing lung volumes using the interruptor technique, and found that it rose abruptly in the lower 20 percent of the vital capacity (241). These results have since been confirmed (44) and suggest that complete closure of airways may take place at residual volume.

Poorly ventilated regions within the lung have also been demonstrated by a number of manoeuvres which have in common a reduction in the end-tidal volume of the lung. Probably the first investigation into the effects of shallow breathing was that of Haldane et al. (119). These authors studied the effect of restricting abdominal movements during respiration by means of corsets, and showed that breathing became periodic. This they attributed to anoxaemia secondary to uneven ventilation of the lung. Lewis and co-workers (165) exposed subjects, from the level of the

xiphisternum downwards, to a positive pressure of 75 mm Hg. Pulmonary arterial and pulmonary wedge pressures were raised by 25 mm Hg or so, and the end-tidal lung volume was reduced. When the volume of gas forced out of the lungs during the process of pressurisation was compared with changes in functional residual capacity determined by helium dilution, it was found that a volume of gas was present in the lungs (610 and 376 ml respectively in two subjects) which did not exchange with the inspired air. Confirmation that this gas was physically trapped was obtained by releasing the pressurisation near the end of a nitrogen wash-out, whereupon the expired nitrogen curve showed a transient rise.

A similar technique was used to demonstrate the presence of gas-trapping when the chest was strapped tightly at full expiration (42), and when an anti-G suit was inflated at $+1G_z$ (114). A fall in the oxygen tension of arterial blood, attributed to complex ventilation-perfusion abnormalities, was obtained when the functional residual capacity was reduced by up to one litre by inflating balloons under a rubber corset (171). The result of these procedures sets a precedent for the occurrence of unventilated but gas containing lung under conditions of reduced end-tidal lung volume, and point to a possible mechanism for the role played by an anti-G suit in the development of acceleration atelectasis.

Superficially, the effect of positive acceleration on the distribution of pulmonary ventilation suggests that the ventilation of the lower lung is improved at $+3G_z$ (chapter 4). However, radioisotopic techniques for the measurement of the distribution of ventilation usually rely on some degree of ventilation to bring the isotope into the alveoli, before rates of wash-in or wash-out, or the distribution of the inspired gas, can be determined. Regions of air trapping will not be visualised by any of these procedures.

In order to overcome this problem, regional ventilation was studied by recording radioactivity wash-out curves after ^{133}Xe had been brought to all perfused alveoli in the pulmonary blood stream (99). Under resting conditions, ventilation within a small counting field in the lower lung was found to be uniform, but under conditions which would have led to atelectasis had oxygen been the gas breathed ($+3G_z$ for 2.5 min with inflated anti-G suit, but breathing air), the wash-out curve was found to contain two exponential components, one with a half-clearance time of 190 seconds (see Fig. 4-8, p. 61). This slow component was found to correspond to the rate at which xenon was removed from the lower lung during breath-holding, and was considered to represent the rate at which xenon was lost to the pulmonary capillary blood from alveoli lacking effective ventilation. The fact that these alveoli were initially able to take up xenon from the capillary blood, and so contribute to the recorded radioactivity, shows that they must have contained gas: this, together with their non-ventilation, suggests air-trapping.

When oxygen was breathed under identical conditions, the slow component disappeared from the recorded wash-out curve and the vital capacity was reduced by over two litres - this run is illustrated in the right hand graph in fig. 8-5. Disappearance of the slow component was also associated with an increase in the quantity of xenon appearing in pulmonary venous blood (this was inferred from the greater radioactivity recorded by a scintillation counter placed over the abdomen (Fig. 8-5)). It was considered that the increased quantity of xenon which appeared in the systemic circulation was due to this gas being shunted through atelectatic lung. Since the development of atelectasis was accompanied by the disappearance of the unventilated alveoli (no slow wash-out component), it was concluded that the collapsed alveoli were the same as those previously demonstrated to be unventilated. As these alveoli became collapsed and free of trapped gas, xenon would no longer be able to diffuse into them from the pulmonary capillary blood and they would no longer be detectable by external scintillation counting. The process of collapse also implies trapping of gas rather than a simple lack of ventilation, for in this

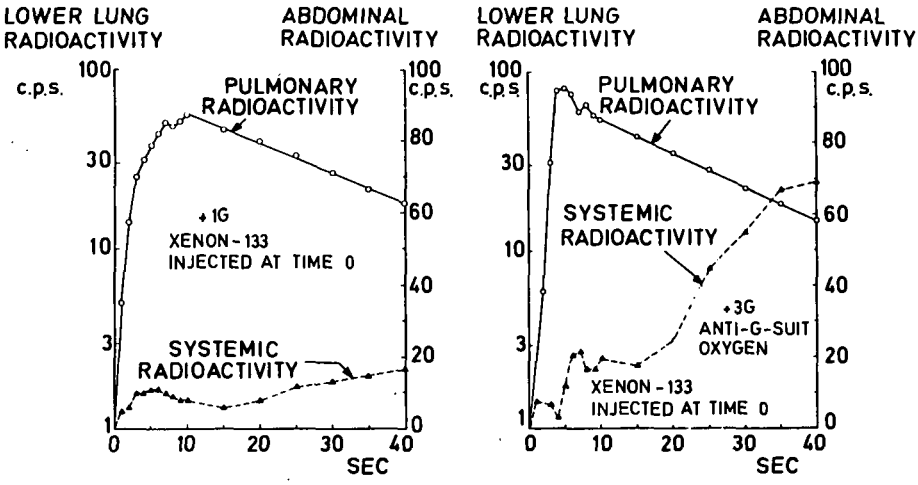

Fig. 8-5 The appearance of radioactivity in, and its subsequent wash-out from the lower lung (solid line), and its appearance in the systemic circulation (dashed lines), following i.v. injection of ^{133}Xe under the experimental conditions noted on each graph. The wash-out of pulmonary ^{133}Xe remains a simple exponential function (a straight line on the semilogarithmic plot) even after atelectasis has been induced (right hand graph), but more of the isotope then enters the systemic circulation. The wash-out curves contrast with the compound exponential form recorded in the same subject during positive acceleration when breathing air (see Fig. 4-8).

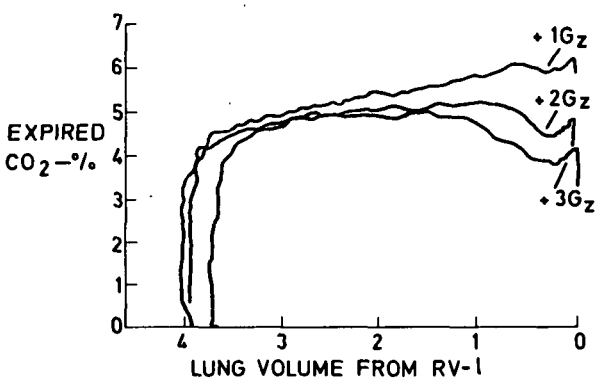

Fig. 8-6 Concentration of carbon dioxide appearing at the lips recorded against volume of gas expired, during maximal expirations from TLC, at accelerations of +1, +2, and $+3G_z$. Positive acceleration reduces the peak expired CO_2 concentration and leads to a reversal in the slope of the terminal portion of the plateau.

latter case, oxygen would flow down the patent airways as fast as it was absorbed into the pulmonary capillary blood.

It appears from these observations that the combination of positive acceleration and anti-G suit inflation leads to the trapping of gas in a fraction of the alveoli present within the lower lung. This fraction was estimated at 10 to 15 percent of the alveolar gas volume present in the lower lung counting field. If the trapped gas were oxygen, its great solubility would lead to absorptional atelectasis, whereas if the trapped gas were air, the presence of nitrogen would delay the development of atelectasis.

Some further light is thrown upon the mechanism of gas-trapping, and the role of an anti-G suit in the generation of acceleration atelectasis, by the results of single breath carbon dioxide tests carried out during centrifugation (96). Figure 8-6 shows the concentration of CO_2 which appears at the lips during slow expirations of the vital capacity at +1, +2 and $+3G_z$, recorded against expired volume on an X-Y plotter. The effect of positive acceleration is to reduce the peak expired CO_2 concentration, and to bring about a fall in the slope of the expired CO_2 plateau towards the end of the expiration.

The reduction in the peak expired concentration of CO_2 cannot be explained on a straightforward basis of hyperventilation, since breath by breath integration of the recorded concentration and expired volume curves failed to demonstrate any preceding excess elimination of this gas (96). It is, however, accounted for by an increase in dead-space (alveolar dead-space), as would occur if the upper lung were unperfused (see chapter 7). Estimates of alveolar dead space, based on the areas of expired CO_2 recordings made at +1 and $+3G_z$, showed that as much as one third of the ventilation could have come from unperfused lung at the higher level of acceleration. Thus, during expiration, CO_2 in alveolar gas coming from the lower lung undergoes continual dilution by CO_2-free gas coming from the upper, unperfused lung.

The fall in expired CO_2 concentration, which is seen towards the end of an expiration at +2 and $+3G_z$, is due to a diminishing contribution to the expirate of gas coming from a region of low ventilation-perfusion ratio (the lower lung). Such an effect has been demonstrated in the dog by tying off the pulmonary artery leading to one lobe of the lung, and constricting the bronchus leading to the same lobe to delay its emptying (270). During acceleration, the plateau reversal takes place quite abruptly (see also Fig. 8-7), as if at some specific lung volume gas were to stop flowing from alveoli within the well perfused lower lung. Again, this suggests the sudden development of airway closure in the dependent lung.

A terminal fall in the plateau concentration of expired CO_2 has also been reported during normal breathing in two subjects exposed to a forward acceleration of $+5G_x$ (141). This observation suggests that gas-trapping occurs during $+G_x$ acceleration in the same way as has been suggested for positive acceleration, and also that the alveolar dead-space increases under these conditions. The effect has also been seen occasionally in subjects riding on the R.A F. centrifuge at accelerations in the range of +5 to $+7G_x$ (Fig. 7-8, p.113).

By making similar expired CO_2 concentration recordings during maximal expirations, the lung volume at which plateau reversal occurred could be determined under varying conditions of acceleration (105). Figure 8-7 illustrates a series of such recordings made at accelerations of +1 to $+4G_z$, the three and four G runs being repeated with the subject wearing an inflated anti-G suit. The point of plateau reversal indicated in each tracing required correction for the response time of the gas analyzer, as well as for the time taken for a sample of alveolar gas to appear at the lips. The relevant lung volume can then be calculated, and as may be seen,

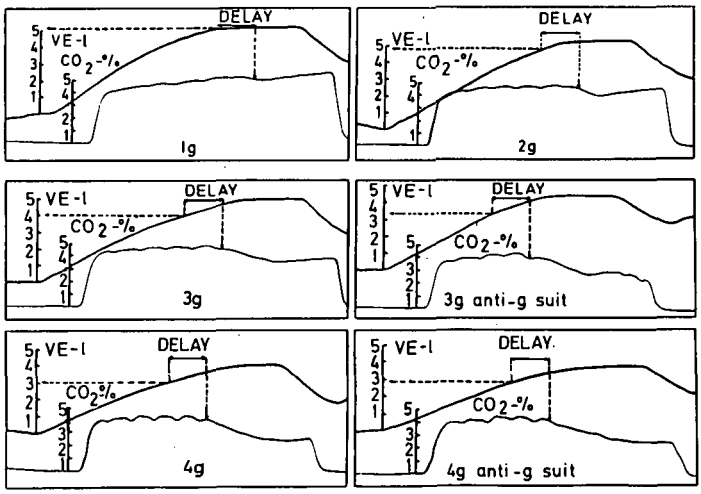

Fig. 8-7 Single breath CO_2 tests carried out from TLC to RV during exposure to increasing levels of positive acceleration (+1 to +4G_z). Arrows indicate the expired volumes, in litres from TLC, at which the slope of each CO_2 plateau shows a reversal, allowance being made for the response time of the gas analyser. Each recording lasts for 9.8 seconds. Amplitude of cardiogenic oscillation is also increased by acceleration.
(From (105), by courtesy of Br. J. hosp. Med.).

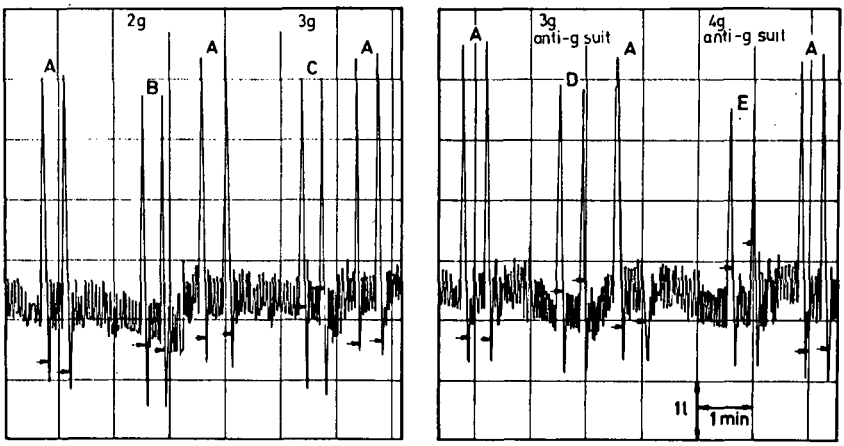

Fig. 8-8 Spirogram showing tidal breathing and maximal expirations from total lung capacity, during which expired CO concentration was monitored (Fig. 8-7).
Each arrow indicates the lung volume at which the expired carbon dioxide concentration started to fall. Oxygen was added to the air in the spirometer circuit at a constant rate of 300 ml/min. This subject developed gross atelectasis whenever he breathed oxygen at +3 or + +4G while wearing an anti-G suit.

it increases with acceleration, but is not affected by the inflation of an anti-G suit. At $+1G_z$, the expiratory reserve volume at plateau reversal averaged 295 ml in the four of the six subjects investigated in whom this point was identifiable. At $+2G_z$, this point could be identified in five subjects, and the volume averaged 870 ml. At $+3G_z$, plateau reversal was seen in all six subjects, and the volume at reversal averaging 1,150 ml without, and 1,110 ml with, an inflated anti-G suit. At $+4G_z$ with the anti-G suit inflated, the ERV at plateau reversal averaged 1,245 ml, or 40 percent of the vital capacity. If the interpretation of the mechanism of plateau reversal given above is correct, then gas-trapping will occur in the lower lung at a volume which increases with acceleration, and at higher levels of acceleration trapping may occur during resting tidal breathing.

When an anti-G suit is inflated, the end-expiratory volume of the lung is decreased, and trapping of alveolar gas may persist throughout the respiratory cycle. This effect is demonstrated in fig. 8-8, where the lung volumes at CO_2 plateau reversal have been indicated on the spirogram. Under one G conditions, trapping only occurs close to residual volume, and alveoli remain open and ventilated throughout normal respiration. At $+2G_z$ (marked B on Fig. 8-8), trapping occurs earlier in expiration, and at $+3G_z$(marked C) it takes place within the resting tidal volume. Under these conditions airways in the lower lung would open and shut with each breath. When the anti-G suit is inflated at +3 or $4G_z$ (marked D & E on Fig. 8-8), the FRC is decreased, and alveoli remain closed off during resting respiration. Under these conditions, this subject did develop atelectasis when he had breathed oxygen prior to the onset of acceleration.

A further feature of the expired CO_2 recording, which is shown clearly in fig. 8-7, is the increase in the amplitude of cardiogenic oscillations (ripple) with exposure to positive acceleration. These ripples are caused by variations in regional gas flows during expiration which result from the action of the heart (85). Their amplification during acceleration suggests a greater inequality in ventilation-perfusion ratio between upper and lower lung. Thus, a peak in CO_2 concentration occurs when a greater fraction of the expired gas has come from a region of lung with a low ventilation-perfusion ratio (the lower lung), and a trough when proportionally more gas has come from a region of high ventilation-perfusion ratio (the upper lung). Assuming that the influence of the heart's action on regional gas flow is unaffected by acceleration, then acceleration causes there to be greater differences in the CO_2 contents of alveolar gas in the upper and lower lung.

A rather similar phenomenon to the terminal fall in the concentration of expired carbon dioxide discussed above is seen in single breath nitrogen tests (32). The subject takes a breath of oxygen and then expires to residual volume while the concentration of nitrogen in the expirate is recorded against expired volume. A sharp rise in nitrogen concentration is seen after about 90 percent of the vital capacity has been expired (Fig. 8-9). In contradistinction to the CO_2 findings, this change does not appear to be so clearly advanced by positive acceleration, though the trace does begin to rise earlier at $+3G_z$, though at a lesser rate. A possible explanation for the discrepancy is that the CO_2 single breath test is more sensitive to sequential emptying of the lung, because of the enormous range in alveolar concentrations existing prior to expiration. The nitrogen gradient which results from the uneven distribution of the preceding breath of oxygen is much smaller.

A further single breath technique has recently been adapted for centrifuge studies, and the findings support the above conclusions(145). In this test, the uppermost parts of the lung are labelled by inspiring 100 ml of a tracer gas (argon) from residual volume, and washing it in to total lung capacity with air. The concentration of tracer appearing at the lips is then recorded during the subsequent expiration (144). The apical distribution of tracer when inspired in this way by seated subjects has been confirmed by experiments in which a bolus of ^{133}Xe was

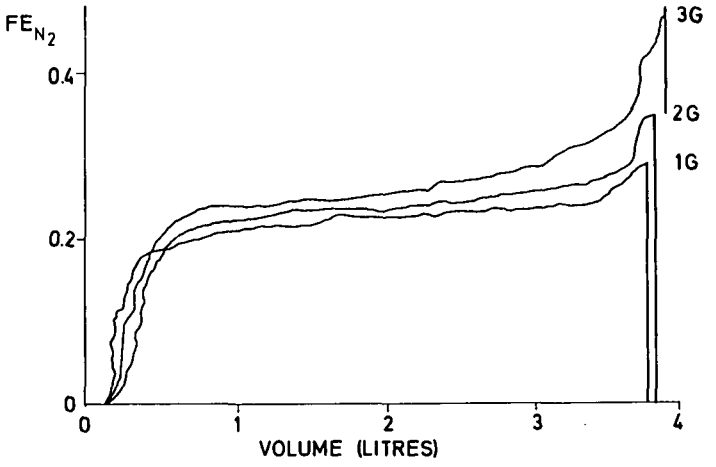

Fig. 8-9 Single breath nitrogen tests obtained by expiring to residual volume after a breath of 100% oxygen. The fraction of nitrogen present in the expirate is recorded against volume of gas expired using an X-Y plotter. Note the terminal rise in nitrogen concentration which results from a reduced contribution to the expirate of gas from units in the lower lung having a low nitrogen content.
(From Bryan and Anthonisen (32), by courtesy of Aerospace Med. Ass.).

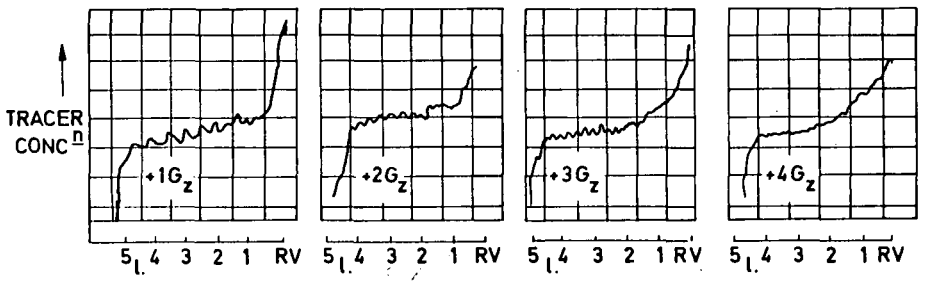

Fig. 8-10 Expired tracer concentration recorded against expired volume during maximal expirations at a low flow rate, after tracer had been introduced into the lung at RV at +1G$_z$. There is an abrupt terminal rise in tracer concentration which starts earlier in expiration with increasing positive acceleration.

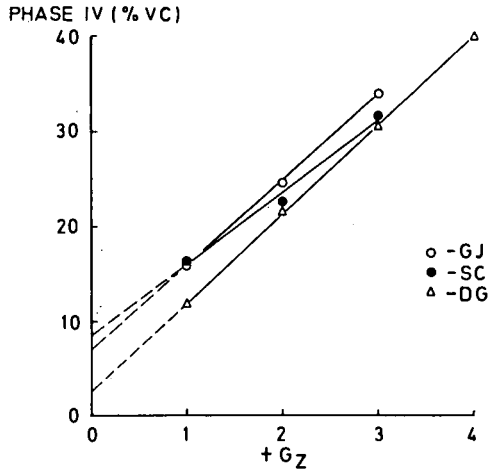

Fig. 8-11 The volume of expirate contributing to the terminal rise in plateau concentration of tracer (phase IV) expressed as a fraction of the vital capacity, plotted against acceleration for three subjects. Extrapolation to zero-G suggests that little gas trapping would occur during weightlessness.
(From Jones et al (145), by courtesy of J. appl. Physiol.).

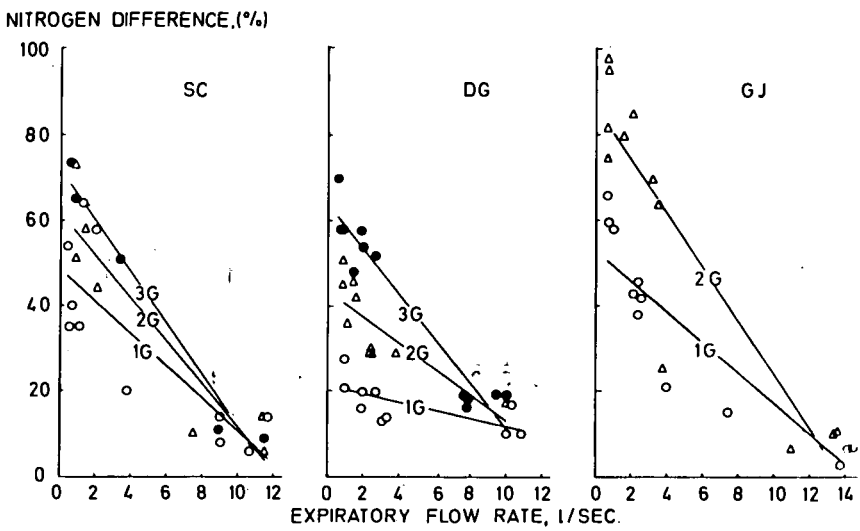

Fig. 8-12 The effect of expiratory flow rate on the magnitude of the terminal rise in plateau concentration of tracer, at differing levels of positive acceleration, for three subjects. A nitrogen difference of 100% indicates that the terminal litre of expirate would contain twice as much tracer gas as the penultimate litre.
(From Jones *et al* (145), by courtesy of J. appl. Physiol.).

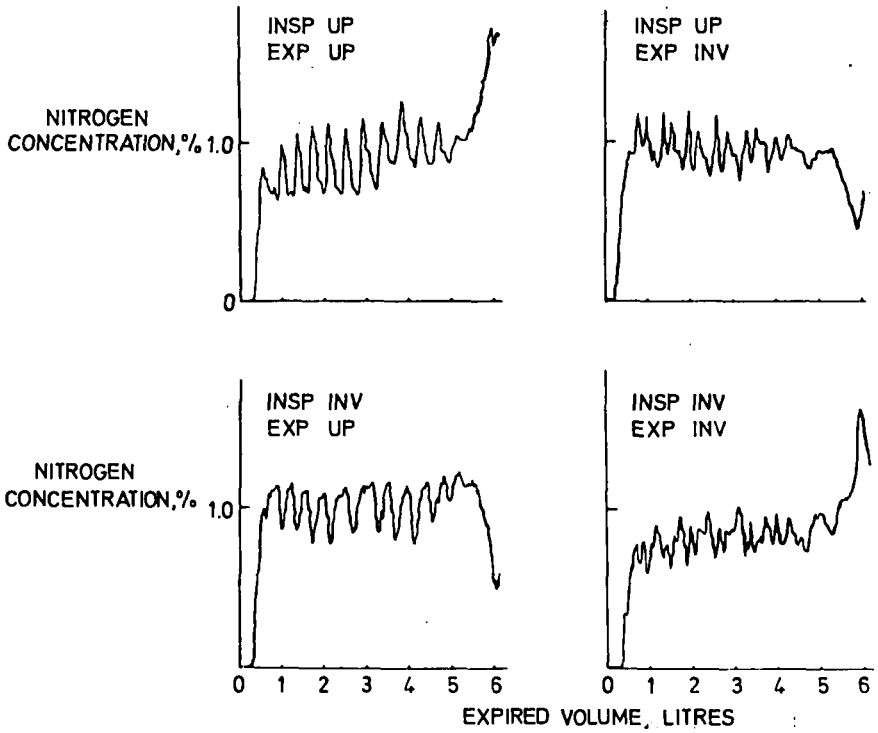

Fig. 8-13 Recordings of expired tracer gas concentration plotted against expired volume for different postures, obtained at flow rates of about 0.5 litres/sec. When the entire procedure was carried out with the subject upright (insp. up; exp. up) or inverted (insp. inv; exp. inv.), a terminal rise in tracer concentration was seen. When the subject was rotated through 180° between inspiration and expiration (insp. up; exp. inv. or insp. inv; exp. up), the reverse pattern was seen. Thus, the tracer always went to the uppermost lung tissue, regardless of anatomy, and dependent airways always became closed off towards the end of expiration. (From Clarke *et al* (50), by courtesy of Clin. Sci.).

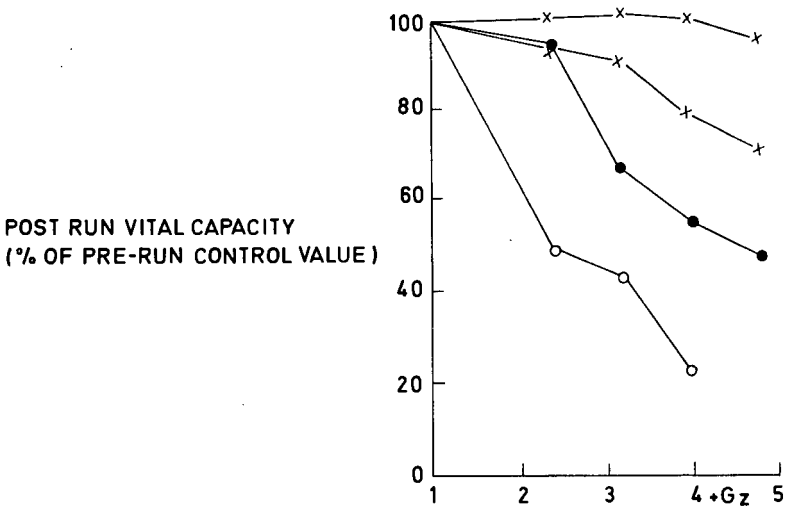

Fig. 8-14 Reductions in vital capacity plotted against the level of acceleration imposed ($+G_z$). The centrifuge runs each lasted for one minute, and subjects wore anti-G suits and breathed oxygen for 15 minutes and during the runs. Note the differing sensitivity to acceleration exhibited.

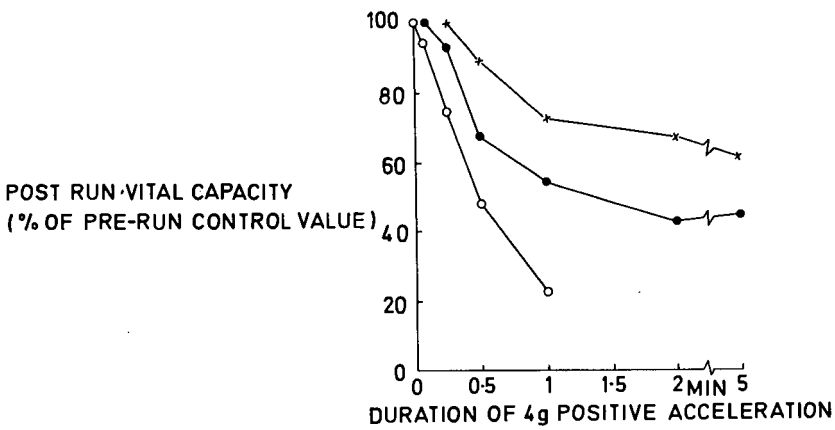

Fig. 8-15 Reductions in vital capacity plotted against the duration of exposure to an acceleration of $+4G_z$. The three subjects (omitting the least susceptible one whose results were given in Fig. 8-14), wore anti-G suits and breathed oxygen for 15 minutes before and during the runs. Note that one subject developed a significant reduction in VC after only five seconds at peak acceleration.

inspired at RV (66), but the use of conventional gas analysers eliminates the random scatter inherent in radioisotope counting.

On the centrifuge, the tracer gas employed was nitrogen, and ambient nitrogen was excluded by breathing an argon/oxygen mixture. As in the single breath CO_2 and N_2 tests described above, a terminal phase in expired tracer concentration was seen where the slope of the plateau changed abruptly (Fig. 8-10). This point is again taken to represent closure of dependent airways, and an increasing contribution to the expirate of alveolar gas from the upper, labelled lung. With $+G_z$ acceleration, this terminal phase occurred at a greater lung volume. This feature may be seen in the recordings, obtained from a single subject at up to $+4G_z$, illustrated in fig. 8-10. The volume of expirate making up the terminal phase is plotted against the imposed acceleration, for three subjects, in fig. 8-11. Lung volume at the onset of airway closure increases linearly with acceleration and extrapolates back to a small fraction of the vital capacity at zero-G. At high expiratory flow rates this effect is abolished (Fig. 8-12), showing that with high transpulmonary pressures the gravitational dependence of regional airway closure becomes of secondary importance. Extrapolation of fig. 8-11 to total lung capacity suggests that, at $+9G_z$, ventilation of the upper lung will be predominant at all lung volumes, and alveoli in the most dependent lung will be at minimal volume even at total lung capacity.

It is interesting to note here that identical test results are obtained at one G in upright or inverted subjects (50), and when the posture is altered through 180°between inspiration and expiration, the terminal rise in tracer concentration is converted into a terminal fall (Fig. 8-13). A similar reversal has been reported in the conventional single breath nitrogen test (32). These results indicate that, at low flow rates (up to two litres per seond), the pattern of lung emptying is dictated by inertial closure of dependent airways and is insensitive to the anatomy or physical dimensions of the lung. There are, however, changes in the earlier part of the expired tracer plateau which are not so easily explained and which require the assumption of a small difference in compliance between the upper and lower lung (50). The ventilatory behaviour of the inverted lung will be considered further in chapter 11.

Factors modifying the development of acceleration atelectasis

Acceleration

As mentioned earlier in this chapter, atelectasis has been produced on centrifuges by exposure to positive, as well as forward accelerations, of the order of +3 to $+3.5G_z$ and +5.6 to $+6.4G_x$, with durations of three to 3.5 minutes. Oxygen must be breathed at all times and an anti-G suit is required for the syndrome to develop during positive acceleration. Atelectasis can occur at lower levels of acceleration in susceptible subjects, and fig. 8-14 illustrates percentage reductions in vital capacity recorded in four subjects following accelerations of from $+2.4$ to $+4.8G_z$, each exposure lasting for one minute. Oxygen was breathed for 15 minutes before as well as during the runs, and anti-G suits were worn on all occasions. One subject halved his vital capacity following exposure to only $+2.4G_z$. One subject was very resistant to the development of atelectasis and showed only a small reduction in vital capacity following $+4.8G_z$. In all four subjects, however, the reduction in vital capacity was related to the magnitude of the applied acceleration.

The mechanism by which acceleration could lead to atelectasis has already been discussed, gas-trapping taking place at greater lung volumes with increasing acceleration. The mechanism responsible for trapping is probably mechanical, alveoli and their ducts (or even large airways) becoming unstable when they are

compressed below a certain critical size. The factors responsible for alveolar stability, namely geometry, surface forces and tissue forces (178), become less effective as the radius of curvature of the alveolus is reduced. Therefore small alveoli may behave like balloons or bubbles placed in parallel, some shrinking further as others expand. It has been shown theoretically that, if the gas pressure is reduced in a unit of lung consisting of a hemispherical alveolus on a cylindrical duct, the duct will be closed by surface retractive forces when the radius of curvature of the alveolus becomes more than double that of the duct (51). At this point the alveolus becomes closed off while still containing some 20 percent of its initial volume. This mechanism was suggested to be important in determining the residual volume of the lungs.

If the lungs are not evenly compressed during expiration, but, due to inertial forces, the lower lung is more compressed than the upper lung (see chapters 3 & 4), then minimal volume will be attained first by alveoli within the most dependent lung tissue. As expiration continues, this region will extend up the lung to reach the apex at a lung volume which is the overall residual volume of the lung. Residual volume, as measured by helium dilution, is not affected by acceleration (see chapter 2), and is also not changed significantly in acceleration atelectasis (114).

An alternative mechanism would also explain gas-trapping in the lower lungs. This is that airways close when the pressure outside them exceeds the pressure inside. With a decrease in lung volume this would occur first in the most dependent lung tissue, where interstitial pressure is increased to the greatest extent by the weight of overlying lung.

Anti-G suit inflation

An anti-G suit exerts its entire effect on the development of acceleration atelectasis by virtue of abdominal compression, since atelectasis does not develop when only the leg bladders of the suit are inflated during acceleration (97). During exposure to forward acceleration, a similar rise in intra-abdominal pressure is caused by the weight of the abdominal viscera, so that in either case the diaphragm will be forced upwards and the resting end-tidal volume of the lung will be reduced. As discussed earlier, such a reduction in lung volume could lead to the persistence of gas-trapping throughout normal respiration, depending upon the level of acceleration imposed.

Oxygen

The effect of oxygen on the development of acceleration atelectasis has already been discussed and, in the presence of trapping, is satisfactorily explained by the solubility of this gas. Oxygen must be breathed for some 15 minutes prior to acceleration so that alveolar nitrogen is reduced to an ineffective concentration (113), but once peak acceleration is attained, the development of atelectasis is no longer sensitive to the composition of the inspired gas. Thus, if air is pre-breathed, atelectasis will not develop even if oxygen is breathed during prolonged exposures to acceleration; nor does the change from breathing oxygen to air with the onset of acceleration prevent the development of atelectasis (97). This observation provides additional evidence that alveoli which collapse are unventilated.

Length of exposure to acceleration

Most centrifuge runs reported to have led to the development of atelectasis have lasted for three minutes or more, but it has been shown that, in a susceptible subject, significant atelectasis can develop within five seconds at $+4G_z$ (97). This subject suffered a loss of vital capacity at a rate of 4.8 litres/min. In three subjects investigated, the reduction in VC followed an approximately exponential time course

with a half-time of 25 seconds, though the asymptotic values varied widely (Fig. 8-15).

The volume of gas that can be absorbed from the lung during the development of atelectasis can be estimated from the fact that each 100 ml. of blood perfusing the lung can only take up some eight millilitres of oxygen. If the total pulmonary blood flow is five litres per minute, oxygen can be absorbed at a maximum rate of 400 ml/min. Much of this blood will be perfusing ventilated lung and will not contribute to atelectasis, and it is unlikely that oxygen could be absorbed from unventilated alveoli at a rate greater than 100 to 200 ml/min. This requires one quarter to one half of the pulmonary blood flow to perfuse unventilated alveoli, and if this fraction were to remain unchanged following atelectasis, a 25 to 50 percent pulmonary shunt would result. This may be compared with actual values of shunts obtained during exposure to acceleration, and these will be discussed in chapter 10.

In fact, this perfusion of unventilated lung may actually be increased by the development of atelectasis (193), with result that the shunt may be greater than predicted. It appears that a reduction in VC, which can occur at a rate of nearly five litres per minute, must be caused by a loss of alveolar volume of no more than 100 to 200 ml/min. This discrepancy can only partly be explained by the regional variations in alveolar volume which result from acceleration, and it must be concluded that the reduction in VC is largely a reflex limitation to inspiration.

Positive pressure breathing

The degree of atelectasis (as measured by the reduction in VC which follows exposure to an acceleration of $+6G_x$) is unaffected by breathing oxygen at a positive pressure of 12.5 mm Hg (see table 8-1, p.149), though the runs were described as being 'more comfortable' than when oxygen was breathed at ambient pressure (140). When judged from radiographs, changes 'indicative of atelectasis' appeared more pronounced when air or oxygen was breathed at a positive pressure of 33 mm Hg during exposure to an acceleration of $+5.3G_x$ (194); though two of the three subjects investigated noted subjective improvement during the run. The situation was somewhat confused, since the subjects had undergone previous acceleration exposures, breathing both air and oxygen at ambient pressure, before the chest radiographs were taken.

During exposure to $+4G_z$ acceleration, the breathing of oxygen at a positive pressure of 13 mm Hg did not modify the development of atelectasis but, in four subjects who breathed oxygen at a positive pressure of 22 mm Hg, the resulting loss of VC was halved in three of them and abolished in the fourth, when compared to identical runs in which oxygen was breathed at ambient pressure (97). This improvement was interpreted as being due to the increase in FRC which resulted from pressure breathing.

Lung volume

The development of acceleration atelectasis is modified by a number of manoeuvres which alter the end-tidal lung volume, and there is a sound theoretical basis for this effect (see p. 59). The development of atelectasis should therefore be sensitive to a voluntary change in FRC, and this has indeed been found to be the case. Atelectasis will not occur during exposure to $+4G_z$ acceleration, even if oxygen is breathed and an anti-G suit worn, if the subject breathes at an unnaturally large lung volume; it will, however, occur even without the inflation of an anti-G suit, if the subject breathes at an unnaturally small lung volume. Positive centrifugal acceleration is not essential for the development of atelectasis, for, if the subject breathes oxygen close to his minimal lung volume for two minutes, a reduction in vital capacity may be recorded (100).

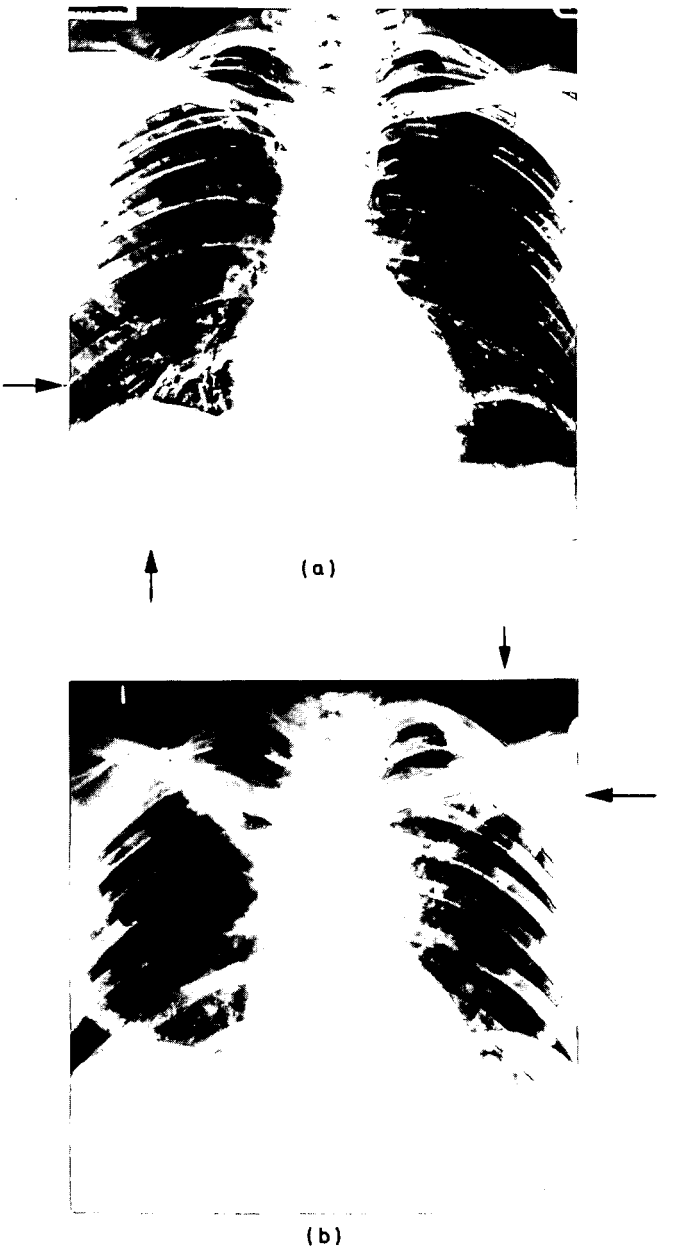

Fig. 8-16 Chest radiographs taken after the induction of low lung volume atelectasis with the subject erect (a) and inverted (b). Areas of atelectasis (arrowed) always develop in the dependent lung.
(From (105), by courtesy of Br. J. hosp. Med.).

A similar result has been reported by Burger and Macklem (38), who obtained symptoms typical of acceleration atelectasis, as well as shifts in inflation pressure-volume curves, following two basically similar manoeuvres carried out in normally seated subjects. In the first of these, the subject pre-breathed oxygen, then hyperventilated on oxygen before holding his breath at residual volume for 90 seconds. In the second experiment the subject breathed voluntarily between RV and 750 ml. above RV for two minutes. If oxygen had been breathed prior to the start of low lung volume breathing, then symptoms and signs attributed to absorptional atelectasis developed in five of seven subjects investigated. A mechanism involving airway closure at low lung volumes was invoked to explain these findings.

Posture

When acceleration atelectasis develops during exposure to positive acceleration, the collapse is seen, radiographically, to occur in the lowermost parts of the lung (114). Typical changes may be seen in figs 8-1 and 8-16a, though this second radiograph actually illustrates a case of low lung volume breathing atelectasis (see below). Linear areas of increased density were also seen in the lower lung fields after exposure to forward acceleration whilst breathing oxygen (194). If these changes result from airway closure in a region of lung prematurely attaining its minimal volume, then they should appear first in the most dependent lung tissue. During exposure to forward acceleration, this region would be expected to be the posterior lung fields. In the study reported above, the acceleration imposed was not strictly forwards, since the trunk was inclined by 12°, and a positive acceleration component was thereby introduced. Under these conditions, the most dependent lung tissue would have been the posterior parts of the lower lobes, and it is not surprising that the radiographic changes were found in the lower lung fields. It is unfortunate that lateral films were not taken as these would have demonstrated any antero-posterior distribution of atelectasis. It may be noted, however, that the radiographic signs of atelectasis were less restricted to the extreme base of the lung than those seen following exposure to positive acceleration, where the areas of increased density are generally to be seen 'hugging the diaphragm' (114).

In order to demonstrate a gravitational, rather than anatomical basis for the distribution of atelectasis, three subjects were investigated during exposure to positive and negative accelerations of one G (seated erect and 'seated' inverted), collapse being induced by breathing oxygen at a minimal lung volume for two minutes. The subjects prebreathed oxygen for 15 minutes and the inverted posture was only maintained for the relevant period of low lung volume breathing. The procedure was found easier to carry out when inverted, presumably because headwards displacement of the diaphragm aided the maintenance of a small lung volume. This is also, probably, the reason why the resulting changes in vital capacity were greater, the reduction averaging 36 percent compared with the 20 percent found when the subjects had remained seated upright. Chest radiographs were taken following similar manoeuvres, and when the apex had been the most dependent part of the lung during the procedure (subject inverted), all three films obtained showed clear signs of apical atelectasis, the lung bases being unaffected. Figure 8-16 illustrates two films taken from one subject after the development of symptoms firstly when seated erect (a), and secondly when inverted (b). The first film shows 'evidence of bilateral segmental atelectasis at the bases', whereas the second shows 'an extensive degree of atelectasis in both upper zones'.

While these findings support the hypothesis that airway closure occurs in dependent lung tissue at low lung volumes, a second interpretation is theoretically feasible. Even if airway closure occurred in areas scattered throughout the lung, absorptional atelectasis would only take place in regions having an adequate blood flow - that is, the dependent lung (see chapters 6 & 7). Studies on the influence of posture on the distribution of blood flow within the lung show a rather different pattern from that

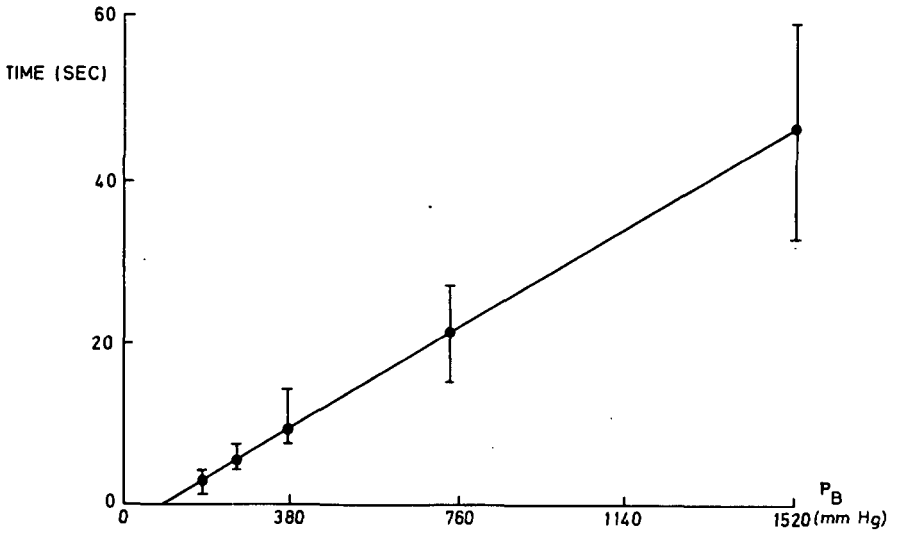

Fig. 8-17 Effect of barometric pressure on the time taken for complete collapse of oxygen filled lungs following tracheal occulusion, in the rat. (From Rahn and Farhi (216), by courtesy of Fedn Proc.).

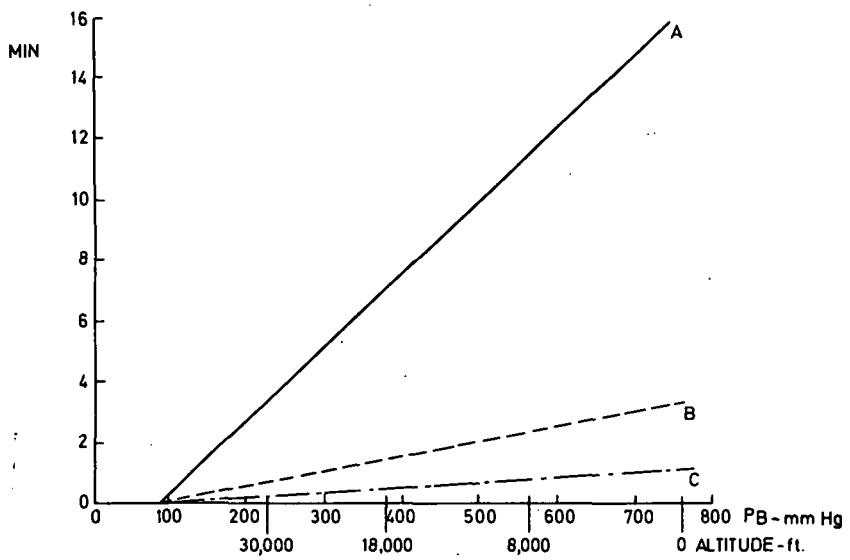

Fig. 8-18 Line A. The effect of altitude on the time of complete collapse of oxygen filled lung, assuming that the breath is held at full inspiration and that the oxygen uptake is 340 ml/min.
(From data of Rahn and Farhi (216)).
Line B takes into account the smaller volume of alveoli under conditions appropriate to the development of acceleration atelectasis.
Line C takes into account the added effect of uneven blood flow distribution, and may be used to predict the rate of development of atelectasis in the dependent lung during exposure to positive acceleration.

which would be required to explain the X-ray findings, however. During inversion, blood flow is more uniformly distributed than in erect subjects (65, 102), but atelectasis is still restricted to the extreme apex of the lung. Furthermore, recent evidence suggests that, at FRC in seated subjects, the blood flow to the extreme base of the lung may actually be less than that some 10 cm higher up (136), but again atelectasis appears maximal at the base.

Barometric pressure

While much experimental work shows that the rate of loss of lung volume during breath-holding or tracheal occlusion is critically dependent upon barometric pressure, no studies on acceleration atelectasis have so far been made at simulated altitude. Robertson and Farhi studied the effect of barometric pressure upon the lung collapse which resulted from tracheal occlusion in rats which had been breathing pure oxygen (226). They found that the time taken for complete collapse was directly proportional to the ambient pressure, and this relationship is illustrated in fig. 8-17. It was concluded that, for any segment of lung where blood flow is proportional to lung volume, the time of collapse $(t) = k(P_B - 87)$, where k is a constant proportional to the ratio of lung volume to oxygen uptake, and 87 is the sum of the partial pressures of carbon dioxide and water vapour present in the alveolar gas (216). These findings have been confirmed in man at simulated altitudes of up to 40,000 ft, by measuring the changes in lung volume which took place during breath-holding, after oxygen had been breathed to wash-out lung nitrogen (161).

The time for complete collapse, assuming that the breath is held at maximum inspiration and that the oxygen uptake is 340 ml/min, is indicated by the solid line in fig. 8-18, taken from the work of Rahn and Farhi (216). Under these conditions, a period of 16 minutes is required for complete collapse at sea-level, but this is reduced to seven minutes at an altitude of 18,000 ft, and to only 3.5 minutes at an altitude of 30,000 ft. These figures are unrealistic in relation to the development of acceleration atelectasis for several reasons. Firstly, the breath is not held at full inspiration, but a subject exposed to an acceleration of $+3G_z$ and wearing an anti-G suit will in fact be breathing at a lung volume of about 2.4 litres. Secondly, alveoli in the lower lung where atelectasis develops are at their minimal volume: that is, at the volume they would adopt if the subject were to expire to residual volume at one G. Line B in fig. 8-18 has been drawn by substituting an effective lung volume of 1.4 litres, and assuming the same oxygen uptake of 340 ml/min. Now, only 3.2 minutes are required for complete collapse at sea level, but this is still rather long in comparison with the 25 seconds half-time found for the time course of vital capacity reduction during the development of acceleration atelectasis. A third correction is required, however, since the pulmonary blood flow is not uniformly distributed during acceleration. At $+3G_z$, alveoli within the dependent lung will receive about three times the blood flow per unit alveolar volume which would be present under conditions of uniform distribution (103). Line C in fig. 8-18 has been drawn taking this factor into account, and it may be seen that complete collapse now requires but 64 seconds at sea-level, and a mere 28 seconds at an altitude of 18,000 ft. The rate of collapse predicted under sea-level conditions agrees very well with the rates of vital capacity reduction recorded during exposures to positive acceleration (Fig. 8-15).

Mechanism of acceleration atelectasis

The changes in the regional ventilation of the lung which result from exposure to positive acceleration, and the way in which these changes could lead to the development of atelectasis, are summarised in fig. 8-19. The first diagram illustrates the resting situation in an upright lung subjected to normal gravitational acceleration $(+1G_z)$. Alveoli in the lower lung are smaller and better ventilated than those

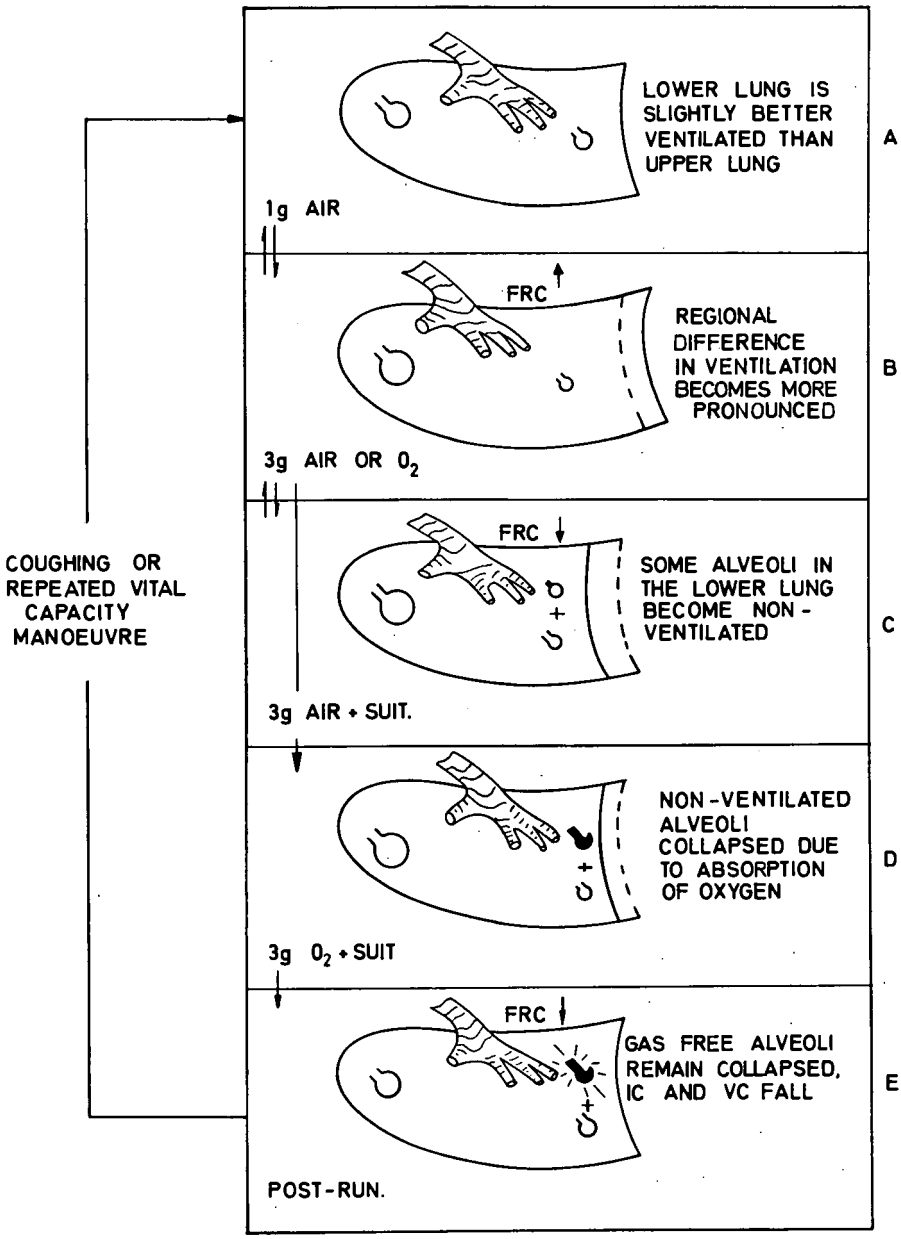

Fig. 8-19 Diagram illustrating changes which may take place in alveoli within the lower lung during exposure to positive acceleration, and the dependence of these changes on the gas breathed (air or oxygen), and on whether or not an anti-G suit is worn. The possible directions in which changes may take place are shown by arrows. Symbols indicate the relative sizes of alveoli in the lung and their relative ventilations (inversley related to size).

in the upper lung, the difference being due to the weight of the intervening lung tissue (chapter 3). When the lung is exposed to a positive acceleration of, for example, $+3G_z$, these changes become exaggerated; but the simultaneous increase in the end-tidal lung volume, which results from a fall in the resting level of the diaphragm, reduces the degree to which alveoli in the lower lung are compressed (diagram b, Fig. 8-19). When an anti-G suit is inflated (or the lung volume reduced voluntarily), the lower lung is compressed further and some alveoli attain their minimal volume and become closed off (diagram c). There is no evidence at the present time to suggest whereabouts in the airway this closure takes place, though theory suggests that smaller airways may be the first to close (51).

When alveoli became closed off, they contain trapped gas. If the trapped gas contains a significant fraction of nitrogen, 20 percent or more, then absorption is delayed and the trapping is reversible. If the alveoli contained oxygen prior to becoming closed off, then rapid absorption of the trapped gas into the pulmonary capillary blood leads to further shrinkage until the unit becomes gasless and atelectatic. This situation is illustrated by diagram d in fig. 8-19. Atelectasis is not progressive, but its development follows an exponential time course to a final value determined by the conditions applied, and by the individual susceptibility of the subject, at which time all unventilated alveoli will have been rendered gasless. The resulting atelectasis is irreversible, or only very slowly reversed, during quiet breathing, presumably because a critical opening pressure must be exceeded within the airways in order to overcome surface forces, and this is only achieved during a forced inspiration or cough.

Returning to normal gravitational acceleration results, in the situation shown in the final diagram of fig. 8-19, the continued presence of collapsed alveoli leads to a restriction in inspiratory capacity and to a reduction in vital capacity. This reduction is largely reflex, since the loss in VC is far greater than the volume of lung rendered atelectatic.

A situation identical to that illustrated in diagram c of fig. 8-19 occurs at one G when the volume of the lung is reduced, excessive upwards displacement of the diaphragm having the same effect as downwards compression of the lung. As before, if the trapped gas is oxygen, absorptional atelectasis will develop with an identical symptomatology. Such a situation can be produced experimentally by a variety of techniques which have already been referred to. It may also occur during anaesthesia owing to the high solubility of nitrous oxide (57), or if high concentrations of oxygen are administered (195), especially when depressive drugs or muscle relaxants are employed. Massive lung collapse attributable to absorptional atelectasis has been described under such conditions (215), though atelectasis may not always be detectable by radiography (195). The terms 'miliary collapse' or 'dispersed absorption collapse' have been used to describe the condition (214). Atelectasis could be prevented by maintaining a normal, or larger than normal end-tidal lung volume, and by occasional hyperinflations of the lung to ensure that all alveoli are open and ventilated. This procedure should also prevent the development of the alveolar shunt caused by perfusion of closed-off or atelectatic alveoli (see chapter 10).

Although not strictly the subject of this chapter, the atelectasis which develops during prolonged exposure to 100 percent oxygen atmospheres, in subjects seated at rest, must be considered in relation to acceleration atelectasis or low lung volume atelectasis, since it has many features in common. The symptons of cough and of chest pain aggravated by deep inspiration, the X-ray findings of basal lung collapse, the reduction in vital capacity and the shift in inflation pressure-volume curves, may all require several hours to develop while breathing oxygen at sea level (37, 73, 244), but otherwise appear identical to phenoma produced by one or two minutes of centrifugation or low lung volume breathing (38, 196). Furthermore, individuals

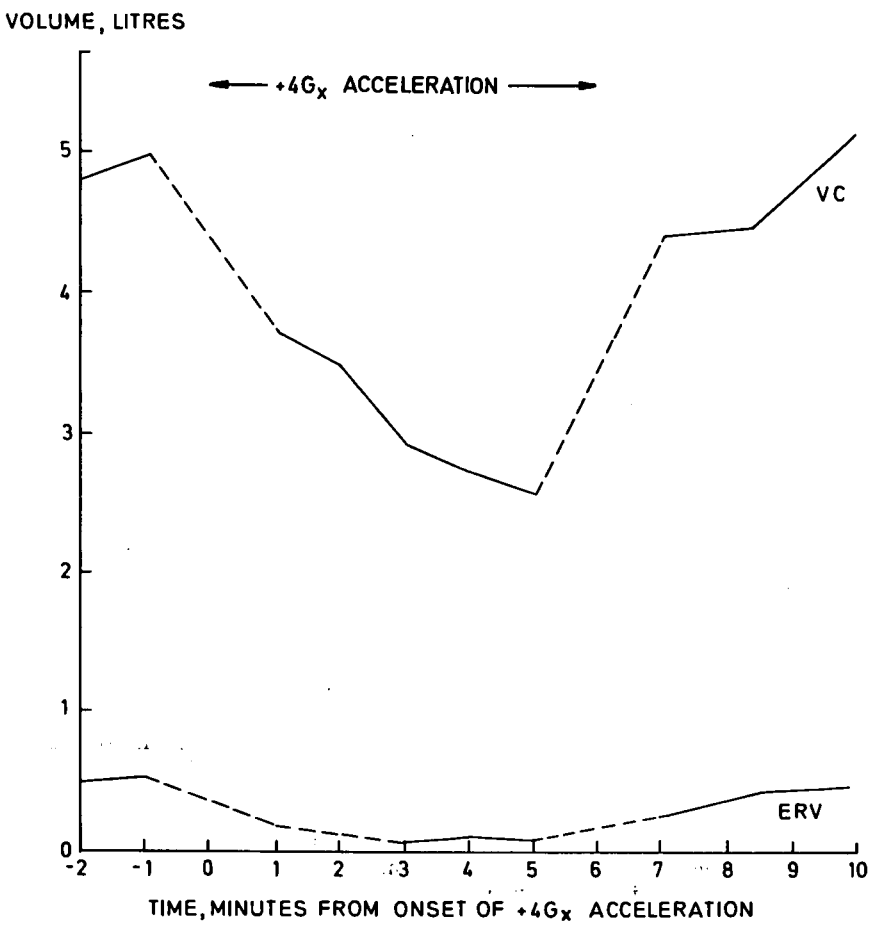

Fig. 8-20 Changes in vital capacity (VC) and expiratory reserve volume (ERV) induced by a six minutes exposure to $+4G_x$. VC was determined at one minute intervals throughout the run.

showing a pronounced susceptibility to the effects of simple oxygen breathing, show a similar susceptibility to low lung volume breathing (37). It is probable that gas-trapping, which occurs extensively in the lower lung during positive acceleration or low lung volume breathing, also occurs to a far lesser degree at normal lung volumes during quiet breathing. The relatively irreversible changes which follow longer exposures to 100 percent oxygen, or the breathing of oxygen at two atmospheres (37), may be attributed to a direct toxic action of this gas, with the possible intervention of pulmonary oedema or of changes in pulmonary surfactant.

Collateral Ventilation

Collateral ventilation has been shown to occur within the lung, and has been suggested as one mechanism which normally resists the development of atelectasis (4). Recently, Henderson and co-workers have confirmed the presence of significant collateral ventilation between segments in the human lung, and have demonstrated communications with diameters of up to 60 microns (121). For absorptional collapse to develop, therefore, the obstruction would have to be in a lobar bronchus, or in all the segmental bronchi of one lobe. This raises the problem of why, if absorptional atelectasis is caused by the closure of airways in the dependent lung, it is not prevented by collateral ventilation; for the production of a low pressure in collapsing alveoli should draw fresh gas in from neighbouring segments. A possible answer is that during acceleration, compression of the dependent lung tissue is such that closure occurs in airways of differing size, and so cuts right across anatomical boundaries. If this is the case, then the communicating passages may also become closed off, and atelectasis can occur.

It is also possible that the existence of interlobular communications may actually assist the lung to collapse during acceleration, for these passages may allow gas to be forced out of dependent alveoli even after their usual airways have become closed off. In this way, 'trapped'gas could leave the lung via an open segmental bronchus supplying a superior part of the same lobe, in which closure had not occurred, or 'trapped' gas could be displaced into other closed-off alveoli higher up the lung. Either mechanism would account for the immediate development of right-to-left shunting seen in some subjects during exposure to forward acceleration (see p.173).

Forward acceleration

So far in this chapter, little mention has been made of atelectasis caused by exposure to forward acceleration. This is because, in aviation, accelerations acting in this direction are too slight, or if severe enough too brief, for absorptional atelectasis to develop. The advent of space-flight has, however, introduced a situation where oxygen is breathed prior to forward acceleration exposures lasting for several minutes, with peaks of up to $+8G_x$. Experimental exposures to G-time profiles equivalent to those required in space missions (820 G seconds for an orbital velocity of 18,000 mph; 1140 seconds for an escape velocity of 25,000 mph) have produced marked reductions in vital capacities and symptoms of acceleration atelectasis when oxygen had been breathed (140, 194, and own observations). Atelectasis is to be expected for the following reasons:-

(a) Forward acceleration produces similar inequalities in alveolar size as does positive acceleration (chapter 4), and dependent airways will close at a larger lung volume. Gas-trapping will, therefore, occur in the posterior parts of the lung.

(b) Forward acceleration reduces the functional residual capacity (chapter 2), and tidal breathing will be carried out at a lung volume at which trapping is present (Fig. 4-10).

(c) Forward acceleration increases the blood flow per unit alveolar volume at

the back of the lung (Fig. 7-9), so that trapped oxygen will be rapidly absorbed.

Figure 8-20 illustrates a centrifuge run in which a subject, breathing oxygen, was exposed to $+4G_x$ for six minutes. There is an initial reduction in both vital capacity and expiratory reserve volume caused by mechanical factors (chapter 2), and this is followed by a progressive reduction in VC due to absorptional atelectasis, despite the fact that maximal inspiratory efforts were being made every minute. While lung function studies have not been carried out early in space flights, it is apparent that atelectasis will occur then, as well as during the re-entry deceleration. To what extent symptoms of, and subsequent recovery from, atelectasis will be influenced by weightlessness is unknown, but the resulting even distribution of blood flow should reduce the magnitude of the alveolar shunt, since atelectatic lung will no longer be in a region of increased blood flow. Re-expansion of collapsed alveoli may also be aided by a uniform pleural pressure, since the pressure surrounding the atelectatic region will fall.

If atelectasis should present a problem, its severity can be reduced by introducing a poorly soluble inert gas into the lung alveoli prior to acceleration exposure (i.e., an oxygen/nitrogen or oxygen/helium mixture could be breathed), and possibly by adoption of the prone position, since the functional residual capacity of the lung is not decreased by backward ($-G_x$) acceleration.

Table 8-1. Effect of acceleration, anti-G suit inflation and inspired gas composition and pressure on the development of atelectasis (as deduced from a reduction in vital capacity in excess of 0.5 l.). From (140).

Experimental conditions (each applied for 3 min)		Percent change in VC ($\frac{\text{control - post-run}}{\text{control}}$ x 100)	
		Air	Oxygen
$+1G_z$	With anti-G suit		NC
	Without anti-G suit		NC
$+3G_z$	With anti-G suit	NC	-20 percent
	Without anti-G suit	NC	NC
$+6G_x$	Ambient pressure	-6 percent	-40 percent
	Positive pressure breathing at 2 mm Hg per G		-40 percent

Note: NC means no significant change.

9

Ventilation-perfusion ratio inequality and gas exchange

Positive acceleration

It was shown in chapter 3 that alveolar ventilation was not uniformly distributed, even under normal resting conditions, but at lung volumes greater than functional residual capacity, alveoli in the lower lung were better ventilated than alveoli in the upper lung. At smaller lung volumes gas-trapping occurred in the lower lung and the pattern of ventilation was reversed. These differences were gravitational in origin, so that their exaggeration by positive acceleration, as demonstrated in chapter 4, was to have been expected. An even greater inequality exists in the distribution of blood flow within the lung (chapter 6), and this too, and for the same reason, is exaggerated by positive acceleration (chapter 7). It follows that alveoli in the upper lung are relatively over-ventilated, while those in the lower lung are relatively over-perfused. The distribution of ventilation-perfusion ratios found at varying levels of positive acceleration are illustrated in fig. 9-1. It should be noted that the values given are relative, since the cardiac output was unknown, but a reasonable estimate of absolute values is obtained by reducing the one G ratios by a factor of 0.85 (alveolar ventilation assumed to be 5.1 litres/min, pulmonary blood flow assumed to be 6.0 litres/min), and by increasing the $+3G_z$ ratios by a factor of 1.37 (alveolar ventilation rising to 6.6 litres/min, pulmonary blood flow falling to 4.8 litres/min). Regional ventilation-perfusion ratios are then seen to range from infinity at the apex of the lung, to approximately 0.7 at the lung base.

The effect that such variations in ventilation-perfusion ratio have upon regional gas exchange is best demonstrated by considering the extreme conditions of a ventilated alveolus without blood flow, and a perfused alveolus without ventilation (Fig. 9-2). In neither case can gas exchange be achieved, but in both cases there will be profound changes in either alveolar gas or capillary blood. If an alveolus is ventilated but unperfused, its gaseous contents will come into rapid equilibrium with inspired gas (Fig. 9-2a). Actually, such an alveolus will continue to contain some carbon dioxide, since it will 'inspire' a fraction of the dead-space gas left in the airways at the end of the preceding expiration. For simplicity, this effect will be ignored in subsequent discussion and calculation. While ventilated but unperfused alveoli do not contribute to gas exchange, they do contribute to the dead-space of the lung, and the term 'alveolar dead-space' may usefully be applied (274).

At the other end of the scale of possible ventilation-perfusion ratios lies an alveolus that is perfused but unventilated. Under these conditions alveolar gas will rapidly attain equilibrium with the mixed venous blood (Fig. 9-2c). Again, such an alveolus could not contribute to gas exchange, nor, directly, could it have any influence on expired gas composition. It will, however, have a profound influence on arterial blood, for it serves as a shunt whereby mixed venous blood can traverse the lungs without undergoing any alteration in its gas composition. The effect that such an 'alveolar shunt' (274) has on the composition of arterial

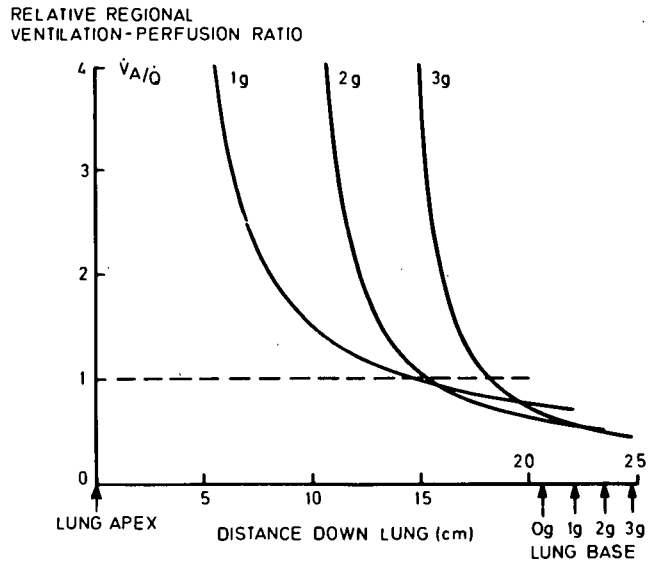

Fig. 9-1 The effect of positive acceleration on the variation in ventilation-perfusion ratio ($\dot{V}_A/\dot{Q}$) down the lung. The +1 to +3G values were obtained by radioisotope scanning after inhalation and intrevenous injection of ^{133}Xe, and the zero G values by extrapolation of this data. Values given are relative, the $\dot{V}_A/\dot{Q}$ of the whole lung being taken as 1.0.

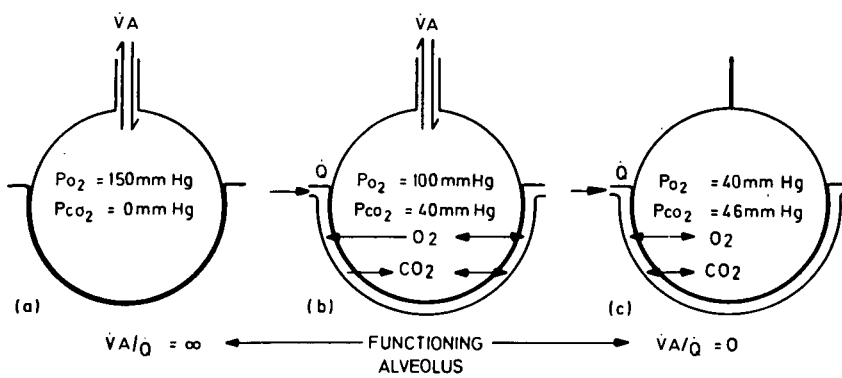

Fig. 9-2 Extremes of ventilation-perfusion ratio ($\dot{V}_A/\dot{Q}$) inequality as exhibited by a ventilated but unperfused alveolus (a) and by a perfused but unventilated alveolus (c), compared with an alveolus having normal ventilation and perfusion (b). Directions in which gas exchange takes place, and the alveolar gas contents which result, are indicated for each situation.

blood will depend upon the fraction of the total pulmonary blood flow shunted, upon the composition of the shunted (mixed venous) blood, and upon compensatory changes in gas exchange which may take place in normally ventilated and perfused regions of the lung. Owing to the shape of the oxygen dissociation curve, a compensatory increase in the ventilation of functioning lung can do little to correct the desaturation which results from shunting, since blood leaving normally ventilated alveoli is already about 97 percent saturated at an oxygen tension of 100 mm Hg. This is not the case with carbon dioxide, the excretion of which can be readily increased by raising the ventilation of functioning lung units. It may be predicted that, if exposure to acceleration does lead to pulmonary shunting - due to the presence of alveoli with $\dot{V}_A/\dot{Q}$ ratios of zero, then the oxygen tension and saturation of arterial blood must fall, but the carbon dioxide content may rise, remain constant or fall, depending upon coincident changes in overall alveolar ventilation. The actual changes in gas composition that have been observed during exposure to acceleration will be discussed in the next chapter.

Two further features of perfused but unventilated alveoli must be considered. Firstly, and for reasons discussed in the preceding chapter, any such alveoli are likely to be situated in the dependent lung, and so will be able to partake of the high blood flow in this region. This will exaggerate their contribution to venous admixture. Secondly, if alveoli contain a high fractional concentration of oxygen at the moment that they become unventilated, then this gas will be trapped and will serve as a reservoir of diffusible oxygen until such time as equilibrium with mixed venous blood is achieved. This will lead to a reduction in the volume of the alveolus. The significance of this process in relation to atelectasis has already been considered (chapter 8).

In an ideal lung, every alveolus should have a ventilation-perfusion ratio equal to that of the whole lung, and it has been suggested that this value, in practice, corresponds to the ratio required to achieve gas exchange with the minimum expenditure of work (79). Even in the absence of overtly unperfused or unventilated alveoli, ventilation-perfusion ratios may vary over a wind range, and these variations will cause regional differences in alveolar gas composition, gas exchange and blood-gas contents (265). In fig. 9-1, ventilation-perfusion ratios were seen to range from infinity at the apex of the lung to a value of about 0.7 at the lung base, during exposure to $+3G_z$ acceleration. The influence that ventilation-perfusion ratios of between 0.1 and 10 have on alveolar gas composition and capillary blood gas contents is illustrated in fig. 9-3. It may be seen that, as the ventilation-perfusion ratio falls, the situation approaches that found in an unventilated alveolus (Fig. 9-2c), and as this ratio rises, the situation approaches that of an unperfused alveolus (Fig. 9-2a). Since the composition of expired gas will be governed largely by alveoli having high ventilation-perfusion ratios, and the composition of arterial blood by alveoli possessing low ratios, it may be seen that considerable differences in gas tensions may occur between mixed alveolar gas and arterial blood, whenever there is a spread of ventilation-perfusion ratios present in the lung.

The overall function of the lung depends upon the relative numbers of alveoli having various ventilation-perfusion ratios, and can only be determined by considering numerical examples. It is assumed that, in every individual alveolus and over the normal range of ventilation-perfusion ratios, end-capillary blood achieves equilibrium with alveolar gas. It must be appreciated that this is an assumption, and that it may not hold true for alveoli having a low ratio of ventilation to perfusion, where the partial pressure of oxygen in the alveolar gas is low (223). Calculations which provide a basis for considering that equilibration does take place within the time taken for blood to transverse the pulmonary capillaries have been reviewed by Forster (84) and, on balance, support the assumption that this process is not diffusion limited under the conditions being considered.

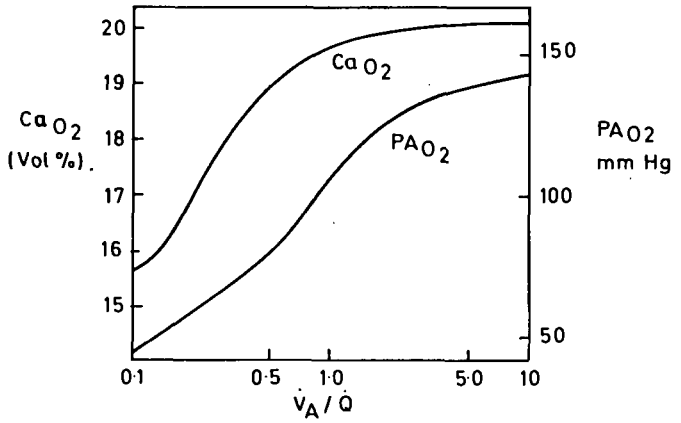

Fig. 9-3 Top. The effect of ventilation-perfusion ratio ($\dot{V}_A/\dot{Q}$) on the partial pressure of oxygen in alveolar gas ($P_{A_{O_2}}$), and on capillary blood oxygen content ($C_{a_{O_2}}$).

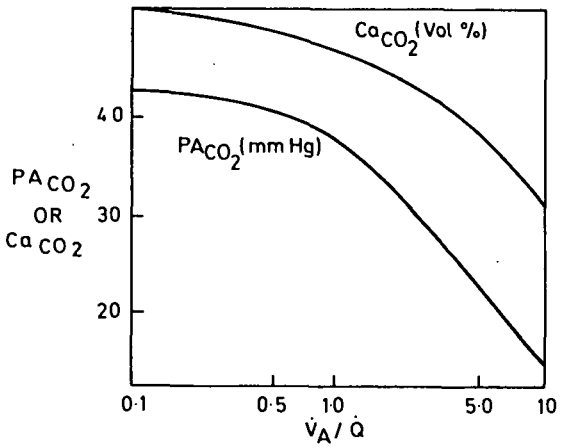

Bottom. The effect of ventilation-perfusion ratio on the partial pressure of carbon dioxide in alveolar gas ($P_{A_{CO_2}}$), and on capillary blood carbon dioxide content ($C_{a_{CO_2}}$). Note that for low ventilation-perfusion ratios the values approach those for an unventilated alveolus (Fig. 9-2c), and that for high ratios the values approach those for an unperfused alveolus (Fig. 9-2a).
From Fahri (79), by a courtesy of Edward Arnold Ltd.

West has calculated that the variations in ventilation-perfusion ratio, which exist in the normal upright lung, lead to an overall alveolar-arterial oxygen difference of four millimetres of mercury, and reduce the oxygen uptake by two percent below that of a lung having even distributions of blood and gas (265). As mentioned earlier, the shape of the oxygen dissociation curve acts as a buffer, so that considerable regional differences in the partial pressure of oxygen in the alveolar gas cause relatively small variations in the oxygen saturation of arterial blood. By combining data for the anatomical distribution of the lung volume in relation to the vertical height of the lung (267), with data obtained by radioisotope scanning of the lung during exposure to positive acceleration (103); and by making reasonable assumptions about the overall values of ventilation and pulmonary blood flow (see p. 151), it is possible to calculate the alveolar-arterial oxygen difference which must occur across the lung at + $3G_z$, solely due to ventilation-perfusion inequalities.

In order to allow comparison with earlier calculations, lung tissue lying between the apex and the dome of the diaphragm was considered in nine horizontal slices. The relevant function of each slice is given in table 9-1. As would be expected, the range of regional ventilations is greater than that calculated by West for the upright lung at one G (from 0.24 litres/min in the top slice to 0.82 litres/min in the bottom slice), and the range of regional blood flows is greater still, with 54 percent of the lung volume unperfused at $+3G_z$. The spread of ventilation-perfusion ratios which results (from infinity at the apex to 0.6 at the extreme base of the lung) leads to regional differences in the partial pressure of oxygen in alveolar gas, the pressure differential between the top and the bottom slice being 65 mm Hg (table 9-1). Arterial blood oxygen contents, also given in the table, vary much less, since blood leaving even the lowermost slice is 96 percent saturated. The result is that the mixed alveolar oxygen tension is 120 mm Hg at $+3G_z$, compared to a value of 101 mm Hg obtained by similar calculation at $+1G_z$ (265); and the arterial oxygen tension is 94 mm Hg compared to the $+1G_z$ value of 97.5 mm Hg.

The surprising feature of these calculations is that, while the overall alveolar-arterial oxygen difference has been increased by 22 mm Hg by exposure to acceleration, this has been achieved with only a minimal lowering of the arterial oxygen tension, which falls by a mere 3.5 mm Hg. It appears that, at an acceleration of $+3G_z$, the considerable spread of ventilation-perfusion ratios has been largely compensated for by the fact that blood is distributed preferentially to the better ventilated lower lung. At $+3G_z$, the lower third of the vertical height of the lung (slices 7 to 9 in table 9-1), receives 52 percent of the available ventilation and virtually all (96 percent) of the pulmonary blood.

Any greater reduction in arterial oxygen saturation than this; found during exposure to positive acceleration, cannot, therefore, be explained on a basis of the observed ventilation-perfusion inequalities *per se*, but must be ascribed to shunting. Shunts could be formed by the perfusion of unventilated or closed-off alveoli, by the perfusion of collapsed and gas-free alveoli (atelectasis), or by extra-alveolar or extra-pulmonary blood flow. Several techniques exist for the differentiation of these various mechanisms, but most require steady-state conditions difficult to achieve during centrifugation. Thus, a simultaneous measurement of alveolar-arterial oxygen, carbon-dioxide and nitrogen differences would be of great value, since the oxygen difference is most affected by venous admixture, the carbon dioxide difference by regions of high ventilation-perfusion ratio, and the nitrogen difference by regions of low ventilation-perfusion ratio (79).

An alternative approach makes use of multiple inert gas wash-outs, with measurements of arterial, mixed venous and alveolar concentrations. By use of a methane-ethane system in this way, a lung compartment has been demonstrated in the anaesthetised dog which has a ventilation-perfusion ratio of less than 0.1, and which receives 10 to 29 percent of the total pulmonary blood flow (275). It is

Table 9-1

Lung slice	Slice volume (% total)	Alveolar ventilation (l./min)	Perfusion (l./min)	$\dot{V}_A/\dot{Q}$	Alveolar PO_2 (mm Hg)	Arterial O_2 content (vol. %)
1	5	0.18	0.0	∞	150	20.0
2	7	0.30	0.0	∞	150	20.0
3	9	0.45	0.0	∞	150	20.0
4	11	0.61	0.0	∞	150	20.0
5	12	0.72	0.0	∞	150	20.0
6	14	0.93	0.18	5.2	140	20.0
7	14	1.04	0.87	1.2	113	19.6
8	14	1.13	1.55	0.7	93	19.4
9	14	1.24	2.20	0.6	85	19.2
Whole lung	100	6.60	4.80	1.4	120	19.36

Analysis of the function of an upright human lung at $+3G_z$. The average arterial oxygen content of 19.36 vol. % corresponds to a tension of 94 mm Hg, and this is only marginally less than that found at $+1G_z$, but the overall alveolar-arterial oxygen difference has risen to 26 mm Hg.

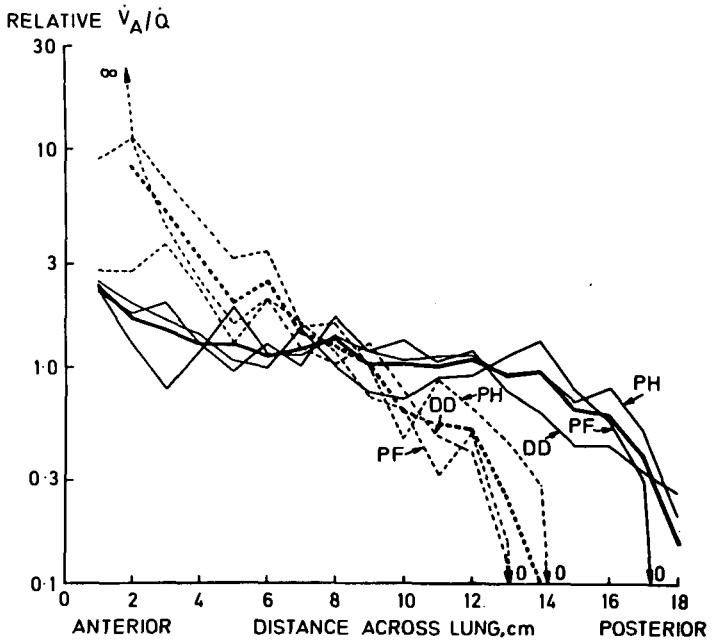

Fig. 9-4 Regional ventilation-perfusion ratios at accelerations of $+1G_x$ (continuous lines) and $+5G_x$ (dotted lines). Individual values from three subjects are given by thin lines, and average values at each level of acceleration by thick lines. The overall ventilation-perfusion ratio of the lung is taken as 1.0, and the graphs are aligned so that the backs of the lungs coincide.

tempting to equate this with the unventilated but well perfused compartment considered to be responsible for acceleration atelectasis. Evidence for the existence of perfused but unventilated alveoli during exposure to positive acceleration was presented in chapter 8, and it was demonstrated that such alveoli could contain trapped gas, or be completely collapsed, depending upon their initial gas contents. Measurements of pulmonary shunting, made using hydrogen or tritium solutions injected intravenously, will be described in the next chapter.

Forward acceleration

With $+G_x$ acceleration the situation is simpler, since a non-ventilated but perfused zone has been clearly demonstrated in the dependent lung. This compartment may be seen by comparing the distribution of ventilation at $+5G_x$ (Fig. 4-12, p. 66) with that of perfusion at the same level of acceleration (Fig. 7-9, p.114). The comparison has been carried out on three subjects common to both determinations in fig. 9-4, where ventilation-perfusion ratios (taking the ratio of the entire lung as 1.0) have been plotted against distance across the lung at +1 and $+5G_x$. At $+1G_x$, the regional ventilation-perfusion ratio varies from two at the front of the lungs to 0.2 at the back, and the effect on regional gas exchange will not be very great (Fig 9-3). However, at $+5G_x$ the ventilation-perfusion ratio varies from 10 to zero, and it is the zone of non-ventilated but still perfused alveoli, at the back of the lungs, which constitutes an alveolar shunt and exerts the greatest influence on gas exchange.

It is interesting to note that the poor ventilation of the dependent lung (Fig. 4-12) is to some extent compensated for by the decreased blood flow per alveolus in this region (Fig. 7-11, p.115). The fraction of the pulmonary blood which perfuses unventilated lung at $+5G_x$ may be calculated by combining the distribution of blood flow per unit lung volume (Fig. 7-9), with the values of regional lung volume given in fig. 7-13 (p. 116). The result is that, despite a compensatory reduction in blood flow per alveolus in the dependent lung, 42 percent of the total flow goes to unventilated alveoli. Direct measurements of left-to-right and physiological shunts will be described in the following chapter, but it may be noted that shunts of the same order of magnitude were found in both men and dogs at accelerations of from +4 to $+7G_x$.

10

The effect of acceleration on gas exchange, arterial oxygen saturation and alveolar shunting

The overall respiratory gas exchange of the body - that is the quantity of oxygen taken up from, and the quantity of carbon dioxide given up to the respired air - can be modified by a number of factors. In a steady state, oxygen uptake must equal the metabolic consumption of oxygen, but over short periods of time there is no reason for this relationship to be adhered to, since the quantities of oxygen stored in blood, tissue fluids and myohaemoglobin may all vary. In this way, oxygen consumption may temporarily exceed oxygen uptake, the difference being taken at the expense of falling body stores. Eventually, any excess must be repaid on a one to one basis and the stores returned to normal. The occurrence of anaerobic metabolism provides an alternative mechanism for a transient fall in oxygen uptake but, owing to the lower efficiency of glycolysis vis-a-vis oxidative energy production, the incurred debt must be repaid on an approximately two to one basis (125). These considerations are important in relation to the relatively brief exposures to acceleration during which measurements of oxygen uptake have been made, since it is extremely unlikely that steady-state conditions will have been achieved.

Similar arguments can be applied to measurements of carbon dioxide excretion. Because of the greater size of the stores of this gas, and due to the extreme sensitivity of these stores to changes in pulmonary ventilation, transient differences between production and output may be very large indeed. Thus, if a man weighing 70kg doubles his resting ventilation, his carbon dioxide stores fall by 1,600 ml, but his oxygen stores increase by only 20 ml. If he halves his resting ventilation, the quantity of carbon dioxide in his body goes up by 4,000 ml, but its oxygen content falls by only 260 ml (80).

Gas exchange

Few measurements of oxygen uptake have been carried out during exposure of man to positive acceleration. Those carried out at rather high levels of acceleration (+4 to +6G_z) (10, 19), show the increase in uptake that would be expected from the muscular effort required to maintain posture, to breathe against added elastic resistance (chapter 2), and to strain to prevent pooling of blood in the abdomen and lower limbs and loss of consciousness. At lower levels of acceleration (+2 to +3G_z) imposed for up to three minutes, resting oxygen uptake falls, though the fall is made up within the first minute of recovery, and overall there is usually a slight increase in uptake (95). The appearance is that of an oxygen debt, built up during the exposure to acceleration and repaid immediately upon return to one G. A similar conclusion was reached by Barr (19), though in his studies at +5G_z, an increase in oxygen uptake was seen during the two minute acceleration exposures.

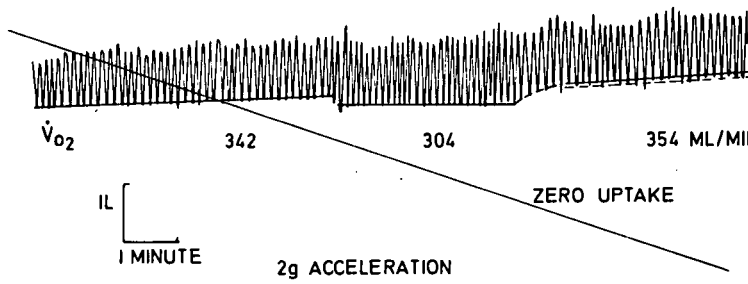

Fig. 10-1 Oxygen uptake ($\dot{V}_{O_2}$) measured by closed circuit spirometry over a three minute exposure to $+2G_z$ acceleration. The subject was breathing air, and oxygen was added to the circuit at a constant rate of 315 ml/min. Note the reduction in oxygen uptake during acceleration, and the rise early in the recovery period.

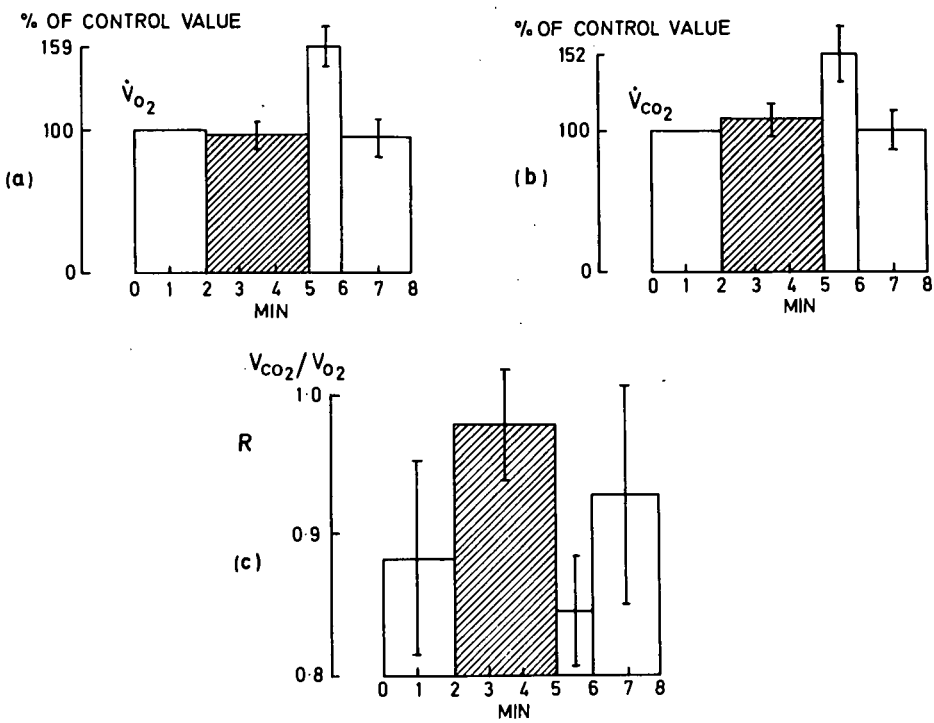

Fig. 10-2 Effect of $+3G_z$ acceleration lasting for three minutes on (a), oxygen uptake (V_{O_2}), (b), carbon dioxide excretion (V_{CO_2}) and (c), respiratory gas exchange ratio (R). The period of acceleration is indicated by shading. Values are the average results found in five subjects, and plus and minus one standard deviation of the mean is indicated by barred vertical lines.

Figure 10-1 shows a spirometer recording obtained during exposure of a resting subject to an acceleration of $+2G_z$, lasting for rather more than three minutes. Oxygen uptake falls from 342 ml/min to 304 ml/min at $+2G_z$. Immediately upon return to normal gravity there is a brief increase in uptake, and this lasts for about one minute before it returns to near the control value. These findings were confirmed by collecting expired air during similar runs at $+3G_z$, and the resulting oxygen uptakes, carbon dioxide outputs and respiratory gas exchange ratios, averaged from five subjects, are illustrated in fig. 10-2. Oxygen uptake fell only slightly at $+3G_z$, but the fall was observed in all five subjects. More striking were oxygen uptakes recorded during the first minute of the recovery period, which averaged 160 percent of the control value ($P < .001$). When an oxygen debt of this magnitude results from moderate exercise , an increase in uptake is also seen at the time of the stress: it is the lack of such an increase during acceleration stress that is the curious feature of these results.

In other experiments, the oxygen debt was found to increase with duration of exposure to $+3G_z$ acceleration, and these results are illustrated in fig. 10-3. Two facts emerge. Firstly, when the oxygen debt was calculated per minute of acceleration, the debt fell with increasing exposure time. Secondly, the uptake did not fall over a five minute exposure to acceleration. These two observations suggest that the oxygen debt is caused by measurements being made in an unsteady state: it is probable that if subjects were exposed to acceleration for greater periods of time, a rise in oxygen uptake would be recorded (see below). Nevertheless, in no run did the average oxygen uptake at $+3G_z$ exceed the resting control value, though an uptake of 770 ml/min was seen in the first minute of recovery after five minutes exposure to this level of acceleration.

Oxygen debts also rose with the level of acceleration, and were reduced by the inflation of an anti-G suit (fig. 10-7). Measured in terms of the oxygen debt built up during a three minute exposure to positive acceleration, an anti-G suit gave a protection of one G, very similar to the protection afforded when measured in terms of a rise in blackout threshold. In these three minute centrifuge runs, collection of expired air was made in two fractions, and oxygen uptakes were found to be less in the first minute than in the subsequent two minutes. This again suggests that steady-state conditions were not attained early in the acceleration exposures.

Oxygen uptake can be raised during brief exposure to positive accelerations of $+2$ to $+3G_z$, but only by carrying out external work (95). Oxygen uptake was less when a standard work load was carried out at $+3G_z$ than at one G, however, and the accrued oxygen debt was also much greater. It was concluded that oxygen uptake could be increased at $+3G_z$, but only after a debt of some 500 ml had first been built up. These findings would be explicable if exposure to $+3G_z$ decreased the body's total oxygen store by 500 ml, and possible mechanisms for such a decrease will be discussed later (see p. 163).

Changes in carbon dioxide outputs found in these studies were more variable, but outputs always rose during the exposure to acceleration. Pulmonary ventilation also increased, despite the fall in oxygen uptake, and it was concluded that the increase in carbon dioxide output was caused by hyperventilation. The changes in ventilation recorded during the runs illustrated in fig. 10-2 have already been discussed in chapter 2, and are illustrated in fig. 2-1 (p. 20).

Recent measurements of gas exchange, made with subjects at rest during the fifth to seventh minute at $+3G_z$, have shown that oxygen uptake rises at this time, and the increases found averaged 54 ml/min in 10 subjects (228). When exercise was carried out at work levels of 300 and 600 kpm/min, exposure to the same level of acceleration increased the oxygen uptake by 203 and 222 ml/min, from control

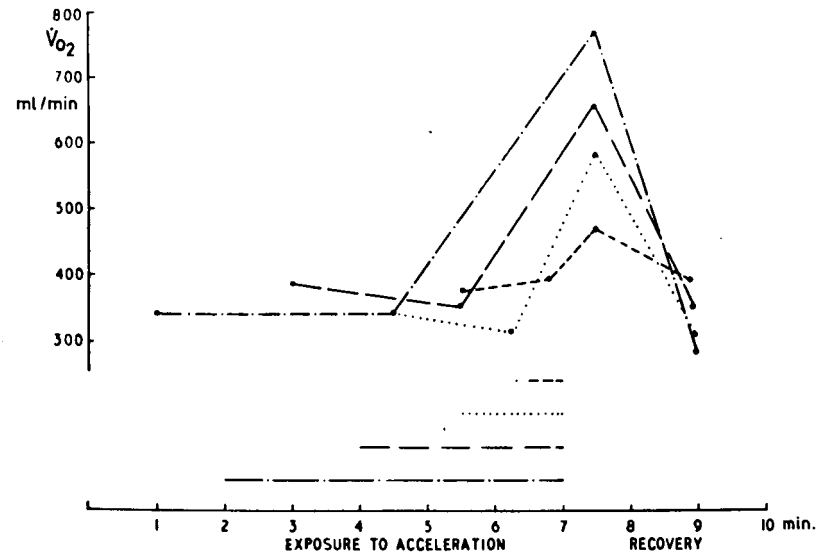

Fig. 10-3 Effect of duration of exposure to $+3G_z$ acceleration on oxygen uptake (V_{O_2}). Runs vary in length from 30 seconds to five minutes as indicated above the time scale, and they are plotted so that the recovery periods coincide

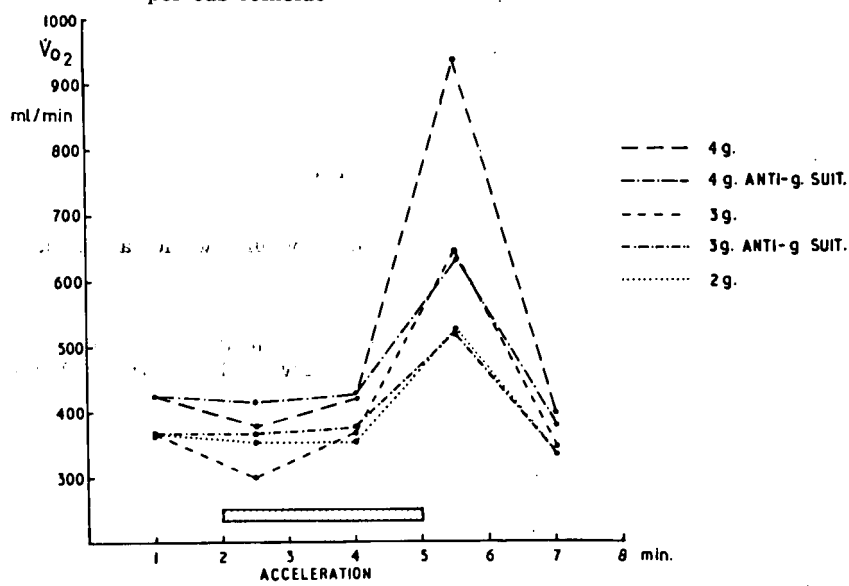

Fig. 10-4 Effect of anti-G suit and level of acceleration on oxygen uptake ($\dot{V}_{O_2}$) during centrifuge runs lasting three minutes. Two collections of expired air were made during the period of acceleration.

values of 879 and 1434 ml/min respectively. It can be assumed that these observations were made during steady-state conditions, and they provide additional evidence that the falls reported earlier were due to measurements being made over a period of transition from one steady state to another.

Gas exchange has also been recorded during exposure to forward acceleration, with results very similar to those described for brief positive acceleration exposures where an oxygen debt had developed. Using a three minute acceleration plateau, Steiner and co-workers (249) found the oxygen uptake to decrease by 16 ml/min at $+6G_x$ and by 71 ml/min at $+8G_x$. Carbon dioxide excretions rose by 62 ml/min and 30 ml/min respectively. As would be expected from the raised respiratory gas exchange ratio found (1.24 at $+8G_x$), there was a marked increase in the minute volume of ventilation at both levels of acceleration. During the recovery period, an additional 470 ml of oxygen was consumed following the exposure to $+6G_x$ acceleration, and an additional 650 ml following the $+8G_x$ exposure. The additional carbon dioxide excretions were 360 and 580 ml respectively. Oxygen debts incurred by three minute exposures to +6 to $+8G_x$ are, therefore, comparable to those reported following the same duration of exposure to $+3G_z$ acceleration. Studies made at up to $+12G_x$ have yielded similar results.

In experiments where the expired oxygen concentration was monitored continuously (45), oxygen uptake was found to fall during three minute exposures to +6 and $+8G_x$, typical reduction being 62 and 86 ml/min at these two levels of acceleration. When the oxygen uptake of the recovery period was included, all levels of acceleration investigated (from +5 to $+12G_x$) led to an increased overall consumption, the additional oxygen requirement per minute acceleration averaging 46 ml at $+5G_x$, 188 ml at $+8G_x$, 310 ml at $+10G_x$ and 716 ml at $+12G_x$. Oxygen uptake at $+12G_x$ may, however, be less than that recorded in the same subjects at an acceleration of only $+8G_x$ (109), a hardly suprising result in view of the extreme reduction in tidal volume provoked by these high levels of forward acceleration (see chapter 2).

Of the possible mechanisms which could be invoked to explain a decrease in oxygen uptake during short exposures to acceleration, a reduction in metabolic requirement can be dismissed in view of the overall increase in uptake, and in view of the finding that the uptake rises if the exposures are prolonged. Furthermore, postural muscle activity has been shown to be increased during positive acceleration (9), and additional work is required for respiration (chapter 2). A second possibility is that blood with a low oxygen content is pooled during acceleration and only returns to the lung when the acceleration stress is lifted. However, to explain an oxygen debt of 500 ml, about half the circulating blood volume would have to be pooled, and this reduced to an oxygen saturation of less than 50 percent, a degree of pooling and desaturation impossible to achieve in the tissues concerned - i.e., the muscles of the lower limbs. This mechanism has, however, been invoked to explain the fall in oxygen saturation which may be seen immediately on return to normal gravity, following prolonged exposure to high levels of forward acceleration (109).

A third possibility is that underperfusion of some tissues could lead to anaerobic metabolism and to the development of an oxygen debt. No measurements of blood lactate have been made during acceleration stress, but it is difficult to see how changes of the required magnitude could be achieved by resting muscle. If blood flow to one leg is occluded for three minutes, the additional flow which follows restoration of the circulation is 1.5 ml per 100 ml of limb volume (2): the maximum oxygen debt which could have been built up is only one or two millilitres per kilogram of leg tissue. A fall in whole blood carbon dioxide content has, however, been observed during exposure to forward acceleration, and at $+8G_x$ it was corrected by breathing oxygen (248). The fall was attributed to the production of anaerobic metabolites in tissues having an inadequate blood supply. A final

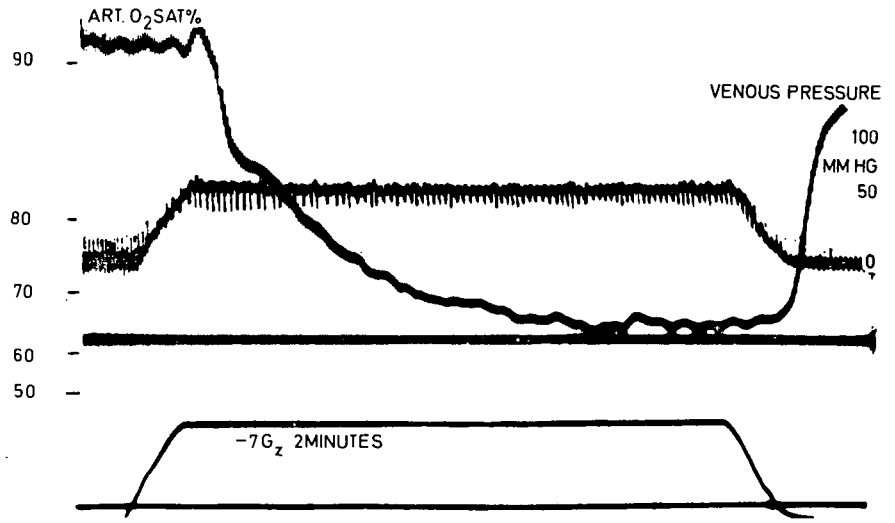

Fig. 10-5 Effect of exposing an anaesthetised dog to an acceleration of $-7G_z$ for two minutes, on arterial oxygen saturation and venous pressure. Note the fall in saturation during the period of acceleration. (From Henry (122), by courtesy of the U.S.A.F.).

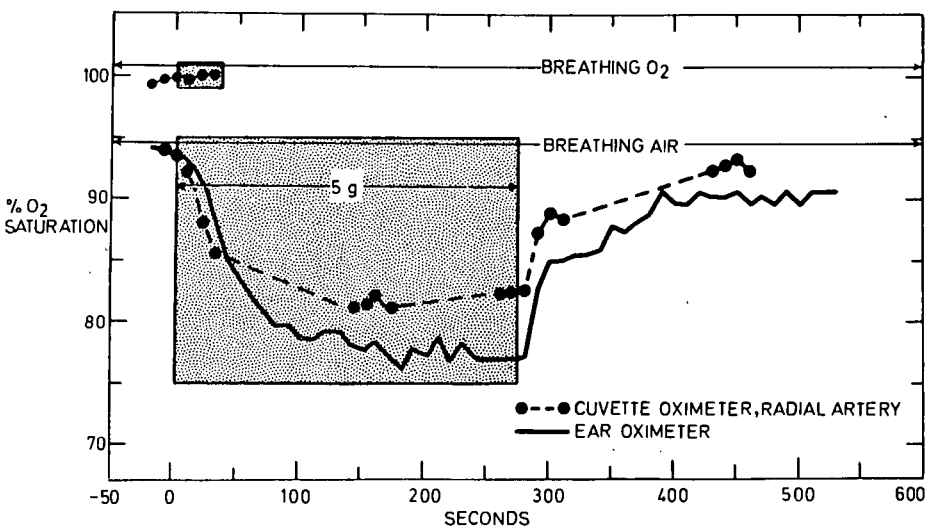

Fig. 10-6 Changes in arterial oxygen saturation during acceleration when breathing oxygen (30 seconds exposure to $+5G_x$) or air (4.5 minute exposure to $+5G_x$). The lack of response when the subject breathed 99.6% oxygen was presumably due to the run being terminated after only 30 seconds, at which time oxygen trapped in unventilated alveoli was still available for diffusion.
From Wood *et al* (272), by courtesy of U.S.A.F.).

possibility is that, during the first few minutes of exposure to acceleration, there is a dramatic decrease in the oxygen stores of the body.

As already stated, the oxygen stores of a 70 kg man will fall by 260 ml if his resting ventilation is halved. However, all observations are consistent in showing an increase in ventilation during exposure to positive as well as forward acceleration. A comparable fall in oxygen stores (220 ml) would result from a halving of the cardiac output, since there will then be a significant reduction in the oxygen contents of the tissues and venous blood. This mechanism could explain the development of an oxygen debt during exposure to positive acceleration, but could not explain the debt seen during forward acceleration, where there is little change in cardiac output (chapter 5). Even during exposure to positive acceleration the fall in output recorded at $+3G_z$ is too small to account for more than a small fraction of a total oxygen debt of 500 ml. We are left with the possibility that a fall in oxygen stores could be caused by a reduction in the oxygen content of arterial blood. Ultimately, this could lead to the unloading of oxygen from myohaemoglobin. Before making any calculations, we must first consider what changes in arterial oxygen saturation do, in fact, occur during exposure to acceleration.

Arterial oxygen saturation

The observation that exposure of a human subject to negative acceleration led to an increase in the radiographic density of the apical regions of the lungs, attributed to an accumulation of blood in these regions, led Henry and co-workers to look for changes in the oxygen saturation of arterial blood. Using a Kramer glass cuvette oximeter, arterial oxygen saturation was found to fall to 60 to 65 percent during exposure of an anaesthetised dog to an acceleration of $-7G_z$ (122). The recording obtained is illustrated in fig. 10-5, and shows that oxygen saturation fell dramatically with the onset of acceleration, the slight delay being due to the time taken for blood to flow from the lungs to the oximeter. On return to normal gravity, there was an equally dramatic recovery in saturation, though recovery was not complete by the end of the recording. Similar, though less profound, changes were found in man during exposure to positive acceleration, the arterial oxygen saturation falling from 97 percent to 90 percent after 15 seconds at $+4.5G_z$ (91).

Further studies carried out in Sweden showed that falls in oxygen saturation were progressive during the exposure of dogs to accelerations of $+3G_z$ for up to five minutes, and could be abolished by prior vagotomy (21). This last observation was not explained, but a possible mechanism is suggested on page 171. A secondary fall in saturation was sometimes seen during the recovery phase, and this phenomenon will also be discussed later. At +4 to $+5G_z$, desaturation occurs despite the breathing of 100 percent oxygen (though reduced in extent); repeated exposures to acceleration have a cumulative effect; and desaturation is more pronounced when an anti-G suit is worn (18).

In the United States, most interest centred round the effects of forward acceleration. Steiner and co-workers (250) noted blueing of arterial blood in dogs during exposure to acceleration of +10 to $+14G_x$, and similar but less marked changes were seen at $+6G_x$. In man, using arterial sampling and manometric analysis, they found that the oxygen saturation fell to average values of 84 percent at $+6G_x$ and to 75 percent at $+8G_x$, the acceleration plateaux being maintained for three minutes (248). Breathing 100 percent oxygen for 15 minutes prior to acceleration, with continued inhalation during the acceleration plateau, only partially corrected the desaturation, the average value found then being 86 percent at $+8G_x$. Recovery was slow and was not complete within three minutes, unless oxygen was administered. Since cardiac output and pulmonary ventilation were considered to be

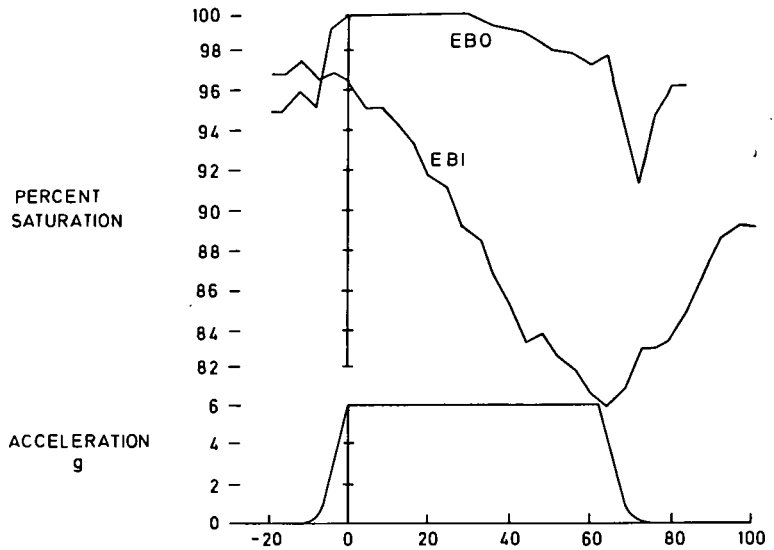

Fig. 10-7 Changes in arterial oxygen saturation recorded during exposure to transverse accelerations with the subject supine (EBI) and prone (EBO). Note that a profound desaturation is seen with the subject supine ($+6G_x$) but that $-G_x$ acceleration has cirtually no effect. From Smedal *et al* (243), by courtesy of Aerospace Med.).

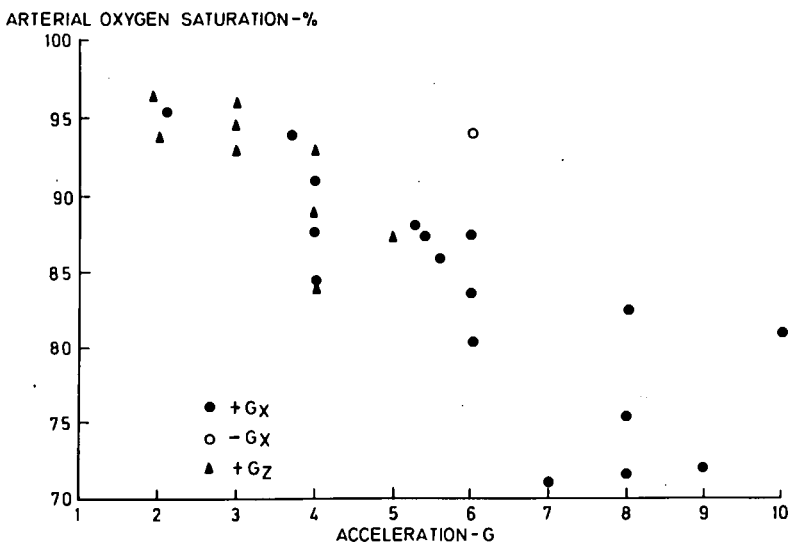

Fig. 10-8 Arterial oxygen saturations reported in man during exposure to varying levels and axes of acceleration. Each point represents the average of at least three, and up to 31 determinations made during exposures lasting from 50 seconds to six minutes with subjects breathing air.

essentially unchanged at these levels of forward acceleration, it was concluded that desaturation was caused by up to 50 percent of the cardiac output being shunted through unventilated areas of lung.

Similar changes in arterial oxygen saturation were reported by Wood and co-workers using cuvette oximetry (273), and fig. 10-6 illustrates the changes found in one subject during exposure to an acceleration of $+5G_x$, breathing air. Recovery was slow and was not completed within three minutes. Breathing 100 percent oxygen prevented desaturation during a 30 seconds exposure to $+5G_x$, and this run is also illustrated in fig. 10-6. Later studies (194) showed that desaturation did still occur with oxygen, but its onset was delayed and its magnitude never as great as when air was breathed. A secondary fall in oxygen saturation was also occasionally seen during the recovery phase, which was attributed to the subject's resuming more normal breathing after a deep breath had led to a temporary rise in saturation. Arterial oxygen saturation was also found to fall within 10 seconds of the onset of exposure to positive acceleration, and reached 93 percent during a one minute run at $+4G_z$. The degree of desaturation was enhanced by inflation of an anti-G suit, when it averaged 89 percent. This effect was seen consistently at +2, +3 and $+4G_z$.

Smedal and co-workers demonstrated that body posture has a considerable influence on the degree of desaturation which results from exposure to transverse accelerations; $+G_x$ acceleration having a much more profound effect than $-G_x$ acceleration (242, 243). This phenomenon is illustrated in fig. 10-7, and similar results were found in eight pairs of runs made at ± 6 and $\pm 8G_x$. At $6G_x$, the lowest value of oxygen saturation averaged 80.3 percent with subjects supine ($+G_x$), and 93.9 percent with them prone ($-G_x$).

The earlier observation that forward acceleration produced arterial desaturation, even when 100 percent oxygen was breathed, has been confirmed in man (3, 131, 220), as well as in the dog (12, 13), though the fall in saturation is delayed and reduced in extent. Hoppin and co-workers found that the administration of oxygen prevented desaturation for up to two minutes at $+4G_x$, and at $+8G_x$ it delayed the onset of desaturation by 60 to 90 seconds. Thereafter, the saturation fell rapidly, though it remained some 20 percent higher than when air was breathed (131). Rates of resaturation were not studied, but it was shown that saturations recorded during acceleration were influenced for up to two minutes by the nature of the gas breathed prior to the onset of acceleration. This observation was taken to indicate that gas inspired prior to acceleration was trapped in parts of the lung from which it could subsequently be taken up in the pulmonary capillary blood.

Breathing oxygen at a pressure of five pounds per square inch, during relatively prolonged exposures to acceleration in the range +4 to $+8G_x$, causes less desaturation than when air is breathed at atmospheric pressure (3). The difference is explicable on the basis of the differing inspired oxygen partial pressures (260 mm Hg with oxygen at five pounds per square inch), and this suggests that the size of the shunt was unaffected by the gas breathed in this instance. The greatest difference between the effect of the two gases lay in the rates of recovery following return to normal gravity. When oxygen was breathed at five pounds per square inch, the degree of resaturation which took place within the first 30 seconds was more than halved. This effect was attributed to the enhancement of collapse caused by the absorption of trapped oxygen. A similar effect has been noted in dogs following exposure to positive acceleration, resaturation being delayed when oxygen was breathed at atmospheric pressure.

The experiments referred to above suggest that inspired gas pressure may have little effect on pulmonary shunting and arterial oxygen saturation. A similar lack of effect was demonstrated when air was breathed at a positive pressure of three

millimetres of mercury per G, during exposure to forward acceleration of from +7 to +10G_x (220).

The degree of arterial oxygen desaturation which results from the exposure of man to acceleration is illustrated in fig. 10-8. Each point, taken from the literature, represents the average of at least three, and up to 31 determinations made during exposures lasting from 50 seconds to six minutes, with the subjects breathing air. Steady-state conditions would not have been achieved in many cases, and it was often noted that saturations were still falling at the end of the periods of observation. For example, Golov (109), whose data are not included owing to insufficient experimental detail, noted an arterial oxygen saturation of 72 percent after two minutes exposure to +8G_x acceleration, but when the run was terminated at five minutes, the saturation had fallen further to 65 percent. The first of these values lies on the general curve of fig. 10-8, but the second lies below it. The curve cannot, therefore, be taken to prepresent the minimum values of saturation which could result from acceleration exposure. While data appertaining to positive acceleration is scant and restricted to low levels, it does appear that the desaturations which result are comparable to those produced by equivalent levels of +G_x acceleration. Under comparable experimental conditions, we have found the arterial oxygen tension to average 52 mm Hg (range 44 to 68 mm Hg) after two minutes at an acceleration of +4G_z, and 53 mm Hg (range 40 to 69 mm Hg) in the same subjects at +4G_x.

As may be seen from fig. 10-8, the degree of desaturation is closely related to the magnitude of the imposed acceleration, a somewhat surprising observation in view of the differences in technique, methods of measurement, precise posture and timing. Desaturation starts at a threshold acceleration of about three G, and then increases progressively, showing no signs of levelling off up to the highest level of acceleration investigated. It may be predicted that saturations would continue to fall at a rate of four to five per cent per G beyond 10G, and an isolated observation of a saturation of 63 percent, obtained after one minute of exposure to an acceleration of +12G_x, confirms this prediction (109). Backward acceleration (-G_x), appears to have significantly less effect on arterial oxygen saturation than the other axes of acceleration investigated, as shown by the single observation which lies well above the general curve. The probable reason for this discrepancy will be discussed later. No studies of negative acceleration (-G_z) have been reported in man, but a single observation made in the dog (65 percent saturation after two minutes at -7G_z (122)), suggests that this stress may provoke a more profound desaturation than does positive acceleration, since other dog data obtained during exposure to forward acceleration fits the human curve tolerably well.

The mechanism of arterial oxygen desaturation during acceleration

Most of the workers referred to above have attributed the arterial desaturation of acceleration to pulmonary shunting and venous admixture, the usual argument being that no other explanation fits the fact that the saturation still falls when 100 percent oxygen is breathed. In a study of the available literature, Hoppin and co-workers (131) concluded that administration of 100 percent oxygen raised arterial oxygen saturations by about 20 percent during brief exposures to acceleration (less than two minutes), but by only 10 percent during more prolonged exposures: oxygen delays the onset of desaturation as well as reducing its extent. If the desaturation is to be explained by simple shunting, then administration of oxygen should raise the saturation by no more than 10 percent, the additional 10 percent found early in the exposure to acceleration being attributed to areas of lung with inadequate ventilation. The most reasonable explanation for the different benefit obtained from oxygen during brief and prolonged exposures to acceleration is that shunting is caused by the perfusion of unventilated alveoli containing trapped gas. When the trapped gas is oxygen, arterial desaturation will not develop until most

of it has been absorbed. Even when the partial pressure of oxygen in the trapped gas has been reduced to 60 mmHg, blood will leave pulmonary capillaries 90 percent saturated.

It is not possible to calculate the time course of gas absorption without knowing the volume of gas trapped and the relevant perfusion. It is reasonable to assume that the time course for oxygen absorption would be similar to that for the development of atelectasis. The half-time of this process, as gauged from the rate of loss of vital capacity, is 25 seconds (see chapter 8). Absorption of trapped oxygen should, therefore, be 96 percent complete within two minutes, a time comparable to the delay in desaturation which results from the administration of oxygen prior to acceleration.

Attempts to find mechanisms other than shunting to explain the arterial oxygen desaturation of acceleration have not been successful. Although pulmonary diffusing capacity is reduced in man by 35 percent at $+8G_x$, this reduction would not depress arterial oxygen saturation below 92 percent (211). The effective pulmonary capillary blood flow also falls by 35 percent at $+8G_x$, but this fall was considered to represent perfusion of unventilated alveoli, rather than an absolute fall in pulmonary blood flow.

In order to estimate the magnitude of the pulmonary shunt required to account for the observed desaturation, it is necessary to know the oxygen content of the mixed venous (shunted) blood. Very few relevant observations have been made, but Banchero and co-workers (12) carried out measurements in dogs and, at an acceleration of $+6G_x$, found shunts which ranged from 11 to 31 percent (average 17 percent) of the systemic blood flow. These values were unaffected by the administration of 100 percent oxygen. Figure 10-9, taken from this study, illustrates the effects of accelerations of +2, +4 and $+6G_x$. Control shunts are shown as zero, this presentation being necessitated by the very high and variable resting arteriovenous shunts found in these dogs after prolonged anaethesia and experimentation (from five to 32 percent of the cardiac output). In a later study (13), shunts of from 40 to 80 percent of the cardiac output were observed in dogs during transverse accelerations ($+G_{x \text{ and } y}$) of 4.4G and 6.7G, though control shunts were again large.

Factors influencing arterial oxygen saturation during acceleration

If the arterial oxygen desaturation which occurs during exposure to acceleration is caused simply by the perfusion of unventilated lung units, then it should be influenced by the same factors which determine the development of atelectasis during acceleration (see chapter 8), as the two phenomena share a common origin.

A simple relationship between desaturation and level of acceleration has already been demonstrated (Fig. 10-8), and this can be explained in terms of increasing numbers of alveoli attaining minimal volume and becoming closed-off and unventilated. The effect that such closure has on regional blood flow is not known, but it is unlikely to be great in view of the undramatic effect of subsequent collapse. Thus, the observation that the magnitude of the shunt is unaffected by the administration of oxygen (12, 13) suggests a lack of effect, whereas Niden has shown, also in the dog, that localised atelectasis produces a fall in pulmonary resistance and an increase in regional blood flow (193). A similar failure, to correct the ventilation - perfusion ratio of poorly ventilated alveoli by a corresponding reduction in perfusion, has been noted in the underventilated compartment of the lungs of asthmatic children (160).

Recent measurements of arteriovenous shunting, in dogs exposed to tranverse acceleration, showed that the total shunt tended to decrease during prolonged exposures though the oxygen saturation of blood leaving the dependent lung remained

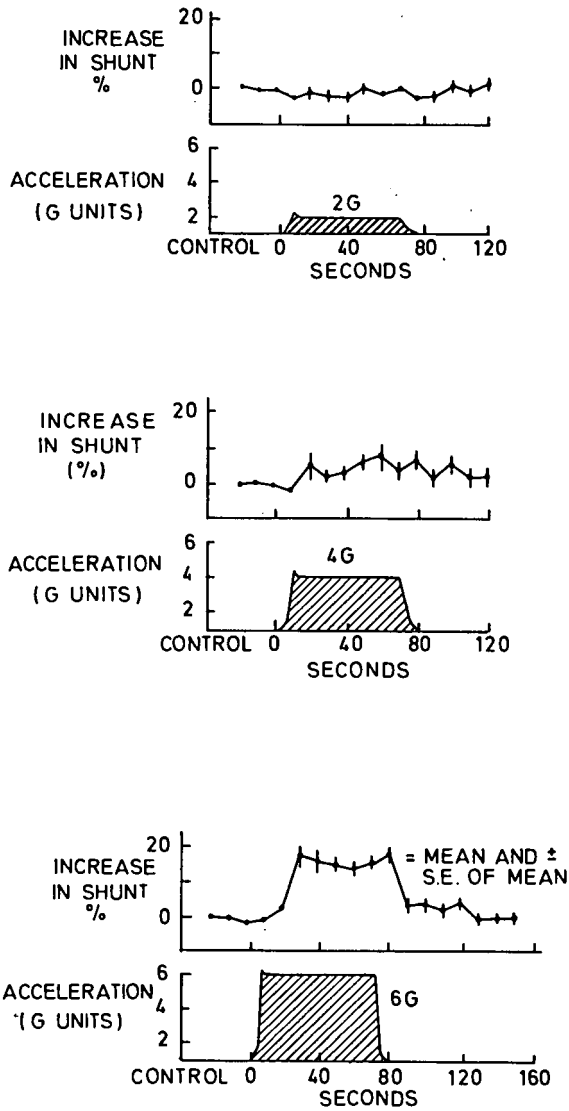

Fig. 10-9 Increase in pulmonary shunt (percent cardiac output) observed in anaesthetised dogs during exposure to forward accelerations of +2, +4 and $+6G_x$. Control values are taken as zero.
(From Banchero *et al.* (12), by courtesy of Aerospace Med.).

low or even fell further (259). This observation suggests that the fraction of the total pulmonary arterial blood which was perfusing unventilated lung actually decreased as atelectasis developed. This may be related to the genesis of a perfusion zone 4 in the lower lung (see fig. 6-13), which under these conditions could be caused by interstitial oedema or by lung collapse.

Should an increase in perfusion accompany atelectasis, then measurements of shunt will overestimate the proportion of lung which is unventilated or collapsed. On the other hand, if unventilated alveoli are present in the unperfused upper lung - though as discussed in chapter 8 this is unlikely - they will not contribute to shunting.

The effect of oxygen on the development of arterial desaturation during acceleration has already been considered in so far as the desaturation is delayed and reduced in extent. It was also noted that administration of oxygen led to slower recovery on return to normal gravity. This phenomenon can be related to the dramatic effect of oxygen on the development of acceleration atelectasis, and the mechanism must be the same. If unventilated alveoli contain oxygen, continued absorption will lead to atelectasis and the ensuing shunt will persist until this has been resolved. As noted in the preceding chapter, re-inflation of collapsed lung is slow, and is dependent upon forced inspirations or coughs.

The recovery of arterial oxygen saturation after a period of acceleration is also slow and dependent upon deep breathing and coughing. Green (112) noted a continuing fall in arterial oxygen tension when no deep breaths were taken over a period of one hour, following the development of acceleration atelectasis (subject exposed to $+4G_z$ for 75 seconds while breathing oxygen and wearing an anti-G suit). At the end of this period the shunt was estimated at 31 percent of the cardiac output. It is probable that atelectasis was continuing to develop while this subject was breathing shallowly on oxygen at $+1G_z$. On other occasions, normal oxygen tensions were regained rapidly on deep breathing and coughing. In another study it was noted that after exposures to forward acceleration breathing 100 percent O_2, saturations could be raised by as much as five to 10 percent by a single deep breath taken during the recovery period. It was also noted that three subjects, who developed marked acceleration atelectasis when breathing oxygen at five pounds per square inch, also exhibited precipitous falls in arterial oxygen saturation, and in one subject this lead to unconsciousness (3).

The inflation of an anti-G suit increases the degree of arterial desaturation which develops during exposure to positive acceleration. This finding is explained by the concomitant reduction in lung volume since, as discussed in chapter 8, alveoli in the lower lung will be further reduced in size, and a greater number will attain their minimal volume and become closed off. Barr and his colleagues have shown that, in dogs, vagotomy prevents arterial desaturation during exposure to positive acceleration (20). This effect was not explained but, since vagotomy results in a slowing and deepening of the respiration, it is probable that alveoli will come to be ventilated at some point in each respiratory cycle. The marked difference in desaturation recorded during human exposures to $+G_x$ and $-G_x$ acceleration (242, 243) can be explained on a similar basis of lung volume change. With the subject supine and the hips flexed 90°, the diaphragm is forced up and the volume of the lung decreased. With the subject prone, the diaphragm is displaced little and the lung volume may even be increased (243). The effect that such lung volume changes have on the ventilation of alveoli in the lower lung has already been considered in chapter 8, and trapping, atelectasis and pulmonary shunting will all be greater in the supine ($+G_x$) position. No studies have, however, been made of the development of atelectasis during exposure to $-G_x$ acceleration. In dogs, no significant differences were noted in oxygen saturations, nor in estimates of pulmonary shunts, with accelerations of 4.4G or 6.7G applied in the forward,

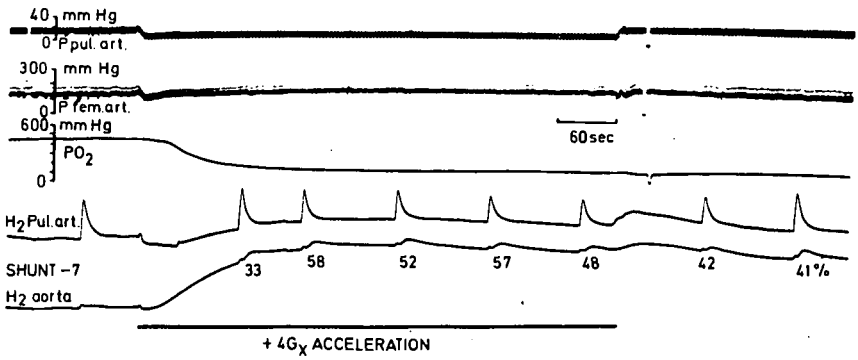

Fig. 10-10 Effect of an acceleration of $+4G_x$ on pulmonary and femoral arterial pressures, on arterial oxygen tension, and on potentials recorded from platinum electrodes in the pulmonary artery (H_2 pul. art.) and aorta (H_2 aorta). During the recording, repeated injections of H_2 solution were made into the right atrium of an anaesthetised dog artificially ventilated on 100% O_2. Right-to-left shunts have been calculated for each H_2 injection, and the values are given as percentages of the cardiac output.

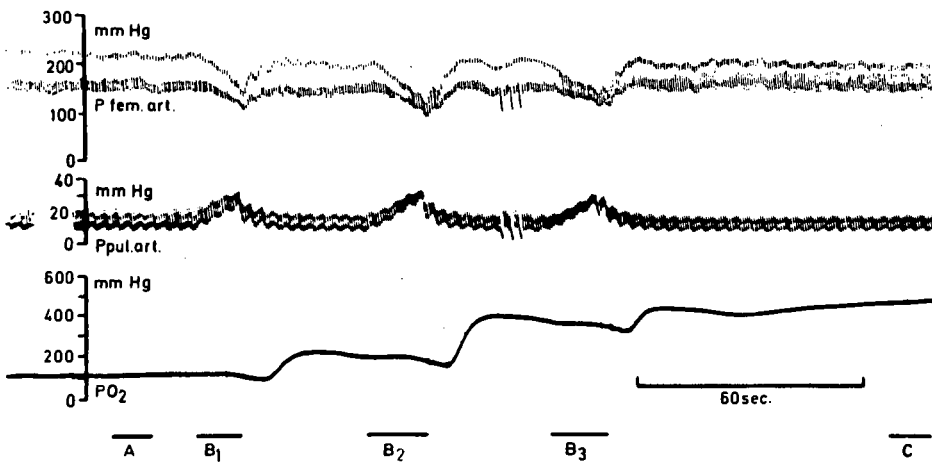

Fig. 10-11 Recording of femoral and pulmonary arterial pressure and arterial oxygen tension, starting seven minutes after the end of the centrifuge run illustrated in Fig. 10-10. At A, the H_2 shunt was 43%. At B_1, B_2 and B_3 the lungs were hyperinflated (VI = 960 ml), and at C, the H_2 shunt had fallen to three percent of the cardiac output. (From (105), by courtesy of Br. J. hosp. Med.).

backward, or left or right lateral directions (13). Lung volumes were not measured, however.

In other studies on dogs at accelerations of up to seven G, desaturation appeared more pronounced in left and right lateral decubitus, than in prone or supine body positions, especially when 100 percent 0_2 was breathed (259). Calculated arterio-venous shunts were greater than 60 percent of the cardiac output during exposure to accelerations of ±5 or $\pm 7G_y$, but were only 36 percent at $+6G_x$ and 41 percent at $-6G_x$. Furthermore, in all postures, shunting was restricted to dependent lung tissue, for blood sampled from a superior pulmonary vein remained well oxygenated, while that from an inferior vein became desaturated to an essentially mixed venous level. Postural differences in total shunt were attributed to differing degrees of lung collapse, though the reason for this was not clear.

A further observation on arterial desaturation, which may be related to changes in lung volume, is the very pronounced effect that negative ($-G_z$) acceleration has in the dog (122). Though unconfirmed, this single observation is again explicable in terms of a reduced lung volume. The different order of effect of $+G_z$ and $-G_z$ acceleration stress on pulmonary shunting may be compared to the greater ease with which atelectasis may be induced in inverted subjects by having them breathe at a small lung volume (see p. 142).

Right-to-left shunt

It is difficult to estimate absolute values of right-to-left shunt by following the transport of oxygen through the lung, because of the multiplicity of factors which govern the uptake of this physiological gas. Most of the problems can be overcome, however, by the use of a foreign, inert gas of low solubility. Attempts to make use of ^{133}Xe in this way have already been described (see p. 129) but, in dogs, the fate of ^{133}Xe passing through the pulmonary circulation is dependent upon pulmonary ventilation (104). This indicates that alveolar back-pressure of xenon in poorly ventilated units is sufficient to limit its escape from the capillary blood. In fact, under normal conditions, only 90 to 95 percent dissolved xenon is extracted from the pulmonary arterial blood on a single passage through the lungs (210).

Hydrogen has a water-gas partition coefficient of 0.02, about one sixth that of xenon, and the difference between their blood-gas partition coefficients is even greater (about one to 12), for xenon has an affinity for the haemoglobin molecule (56). The blood-gas partition coefficient of the radioactive isotope of hydrogen, $^3H_2$ (tritium), is similar to that of hydrogen (183). Either gas should be 99 percent cleared from the blood after a single passage through the pulmonary capillaries, even during breath-holding at a small lung volume (159). These gases should, therefore, be suitable for the estimation of right-to-left shunts.

In dogs, rapid injections of hydrogen, dissolved in saline, were made into the right atrium, and the concentration of H_2 in the pulmonary arterial and aortic blood was monitored by recording potentials developed by indwelling platinum electrodes.

In animals breathing air, physiological shunts of 30 to 50 percent were estimated from arterial oxygen tensions recorded at $+4G_x$, but less than five percent of the injected dose of H_2 appeared in the arterial blood. This indicates that the lung units responsible for the physiological shunt were still able to extract H_2 from the capillary blood. These units must have contained gas, but must have been very poorly ventilated. When the dogs were ventilated on 100 percent oxygen, H_2 shunts of up to 20 percent were obtained at $+4G_x$, and in one experiment (Fig. 10-10),

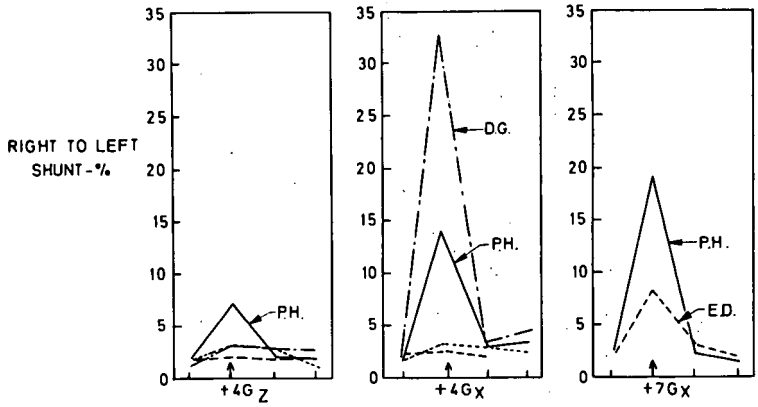

Fig. 10-12 Right-to-left shunts obtained with tritium in four subjects before, during and one and five minutes after exposure to accelerations of $+4G_z$ and +4 and $+7G_x$.

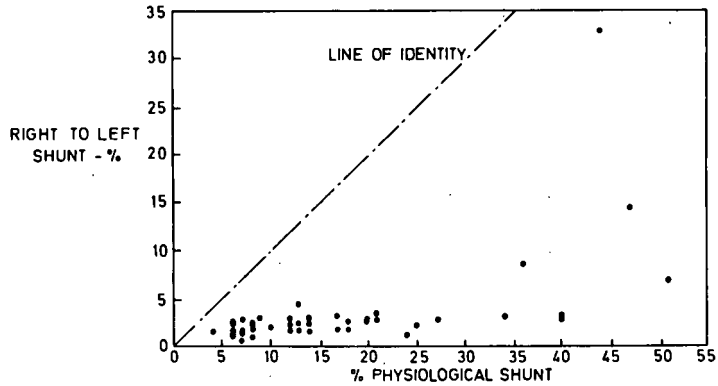

Fig. 10-13 Comparison of right-to-left shunts obtained using tritium with physiological shunts estimated from measurements of arterial oxygen tension. Points were obtained from four subjects at +1 and $+4G_z$ and +1, +4 and $+7G_x$.

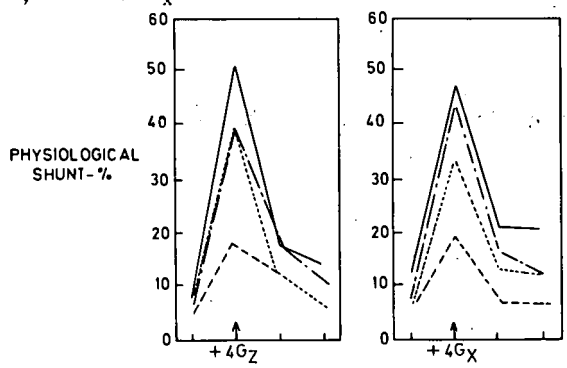

Fig. 10-14 Physiological shunts estimated from measurements of arterial oxygen tension in four subjects before, during and one and five minutes after exposure to accelerations of $+4G_z$ and $+4G_x$.

a shunt in excess of 50 percent was seen when the dog was artifically ventilated at a reduced tidal volume (100 ml). This H_2 shunt was similar to the computed physiological shunt, and must have resulted from the perfusion of atelectatic lung. It is considered that collapse was caused by the absorption of oxygen trapped in unventilated alveoli. Further evidence for this supposition comes from the observation that the shunt persisted on return to normal gravity, and remained until the lungs were over inflated. Disappearance of the H_2 shunt then coincided with the return of the arterial oxygen tension to normal (Fig. 10-11).

It was concluded from these studies that, in the dog, exposure to acceleration led to the trapping of alveolar gas, rather than to lung collapse *per se*; absorption collapse developing subsequently when oxygen has been breathed. This view is at variance with that of Wood and his colleagues who attributed part of the shunting they recorded at seven G to 'immediate collapse of a significant fraction of the alveoli in dependent regions as a consequence of the sevenfold increase in weight of the overlying thoracic contents' (259). However, 'some degree of gas trapping' was also invoked to account for the 40 to 90 second delay observed before shunting became fully developed.

Measurements of right-to-left shunt have also been made in men exposed to positive, as well as forward acceleration (unpublished observations of Mellemgaard and the present author). The gas used was tritium, and an intravenous injection of a saline solution of this gas was made after two-minute exposures to $+4G_z$ or to +4 or $+7G_x$. The injectate also contained tritiated water, and the right-to-left shunt was estimated by comparing the ratio of $^3H_2$ to ^3H_2O in the injectate, with that in arterial blood collected during maintained acceleration. Figure 10-12 shows the shunts obtained in four subjects. While significant increases in right-to-left shunt occurred in half the centrifuge runs, measurements of arterial oxygen tension showed that the majority of physiological shunts were very much larger (Fig. 10-13). It was considered that the physiological shunt was the result of gross ventilation-perfusion inequalities caused by a lung compartment having zero ventilation, but that, in subject DG at $+4G_x$, and to a lesser extent in subject PH at +4 and $+7G_x$ (Fig. 10-12), some alveoli had been squeezed empty of gas. Arterial oxygen tensions were virtually identical at $+4G_z$ and $+4G_x$ (Fig. 10-14), so that the difference in the tritium shunts must be ascribed to the reduction in lung volume caused by $+G_x$ acceleration.

From these limited observations it may be concluded that, in both men and dogs, exposure to acceleration leads to the development of an unventilated compartment in the lung. Usually this compartment contains trapped gas, and it will only become atelectatic after this gas has been absorbed. However, it is possible that, in some subjects, exposure to forward acceleration leads directly to atelectasis, a phenomenon which requires further study.

Transient changes in arterial oxygen tension following acceleration

If the arterial oxygen desaturation which results from acceleration is explicable simply in terms of perfusion of unventilated or collapsed alveoli, the same cannot be said of transient changes observed early in the recovery phase and, unlike those discussed above, independent of respiration. Such changes have been observed in man (18), as well as in the dog (21), and have recently been studied in detail in dogs exposed to positive acceleration, using an indwelling oxygen microelectrode (104). A typical recording of arterial oxygen tension taken during such an experiment is illustrated in fig. 10-14, and the tension changes can be divided into three phases. Firstly, as already discussed, arterial oxygen tension falls during exposure to acceleration. This fall is usually progressive, though it may

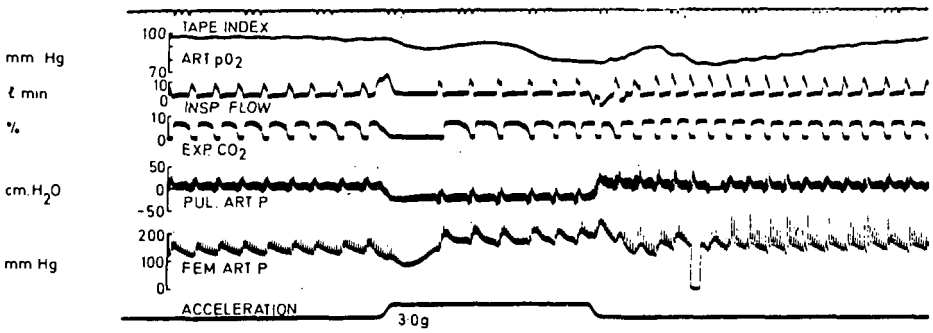

Fig. 10-15 Effect of a 50 second exposure to $+3G_z$ acceleration on an anaesthetised dog breathing air. From above, downwards, the traces show tape index (recorded every 20 seconds), arterial oxygen tension, inspiratory gas flow, expired carbon dioxide concentration, pulmonary and systemic arterial pressures, and imposed acceleration. Pressures are referred to the level of the pulmonary trunk and left ventricle respectively. The arterial oxygen tension falls in three distinct phases. (From (104), by courtesy of Aerospace Med.).

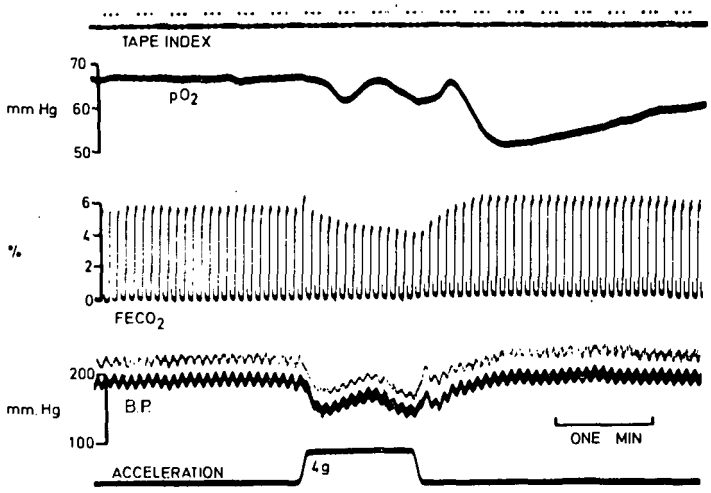

Fig. 10-16 Effect of an acceleration of $+4G_z$ lasting one minute on an anaesthetised dog artificially ventilated with air. From above, downwards, the traces record tape index, arterial oxygen tension (P_{O_2}), expired carbon dioxide concentration (FE_{CO_2}), and systemic blood pressure referred to heart level. During acceleration (lowermost trace), the arterial oxygen tension recovers transiently together with blood pressure, but on return to one G tension falls despite a rise in blood pressure. Expired carbon dioxide concentration falls during acceleration despite constant ventilation.
(From (104), by courtesy of Aerospace Med.).

be interrupted by partial recovery at the time that the systemic blood pressure rises. Such a transient recovery can be seen in fig. 10-14, and is shown more clearly in the experiment illustrated in fig. 10-15, where ventilation has been kept constant. The transient rise in arterial oxygen tension is attributed to a partial recovery in the cardiac output as discussed in chapter 5 (see p.73 and Fig. 5-1).

Following the return to normal gravity there is a further transient recovery in arterial oxygen tension, the peak of which occurs some 10 to 15 seconds after the centrifuge has stopped. A similar rise is not seen in mixed venous blood, nor is there any dramatic change in cardiac output which could explain it. It is attributed to the reperfusion of alveolar dead space in which alveolar gas had equilibrated with inspired gas and so, in the absence of carbon dioxide, come to contain a higher partial pressure of oxygen than normally present in perfused lung. The recovery of normal alveolar gas composition, with the return of carbon dioxide, heralds the end of this phase. Finally, there is a delayed recovery in tension which takes one to two minutes to return to normal. As discussed above, this delay can be attributed to a persistence of pulmonary shunting due to the failure of closed-off alveoli to reopen spontaneously on return to normal gravity.

As shown in fig. 10-17, the changes in arterial oxygen tension described above are still seen in dogs ventilated at a constant rate and depth on oxygen. It is concluded that, in the dog at any rate, much of the change in arterial oxygen tension seen during exposure to positive acceleration is due to a fall in cardiac output, a concomitant reduction in mixed venous oxygen content exaggerating the effect of a relatively small shunt.

A further feature which is also apparent in fig. 10-17, and which was very pronounced in the previous illustration (Fig. 10-16), is that the arterial oxygen tension seen following the return to normal gravity may fall below the lowest value recorded during acceleration stress. This phenomenon is not easy to explain, but may be due to a redistribution of pulmonary blood flow as the cardiac output recovers, so that a larger fraction comes to perfuse atelectatic lung. A similar effect has been noted in man, which was attributed to the return, to the lung, of blood which had been desaturated and pooled during the preceding acceleration (109). This explanation is not tenable in the dog where the mixed venous oxygen tension does not fall following acceleration, nor, if lung function had fully recovered, should desaturation be seen in man.

The effect of acceleration on gas stores in the body

The magnitude of the oxygen debt which would develop during exposure to acceleration due to a decrease in the quantity of oxygen stored in the body, may be calculated from changes in blood gas tensions (80). Pertinent data is scarce, since only arterial oxygen saturations are known in man. However, arterial as well as mixed venous tensions have been recorded in dogs during exposure to both positive and forward acceleration, so that reasonably accurate estimates of gas stores can be made in this species. The quantitatively similar arterial desaturations which result from exposure of the two species to acceleration, suggests that it should be possible to estimate the order of changes which must take place in man by collating all the available data. This procedure has been carried out with the results shown in table 10-1, the two situations considered being three minute exposures to accelerations of $+3G_z$ and $+8G_x$. For the calculation of oxygen stores, a body weight of 70 kg has been assumed. The sources of the data are indicated in the table; where no source is given the relevant figures have been calculated. Values for mixed venous oxygen tension may be approached in two ways; firstly, by direct measurement but as already mentioned, such measurements are few and far between. Secondly, by calculating how much oxygen must have been extracted

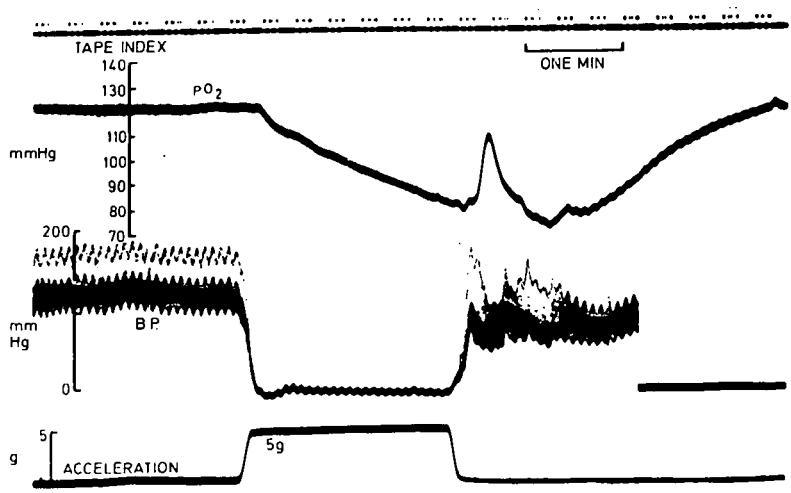

Fig. 10-17 Effect of an acceleration of $+5G_z$ lasting two minutes on an anaesthetised dog, relaxed and ventilated at a constant rate and depth with oxygen. From above, downwards, the traces record tape index, arterial oxygen tension (P_{O_2}), systemic blood pressure referred to heart level (B.P.), and imposed acceleration. Note progressive fall in oxygen tension during acceleration, transient recovery on return to one G, and the slow final recovery. The pressure transducer was open to atmosphere for the last 90 seconds of the recording. (From (104), by courtesy of Aerospace Med.).

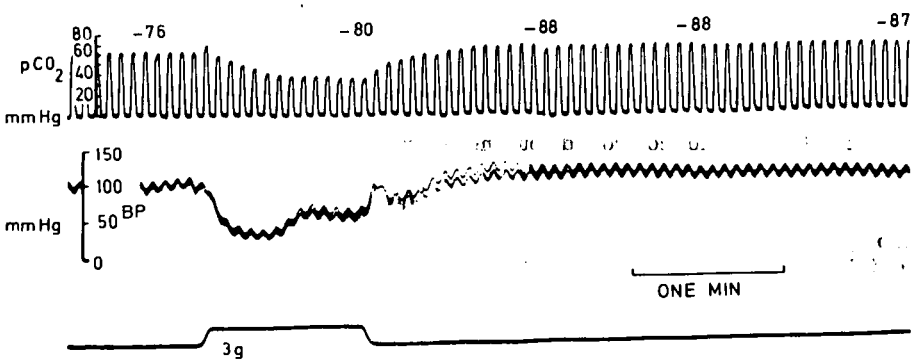

Fig. 10-18 Effect of positive acceleration on the overall arterio-alveolar carbon dioxide difference in the dog. The upper trace records the partial pressure of carbon dioxide in expired gas, and above it are the tensions of this gas in samples of arterial blood plotted to the same scale. The lower traces record systemic blood pressure and the imposed $+3G_z$ acceleration. Expired carbon dioxide concentration falls dramatically during acceleration but the arterial tension actually rises to give an apparent pressure difference of 47 mm Hg. The dog was anaesthetised, relaxed and ventilated at a constant rate and depth with air.

from blood by the tissues, using estimates of total oxygen consumption and cardiac output. While the second procedure was adopted in compiling table 10-1, it is satisfactory to note that the value for mixed venous oxygen saturation obtained at $+8G_x$ is very similar to values recorded in dogs exposed to acceleration of $+5.9G_x$ (12). However, the $+3G_z$ value for mixed venous oxygen tension is nearly double that recorded in dogs exposed to this same level of acceleration (104). The difference is explained by the finding that the reductions in cardiac output recorded in the dog were far greater than the values assumed for man. If cardiac output is assumed to fall by 50 percent at $+3G_z$ (as is likely in the dog), the discrepancy in mixed venous oxygen tension becomes insignificant.

The total oxygen stores of the body (oxyhaemoglobin plus oxygen present in tissues), when calculated from the best estimates of oxygen tensions, fall from their normal value of 905 ml, to 545 ml at $+3G_z$ and to 595 ml at $+8G_x$. These changes are also noted in table 10-1, and they should be 75 percent complete within one minute (80). Thus, over the course of a three minute centrifuge run, oxygen uptake could fall by up to 120 ml/min at $+3G_z$, and by up to 103 ml/min at $+8G_x$. If the metabolic consumption of oxygen were to rise during acceleration, the observed uptakes would be reduced to a smaller extent, and oxygen debts would be accrued of magnitudes very similar to those recorded following actual exposures to acceleration. The agreement is again particularly good at $+8G_x$, where a calculated debt of 745 ml oxygen may be compared with a measured debt of 650 ml oxygen (249). In each example, however, the calculated debt is more than adequate to account for the sequence of gas exchange observed during and after exposure to acceleration, and no additional mechanism needs to be invoked to explain the experimental findings.

It will be noted that no reference has been made to carbon dioxide in table 10-1, and oxygen figures have been calculated on the assumption that blood carbon dioxide tensions have not changed to a significant extent. Striking changes in expired carbon dioxide concentrations are seen during exposure to positive as well as to forward acceleration but, as discussed in chapter 8, they are explicable in terms of an increased alveolar dead space. Figure 10-16 illustrates such a finding in an anaesthetised, constantly ventilated dog, during exposure to an acceleration of $+4G_z$. A similar effect is illustrated in fig. 10-18, where the partial pressure of carbon dioxide in the expired gas fell from 60 mm Hg to 33 mm Hg after one minute at an acceleration of $+3G_z$, but an arterial blood sample showed that its carbon dioxide tension had actually risen from 76 mm Hg to 80 mm Hg. Similar results have been reported in man, the arterial carbon dioxide tension rising by seven millimetres of mercury at $+6G_x$ and by two millimetres of mercury at $+8G_x$ (248). Here ventilation was not controlled, but increased, during identical centrifuge runs, by 70 percent and 45 percent respectively.

Carbon dioxide excretions recorded in men during acceleration have been very variable, and this finding may be explained by the extreme sensitivity of the washout of this gas to ventilation, and by the very variable response of ventilation to acceleration (see chapter 2). For these reasons, no attempt has been made to calculate changes in carbon dioxide stores during acceleration. Thus, oxygen exchange is affected primarily by regions of low ventilation-perfusion ratio, but the elimination of carbon dioxide is more sensitive to regions of lung having a high ratio (238). Also, because of the larger size of the carbon dioxide stores present in the body, changes take place more slowly than with oxygen, and the process requires, in the dog, eight minutes to be 75 percent completed (80). It is therefore unlikely that steady-state conditions would be attained within the time course of the acceleration exposures being considered.

Table 10-1 Oxygen exchange under various conditions of acceleration.

	$+1G_{z \text{ and } x}$ (78)	$+3G_z$	$+8G_x$
Arterial blood			
oxygen content (vol. %)	20.3	19.9	16.1
oxygen saturation (%)	97.1	95.1 (228, 273)	77.0
oxygen tension (mm Hg)	95	80	42
Mixed venous blood			
oxygen content (vol. %)	15.5	12.9	10.0
oxygen saturation (%)	75.0	61.8	47.8 (12)
oxygen tension (mm Hg)	40	32	26
Mean tissue capillary blood			
oxygen tension (mm Hg)	58	48	31
Oxygen uptake (ml/min)	275	265 (95)	205 (249)
Oxygen consumption (ml/min)	275	320	420
Oxygen stores (ml)	905 (80)	545	595
Oxygen debt (ml)	0	495	745
Cardiac output (l/min)	5.7	4.6 (228, 273)	6.8 (273)

Note: Oxygen uptake and oxygen consumption values are averaged over 3 minute acceleration exposures; all other values apply to the end of such exposures. Where values are taken from the literature, appropriate references are given in brackets.

11

Summary and conclusions

All the breathing Spring William Collins

In the preceding chapters, the effects of acceleration on the behaviour and function of the lung have been considered in detail. The purpose of this final chapter is to gather these findings together and to try and paint a co-ordinated picture of the way in which gravity and acceleration act. In carrying out this process, some anomolies and differences of opinion - or interpretation, since the experimental findings are not disputed - must inevitably come to light. Such differences should constitute suitable subject matter for future research. The mechanics and ventilation of the lung will be considered first.

Lung mechanics

When the lung is considered as a whole, acceleration has remarkably little effect. Its compliance is unaltered and changes in pulmonary ventilation are small and variable. More significant is the effect of the increased weight of the chest wall which, in the supine posture, leads to a reduction in inspiratory capacity and to the virtual disappearance of the expiratory reserve volume. In the erect position ($+G_z$), vital capacity is better maintained, and the expiratory reserve volume is increased by the passive descent of the diaphragm. The effect of posture is simply explained by the fact that, on inspiration, the centre of gravity of the anterior chest wall moves forwards rather than upwards; and by the fact that, in the two body positions considered, the weight of the abdominal viscera tends to displace the diaphragm in opposite directions.

The residual volume of the lung is unchanged by acceleration in either body posture ($+G_z$ or $+G_x$), a finding which is taken to indicate that this volume is a function of the lung *per se*, rather than of the chest wall. It appears that residual volume may be attained when only some half of the lung alveoli are at minimal volume and their airways closed (Fig. 3-10, p.46), so that reflex inhibition of expiratory effort must intervene before complete closure of all the airways occurs. However, the fraction of the lung which is closed off increases rapidly as residual volume is approached and it is difficult, even in trained subjects, to make measurements absolutely at residual volume. It is possible that, ultimately, expiration is limited by complete closure of airways, so trapping all the gas remaining in the lung.

Regional ventilation

It is only when regional behaviour of the lung is considered that the profound influence of gravity and acceleration becomes apparent. Evidence presented in chapters 3, 4 and 8 suggests that a weightless lung would be uniformly ventilated, but that acceleration produces inequalities in ventilation, and can even cause gas

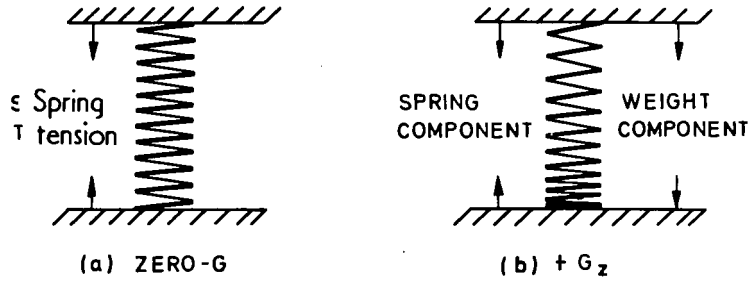

Fig. 11-1 Behaviour of a loosely coiled spring when weightless (a) and when exposed to acceleration (b). Coil spacing is taken to indicate the relative sizes of alveoli within the lung.

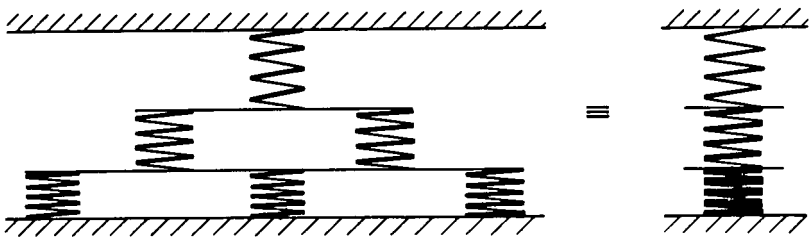

Fig. 11-2 a) Compound spring model of the lung used by Proctor *et al* (213) to account for a uniform distribution of pressure along the inverted dog lung (coil spacings are equal when this model is turned upside down). b) An equivalent model made up by three springs of differing stiffness in series.

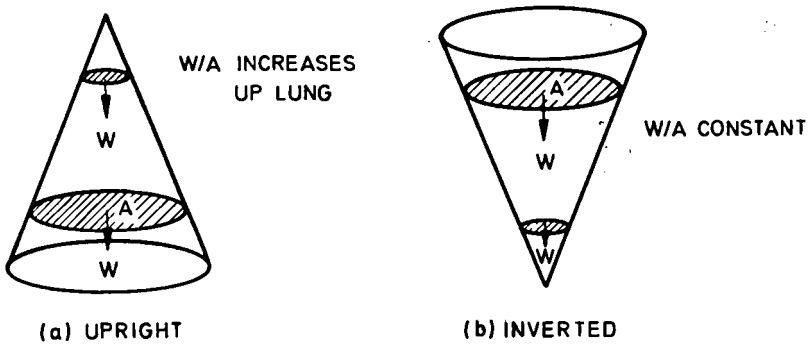

Fig. 11-3 A model of the lung in which pressure (or alveolar size) at any level is given by the appropriate depending weight (W) divided by the cross-sectional area at that level (A). W/A increases with distance up the upright lung (a), but is constant throughout the inverted lung (b).

to be trapped behind closed airways during normal breathing.

In order to discuss the way in which gravity and acceleration act upon lung tissue, it is necessary to have a simple model, the behaviour of which can be predicted. This behaviour can then be compared with the response to acceleration of the human lung, so that the validity of the model can be assessed. To be acceptable, the model must predict regional ventilations correctly during weightlessness, at differing levels of acceleration, and in various body postures under normal gravity. Two simple models have already been referred to in chapter 3 and were illustrated in fig. 3-12 (p. 50). One likens the lung to a loose coiled spring supported at either end, the other considers the lung as a sponge supported solely from its upper surface.

The lung as a simple spring

The spring model has been redrawn in fig. 11-1, where it is considered to represent a lung at functional residual capacity, first weightless (a) and then under the influence of acceleration (b). When weightless, the only force acting is tension due to stretch of the spring. This tension is uniform along the spring's length and equally and oppositely applied to the two supports. Since the spring has mass, a downwards acting inertial force will be developed when the spring is accelerated upwards. When the acceleration is due to gravity, this force is referred to as weight. It acts on each part of the spring and always in the same direction, so that tension in the spring is increased above and decreased below, and the coils become more widely spaced at the top and closer together at the bottom (Fig. 11-1b).

Coil separation in this model is taken to indicate alveolar size and, due to the non-linear compliance of lung tissue, smaller alveoli at the lung base will be better ventilated than larger ones at the apex. As the level of acceleration is increased, the lowermost coils of the spring close up completely. The number of coils closed then increases and the upper level of closure rises steadily up the spring.. Shortening of the spring assists this process as it reduces tension in the upper, stretched coils. Closure of dependent coils will then take place at a lesser level of acceleration. In all these respects the behaviour of the spring mimics that of the lung, only alveoli do not close completely, but become shut off at a certain minimal volume, set apparently by the mechanics of the alveoli and airways.

Further analysis of the spring model suggests that, at high levels of acceleration, it is quite possible for alveoli at the top of the lung to be at their maximum capacity, while alveoli at the bottom are at their minimal volume. Experiments reported in chapter 8 suggest that this may occur at accelerations greater than $+9G_z$ (see p.138).

In the spring, spacing of the upper coils continues to widen as the level of acceleration is increased. This suggests that alveoli at the lung apex could be expanded beyond the volume they normally occupy at total lung capacity. In fig. 4-2 (p. 56), regional lung volume was plotted against total lung volume for the upper, middle and lower lung. At $+2G_z$ and maximum inspiration, all three regions achieved just 100 percent of their $+1G_z$ maximum volume. However, there is no evidence to show that the same must hold true at greater accelerations.

If the spring is laid on its side, its coils become equally spaced, independent of acceleration. In the supine posture the apex and base of the lung receive approximately equal ventilations. If the spring is turned upside down, the roles of top and bottom are simply reversed and the new lower lung (anatomically the apex) should be better ventilated than the new upper lung (anatomically the base). If the volume of the lung is then reduced, airway closure and gas trapping should occur first in the new lower lung: if the trapped gas is oxygen, this is where absorptional atelectasis should be expected.

Unfortunately, the behaviour of the inverted lung is not quite so clear cut as would be liked, but the majority of observations conform with these predictions. When the rate of wash-in of radioactive xenon is used as an index, the dependent lung is better ventilated than the uppermost lung, regardless of posture (102). Single breath tests in which a small bolus of tracer gas is inspired from residual volume demonstrate that the pattern of expiration, and that of inspiration, is almost exactly reversed when the experimental subject is inverted; and indicate that, during expiration, closure always starts in dependent airways (Fig. 8-13, p.136). When inverted subjects breathe oxygen at a low lung volume, atelectacis develops at the dependent lung apex (Fig. 8-16, p.141). The distribution of inspired gas has been reported to be uniform in inverted subjects (Fig. 3-4, p. 40), but it may be noted that these subjects were only 60° head down, and a reversed pattern of inspired gas distribution was actually found in some of them (Milic-Emili, personal communication).

It appears that the simple spring model can account for the influence of gravity and acceleration on the regional ventilation of the lung with a considerable degree of accuracy but, intuitively, one hesitated to accept a model which ignores, so blatantly, two of the three dimensions of the lung.

The lung as a compound spring

Recently, Proctor and his colleagues (213) have modified the simple spring model to take some account of lung shape, by arranging a number of similar springs in a series-parallel configuration (Fig. 11-2). The effect of this is to exaggerate differences in coil spacing when the model is upright, but since the tension applied to the top spring must be shared equally between the lower three springs (Fig. 11-2a), these will still be less stretched when the model is placed on its side, or even when weightless. Thus, such a model does not accurately predict the behaviour of the human lung as outlined above. While the greater thickness of the lower lung appears to have been taken into account in the compound model, spring tensions are still all acting along a single axis as they were in the simple spring. The model can, therefore, be simplified to that illustrated in fig. 11-2b, where three springs of differing stiffness are arranged in series. The use of such a model implies that the lower lung is less compliant than the upper lung but, at least in man, regional differences in compliance appear small compared to the effect of gravity (50).

Neither the simple nor compound spring models described above can be used to make predictions about intrapleural pressures, for lateral forces are not considered. A further model has, however, been used for this purpose.

The lung supported from above

Mead (179), and more recently West and his colleagues (107), have developed a model of the lung in which it is considered to be supported solely from its upper surface. This model takes account of lung shape, since the pressure due to gravity at any level is given by the weight of lung tissue below that level, divided by the appropriate cross sectional area. Since the lung approximates to a cone, rather than to a cylinder, the cross sectional area decreases up the lung as the depending weight increases, and a steep pressure gradient is generated (Fig. 11-3a). This interstitial pressure gradient will produce regional differences in alveolar size, and therefore, in ventilation, as in the previous models.

When laid on its side, the apical support model predicts uniform ventilation from apex to base, again in agreement with experimental findings in man. However, when inverted, cross sectional area increases with depending weight (Fig. 11-3b), and ventilation will again be uniform from apex to base. This prediction is not in accord with the majority of the experimental findings as outlined above.

The apical support model has been invoked to account for a uniform distribution of alveolar size found in dogs frozen while inverted (107). This finding could also be explained by the lower lobes of dog's lungs being less compliant than the upper lobes, as has been demonstrated in lungs isolated from this species (82, 88). The uniform distribution of alveolar size could also have been the result of a postural change in lung volume. The same model has been used to account for the absence of an intra-oesophageal or intrapleural pressure gradient in inverted dogs (213), but the assumption that the lung derives its sole support from its upper surface denies the existence of these pressure gradients in any body position. Thus, the existence of a pressure gradient implies that the lung is obtaining varying support from the pleural surface. It follows that the apical support model can only be used, logically, to account for the behaviour of an isolated lung, suspended in this manner.

The fluid lung

Krueger and co-workers (153) suggested that the lung behaved like a fluid poured into the thoracic cavity, and that the interstitial and intrapleural pressure gradients were the equivalent of a hydrostatic pressure gradient. These gradients should therefore be independent of lung shape, just as the vertical hydrostatic pressure gradient in a vessel filled with water is independent of the shape of the vessel, and pressure must always increase down the gravitational axis. The behaviour of the lung predicted by this model is identical to that of the simple spring considered above, for if the 'fluid' is allowed to be compressible, alterations in alveolar size and ventilations will occur as before. In addition, the fluid model allows pressures surrounding the lung to be predicted.

Intrapleural pressure

Unhappily, there is considerably less agreement about the effects of posture on intrapleural and intra-oesophageal pressure gradients, or even upon the magnitude of the gradient in the normal upright chest, than there is about the effects of posture on the distribution of ventilation. One problem, recently highlighted (208), is a possible difference between fluid and surface pressure, and this probably accounts for some of the discordant results. Nevertheless, pressure gradients with magnitudes appropriate to the density of lung tissue have been recorded in seated subjects. These gradients are increased in proportion to applied acceleration and disappear upon adoption of the supine posture. In all these respects the 'fluid' lung proves to be an adequate model.

Fewer measurements have been made in inverted subjects, but in the dog, and by using calibrated Starling resistors to measure surface pressures, Proctor and co-workers found that the intra-oesophageal pressure gradient was absent whether the animals were supine or supported head down (213). The compound spring model was developed to account for this finding, but has already been shown to suffer from greater failures in prediction when applied to man. The fluid model predicts a simple reversal in the gradient of intra-oesophageal and intrapleural pressure when the lung is inverted, as some other workers have in fact found (257), and this model should not be discarded until the conflicting observations have been confirmed in man.

The reason for difficulties in predicting the regional distribution of intrapleural pressure, as well as for possible discrepancies between the regional pressure and the ventilation of the underlying lung, is apparent when the factors which must determine the pressure at any point on the pleural surface are considered. Firstly, if an isolated lung is inflated to the volume it would occupy in the relaxed thorax (functional residual capacity), a positive pressure is required. In life,

alveolar pressure is equal to atmospheric pressure, and the lung is kept inflated by virtue of the fact that it has to fill the pleural cavity by default as it were, since both gases and liquids are absorbed from the intrapleural space and cannot constitute a stable filling (178). A sub-atmospheric or 'negative' pressure is therefore generated and, in theory, this is equal throughout the intrapleural space.

A second factor which causes local variations in intrapleural pressure is that when the lung is inflated as described above, its shape does not exactly match the cavity in which it has to fit. A balloon inflated within the thoracic cavity would exert the greatest surface pressure at the points where it first made contact with the parietal pleura. At other places, such as the costo-phrenic angles, it would be unlikely to make contact at all. Steep gradients of pleural pressure would therefore be generated around regions of greatest miss-fit. While the lung is obviously better shaped to fit the thoracic cavity than a simple balloon, this factor could account for steep gradients of pressure recorded at the lung apex and in the costo-phrenic angles. These local pressure gradients should be largely independent of gravity, and should still occur during weightlessness.

A third factor is that, due to gravity, the lung is not weightless, but has a density of 0.2 to 0.3 g/cm^3, the two lungs together, in man, weighing about one kilogramme. If the thoracic cavity were filled with a fluid of specific gravity 0.2 to 0.3, the pressure recorded at the pleural surface (or at any point within the fluid) would rise by 0.2 to 0.3 cm water/cm vertical descent, and the pressure at the base would be about 7.5 cm water higher than that at the apex. If the fluid is poured, not directly into the thoracic cavity, but into a balloon previously inflated there, a hydrostatic pressure gradient will still be present, but it will only be transmitted to the intrapleural space at those points where the balloon makes contact with the parietal pleura. Elsewhere, hydrostatic pressures will be supported by tension developed in the wall of the balloon (that is, by the visceral pleura).

The result is that most of the intrapleural space will be exposed to a gravity dependent pressure gradient, some of it will be protected, and other parts will exhibit non-gravity dependent gradients due to local distortions of the lung surface. Surface pressures actually recorded in any posture will depend upon the relative magnitude of these factors: this probably varies from species to species and even at different lung volumes in the same species.

It is probable that the pressure gradients which result from local distortion of the lung surface do not act deep within the lung parenchyma, just as the surface of an inflated balloon can be indented without causing a local rise in underlying gas pressure. Mead, in his recent analysis of the transmission of pressures through the lung (179), showed that local variations in alveolar size tend to be smoothed out. Thus, the pressure gradient which determines alveolar size, and hence the ventilation of the bulk of the lung tissue, is that due to lung density. Ventilation should therefore be more uniform, and more consistent in its gravity dependence, than measurements of intrapleural pressure might suggest. This prediction is borne out by the experimental results already discussed.

Finally, since the intrapleural space is filled with a liquid having a specific gravity of about one, the pleural fluid, there will be a liquid pressure gradient of one centimetre of water per centimetre vertical distance, due to gravity. Such a gradient has been demonstrated to exist even in thin capillary films, and is measurable when liquid filled catheters and pressure gauges having a very low compliance are used (251). These pressures will not have any significance in relation to the function of the underlying lung, but explain the steep gradients sometimes recorded. A similar difference between liquid and surface pressure has been demonstrated in the oesophagus (208).

To sum up, the regional distribution of ventilation is modified by posture, and by increased acceleration, in a manner predictable on the basis that the lung behaves like a loosely coiled spring or compressible fluid. Interstitial pressures are explicable on the basis of the density of a fluid-like lung parenchyma, while intrapleural pressures are subjected to superimposed local stresses. The interstitial pressure gradient will also be invoked to account for a reduced blood flow to the lower lung (see below). More significant in determining regional changes in ventilation is the occurrence of airway closure, since this can convert a region of good ventilation at the bottom of the lung to one of zero ventilation, simply because of a further small reduction in regional lung volume. Such a reduction could result from a decrease in total lung volume - voluntary, postural, or due to inflation of an anti-G suit - or be caused by acceleration.

The subsequent behaviour of closed-off alveoli depends upon the solubility of the gas trapped, the regional blood flow, and the length of time before the factors which led to airway closure are alleviated. If this time is shorter than that required for complete absorption of trapped gas, then airways will simply re-open and normal ventilation will be resumed. If, on the other hand, sufficient time is available for complete absorption - and this may be predicted quite simply (Fig. 8-18, p.143) - surface tension forces will maintain the collapse until an adequately high transpleural pressure has been generated. This may result from a cough, or from a maximal inspiratory effort, and collapsed alveoli will then be cracked open and ventilated. The degree of reduction in vital capacity caused by absorptional collapse appears to be much greater than the volume of gas absorbed (p.140), and is presumably largely due to a reflex limitation to inspiration, though the neuronal pathway responsible is unknown.

Regional perfusion

The gravitational dependence of pulmonary blood-flow distribution was recognised some 70 years before that of the distribution of pulmonary ventilation yet the precise mechanisms by which relatively small variations in arterial, venous and alveolar pressures could lead to gross differences in regional blood flow have only recently been elucidated. They were described in chapter 6. Confirmation, that regional differences in perfusion are primarily the result of hydrostatic pressure gradients within the pulmonary vasculature, is given by the finding that they increase in direct proportion to applied acceleration (chapter 7). However, this is not true of a zone of decreasing blood flow sometimes found at the bottom of the lung and referred to as zone 4 (p. 97).

It is apparent that two separate indices of blood flow are required in order to assess fully the mechanisms responsible for its distribution, as well as the effect that this distribution has upon lung function. Measurement of blood flow per unit lung volume allows the relationships between flow and pressure, and between regional flow and regional ventilation, to be determined: measurement of blood flow per alveolus is needed in order to assess the relative contributions of regional differences in capillary density and dimensions.

There are two possible explanations for the observed distribution of blood flow and the influence, thereupon, of acceleration. The first is the three-zone model described in chapter 6. This model explains most of the experimental observations made on isolated lungs, as well as in intact man, but to do so, ascribes a high degree of distensibility to capillaries in the dependent lung. Evidence is beginning to accumulate which suggests that these capillaries are not so distensible (Permutt, personal communication), and this is also suggested by the rather flat blood-flow per alveolus curve recorded down the lung at $+5G_x$ (Fig. 7-11, p. 115). An

alternative explanation is given by a choice of mechanisms which have the effect of stretching the waterfall effect region (zone 2), so that the whole of the perfused lung is involved. These mechanisms were discussed in detail in chapter 7 (p.109) and they warrant further investigation. In this connection, it may be noted that, in the isolated lung, histological studies have shown that not all capillaries are open even under zone 3 conditions (see p. 95), a fact which could be taken to imply that this zone is really a downwards extension of zone 2.

Finally, there is the rather awkward region at the bottom of the lung (zone 4), where blood flow per alveolus decreases despite a further rise in hydrostatic pressures. This phenomenon has been ascribed to the action of interstitial pressure on extra-alveolar vessels (p.101), but, since the gradient of interstitial pressure depends upon lung density (0.2 to 0.3 g/cm^3), and vascular pressures upon the density of blood (1.06 g/cm^3), it is difficult to see how interstitial pressure, acting from outside the vessels, can ever exceed the hydrostatic pressure, acting from within. Even if the interstitial pressure gradient is considered to be due to a column of tissue fluid, this would merely balance the intravascular pressure gradient, and blood flow would be uniform throughout zone 4. It is conceivable, however, that interstitial pressure acts by distorting the blood vessels in some way, just as a kink will occlude a high pressure hose. In favour of such a mechanism is the observation that, during forward acceleration, zone 4 appears to coincide with a region of gas-trapping in which distortion of the lung parenchyma is presumably at a maximum. A further factor which must be considered is that, in such a region, alveolar pressure need no longer remain at effectively atmospheric pressure, but could rise to equal interstitial pressure. In this way the influence of interstitial pressure does not have to be restricted to extra-alveolar vessels. More needs to be known about the factors which influence the development and extent of zone 4. For example, can it be identified at the apex of an inverted lung like gas-trapping, and how is it modified by absorptional atelectasis?

A decrease in the quantity of blood going to unventilated units is of obvious benefit to the gas exchange function of the lung, for alveolar shunting will be reduced. Such a decrease could be caused by constriction of pulmonary resistance vessels, initiated by changes in alveolar or capillary blood gas tensions. Though these reflex mechanisms undoubtedly exist (8, 127), they seem too feeble to produce a zone 4. Thus, a shift of blood away from hypoxic lung was only obtained when the alveolar oxygen tension was dropped below 35 mm Hg (127), a value less than would occur, initially at any rate, even in a region of gas-trapping.

Despite reservations about zone 4, the effects of acceleration on the distribution of pulmonary blood flow can be simply stated. At the plane of hydrostatic indifference appropriate to the posture (five centimetres below the pulmonary trunk in a seated subject, 15 cm anterior to the back of the chest in a supine one), mean pulmonary arterial pressure remains constant at about 15 cm water. At a vertical distance above this plane given by that pressure (cm water) divided by the relevant hydrostatic pressure gradient (cm water/cm), blood flow falls to zero. Any lung above this level is unperfused and constitutes alveolar dead space. Below this level blood flow per unit lung volume increases linearly with vertical distance down the lung, the rate of increase being proportional to acceleration up to some three G, but appearing to fall off at greater levels of acceleration. The increase in flow continues right down the lung, with no evidence of discontinuity. However, when blood flow is expressed per alveolus and hence, presumably, per capillary, there is a marked discontinuity in its rate of increase; to the extent that blood flow actually falls in the lowermost lung. The difference between the two sets of measurements is a striking demonstration of the distortion to which the lung must submit during exposure to high levels of acceleration.

The extreme sensitivity to acceleration exhibited by regional blood flow, and the

ready production of alveolar dead space (and wasted ventilation), raises the question of why normal pressures are so low in the lesser circulation. The answer may be found by considering fluid exchange in the lung, since extravasation into the tissues, and possibly into alveoli, will occur if capillary pressures exceed alveolar gas pressure by as little as 30 to 40 cm water (p.119). This figure sets an upper limit to capillary pressures at the base of the lung, and hence to pressures at all other levels. A second feature which requires the pulmonary circulation to function at a low pressure, is that the diffusion distance between blood and gas must be short. Capillaries must, therefore, be thin walled, and can obtain only minimal support from other tissues. Rather surprisingly, these vessels do appear able to withstand quite high pressures without evidence that they have been overstressed. For example, in man, capillary pressures at the back of the lung may reach 120 cm water (90 mm Hg) or more at $+8G_x$, without evidence of failure, though a rise in gas pressure in closed-off alveoli could have afforded them some protection. Haemorrhages have been demonstrated in the lungs of dogs, however, following a three minute exposure to the same level of acceleration (151), though these were not restricted to the dependent parenchyma where rupture would be expected, but appeared to be caused by tearing of tissues at the lung root.

Regional ventilation-perfusion ratio

As discussed in chapter 9, blood flow must be related to ventilation on a regional basis in order to evaluate the function of the lung in terms of gas exchange. When this is done, it is apparent that gravitational dependence of ventilation is an advantage, once the need for a gravity dependent distribution of blood flow has been established. The matching of ventilation to perfusion is not perfect, however, even at one G, and at higher levels of acceleration ventilation-perfusion inequalities become pronounced (Figs. 9-1, p.152 and 9-4, p.156). Even so, the shape of the oxyhaemoglobin dissociation curve means that a considerable degree of mis-match can be accommodated with little fall in the oxygen saturation of blood leaving the lungs (p. 155). More aggravating to the gas-exchange function of the lung is the development of a region of zero ventilation-perfusion ratio due to gas-trapping, or to overt atelectasis, since in either case an alveolar, right-to-left shunt is generated, which cannot be compensated for by an increase in the ventilation of functioning lung units.

While exposure to positive acceleration leads to a similar reduction in the saturation of arterial blood as does exposure to forward acceleration (Fig. 10-8 p. 166), the precise mechanisms responsible for desaturation appear to differ. With $+G_z$ acceleration, a modest right-to-left shunt is aggravated by a reduced cardiac output, tissue hypoxia, and a further desaturation of shunted blood. With $+G_x$ acceleration the cardiac output is well maintained, but a postural reduction in lung volume increases the extent of airway closure and gas-trapping, and alveolar shunting is enhanced.

Radioactive xenon studies, to which frequent references have been made, allow the function of relatively small volumes of lung tissue to be studied. Even so, resolution of radiation detecting systems is limited, and the field of view is large compared to the size of an alveolus, or even to the functional unit of lung comprising a single terminal bronchiole and its divisions. For example, in the rat's lung, autoradiographic techniques have demonstrated large gradients of ventilation and perfusion within a secondary lobule (263). However, since these gradients appear to be the same for both gas and blood, the fact that they would be missed by conventional ^{133}Xe techniques is probably unimportant.

Unfortunately, the resolution of detecting systems for gamma radiation cannot be improved without reducing their overall sensitivity, and the practicable limit of

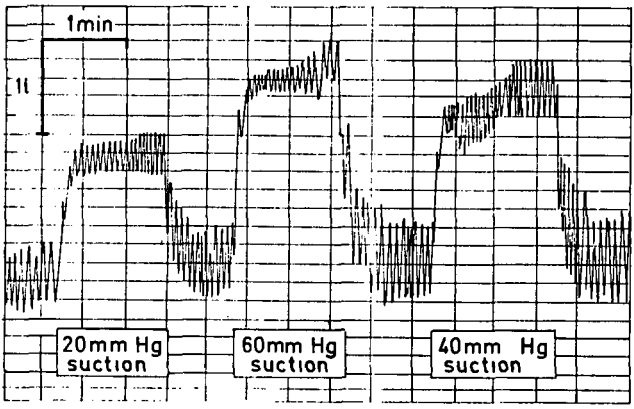

Fig. 11-4 Lung volume changes recorded when a relaxed, quietly breathing subject, lying supine, is exposed to a sub-atmospheric pressure to the body below the level of the lower ribs (xiphisternal suction).

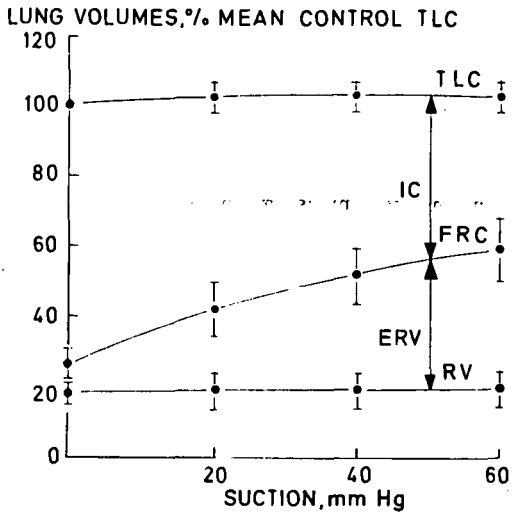

Fig. 11-5 Effect of xiphisternal suction on total lung capacity (TLC) and its subdivisions - inspiratory capacity (IC), functional residual capacity (FRC), expiratory reserve volume (ERV) and residual volume (RV).

resolution has probably been obtained with existing collimators (101). An apparently homogeneous region of lung could, in theory, still contain alveoli exhibiting a wide scatter of ventilation-perfusion ratios. Radioisotope techniques are, therefore, complementary to other methods which may be used to compartmentalise ventilation-perfusion inequality. A method which makes use of the rates of washout of pairs of inert gases of differing solubilities (81) could usefully be applied to centrifuge studies, and would allow an independent assessment of ventilation-perfusion inequality to be made.

The evidence so far presented supports the view that regional distributions of ventilation and perfusion within the lung are dependent upon inertial forces. This implies that all alveoli on a given horizontal plane should be functionally homogeneous, and that differences will only occur along the gravity or acceleration vector. This is the reason for the development of flat-beam collimators for radioisotope studies of the lung, since they combine high sensitivity with good vertical resolution (101). However, once constructed and used for scanning the lung vertically, their employment does not allow the underlying hypothesis to be proved to the extent of excluding all other factors which might affect the distribution of gas or blood across, rather than up and down the lung. Fortunately, studies using multiple detectors arranged in horizontal as well as vertical rows (146), and more recently, the employment of scintillation cameras to allow two-dimensional analyses (192), have clearly shown that the horizontal distributions are effectively uniform, at least at a macroscopic level.

Methods for increasing G-tolerance

The opening chapter referred to the place of acceleration in aerospace medicine. The present day, well tolerated acceleration stresses of space flight allow high velocities to be achieved - 24 200 mph (35 500 ft./sec) on the outward leg of the historic flight of Apollo 8 - but, even so, it took $2\frac{1}{2}$ days to reach the moon. If minimum acceleration is the criterion, a flight to Mars would take almost nine months, and it is apparent that, if man is to penetrate beyond the immediate confines of the solar system, he must travel much faster. A property of rockets is that, to be efficient, they must deliver high thrusts of relatively short duration. This means that the accelerations imposed on man are likely to increase, and it is of interest to speculate on ways in which man's tolerance to acceleration could be increased.

The systemic circulation can be protected by adopting a horizontal posture and, at higher levels of acceleration, by immersing the body in water, so that hydrostatic pressure gradients within the circulation are exactly balanced by similar gradients without (111). Tolerance to prolonged forward acceleration is dictated, initially, by ventilation-perfusion inequality, gas-trapping and atelectasis, subsequently by mechanical difficulty in breathing, and ultimately by the differing densities of air, and of lung tissue and blood, so that the unsupported lungs may be torn from their roots.

Ventilation-perfusion inequalities can be reduced, and gas-trapping and atelectasis minimised, by breathing at a larger lung volume. Possible mechanisms by which this can be achieved include positive pressure breathing, adoption of a slightly head-up attitude (until the $+G_z$ component becomes significant and cerebral blood flow drops), adoption of the prone posture, or the application of a negative pressure to the abdomen. The first three of these techniques have been demonstrated to be beneficial (264, 278, 227), and the last appears promising. Thus, exposure of the body below the level of the lower ribs to a negative (sub-atmospheric) pressure, causes a dramatic increase in the functional residual capacity of the lung (Fig. 11-4). The procedure has no effect on total lung capacity, nor on

residual volume (Fig. 11-5), and systemic effects could be reduced by excluding the lower limbs from suction. An increase in lung volume during forward acceleration should also increase the tidal volume, for the compliance of the thorax will be effectively increased (Fig. 2-14,p. 30).

It is less easy to overcome problems caused by the different density of gas and tissue at high levels of acceleration, though there are two theoretically possible ways in which it might be done. The first makes use of the phenomenon of acceleration atelectasis to de-gas the lungs, collapse being aided by the induction of a bilateral hydrothorax (72). For brief acceleration exposures this might be adequate, but for longer periods an alternative means of achieving gas exchange, such as an extra-corporeal 'lung', would be required. A second possibility is to adopt 'fluid' breathing, in which air is replaced by a low viscosity fluid equilibrated with oxygen. Certain fluorocarbon compounds appear promising for this application, since they combine low viscosity and non-toxicity with high oxygen solubility (47). In either case the systemic circulation would require support at least as effective as that provided by immersion in water, and accelerations of the order of 30G or more could well become tolerable.

References

1. Abernethy, J.D., Maurizi, J.J.,and Farhi, L.E., 'Diurnal variations in urinary-alveolar N_2 difference and effects of recumbency.' J. appl. Physiol. 23, 1967, 875-879.

2. Abramson, D.I., Katzenstein, K.H., and Ferris E.B., 'Observations on reactive hyperaemia in various portions of the extremities.' Am. Heart J. 22, 1941, 329-341.

3. Alexander, W.C., Sever, R.J., and Hoppin, F.G., 'Hypoxemia induced in man by sustained forward acceleration while breathing pure oxygen in a five pounds per square inch absolute environment.' Aerospace Med. 37, 1966, 372-378.

4. Allen, C.M. Van, Lindskog, G.E., and Richter, H.G. 'Collateral respiration. Transfer of air collaterally between pulmonary lobules.' J. clin. Invest. 10, 1931, 559-590.

5. Anthonisen, N.R. and Milic-Emili, J. 'Distribution of pulmonary perfusion in erect man.' J. appl. Physiol. 21, 1966, 760-766.

6. Armstrong, H.G. and Heim, J.W. 'The effect of acceleration on the living organism.' J. Aviat, Med. 9, 1938, 199-215.

7. Asmussen, E., Christiensen, E.H. and Neilsen, M. 'The regulation of circulation in different postures.' Surgery 8, 1940, 604-616.

8. Atwell, R.J., Hickman, J.B., Pryor, W.W. and Page, E.B. 'Reduction of blood flow through the hypoxic lung.' Am. J. Physiol. 166, 1951, 37-44.

9. Babushkin, V.I., Isakov, P.K., Malkin, V.B. and Usachev, V.V. 'An investigation on the biolectric activity of skeletal muscle in man exposed to radial acceleration.' Sechenov physiol. J. U.S.S.R. 44, 1958, 7-10.

10. Babushkin, V.I. Isakov, P.K., Malkin, V.B. and Usachev, V.V. 'Respiration and gaseous exchange in man subjected to radial acceleration.' Sechenov physiol. J. U.S.S.R. 44, 1958, 308-314.

11. Ball, W.C., Stewart, P.B., Newsham, L.G.S. and Bates, D.V. 'Regional pulmonary function studied with xenon 133. J. clin. Invest. 41, 1962, 519-531.

12. Banchero, N., Cronin, L., Nolan, A.C. and Wood, E.H. 'Blood oxygen changes induced by forward ($+G_x$) acceleration.' Aerospace Med. 36, 1965, 608-617.

13. Banchero, N., Cronin, L., Rutishauser, W.J., Tsakinis, A.G. and Wood, E.H. 'Effects on transverse acceleration on blood oxygen saturation.' J. appl. Physiol. 22, 1967, 731-739.

14. Banchero, N., Schwartz, P.E. and Wood, E.H. 'Intraesophageal pressure gradient in man.' J. appl. Physiol. 22, 1967, 1066-1074.

15. Banister, J. and Torrance, R.W. 'The effects of the tracheal pressure upon flow: pressure relations in the vascular bed of isolated lungs.' Q. Jl exp. Physiol. 45, 1960, 352-367.

16. Barach, A.L. 'Effects of atmospheres rich in oxygen on normal rabbits and on rabbits with pulmonary tuberculosis.' Am. Rev. Tuberc. pulm. Dis. 13, (1926). 292-316.

17. Barer, A.S., Golov, G.A., Subavin, V.B., Murakchovski, K.I., Rodin, S.A., Sorokina, E.I. and Tikchomirov, E.P. 'Physiological reactions of the human body to transverse acceleration and some means of increasing the organism's resistance to these effects.' Aerospace Med. 37, 1966, 127-133.

18. Barr, P.O. 'Hypoxaemia in man induced by prolonged acceleration.' Acta physiol. scand. 54, 1962, 128-137.

19. Barr, P.O. 'Pulmonary gas exchange in man as affected by prolonged gravitational stress.' Acta physiol. scand. 58, suppl. 207, 1963.

20. Barr, P.O., Bjurstedt, H. and Coleridge, J.C.G. 'Reflex control of respiration in the anaesthetized dog during prolonged exposure to positive radial acceleration.' Acta physiol. scand. 47, 1959, 1-15.

21. Barr, P.O., Bjurstedt, H. and Coleridge, J.C.G. 'Blood gas changes in the anaesthetized dog during prolonged exposure to positive radial acceleration.' Acta physiol. scand. 47, 1959, 16-27.

22. Bates, D.V. 'Measurement of regional ventilation and blood flow distribution.' 'Handbook of Physiology, sect. 3, Respiration' vol.2, Am. Physiol. Soc. Washington 1964, pp. 1425-1436.

23. Beck, E.P., Ernsting, J. and Lythgoe, C. 'A simple technique for the measurement of the residual volume of the lungs and its application to the hydro-static method of determining the specific gravity of human subjects.' Rep. No. 188, R.A.F. Inst. of Aviation Med., Farnborough, 1961, 12 pp.

24. Beddoes, T. 'The effect of breathing oxygene air little diluted.' In Beddoes, T. and Watt. J. 'Considerations on the medicinal use and on the production of factitious airs.' 3rd ed. Bulgin and Rosser, Bristol. 1796, p.13.

25. Behnke, A.R. 'High atmospheric pressures; physiological effects of increased and decreased pressures; application of these findings to clinical medicine.' Ann. intern. Med. 13, 1940, 2217-2228.

26. Bevegârd, S., Holmgren, A. and Jonsson, B. 'The effect of body position on the circulation at rest and during exercise, with special reference to the influence on the stroke volume.' Acta physiol. scand. 49, 1960, 279-298.

27. Bondurant, S. 'Effect of acceleration on pulmonary compliance.' Fedn Proc. Fedn Am. Socs exp. Biol. 17, 1958, 18.

28. Bondurant, S., Mead, J. and Cook, C.D. 'A re-evaluation of effects of acute central congestion on pulmonary compliance in normal subjects.' J. appl. Physiol. 15, 1960, 875-877.

29. Bouhuys, A. 'Distribution of inspired gas in the lungs.' 'Handbook of Physiology, sect. 3, Respiration,' vol. 1, Washington, Am Physiol. Soc. 1964, pp. 715-733.

30. Britton, S.W., Pertzoff, V.A., French, C.R. and Kline, R.F. 'Circulatory and cerebral changes and protective aids during exposure to acceleratory forces.' Am. J. Physiol. 150, 1947, 7-26.

31. Bruderman, I., Somers, K., Hamilton, W.K., Tooley, W.H. and Butler, J. 'Effect of surface tension on circulation in the excised lungs of dogs.' J. appl. Physiol. 19, 1964, 707-712.

32. Bryan, A.C. and Anthonisen, N.R. 'The effect of acceleration on terminal airway closure.' Aerospace Medical Association Annual Scientific Meeting, Washington, April 10-13, 1967.

33. Bryan, A.C., Aspin, N., Levison, H. and Weng, T. 'Ventilation/perfusion distribution studied with the gamma camera.' Proc. int. Union Physiol. Sci. (Wash.), 7, 1968, 64.

34. Bryan, A.C., Bentivoglio, L.G., Beerel, F., MacLeish, H., Zidulka, A. and Bates, D.V. 'Factors affecting regional distribution of ventilation and perfusion in the lung.' J. appl. Physiol. 19, 1964, 395-402.

35. Bryan, A.C., Macnamara, W.D., Simpson, J. and Wagner, H.N. 'Effect of acceleration on the distribution of pulmonary blood flow.' J. appl. Physiol. 20, 1965, 1129-1132.

36. Bryan, A.C., Milic-Emili, J. and Pengelly, D. 'Effect of gravity on the distribution of pulmonary ventilation.' J. appl. Physiol. 21, 1966, 778-784.

37. Burger, E.J. 'Pulmonary mechanics associated with oxygen toxicity and a suggested physiological test for susceptibility to the effects of oxygen.' Aerospace Med. 38, 1967, 507-513.

38. Burger, E.J. and Macklem, P.T. 'The effect on lungs of breathing 100 percent oxygen near residual volume.' Fedn Proc. Fedn Am. Socs exp. Biol. 25, 1966, 566.

39. Burton, A.C. 'On the physical equilibrium of small blood vessels.' Am. J. Physiol. 164, 1951, 319-329.

40. Caldwell, P.R.B., Giammona, S.T., Lee, W.L. and Bondurant, S. 'Effect of oxygen breathing at one atmosphere on the surface activity of lung extracts in dogs.' Ann. N. Y. Acad. Sci. 121, 1965, 823-828.

41. Campbell, E.J.M. 'Nature of the limitation of maximum inspiratory and expiratory efforts.' In 'The Respiratory Muscles and the Mechanics of Breathing.' Lloyd-Luke, London 1958, p.77.

42. Caro, C.G., Butler, J. and DuBois, A.B. 'Some effects of restriction of chest cage expansion on pulmonary function in man: an experimental study.' J. clin. Invest. 39, 1960, 573-583.

43. Cavagna, G.A., Stemmler, E.J., and DuBois, A.B. 'Alveolar resistance to atelectasis.' J. appl. Physiol. 22, 1967, 441-452.

44. Cheng, T.O., Godfrey, M.P. and Shepard, R.H. 'Pulmonary resistance and state of inflation of the lungs in normal subjects and in patients with airway obstruction.' J. appl. Physiol. 14, 1959, 727-732.

45. Cherniack, N.S., Hyde, A.S., Watson, J.F. and Zechman, F.W. 'Some aspects of respiratory physiology during forward acceleration.' Aerospace Med. 32, 1961, 113-120.

46. Cherniack, N.S., Hyde, A.S. and Zechman, F.W. 'Effect of tranverse acceleration on pulmonary function.' J. appl. Physiol. 14, 1959, 914-916.

47. Clark, L.C. and Gollan, F. 'Survival of mammals breathing organic liquids equilibrated with oxygen at atmosphere pressure.' Science 152, 1966, 1755-1756.

48. Clark, N.P. and Bondurant, S. 'Human tolerance to prolonged forward and backward acceleration.' Tech. Rep. No. 58-267, Wright Air Development Division, Wright-Patterson A.F.B. Ohio, 1958, 29 pp.

49. Clark, W.E., Gardiner, I.D.R., McIntyre, A.K. and Jorgensen, H. 'The effect of positive acceleration on fluid loss from blood to tissue spaces in human subjects on the centrifuge.' Rep. No. 468, Committee on Aviation Medicine, Nat. Res. Co. U.S.A., 1945, 3 pp.

50. Clarke, S.W., Jones, J.G. and Glaister, D.H. 'Change in pulmonary ventilation in different postures.' Clin. Sci. 37, 1969, 357-69.

51. Clements, J.A., Brown, E.S. and Johnson, R.P. 'Pulmonary surface tension and the mucus lining of the lungs: some theoretical considerations.' J. appl. Physiol. 12, 1958, 262-268.

52. Coburn, K.R., Craig, P.H. and Beckman, E.L. 'Effect of positive G on chimpanzees immersed in water.' Report No. MA-6139, U.S. Naval Air Development Center, Johnsville, Pa., 1964, 35 pp.

53. Colville, P., Shugg, C. and Ferris, B.G. 'Effects of body tilting on respiratory mechanics.' J. appl. Physiol. 9, 1956, 19-24.

54. Comroe, J.H. 'The Lung,' 2nd ed., Chicago: Year Book Medical Publishers. 1962, p.10.

55. Comroe, J.H., Dripps, R.D., Dumke, P.R. and Deming, M. 'Oxygen toxicity. The effect of inhalation of high concentrations of oxygen for twenty-four hours on normal men at sea level and at a simulated altitude of 18,000 feet.' J. Am. med. Ass. 128, 1945, 710-717.

56. Conn, H.L. 'Equilibrium distribution of radioxenon in tissue: xenon-hemoglobin association curve.' J. appl. Physiol. 16, 1961, 1065-1070.

57. Coryllos, P.N. and Birnbaum, G.L. 'Studies in pulmonary gas absorption in bronchial obstruction. 11. The behaviour and absorption times of oxygen, carbon dioxide, nitrogen, hydrogen, helium, ethylene, nitrous oxide, ethyl chloride, and ether in the lung.' Am. J. med. Sci. 183, 1932, 326-347.

58. Coryllos, P.N. and Birnbaum, G.L. 'Studies in pulmonary gas absorption in bronchial obstruction. III. A theory of air absorption in atelectasis.' Am. J. med. Sci. 183, 1932, 347-359.

59. Cumming, G., Crank, J., Horsfield, K. and Parker, I. 'Gaseous diffusion in the airways of the human lung.' Resp. Physiol. 1, 1966. 58-74.

60. Cumming, G., Horsfield, K., Jones, J.G. and Muir, D.C.F. 'The influence of gaseous diffusion on the alveolar plateau at different lung volumes.' Resp. Physiol. 2, 1967, 386-398.

61. Dale, W.A. and Rahn, H. 'Rate of gas absorption during atelectasis.' Am. J. Physiol. 170, 1952, 606-615.

62. Daly, W.J. and Bondurant, S. 'Direct measurement of respiratory pleural pressure changes in normal man.' J. appl. Physiol. 18, 1963, 513-518.

63. Davy, H. 'Researches Chemical and Philosophical; Chiefly Concerning Nitrous Oxide, or Dephlogisticated Nitrous Air, and its Respiration.' Johnson. London. 1800.

64. Defares, J.G. and Douleben, P.G. 'Relationship between frequency - dependent compliance and unequal ventilation.' J. appl. Physiol. 15, 1960, 166-169.

65. Denison, D., Ernsting, J. and Fryer, D.I. 'The effect of the inverted posture upon the distribution of pulmonary blood flow in man.' J. Physiol. (Lond.) 172, 1964, 49-50P.

66. Dolfuss, R.E., Milic-Emili, J. and Bates, D.V. 'Regional ventilation of the lung studied with boluses of ^{133}Xenon.' Resp. Physiol. 2, 1967, 234-246.

67. Dollery, C.T. and Gillam, P.M.S. 'The distribution of blood and gas within the lungs measured by scanning after administration of ^{133}Xe.' Thorax 18, 1963, 316-325.

68. Dollery, C.T. and West, J.B. 'Regional uptake of radioactive oxygen, carbon monoxide and carbon dioxide in the lungs of patients with mitral stenosis.' Circulation Res. 8, 1960. 765-771.

69. Dollery, C.T., West, J.B., Wilcken, D.E.L., Goodwin, J.F. and Hugh-Jones, P. 'Regional pulmonary blood flow in patients with circulatory shunts.' Br. Heart J. 23, 1961, 225-235.

70. Doyle, A.E., Goodwin, J.F., Harrison, C.V. and Steiner, R.E. 'Pulmonary vascular patterns in pulmonary hypertension.' Br. Heart J. 19, 1957, 353-365.

71. Duane, T.D., Beckman, E.L., Ziegler, J.E. and Hunter, M.N. 'Some observations on human tolerance to exposures of 15 transverse G.' Rep. No. NADC-MA-5305, U.S. Naval Air Development Center, Johnsville, Pa., 1953, 26 pp.

72. DuBois, A.B. 'Exchange of fluids in lungs.' In 'Physiology in the Space Environment,' vol. II. 'Respiration.' chap. 8, Washington: National Academy of Sciences Nat. Res. Cou. pub. 1485 B. 1967, pp. 59-65.

73. DuBois, A.B., Turaids, T., Mammen, R.E. and Nobrega, F.T. 'Pulmonary atelectasis in subjects breathing oxygen at sea level or at simulated altitude.' J. appl. Physiol. 21, 1966, 828-836.

74. **Dyson, N.A., Hugh-Jones, P., Newbery, G.R., Sinclair, J.D. and West, J.B.** 'Studies of regional lung function using radioactive oxygen.' Brit. med. J. 1, 1960. 231-238.

75. **Ernsting, J.** 'Some effects of oxygen breathing on man.' Proc. R. Soc. Med. 53, 1960, 96-98.

76. **Ernsting, J.** 'The ideal relationship between inspired oxygen concentration and cabin altitude.' Aerospace Med. 34, 1963, 991-997.

77. **Ernsting, J.** 'Rate of gas absorption from the lung during rebreathing in the dog.' J. Physiol. (Lond.) 181, 1965, 42-43P.

78. **Ernsting, J.** In 'A Textbook of Aviation Physiology.' Gillies, J.A. ed. Pergamon Press, London, 1965, p. 253.

79. **Farhi, L.E.** 'Ventilation-perfusion relationship and its role in alveolar gas exchange.' In 'Advances in Respiratory Physiology.' Caro. C.G. ed. Edward Arnold. London, 1966, pp. 148-197.

80. **Farhi, L.E. and Rahn, H.** 'Gas stores of the body and the unsteady state.' J. appl. Physiol. 7, 1955, 472-484.

81. **Farhi, L.E. and Yokoyama, T.** 'Effects of ventilation - perfusion inequality on elimination of inert gases.' Resp. Physiol. 3, 1967, 12-20.

82. **Faridy, E.E., Kidd, R. and Milic-Emili, J.** 'Topographical distribution of inspired gas in excised lobes of dogs.' J. appl. Physiol. 22, 1967, 760-766.

83. **Ferris, B.G. and Pollard, D.S.** 'Effect of deep and quiet breathing on pulmonary compliance in man.' J. clin. Invest. 39, 1960, 143-149.

84. **Forster, R.E.** 'Diffusion of gases.' In 'Handbook of Physiology, sect. 3, Respiration.' Vol. 1, Am. Physiol. Soc. Washington, 1964, pp. 839-872.

85. **Fowler, K.T. and Read, J.** 'Cardiac oscillations in expired gas tensions, and regional pulmonary blood flow.' J. appl. Physiol. 16, 1961, 863-868.

86. **Fowler, K.T., West, J.B. and Pain, M.C.F.** 'Pressure-flow characteristics of horizontal lung preparations of minimal height.' Resp. Physiol. 1, 1966, 88-98.

87. **Fowler, W.S.** 'Intrapulmonary distribution of inspired gas.' Physiol. Rev. 32, 1952, 1-20.

88. **Frank, N.R.** 'A comparison of static volume-pressure relations of excised pulmonary lobes of dogs.' J. appl. Physiol. 18, 1963, 274-278.

89. **Gaar, K.A., Taylor, A.E., Owens, L.J. and Guyton, A.C.** 'Effect of capillary pressure and plasma protein on development of pulmonary edema.' Am. J. Physiol. 213, 1967, 79-82.

90. **Gauer, O.** 'The physiological effects of prolonged acceleration.' In 'German Aviation Medicine World War II.' Vol. 1, Department of the Air Force. Washington, 1950, p. 554.

91. **Gauer, O., Henry, J.P., Martin, E.E. and Maher, P.J.** 'Arterial oxygen saturation and intracardiac pressures during acceleration in relation to cardiac damage.' Fedn Proc. Fedn Am. Socs exp. Biol. 8, 1949, 54.

92. **Gell, C.F.** 'Table of equivalents for acceleration terminology.' Aerospace Med. 32, 1961, 1109-1111.

93. **Glammona, S.T., Kerner, D. and Bondurant, S.** 'Effect of oxygen breathing at atmospheric pressure on pulmonary surfactant.' J. appl. Physiol. 20, 1965, 855-858.

94. **Glaister, D.H.** 'The effect of positive acceleration on diaphragm movement as demonstrated by a direct recording technique.' Revue Méd. aéronaut. 2, 1961, 28-29.

95. **Glaister, D.H.** 'Pulmonary gas exchange during positive acceleration.' Rep. No. 1212, Flying Personnel Research Committee, M.O.D. (Air Force Dept.), London, 1963, 14 pp.

96. **Glaister, D.H.** 'The effect of positive acceleration on the inequality of ventilation and perfusion in the lung.' Rep. No. 1231, Flying Personnel Research Committee, M.O.D. (Air Force Dept.), London, 1964, 21 pp.

97. **Glaister, D.H.** 'Acceleration atelectasis - some factors modifying its occurrence and magnitude.' Memorandum No. 220, Flying Personnel Research Committee, M.O.D. (Air Force Dept.), London, 1965, 11 pp.

98. **Glaister, D.H.** 'Regional ventilation and perfusion in the lung during positive acceleration measured with Xe-133.' J. Physiol. (Lond.) 177, 1965, 73-74P.

99. **Glaister, D.H.** 'Regional ventilation and perfusion of the lung during gravitational stress measured with radioactive xenon.' Rep. No. 1236, Flying Personnel Research Committee, M.O.D. (Air Force Dept.), London, 1965, 33 pp.

100. **Glaister, D.H.** 'The effects of positive acceleration on lung mechanics and gas exchange.' Ph.D. thesis, Univ. of London. 1966.

101. **Glaister, D.H.** 'A flat beam collimator for radioisotope scanning of the lung.' Bro. J. Radiol. 40, 1967, 670-675.

102. **Glaister, D.H.** 'The effect of posture on the distribution of ventilation and blood flow in the normal lung.' Clin. Sci. 33, 1967, 391-398.

103. **Glaister, D.H.** 'The effect of positive centrifugal acceleration upon the distribution of ventilation and perfusion within the human lung, and its relation to pulmonary arterial and intraoesophageal pressures.' Proc. R Soc. B. 168, 1967, 311-334.

104. **Glaister, D.H.** 'Transient changes in arterial oxygen tension during positive ($+G_z$) acceleration in the dog.' Aerospace Med. 39, 1968, 54-62.

105. **Glaister, D.H.** 'Lung Collapse in aviation medicine.' Br. J. hosp. Med. 2, 1969, 635-642.

106. **Glaister, D.H.** 'The effect of positive acceleration upon cardiac output and regional blood flow in the dog.' In 'Aviation and Space Medicine.' Universitetsforlaget Oslo: 1969.

107. Glazier, J.B., Hughes, J.M.B., Maloney, J.E. and West, J.B. 'Vertical gradient of alveolar size in lungs of dogs frozen intact.' J. appl. Physiol. 23, 1967, 694-705.

108. Glazier, J.B., Hughes, J.M.B., Maloney, J.E. and West, J.B. 'Measurements of capillary dimensions and blood volume in rapidly frozen lung.' J. appl. Physiol. 26, 1969, 65-76.

109. Golov, G.A. 'Changes in gas exchange and oxygen saturation of arterial blood in man during exposure to transverse acceleration.' Bull. exp. Biol. Med. U.S.S.R. 62, 1966, 1240-1243.

110. Gómez, D.M., Briscoe, W.A. and Cumming, G. 'Continuous distribution of specific tidal volume throughout the lung.' J. appl. Physiol. 19, 1964, 683-692.

111. Gray, R.F. and Webb, M.G. 'High G protection.' Rep. MA-5910, Naval Air Development Center, Johnsville, Pa., 1960, 18 pp.

112. Green, I.D. 'The degree of pulmonary arterial to venous shunt produced by breathing 100 percent oxygen during increased positive acceleration and whilst wearing an anti-g suit.' J. Physiol. (Lond.), 169, 1963, 96-97P.

113. Green, I.D. 'Synopsis of recent work done on the problem of pulmonary atelectasis associated with breathing 100 percent 0_2 and increased positive 'g'.' Rep. No. 230, R.A.F. Institute of Aviation Medicine, Farnborough, 1963, 5 pp.

114. Green, I.D. and Burgess, B.F. 'An investigation into the major factors contributing to post flight chest pain in fighter pilots. Rep. No. 1182, Flying Personnel Research Committee, M.O.D. (Air Force Dept.), London, 1962, 43 pp.

115. Green, J.H. and Howell, J.B.L. 'The correlation of intercostal muscle activity with respiratory air flow in conscious human subjects.' J. Physiol. (Lond.), 149, 1959, 471-476.

116. Greenfield, A.D.M. 'Effect of acceleration on cats, with and without water immersion.' J. Physiol. (Lond.) 104, 1945, 5-6P.

117. Guyton, A.C. and Greganti, F.P. 'A physiological reference point for measuring circulatory pressures in the dog - particularly venous pressure.' Am. J. Physiol. 185, 1956, 137-141.

118. Hackney, J.D., Collier, C.R., Conrad, D. and Coggin, J. 'Pulmonary surface phenomena in oxygen poisoning.' Clin. Res. 11, 1963, 91.

119. Haldane, J.S., Meakins, J.C. and Priestley, J.G. 'The effects of shallow breathing.' J. Physiol. (Lond.) 52, 1919, 433-453.

120. Hayek, H. von. 'The Human Lung.' Haffner Publishing Co. New York: 1960.

121. Henderson, R., Horsfield, K. and Cumming, G. 'Intersegmental collateral ventilation in the human lung.' Resp. Physiol. 6, 1969, 128-134.

122. Henry, J.P. 'Studies of the physiology of negative acceleration.' A.F. Technical Rep. No. 5953, Air Material Command, U.S. A.F. 1950, 59 pp.

123. Henry, J., Jacobs, H., Karstens, A. and Gauer, O. 'Influence of temperature on pressure-volume.' Am. J. Physiol. 159, 1949, 573-574.

124. Hershgold, E.J. and Steiner, S.H. 'Cardiovascular changes during acceleration stress in dogs.' J. appl. Physiol. 15, 1960, 1065-1068.

125. Hill, A.V. 'Recovery heat in muscle.' Proc. R. Soc. B. 127, 1939, 297-307.

126. Hill, L. 'The influence of the force of gravity on the circulation of the blood.' J. Physiol. (Lond.) 18, 1895, 15-53.

127. Himmelstein, A., Harris, P., Fritts, H.W. and Cournard, A. 'Effects of severe unilateral hypoxia on the partition of pulmonary blood flow in man.' J. thorac. Surg. 36, 1958, 369-381.

128. Holland, J., Milic-Emili, J., Macklem, P.T. and Bates, D.V. 'Regional distribution of pulmonary ventilation and perfusion in elderly subjects.' J. clin. Invest. 47, 1968, 81-92.

129. Holley, H.S., Milic-Emili, J., Becklake, M.R. and Bates, D.V. 'Regional distribution of pulmonary ventilation and perfusion in obesity.' J. clin. Invest. 46, 1967, 475-481.

130. Hoppin, F.G., Kuhl, D.E. and Hyde, R.W. 'Distribution of pulmonary blood flow as affected by transverse ($+G_x$) acceleration.' J. appl. Physiol. 22, 1967, 469-474.

131. Hoppin, F.G., Sever, R.J. and Hitchcock, L. 'Pulmonary function in man under prolonged acceleration. II. Correlation of arterial blood oxygen saturation with ventilation and gas being breathed.' Rep. No. NADC-MR-6519 U.S. Naval Air Development Center, Johnsville, Pa., 1965, 16 pp

132. Howard, P. 'Changes in the cardiac output during positive radial acceleration.' J. Physiol. (Lond.) 147, 1959, 49P.

133. Howard, P. 'Visual and cardiovascular effects induced by acceleration.' Ph. D. thesis, Univ. of London. 1964.

134. Howard, P. and Garrow, J.S. 'Changes in the vascular resistance of the forearm and hand during radial acceleration.' J. Physiol. (Lond.) 143, 1958, 83P.

135. Howell, J.B.L., Permutt, S., Proctor, D.F. and Riley, R.L. 'Effect of inflation of the lung on different parts of pulmonary vascular bed.' J. appl. Physiol. 16, 1961, 71-76.

136. Hughes, J.M.B., Glazier, J.B., Maloney, J.E. and West, J.B. 'Effect of lung volume on the distribution of pulmonary blood flow in man.' Resp. Physiol. 4, 1968, 58-72.

137. Hughes, J.M.B., Glazier, J.B., Maloney, J.E. and West, J.B. 'Effect of extra alveolar vessels on the distribution of blood flow in the dog lung.' J. appl. Physiol. 25, 1968, 701-12.

138. Hutchinson, J. 'Vital capacity affected by the position of the body.' In Cyclopaedia of Anatomy and Physiology vol. 4, Todd, R.B. ed. Longman, Brown, Green, Longmans and Roberts. London, 1849, p. 1073.

139. Hyde, A.S. 'The effect of back angle, molded supports, and staged evisceration upon intrapulmonary pressures in dogs and a monkey during forward ($+G_x$) acceleration.' Tech. Rep. No. 62-106, 6570th Aerospace Medical Research Lab. Wright-Patterson A.F.B. Ohio, 1962, 12 pp.

140. Hyde, A.S., Pines, J. and Saito, I. 'Atelectasis following acceleration: a study of causality.' Aerospace Med. 34, 1963, 150-157.

141. Jacquemin, C., Demange, J., Timbal, J. and Varene, P. 'Effects of forward acceleration on anatomical dead space.' J. appl. Physiol. 20, 1965, 1205-1210.

142. Jacquemin, C., Petit, J.M., Varene, P. and Damoiseau, J. 'Influence de la pesanteur du médiastin sur l'élastance oesophagienne.' J. Physiol. (Paris,) 57, 1965, 633.

143. Jones, J.G. 'The effect of preinspiratory lung volume on the result of the single breath 0_2 test.' Resp. Physiol. 2, 1967, 375-385.

144. Jones, J.G. and Clarke, S.W. 'The effect of expiratory flow rate on regional lung emptying.' Clin. Sci. 37, 1969, 343-56.

145. Jones, J.G., Clarke, S.W. and Glaister, D.H. 'The effect of acceleration on regional lung emptying.' J. appl. Physiol. 26, 1969, 827-32.

146. Kaneko, K., Milic-Emili, J., Dolovich, M.B., Dawson, A. and Bates, D.V. 'Regional distribution of ventilation and perfusion as a function of body position.' J. appl. Physiol. 21, 1966, 767-777.

147. Keefe, J.V. 'Post flight respiratory disorder in fighter aircrew.' Rep. No. 20, H.Q. Fighter Command, R.A.F. 1958.

148. Knipping, Von H.W., Bolt, W., Venrath, H., Valentin, H., Ludes, H. and Endler, P. 'Eine neue Methode zur Prüfung der Herzu und Lungenfunktion.' Dt. med. Wschr. 80, 1955, 1146-1147.

149. Knowles, J.H., Hong, S.K. and Rahn, H. 'Possible errors using oesophageal balloon in determination of pressure-volume characteristics of the lung and thoracic cage.' J. appl. Physiol. 14, 1959, 525-530.

150. Knowlton, F.P. and Starling, E.H. 'The influence of variations in temperature and blood pressure on the performance of the isolated mammalian heart.' J. Physiol. (Lond.) 44, 1912, 206-219.

151. Korolev, Yu, N. 'Effect of lateral accelerations on dog lung histology.' In 'Aviation and Space Medicine.' Parin, V.V. ed. NASA TT F-228 Washington' 1964, p. 247-249.

152. Krogh, A. and Lindhard, J. 'The volume of the dead space in breathing and the mixing of gases in the lungs of man.' J. Physiol. (Lond.) 51, 1917, 59-90.

153. Krueger, J.J., Bain, T. and Patterson, J.L. 'Elevation gradient of intrathoracic pressure.' J. appl. Physiol. 16, 1961, 465-468.

154. Lambert, E.H. 'The physiologic basis of 'blackout' as it occurs in aviators.' Fedn Proc. Fedn Am. Socs exp. Biol. 4, 1945, 43.

155. Lambert, E.H. and Wood, E.H. 'Direct determination of man's blood pressure on the human centrifuge during positive acceleration.' Fedn Proc. Fedn Am. Socs exp. Biol. 5, 1946, 59.

156. Lambert, E.H., Wood, E.H. and Baldes, E.J. 'Man's ability to withstand transverse acceleration when in the sitting position.' Rep. No. 418, Committee on Aviation Medicine, Nat. Res. Cou. U.S.A. 1945.

157. Landis, E.M. and Britton, S.W. 'Effects of high gravitational forces.' Progress Rep. No. 3 to Committee on Aviation Medicine, Nat. Res. Cou. U.S.A., 1942, 2 pp.

158. Langdon, D.E. and Reynolds, G.E. 'Postflight respiratory symptoms associated with 100 percent oxygen and G-forces.' Aerospace Med. 32, 1961, 713-718.

159. Lassen, N.A., Mellemgaard, K. and Georg, J. 'Tritium used for estimation of right-to-left shunts.' J. appl. Physiol. 16, 1961, 321-325.

160. Ledbetter, M.K., Bruck, E. and Farhi, L.E. 'Perfusion of the underventilated compartment of the lungs in asthmatic children.' J. clin. Invest. 43, 1964, 2233-2240.

161. Lee, W.L. 'Breath holding, altitude and atelectasis.' 18th Aerospace Medical Panel Meeting, NATO(AGARD), Oslo, July 24-26, 1961.

162. Leverett, S.D., Kirkland, V.E., Schermerhorn, T.J. and Newsom, W.A. 'Retinal circulation in man during $+G_z$ acceleration.' Aerospace Medical Association 38th Annual Meeting, Washington, April 10-13, 1967.

163. Levine, B.E. and Johnson, R.P. 'Effects of atelactisis on pulmonary surfactant and quasi-static lung mechanics.' J. appl. Physiol. 20, 1965, 859-864.

164. Levy, P.M., Jaeger, E.A., Stone, R.S. and Doudna, C.T. 'Aeroatelectasis: a respiratory syndrome in aviators.' Aerospace Med. 33, 1962, 988-994.

165. Lewis, B.M., Forster, R.E. and Beckman, E.L. 'Effect of inflation of a pressure suit on pulmonary diffusing capacity in man.' J. appl. Physiol. 12, 1958, 57-64.

166. Lichtheim, L. 'Versuche über Lungenatelektase.' Arch. exp. Path. Pharmak. 10, 1879, 54-100.

167. Linderholm, H. 'Lung mechanics in sitting and horizontal postures studied by body plethysmographic methods.' Am. J. Physiol. 204, 1963, 85-91.

168. Lloyd, T.C. and Wright, G.W. 'Pulmonary vascular resistance and vascular transmural gradient.' J. appl. Physiol. 15, 1960, 241-245.

169. Lombard, C.F., Roth, H.P. and Drury, D.R. 'The influence of radial acceleration (centrifugal force) on respiration in human beings.' Aerospace Med. 19, 1948, 355-364.

170. Lopez-Muniz, R., Stephens, N.L., Bromberger-Barnea, B., Permutt, S. and Riley, R.L. 'Critical closure of pulmonary vessels analyzed in terms of Starling resistor model.' J. appl. Physiol. 24, 1968, 625-635.

171. McIlroy, M.B., Butler, J. and Finley, T.N. 'Effects of chest compression on reflex ventilatory drive and pulmonary function.' J. appl. Physiol. 17, 1962, 701-705.

172. Macklem, P.T. and Mead, J. 'Resistance of central and peripheral airways measured by a retrograde catheter.' J. appl. Physiol. 22, 1967, 395-401.

173. Macklin, C.C. 'Transport of air along sheaths of pulmonic blood vessels from alveoli to mediastinum.' Archs intern. Med. 64, 1939, 913-925.

174. Macklin, C.C. 'Evidence of increase in the capacity of the pulmonary arteries and veins of dogs, cats and rabbits during inflation of the freshly excised lung.' Revue can. Biol. 5, 1946, 199-232.

175. Maloney, J.E., Bergel, D.H., Glazier, J.B., Hughes, J.M.B. and West, J.B. 'Transmission of pulsatile blood pressure and flow through the isolated lung.' Circulation Res. 23, 1968, 11-24.

176. Maloney, J.E., Bergel, D.H., Glazier, J.B., Hughes, J.M.B. and West, J.B. 'Effect of pulsatile pulmonary artery pressure on distribution of blood flow in isolated lung.' Resp. Physiol. 4, 1968, 154-167.

177. Marchand, P. 'The anatomy and applied anatomy of the mediastinal fascia.' Thorax 6, 1951, 359-368.

178. Mead, J. 'Mechanical properties of lungs.' Physiol. Rev. 41, 1961, 281-330.

179. Mead, J. 'A model of lung elasticity and some of its implications. In 'Form and function in the human lung.' Cumming, G. and Hunt, L.B., eds, Livingstone, London, 1968, pp. 47-56.

180. Mead, J., Turner, J.M., Macklem, P.T. and Little, J.B. 'Significance of the relationship between lung recoil and maximum expiratory flow.' J. appl. Physiol. 22, 1967, 95-108.

181. Mead, J. and Whittenberger, J.L. 'Physical properties of human lungs measured during spontaneous respiration.' J. appl. Physiol. 5, 1953, 779-796.

182. Mead, J. and Whittenberger, J.L. 'Evaluation of airway interruption technique as a method for measuring pulmonary air-flow resistance.' J. appl. Physiol. 6, 1954, 408-416.

183. Mellemgaard, K., Lassen, N.A. and Georg, J. 'Right-to-left shunt in normal man determined by the use of tritium and krypton 85.' J. appl. Physiol. 17, 1962, 778-782.

184. Michel, E.L., Langevin, R.W. and Gell, C.F. 'Effect of continuous human exposure to oxygen tension of 418 mm Hg for 168 hours.' Aerospace Med. 31, 1960, 138-144.

185. Milic-Emili, J., Henderson, J.A.M., Dolovich, M.B., Trop, D. and Kaneko, K. 'Regional distribution of inspired gas in the lung.' J. appl. Physiol. 21, 1966, 749-759.

186. Milic-Emili, J., Henderson, J.A.M. and Kaneko, K. 'Distribution of ventilation as investigated with radio-active gases.' J. nucl. Biol. Med. 11, 1967, 63-68.

187. Milic-Emili, J., Henderson, J.A.M. and Kaneko, K. 'Regional distribution of ventilation in the normal lung.' In 'Form and function in the human lung.' Cumming, G. and Hunt, L.B. eds., Livingstone, London, 1968, pp. 66-75.

188. Milic-Emili, J., Mead, J. and Turner, J.M. 'Topography of esophageal pressure as a function of posture in man.' J. appl. Physiol. 19, 1964, 212-216.

189. Mills, R.J., Cumming, G. and Harris, P. 'Frequency-dependent compliance at different levels of inspiration in normal adults.' J. appl. Physiol. 18, 1963, 1061-1064.

190. Nakamura, T., Takishima, T., Okubo, T., Sasaki, T. and Takahashi, H. 'Distribution function of the clearance time constant in lungs.' J. appl. Physiol. 21, 1966, 227-232.

191. Newhouse, M.T., Becklake, M.R., Macklem, P.T. and McGregor, M. 'Effect of alterations in end-tidal CO_2 tension on flow resistance.' J. appl. Physiol. 19, 1964, 745-749.

192. Newhouse, M.T., Wright, F.J., Ingham, G.K., Archer, N.P., Hughes, L.B. and Hopkins, O.L. 'Use of scintillation camera and ^{135}xenon for study of topographic pulmonary function.' Resp. Physiol. 4, 1968, 141-153.

193. Niden, A.H. 'The acute effects of atelectasis on the pulmonary circulation.' J. clin. Invest. 43, 1964, 810-824.

194. Nolan, A.C., Marshall, H.W., Cronin, L., Sutterer, W.F. and Wood, E.H. 'Decreases in arterial oxygen saturation and associated changes in pressures and roentgenographic appearance of the thorax during forward ($+G_x$) acceleration.' Aerospace Med. 34, 1963, 797-813.

195. Nunn, J.F. 'Factors influencing the arterial oxygen tension during halothane anaesthesia with spontaneous respiration.' Br. J. Anaesth. 36, 1964, 327-341.

196. Nunn, J.F., Coleman, A.J., Sachithanandan, T., Bergman, N.A. and Laws J.W. 'Hypoxaemia and atelectasis produced by forced expiration.' Br. J. Anaesth. 37, 1965, 3-11.

197. Ohlsson, W.T.L. 'A study on oxygen toxicity at atmospheric pressure.' Acta med. scand. 128, suppl. 190. 1947.

198. Orth, J. 'Atiologisches und Anatomisches über Lungenschwindsucht.' Hirschwald, Berlin: 1887, p.20.

199. Otis, A.B. 'The work of breathing.' Physiol. Rev. 34, 1954, 449-458.

200. Otis, A.B., Fenn, W.O. and Rahn, H. 'Mechanics of breathing in man.' J. appl. Physiol. 2, 1950, 592-607.

201. Otis, A.B., McKerrow, C.B., Bartlett, R.A., Mead, J., McIlroy, M.B., Selverstone, N.J. and Radford, E.P. 'Mechanical factors in distribution of pulmonary ventilation.' J. appl. Physiol, 8, 1956, 427-443.

202. **Otis, A.B. and Proctor, D.F.** 'Measurement of alveolar pressure in human subjects.' Am. J. Physiol. 152, 1948, 106-112.

203. **Pain, M.C.F. and West, J.B.** 'Effect of the volume history of the isolated lung on distribution of blood flow.' J. appl. Physiol. 21, 1966, 1545-1550.

204. **Pappenheimer, J.R., Comroe, J.H., Cournand, A., Ferguson, J.K.W., Filley, G.F., Fowler, W.S., Gray, J.S., Helmholtz, H.F. Otis, A.B., Rahn, H. and Riley, R.L.** 'Standardization of definitions and symbols in respiratory physiology.' Fedn Proc. Fedn Am. Socs exp. Biol. 9, 1950, 602-605.

205. **Permutt, S.** 'Effect of interstitial pressure of the lung on pulmonary circulation.' Med. thorac. 22, 1965, 118-131.

206. **Permutt, S.** 'Pulmonary circulation and the distribution of blood and gas in the lungs.' In 'Physiology in the Space Environment, vol. II Respiration.' 6, National Academy of Sciences Nat. Res. Cou. pub. 1485B Washington' 1967, pp 38-56.

207. **Permutt, S., Bromberger-Barnea, B and Bane, H.N.** 'Alveolar pressure, pulmonary venous pressure and the vascular waterfall.' Med. thorac. 19, 1962, 239-260.

208. **Permutt, S., Caldini, P., Bane, H.N., Howard, P. and Riley, R.L.** 'Liquid pressure versus surface pressure of the esophagus.' J. appl. Physiol. 23, 1967, 927-933.

209. **Piorry.** 'Influence de la pesanteur sur le cours du sang; diagnostic de la syncope et de l'appoplexie.' Archs gén. Méd. 2, 1826, 292-294.

210. **Pittinger, C.B., Conn, H.L., Featherstone, R.M., Stickley, E., Levy, L. and Cullen, S.C.** 'Observations on the kinetics of transfer of xenon and chloroform between blood and brain in the dog.' Anesthesiology 17, 1956, 523-530.

211. **Power, G.G., Hyde, R.W., Sever, R.J., Hoppin, F.G. and Nairn, J.R.** 'Pulmonary diffusing capacity and capillary blood flow during forward acceleration.' J. appl. Physiol. 20, 1965, 1199-1204.

212. **Preston-Thomas, H., Edelberg, R., Henry, J.P., Miller, J., Saltzman, E.W. and Zuidema, G.D.** 'Human tolerance to multistage rocket acceleration curves.' J. aviat. Med. 26, 1955, 390-398.

213. **Proctor, D.F., Caldini, P. and Permutt, S.** 'The pressure surrounding the lungs.' Resp. Physiol. 5, 1968, 130-144.

214. **Prys-Roberts, C., Nunn, J.F., Dobson, R.H., Robinson, R.H., Greenbaum, R. and Harris, R.S.** 'Radiologically undetectable pulmonary collapse in the supine position.' Lancet 2, 1967, 399-401.

215. **Raffensperger, J.G., Diffenbaugh, W.G. and Strohl, E.L.** 'Postoperative massive collapse of the lungs.' J. Am. med. Ass. 174, 1960, 1386-1388.

216. **Rahn, H. and Farhi, L.E.** 'Gaseous environment and atelectasis.' Fedn Proc. Fedn Am. Socs exp. Biol. 22, 1963, 1035-1041.

217. Rauwerda, P.E. 'Unequal ventilation of different parts of the lung and the determination of cardiac output.' (Thesis). Univ. of Groningen. 1946.

218. Read, J. 'Alveolar populations contributing to expired gas tension plateaus.' J. appl. Physiol. 21, 1966, 1511-1520.

219. Read, J. 'Stratification of ventilation and blood flow in the normal lung.' J. appl. Physiol. 21, 1966, 1521-1531.

220. Reed, J.H., Burgess, B.F. and Sandler, H. 'Effects on arterial oxygen saturation of positive pressure breathing during acceleration.' Aerospace Med. 35, 1964, 238-243.

221. Reed, J.H., Vandenberg, R.A. and Wood, E.H. 'Effect of gravitational and inertial forces on regional distribution of pulmonary blood flow.' Physiologist (Wash.) 10, 1967, 288.

222. Riley, R.L. 'Effect of lung inflation upon the pulmonary vascular bed.' In 'Pulmonary Structure and Function.' eds. de Reuck, A.V.S. and O'Connor, M. London, Churchill. 1962, pp. 261-279.

223. Riley, R.L. and Cournard, A. 'Analysis of factors affecting partial pressures of oxygen and carbon dioxide in gas and blood of lungs: theory.' J. appl. Physiol. 4, 1951, 77-101.

224. Robertson, J.S., Siri, W.E. and Jones, H.B. 'Lung ventilation patterns determined by analysis of nitrogen elimination rates; use of the mass spectrometer as a continuous gas analyzer.' J. clin. Invest. 29, 1950, 577-590.

225. Robertson, P.C., Ross, W.R.D. and Anthonisen, N.R. 'The effect of inspiratory flow rate on regional distribution of inspired gas.' Physiologist (Wash.) 10, 1967, 290.

226. Robertson, W.G. and Farhi, L.E. 'Effects of ambient pressure on the rate of collapse of the rat's lung.' Physiologist (Wash.) 4, 1961, 95.

227. Rogers, T.A. and Smedal, H.A. 'The ventilatory advantage of backward transverse acceleration.' Aerospace Med. 32, 1961, 737-740.

228. Rosenhamer, G. 'Influence of increased gravitational stress on the adaption of cardiovascular and pulmonary function to exercise.' Acta physiol. scand. 68, suppl. 276 1967.

229. Ross, B.B. 'Influence of bronchial tree structure on ventilation in the dog's lung as inferred from measurements of a plastic cast.' J. appl. Physiol. 10, 1957, 144.

230. Ross, B.B. and Farhi, L.E. 'Dead-space ventilation as a determinant in the ventilation-perfusion concept.' J. appl. Physiol. 15, 1960, 363-371.

231. Rushmer, R.F. 'A rontgenographic study of the effect of a pneumatic anti-blackout suite on the hydrostatic columns in man exposed to positive radial acceleration.' Am. J. Physiol. 151, 1947, 459-468.

232. Rutishauser, W.J., Banchero, N., Tsakiris, A.G., Edmundowicz, A.C. and Wood, E.H. 'Pleural pressures at dorsal and ventral sites in supine and prone body positions.' J. appl. Physiol. 21, 1966, 1500-1510.

233. **Rutishauser, W.J., Banchero, N., Tsakiris, A.G. and Wood, E.H.** 'Effect of gravitational and inertial forces on pleural and esophageal pressures.' J. appl. Physiol. 22, 1967, 1041-1052.

234. **Sandler, H.** 'Hemodynamic and cineradiographic study of transverse ($+G_x$) acceleration.' Rep. No. NADC-ML-6413, U.S. Naval Air Development Center, Johnsville, Pa., 1964, 49 pp.

235. **Sandler, H.** 'Angiocardiographic and hemodynamic study of transverse (G_x) acceleration.' Aerospace Med. 37, 1966, 901-910.

236. **Sapirstein, L.A.** 'Regional blood flow by fractional distribution of indicators.' Am. J. Physiol. 193, 1958, 161-168.

237. **Scatchard, G., Batchelder, A.C. and Brown, A.** 'Chemical, clinical, and immunological studies on the products of human plasma fractionation. VI. The osomotic pressure of plasma and of serum albumin.' J. clin. Invest. 23, 1944, 458-464.

238. **Severinghaus, J.W. and Stupfel, M.** 'Alveolar dead space as an index of distribution of blood flow in pulmonary capilaries.' J. appl. Physiol. 10, 1957. 335-348.

239. **Severinghaus, J.W., Swenson, E.W., Finley, T.N., Lategola, M.T. and Williams, J.** 'Unilateral hypoventilation produced in dogs by occluding one pulmonary artery'. J. appl. Physiol. 16, 1961, 53-60.

240. **Sikand, R., Cerretelli, P. and Farhi, L.E.** 'Effects of $\dot{V}_A$ and $\dot{V}_A/Q$ distribution and of time on the alveolar plateau.' J. appl. Physiol. 21, 1966, 1331-1337.

241. **Slagter, B. and Heemstra, H.** 'Limiting factors of expiration in normal subjects.' Acta physiol. pharmacol. neerl. 4, 1955, 419-420.

242. **Smedal, H.A., Holden, G.R. and Smith, J.R.** 'Cardiovascular responses to transversely applied accelerations.' Aerospace Med. 34, 1963, 749-752.

243. **Smedal, H.A., Rogers, T.A., Duane, T.D., Holden, G.R. and Smith, J.R.** 'The physiological limitations of performance during acceleration.' Aerospace Med. 34, 1963, 48-55.

244. **Smith, C.W., Lehan, P.H. and Monks, J.J.** 'Cardiopulmonary manifestations with high O_2 tensions at atmospheric pressure.' J. appl. Physiol. 18, 1963, 849-853.

245. **Smith, J.L.** 'The pathological effects due to increase of oxygen tension in the air breathed.' J. Physiol. (Lond.) 24, 1899, 19-35.

246. **Staub, N.C., Nagano, H. and Pearce, M.L.** 'Pulmonary edema in dogs, especially the sequence of fluid accumulation in lungs.' J. appl. Physiol. 22, 1967, 227-240.

247. **Steiner, S.H. and Mueller, G.C.E.** 'Heart rate and forward acceleration.' J. appl. Physiol. 16, 1961, 1078-1080.

248. **Steiner, S.H. and Mueller, G.C.E.** 'Pulmonary arterial shunting in man during forward acceleration.' J. appl. Physiol. 16, 1961, 1081-1086.

249. Steiner, S.H. and Mueller, G.C.E. and Cherniack, N.S. 'Pulmonary gas transport as influenced by a hypergravitational environment.' J. appl. Physiol. 16, 1961, 641-643.

250. Steiner, S.H., Mueller, G.C.E. and Taylor, J.L. 'Hemodynamic changes during forward acceleration.' Aerospace Med. 31, 1960, 907-914.

251. Surprenant, E.L. and Rodbard, S. 'A hydrostatic pressure gradient in the pleural sac.' Am. Heart J. 66, 1963, 215-220.

252. Sutherland, P.W., Katsura, T. and Milic-Emili, J. 'Previous volume history of the lung and regional distribution of gas.' J. appl. Physiol. 25, 1968, 566-574.

253. Takats, G. de., Fenn, G.K. and Jenkinson, E.L. 'Reflex pulmonary atelectasis.' J. Am. med. Ass. 120, 1942, 686-690.

254. Tocker, A.M. and Langston, H.T. 'The perivascular space of pulmonary vessels. An anatomic demonstration.' J. thorac. Surg. 23, 1952, 539-545.

255. Torphy, D.E., Leverett, S.D. and Lamb, L.E. 'Cardiac arrhythmias occurring during acceleration.' Aerospace Med. 37, 1966, 52-58.

256. Trop, D., Van de Woestijne, K.P. and Afschrift, M. 'Influence of mediastinal structures on the esophageal pressure gradient in dogs.' J. appl. Physiol. 23, 1967, 426-432.

257. Turner, J.M. 'Distribution of lung surface pressure as a function of posture in dogs.' Physiologist (Wash.) 5, 1962, 223.

258. Ueda, H., Iio, M. and Kaihara, S. 'Determination of regional pulmonary blood flow in various cardiopulmonary disorders.' Jap. Heart J. 5, 1964, 431-444.

259. Vandenberg, R.A., Nolan, A.C., Reed, J.H. and Wood, E.H. 'Regional pulmonary arterial-venous shunting caused by gravitational and inertial forces.' J. appl. Physiol. 25, 1968, 516-527.

260. Varene, P. and Jacquemin, C. 'Les résistances bronchiques au cours des accélérations transverse. C. r. hebd. Séanc. Acad. Sci., Paris. 252, (iii) 1961 3652-3654.

261. Wade, O.L. 'Movements of the thoracic cage and diaphragm in respiration.' J. Physiol. (Lond.) 124, 1954, 193-212.

262. Wagner, H.N., Sabiston, D.C., Iio, M., McAfee, J.G., Meyer, J.K. and Langan, J.K. 'Regional pulmonary blood flow in man by radioisotope scanning.' J. Am. med. Ass. 187, 1964, 601-603.

263. Wagner, P., McRae, J. and Read, J. 'Stratified distribution of blood flow in secondary lobule of the rat lung.' J. appl. Physiol. 22, 1967, 1115-1123.

264. Watson, J.F. and Cherniack, N.S. 'Effect of positive pressure breathing on the respiratory mechanics and tolerance to forward acceleration. Tech Rep. No. 61-398, Aeronautical Systems Division, Wright-Patterson A.F.B. Ohio, 1961, 8 pp.

265. West, J.B. 'Regional differences in gas exchange in the lung of erect man.' J. appl. Physiol. 17, 1962, 893-898.

266. West, J.B. 'Recent observations on the distribution of pulmonary blood flow.' J. nucl. Biol. Med. 11, 1967, 54-62.

267. West, J.B. and Dollery, C.T. 'Distribution of blood flow and ventilation-perfusion ratio in the lung, measured with radioactive CO_2.' J. appl. Physiol. 15, 1960, 405-410.

268. West, J.B., Dollery, C.T. and Heard, B.E. 'Increased pulmonary vascular resistance in the dependent zone of the isolated dog lung caused by perivascular oedema.' Circulation Res. 17, 1965, 191-206.

269. West, J.B., Dollery, C.T. and Naimark, A. 'Distribution of blood flow in isolated lung; relation to vascular and alveolar pressures.' J. appl. Physiol. 19, 1964, 713-724.

270. West, J.B. and Hugh-Jones, P. 'Experimental verification of the single breath tests of ventilatory and ventilation-perfusion ratio inequality.' Clin. Sci. 18, 1959, 553-558.

271. Wilson, W.H. 'The influence of posture on the volume of the reserve air.' J. Physiol. (Lond.) 64, 1927, 54-64.

272. Wood, E.H., Nolan, A.C., Donald, D.E. and Cronin, L. 'Influence of acceleration on pulmonary physiology.' Fedn Proc. Fedn Am. Socs exp. Biol. 22, 1963, 1024-1034.

273. Wood, E.H., Sutterer, W.F., Marshall, H.W., Lindberg, E.F. and Headley, R.N. 'Effect of headward and forward accelerations on the cardiovascular system.' Tech. Rep. No. 60-634, Wright Air Development Division, U.S.A.F., Wright-Patterson A.F.B. Ohio, 1961, 48 pp.

274. Workman, J.M., Penman, R.W.B., Bromberger-Barnea, B., Permutt, S. and Riley, R.L. 'Alveolar dead space, alveolar shunt, and transpulmonary pressure.' J. appl. Physiol. 20, 1965, 816-824.

275. Yokoyama, T. and Farhi, L.E. 'Study of ventilation-perfusion ratio distribution in the anesthetized dog by multiple inert gas washout.' Resp. Physiol. 3, 1967, 166-176.

276. Yudkofsky, P.L. and Zuidema, G.D. 'Human tolerance to one stage rocket acceleration.' Tech. Rep. No. 57-59, Wright Air Development Center, U.S.A.F., Wright-Patterson A.F.B. Ohio, 1957, 5 pp.

277. Zardini, P. and West, J.B. 'Topographical distribution of ventilation in isolated lung.' J. appl. Physiol. 21, 1966, 794-802.

278. Zechman, F.W. 'The effect of forward acceleration on vital capacity.' Tech. Note No. 58-376, Wright Air Development Center, U.S.A.F., Wright-Patterson A.F.B. Ohio, 1958, 6 pp.

279. Zechman, F.W., Cherniack, N.S. and Hyde, A.S. 'Ventilatory response to forward acceleration.' J. appl. Physiol. 15, 1960, 907-910.

Index

Numbers in bold type indicate main references

Absorptional collapse, 125-7, 140, 142, 144
see also Acceleration atelectasis
Acceleration
definition of, 13ff.
effect on arterial oxygen saturation, 165
--cardiovascular system, 69
--gas exchange, 159
--mechanics of breathing, 19
--pulmonary blood flow distribution, 103
--pulmonary shunting, 173
--pulmonary ventilation, 19
--ventilation distribution, 55
see also Backward, Forward, Lateral, Negative and Positive acceleration
Acceleration atelectasis, 121
barometric pressure and, 89, 125-7, 144
effect of inspired nitrogen, 125-7, 139
--lung volume, 140, 142
--positive pressure breathing, 140
--posture, 142, 144
effect on lung volumes, 123-4, 140
--regional blood flow, 169-171
forward acceleration and, 123, 148
mechanism of, 144, 145
positive acceleration and, 121, 138-9
prevention of, 125-7, 149
radiographic appearance, 121, 122, 127, 141, 142
rate of development, 137, 139-40, 144
to increase acceleration tolerance, 191
Acceleration nomenclature, 13, 14
Acceleration tolerance, 17-18, 70, 74, 189
techniques for increasing, 191
Aeroatelectasis, 123
see also Acceleration atelectasis
Air shunt, 63
see also Alveolar dead space
Air trapping, 128ff.
see also Gas trapping
Airway closure
alveolar gas pressure and, 110, 111, 189
effect of acceleration, 59ff, 129ff
--intrapleural pressure, 39
--lung volume, 47-8, 59ff, 128ff
--posture, 48, 142-4
mechanism of, 59-63, 139
regional ventilation and, 47ff
re-opening of, 47, 146
see also Gas trapping
Airway resistance, 31

effect of acceleration, 31-3
--lung volume, 128
interruptor method of measurement, 33
regional variation in, 48-9
Alveolar dead space, 151-3
effect of acceleration, 105, 111, 131
Alveolar dimensions, 41, 42, 43
apparent blood flow distribution and, 110, 117
effect of acceleration, 55, 62, 63, 110
--gravity, 41, 43
--posture, 43
Alveolar gas composition
effect of acceleration, 153-5
--ventilation-perfusion ratio inequality, 151ff
Alveolar lining layer and blood flow distribution, 93
Alveolar oedema, 119
in atelectasis, 121, 127-8
Alveolar shunt, 151-3
see also Pulmonary shunt
Alveolar ventilation and acceleration, 21
see also Pulmonary ventilation
Anaerobic metabolism during acceleration stress, 159, 163-5
Anatomical dead space, 21
distribution of dead space gas, 52-3, 151-3
Anterior chest wall, movement during respiration, 23
Anti-g suit, 16, 18
effect on airway closure, 63, 129
--arterial oxygen saturation, 171
--atelectasis, 121, 128, 139
--functional residual capacity of lung, 18, 133
--gas trapping, 129-131, 133
--intra-abdominal pressure, 29
--lung compliance, 31
--oxygen debt of acceleration, 161
--pulmonary arterial blood pressure, 79
--single breath carbon dioxide test during acceleration, 133
--ventilation distribution, 47, 63
Aortic blood pressure in acceleration, 69-70, 74, 75
Apical support model of lung, 50, 51, 182, 189
Argon single breath test, 138
effect of acceleration, 134, 138
--expiratory flow rate, 135, 138
--posture, 136, 138
Arterial oxygen saturation during acceleration, 166, 165, 168-9
effect of anti-g suit, 165, 167, 171
--inspired oxygen, 167-9, 171
--positive pressure breathing, 167-8
--posture, 167, 168, 171-3
--ventilation perfusion ratio inequality, 151ff.
transient changes following acceleration, 175
Asynchronous (sequential) ventilation, 52
Atelectasis; see Acceleration atelectasis, Low lung volume breathing atelectasis, and Oxygen

Backward acceleration ($-G_x$, transverse prone G, eyeballs out)
definition of, 14
effect on arterial oxygen saturation, 168
--central venous pressure, 118

--pulmonary ventilation, 21
--vital capacity, 23
Baroreceptor reflexes, 21, 70-71, 74
Blackout, 17, 18, 69, 74
Blood shunt, 63
see also Pulmonary shunt, and Right-to-left shunt

Carbon dioxide
output during acceleration, 161, 163, 179
radioactive, in measurement of pulmonary blood flow distribution, 44, 82, 83
single breath test
forward acceleration and, 111, 113, 131
positive acceleration and, 130, 131-3
stores of body, 159-161
acceleration and, 179
Cardiac arrhthmias during acceleration, 74
Cardiac output during positive acceleration, 71-4
during forward acceleration, 74-5
Cardiogenic oscillation, 133
Cardiovascular changes provoked by acceleration, 69
Centrifugal force, 13
Centrifuge, 13, 14
recording from, 15-17
Centripetal acceleration, 13
Chest strapping, 47, 129
Circulating blood volume in acceleration, 70
Collapse of lung; see Acceleration atelectasis, and Low lung volume breathing
Collateral ventilation, 148
Collimation for radioisotope scanning of lung, 105, 106, 191
Colloid osmotic pressure of plasma proteins, 119
Compliance of lung, 31
artifacts in measurement, 31
effect of acceleration, 31, 55, 56
--age, 51
--anti-g suit, 31
--posture, 31
frequency independence of, 48, 52
in atelectasis, 121-3
regional differences in, 48-9, 184, 185
Compliance of thorax, 29
effect of forward acceleration, 29-31
--positive acceleration, 28, 29-31
Compound spring model of lung, 182, 183-4
Conductance of pulmonary capillaries, 96, 97
Critical closing pressure
in pulmonary capillaries, 101, 110
in systemic capillaries, 70

Diaphragm, movement with respiration, 25-9
effect of acceleration, 27, 29
--anti-g suit, 28, 29
recording technique, 26, 25
Diffusion of gas in lung, 53
Diffusing capacity of lung
effect of acceleration, 169
--oxygen, 124-5
Disorientation caused by angular acceleration, 18
Dispersed absorption collapse of lung, 146

Distribution of dead space gas, 52-3
Distribution of pulmonary blood flow, 83
effect of acceleration, 103, 187-9
see also Pulmonary blood flow
Distribution of ventilation, 37, 44, 183-4
effect of acceleration, 55
see also Pulmonary ventilation
Distribution of ventilation-perfusion ratio, 189-91
effect of forward acceleration, 157, 189
--positive acceleration, 151, 189
see also Ventilation-perfusion ratio inequality

Effective pulmonary capillary blood flow, 169
Expiratory effort during acceleration, 33-5
Expiratory reserve volume
effect of forward acceleration, 17, 22, 23
--positive acceleration, 22
regional values, 38
Expired gas composition
effect of acceleration, 131-3, 179
--alveolar dead space, 161
see also Single breath tests
Extra-alveolar vessels, role in blood flow distribution, 98, 99-102

Filtration of blood during acceleration, 70
Flat-lung preparation, 93ff
Fluid breathing, 192
Fluid lung model, 49-50, 185
Fluid pressure, 185, 186
Forward acceleration (+G_x, transverse supine G, eyeballs in)
definition of, 14, 15
effect on arterial oxygen saturation, 165ff
--cardiovascular system, 74
--distribution of pulmonary blood flow, 111
--distribution of ventilation, 63
--distribution of ventilation-perfusion ratio, 157
--gas exchange, 163ff
--gas stores, 177ff
-lung mechanics, 29ff
--lung volumes, 21ff
--pulmonary circulation, 81
--pulmonary shunt, 173ff
--pulmonary ventilation, 21ff
Four-zone model of lung, 100, 102
Functional residual capacity of lung
effect of acceleration, 23-5, 29-31, 67
--lower body negative pressure, 191
--posture, 23-5, 48
regional values, 36, 39
role in acceleration atelectasis, 140

Gas exchange, 159
effect of forward acceleration, 163
--positive acceleration, 159
influence of ventilation-perfusion ratio inequality, 151ff
Gas stores
change with acceleration, 177
--cardiac output, 159-161, 165

--pulmonary ventilation, 159-161, 165
Gas trapping
absorptional collapse and, 128ff
during normal breathing, 48, 148
effect of acceleration, 59ff, 129ff
-anti-g suit, 63, 129, 133
--lung volume, 39, 47, 61, 64, 128-9
mechanism of, 39, 59, 139
volume of gas trapped, 46, 47, 131, 140, 168

Haematocrit, change with acceleration, 70-1
Headward acceleration; see Positive acceleration
Hydrogen for assessment of pulmonary shunt, 173-5
see also Tritium
Hydrostatic indifference level
in pulmonary circulation, 79, 81, 103, 112
in systemic circulation, 70
Hydrostatic pressure gradient
in lung, 186
in pulmonary circulation, 15, 87
effect of acceleration, 79, 103, 104
in systemic circulation, 69, 74

^{131}I-MAA: see Macro-aggregated albumin
Inertial force, definition of, 13, 14
Inspiratory capacity of lung, 22, 23, 24
reduction in atelectasis, 121, 146
regional values, 36
Inspiratory effort during acceleration, 33-5
Interlobular communications in lung, 146
Interstitial oedema in lung, 101, 101, 119
Interstitial pressure in lung, 139, 186-7
blood flow distribution and, 97-102, 188
effect of acceleration, 109-10
Intra-abdominal pressure
effect of acceleration, 25-9
--anti-g suit, 28, 29
Intra-oesophageal pressure measurement, 31, 185
Intrapleural pressure gradient, 39ff, 49-51, 57, 185
blood flow distribution and, 49
effect of acceleration, 55, 59, 59-63, 65
--posture, 39, 49, 184, 185
estimation from alveolar size, 49
--using xenon-133, 49, 50, 59
gas distribution and, 49
nature of, 49, 185-6
regional lung expansion and, 38, 39ff, 46
Isolated lung preparation, 87ff
Isopressure level in lung, 57

Lateral acceleration ($\pm G_y$, eyeballs right and left)
definition of, 14
effect on pulmonary blood flow distribution, 117-8
--pulmonary vascular pressures, 117
Low lung volume atelectasis (collapse), 140-2
in anaesthesia, 146-8
Low lung volume breathing
absorptional collapse in, 140-4, 14-6

airway closure in, 128-9, 142
effect of posture on, 142-4
Lower body negative pressure, 191
Lung compliance, 31
see also Compliance
Lung histology, 91, 94, 95
in absorptional atelectasis, 126, 127
Lung mechanics, 19, 181
Lung tissue viscance, 33
Lung volumes (see also Regional lung volume)
effect of acceleration, 21
regional subdivisions of, 37
see also Expiratory reserve volume, Functional residual capacity, Inspiratory capacity, Minimal volume, Residual volume, Total lung capacity, and Vital capacity

Macro-aggregated albumin for measurement of pulmonary blood flow distribution, 47, 105, 111
Mechanics of breathing, 19, 181
Miliary lung collapse, 146
Minimal volume of lung, 47, 139
mechanism of, 39, 47, 139, 181
Models of lung
for blood flow,
four-zone model, 100, 102
three-zone model, 89ff, 187
for ventilation, 38, 39ff
apical support model, 49-51, 182, 184
compound spring model, 182, 184
fluid model, 51, 185
simple spring model, 50, 182, 183

Negative acceleration (negative G, - G_z, eyeballs up, footward acceleration)
definition of, 14
effect on arterial oxygen saturation, 168, 173
--pulmonary blood flow distribution, 103, 104, 118
Negative pressure breathing
compared with forward acceleration, 21
lung volume change induced by, 47
Nitrogen
absorption from lung, 125ff
role in acceleration atelectasis, 126, 127
single breath test, 133
effect of acceleration, 133, 134
--posture, 138
Nitrogen brake, 125, 127

Osmotic pressure of plasma proteins, 119
Oxygen
cost of breathing during acceleration, 33
debt following acceleration, 159ff
solubility, role in atelectasis, 125, 139, 168-9
stores, effect of acceleration, 165, 177-9
toxicity, role in atelectasis, 124, 148
uptake during forward acceleration, 163ff
--positive acceleration, 159ff
effect of exercise, 161-3
see also Arterial oxygen saturation

Oxygen-15 labelled carbon dioxide, for measurement of pulmonary blood flow distribution, 44, 82, 83

Parallel ventilation theory, 51, 52-3
Periodic breathing, 128
Peripheral resistance, changes during acceleration, 71
Perivascular space of lung, 99-101
Pleural pressure; see Intrapleural pressure
Pooling of blood during acceleration, 70
Positive acceleration (positive G, + G_z, eyeballs down, headward acceleration)
  definition of, 13, 14
  effect on arterial oxygen saturation, 165ff, 175ff
  --distribution of pulmonary blood flow, 105
  --distribution of ventilation, 55
  --distribution of ventilation-perfusion ratio, 151
  --gas exchange, 159-165
  --gas stores, 177ff
  --lung mechanics, 19
  --lung volumes, 21ff
  --pulmonary circulation, 75-81
  --pulmonary shunt, 173-5
  --pulmonary ventilation, 19
  --regional subdivisions of lung volume, 57ff
  --systemic circulation, 69ff
  in acceleration atelectasis, 121ff
Positive pressure breathing
  acceleration atelectasis and, 140
  acceleration tolerance and, 21, 191
Pulmonary arterial pressure, 75-81
  blood flow distribution and, 87ff, 103ff
  effect of anti-g suit, 79
  --forward acceleration, 81
  --positive acceleration, 75-80, 174
  --posture, 79
  --weightlessness, 118-19
  pulse, and blood flow distribution, 94
  pulse, transmission through lung, 92, 93
Pulmonary blood flow, 71ff
Pulmonary blood flow distribution, 83, 84, 103, 187
  effect of alveolar lining layer, 93
  --alveolar size, 115, 117
  --exercise, 86, 87
  --forward acceleration, 111ff
  --interstitial pressure, 97, 101
  --lung volume, 84, 85
  --lung volume history, 91
  --other acceleration vectors, 118
  --pathological factors, 87
  --positive acceleration, 105ff
  --posture, 85
  --pulse pressure, 93-4
  --vascular pressures, 86, 87, 88
  --weightlessness, 118-19
  four-zone model of, 100, 102
  measurement using labelled macro-aggregated albumin, 85, 105, 111
  --xenon-113, 82, 83, 87ff, 105ff, 112ff, 189
  --oxygen-15 labelled carbon dioxide, 44, 82, 83
  three-zone model of, 89ff, 187

Pulmonary blood volume
distribution of ventilation and, 49
Pulmonary capillaries
conductance of, 96, 97
critical closing pressure of, 101, 110
distensibility of, 94, 95, 97, 109, 111, 117, 187
histology of, 91, 94, 95
waterfall effect in, 89, 94-5
Pulmonary circulation during acceleration, 75
Pulmonary diffusing capacity
effect of acceleration, 169
--oxygen, 124
Pulmonary oedema
acceleration and, 119
blood flow distribution and, 101
role in acceleration atelectasis, 127-8
Pulmonary shunt, 151, 155, 173
alveolar collapse and, 140
effect of acceleration, 157, 168ff
estimation from arterial oxygen saturation, 169
--using hydrogen, 172, 173-5
--using tritium, 174, 175
--using xenon-113, 129, 173
Pulmonary surfactant, 128
Pulmonary vascular bed, effect of lung inflation, 99
Pulmonary ventilation, 19
asynchronous, 52
effect of forward acceleration, 21
--backward acceleration, 21
--positive acceleration, 19, 20
reflex control during acceleration, 21
regional distribution of, 37, 44, 181ff
effect of backward acceleration, 67
--forward acceleration, 65-7
--gravity, 39ff, 138-9, 181ff
--inspiratory airflow, 44, 47
--lung volume, 44ff
--positive acceleration, 55, 181ff
--posture, 39ff, 59, 138, 183ff
--weightlessness, 67
factors determining, 48
sequential, 47, 52
series, 52, 53

Radial acceleration, 13
Radioisotopes for lung function studies; see Carbon dioxide, Macro-aggregated albumin, Tritium, Xenon-133
Reference levels for vascular pressure measurement, 74-5
Reflex pulmonary atelectasis, 128
Reflex regulation
in pulmonary circulation, 81
in systemic circulation, 70
of respiration during acceleration, 21
Regional distribution
of pulmonary blood flow, 83
effect of acceleration, 103, 187-9
see also Pulmonary blood flow
of ventilation, 37, 44, 181ff

effect of acceleration, 55, 181ff
see also Pulmonary ventilation
of ventilation-perfusion ratio, 151, 189
effect of acceleration, 153-7
see also Ventilation-perfusion ratio inequality
Regional lung volume, 37ff
effect of forward acceleration, 64, 65, 117
--positive acceleration, 56, 57-9, 61
--posture, 36, 37ff
Regional subdivisions of lung volume, 37
see also Lung volumes, and Regional lung volume
Relaxation pressures, 29
effect of forward acceleration, 29, 30, 31
--positive acceleration, 29, 30
Residual volume of lung
effect of acceleration, 21, 22
--lower body negative pressure, 191
measurement of, 21
mechanism of, 23, 39, 181
regional values of, 36, 39ff
Respiratory frequency
effect of acceleration, 20, 21, 32
--anti-g suit, 29
optimum value during acceleration, 32, 33
Resultant acceleration, 13
Retinal blood flow, 69
Right atrial pressure during acceleration, 77, 79
Right-to-left shunt, 173
see also pulmonary shunt
Ripple in expired gas concentration: see Cardiogenic oscillation
Rubidium-86 for measurement of cardiac output distribution, 71

Sequential (asynchronous) ventilation, 47, 52
Series ventilation theory, 52, 53
Single breath tests, 131ff
see also Argon, Carbon dioxide, and Nitrogen
Sluice flow: see Waterfall effect
Spring model of lung
compound, 182, 184
simple, 50, 182, 183
Starling resistor, 89, 94
for pressure measurement, 185
see also Waterfall effect
Stratification ventilation theory, 52, 53
Surface active material in lung, 128-9
Surface pressure
in oesophagus, 186
in pleural cavity, 185-6
Systemic circulation during acceleration, 69
Shallow breathing, 128-9
see also Low lung volume breathing

Thoracic compliance, 29
see also Compliance
Thoracic elastance
effect of positive acceleration, 29, 30
--weightlessness, 29
Three-zone model of lung, 89ff, 187

effect of acceleration, 103ff
Tidal volume of lung
effect of acceleration, 20, 21
--anti-g suit, 28, 29
Tolerance to acceleration, 17, 69, 74, 189
effect of anti-g suit, 17
techniques for increasing, 191
Total lung capacity, 21
effect of acceleration, 21-5
--lower body negative pressure, 190, 191-2
regional subdivisions of, 37ff
subdivisions of, 21
Transmission of pressure pulse through lung, 92, 93-4
Transudation
in lungs, 111, 119, 127-8
in systemic circulation, 70
Transverse acceleration, 14, 15
see also Backward, and Forward acceleration
Trapping: see Gas trapping, and Airway closure
Tritium for measurement of right-to-left shunt, 174, 175

Urinary-alveolar nitrogen difference, effect of posture, 48

Vagal afferents in lung, 123
Valsalva manoeuvre, 17
Venous admixture: see Pulmonary shunt
Ventilation, 19
asynchronous, 52
collateral, 146
distribution of, 37, 44, 181ff
effect of acceleration, 55, 181ff
sequential, 47, 52
series, 52, 53
see also Pulmonary ventilation
Ventilation-perfusion ratio inequality, 151, 189, 191
airway closure and, 63, 151, 155, 189
effect of forward acceleration, 156, 157
--positive acceleration, 151, 152
--posture, 48
alveolar gas composition and, 151ff
capillary blood gas content and, 153, 154
gas exchange and, 151ff
in secondary lobule, 53
reflex adjustment of, 188
see also Pulmonary blood flow, and Pulmonary ventilation
Vital capacity of lung
effect of backward acceleration, 23
--forward acceleration, 23, 24
--oxygen, 124-5, 146
--positive acceleration, 22, 23
--posture, 15, 23
in acceleration atelectasis, 121, 122, 123, 126, 137, 138, 139, 146, 168, 187
regional values and subdivisions, 36, 37ff
effect of posture, 39, 40, 43

Waterfall effect, 70, 94
see also Zones of blood flow in lung
Weightlessness

atelectasis and, 149
pulmonary arterial pressure during, 119
pulmonary blood flow distribution in, 118-19
ventilation distribution in, 67
Work of breathing, 33-5
oxygen cost during acceleration, 33, 35

Xenon-133
for calculation of intrapleural pressure gradient, 49, 59
for detection of unventilated alveoli, 63, 129-31
for measurement of pulmonary blood flow distribution, 82-3, 87 et seq., 105 et seq., 112ff, 189, 191
--pulmonary shunting, 129, 173
--regional subdivisions of lung volume, 37, 39, 43
--ventilation distribution, 44ff, 57ff 65ff
for monitoring cardiac output, 73
Xiphisternal suction, 191-2

Zero-g, 67, 118-19
see also Weightlessness
Zones of blood flow in lung, 89ff, 105ff, 187-8
1, zone of zero flow, 89, 91-4
effect of acceleration, 103, 104, 105, 109, 112
2, waterfall (sluice flow), 89, 94-5
effect of acceleration, 109, 112, 117, 188
3, passive distension zone, 89, 95, 97
effect of acceleration, 109-11, 112, 117
4, zone of interstitial pressure, 97-102, 188
effect of acceleration, 111, 117-18, 171